Exploration and Manipulation of Cellular Pathways for Treatment of Neurodegeneration

This thesis is submitted for the degree of Doctor of Philosophy at Cardiff University

Kyle Fears

Supervisors:

Professor Riccardo Brambilla

Dr Simon Brooks

Dr Stéphane Baudouin

Professor Stephen Dunnett

January 2019

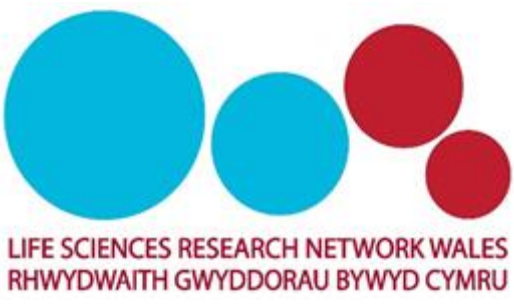

Declaration

This work has not been submitted in substance for any other degree or award at this or any other university or place of learning, nor is being submitted concurrently in candidature for any degree or other award.

Signed …… (candidate) Date ……

STATEMENT 1

This thesis is being submitted in partial fulfillment of the requirements for the degree of ……(insert MCh, MD, MPhil, PhD etc, as appropriate)

Signed …… (candidate) Date ……

STATEMENT 2

This thesis is the result of my own independent work/investigation, except where otherwise stated, and the thesis has not been edited by a third party beyond what is permitted by Cardiff University's Policy on the Use of Third Party Editors by Research Degree Students. Other sources are acknowledged by explicit references. The views expressed are my own.

Signed …… (candidate) Date ……

STATEMENT 3

I hereby give consent for my thesis, if accepted, to be available online in the University's Open Access repository and for inter-library loan, and for the title and summary to be made available to outside organisations.

Signed …… (candidate) Date ……

STATEMENT 4: PREVIOUSLY APPROVED BAR ON ACCESS

I hereby give consent for my thesis, if accepted, to be available online in the University's Open Access repository and for inter-library loans **after expiry of a bar on access previously approved by the Academic Standards & Quality Committee.**

Signed …… (candidate) Date ……

Thesis Summary

Neurodegenerative disorders such as Huntington's disease (HD) and Parkinson's disease (PD) represent a significant and growing public health crisis. In order to combat these devastating illnesses, we must understand the underlying pathophysiology and develop effective treatments.

The aim of Chapter 2 was to establish whether the novel Parkin$^{S65A/S65A}$ knock-in mouse represented a robust model of PD. Despite carrying a mutation analogous to those found in human PD, through extensive behavioural testing it became apparent that the Parkin$^{S65A/S65A}$ mouse did not display a Parkinsonian motor phenotype.

Chapter 3 was directed towards optimising a gene therapy approach for PD by using adeno-associated viral vectors (AAVs) co-expressing tyrosine hydroxylase (TH) and GTP cyclohydrolase 1 (GCH1) to produce L-DOPA directly within the striatum of the 6-hydroxydopamine (6-OHDA) model of PD. The efficacy of linker-separated bicistronic AAVs was compared to a reference bicistronic AAV with tandem promoters by using multiple behavioural readouts to assess the extent of functional recovery. No behavioural recovery was observed with any AAV, likely reflecting administration of an insufficient dose.

In Chapter 4, the effects of the novel peptide RB5 were assessed in wild-type animals. By increasing extracellular protein kinase (ERK) signalling in the striatum, RB5 could represent a disease-modifying strategy for the treatment of HD. RB5 was unsuccessful in increasing striatal ERK signalling when administered systemically or when constitutively expressed within the striatum. Expression of RB5 did not alter the behaviour of mice compared to control mice expressing green fluorescent protein, but a significant number of animals in both groups displayed substantial expression-related neurodegeneration.

The results outlined in these chapters demonstrate the challenging nature of the essential steps towards understanding and treatment of neurodegeneration. Firstly, animal models of disease are an invaluable tool but often do not accurately reflect the human condition. Secondly, the benefit of gene therapy lies within a narrow therapeutic window, with transgene under-expression ineffective and transgene over-expression potentially harmful, necessitating optimisation. Finally, disease-modifying treatments are extremely difficult to formulate and should be extensively characterised in healthy mice before use in disease models.

Acknowledgments

I'd firstly like to thank Anne, Steve, and everyone at the BRG – past and present – for welcoming me for a summer project and letting me stay almost 5 years. Everyone has always been so welcoming, and it's been great to be part of the lab.

Particular office-based thanks go out to Laura for all the cocktail sausage-based laughs, Oly for spilling the lapsang souchong at every opportunity, David for unwillingly teaching me a Northern Irish accent, and Susanne for all the bird-based tomfoolery. Special thanks also go out to Ana Statisticamente for all the ANOVA help and tortillas, to Rachel Hills for teaching me everything I know and not punching me every time I forget it, Harri for fixing everything after I've broken it, and Mariah for all your help and advice. I'd also like to say a big thank you to the cleanroom crew – I couldn't think of a better group of people to sweat and hate my life with in the depths of summer.

Most of all I'd like to thank Stéphane. Thank you for all your help, guidance, and righteous anger. There's no way I'd be writing these words without you stepping in. I know it's been frustrating for you at times, but I hope it's all been worth it for the endless supply of sarcasm and gossip I supply. It's the only way I have to repay you

I'd like to take the opportunity to thank my parents for asking what I do and pretending to care - I appreciate the support. I'd like to also thank my sisters Bethan and Claire for making it so easy for me to be the favourite child.

Finally, I'd like to thank Emeka for all the support and always being there for me. I know you're just in it for the sweets.

Abbreviations

5'UTR	5' untranslated region
6-OHDA	6-hydroxydopamine
AADC	Aromatic L-amino acid decarboxylase
AAV	Adeno-associated viral vector
Akt	Protein kinase B
AD	Alzheimer's Disease
AMPA	α-amino-3-hydroxy-5-methyl-4-isoxazolepropionic acid
ALS	Amyotrophic lateral sclerosis
ATP12A2	PARK9
BACHD	Bacterial artificial chromosome
BDNF	Brain-derived neurotrophic factor
BH4	Tetrahydrobiopterin
CCCP	Carbonyl cyanide *m*-chlorophenyl hydrazone
cDNA	Complementary DNA
D1Rs	D1 dopamine receptors
D2Rs	D2 dopamine receptors
DJ-1	Protein deglycase DJ-1 (PARK7)
ERK	Extracellular signal-regulated kinase
FMDV	Foot and mouth disease virus
GABA	γ-aminobutyric acid
gc/ml	Genome copies per millilitre
GCH1	GTP cyclohydrolase 1
GCPRs	G-coupled protein receptors
GPe	Globus pallidus externalis
GPi	Globus pallidus internalis
GMP	Good manufacturing practice
GOF	Gain-of-function
GTP	Guanosine triphosphate
H_2O_2	Hydrogen peroxide
HOM	Homozygous

HTT	Huntingtin gene
5'UTR	5' untranslated region
HD	Huntington's disease
IEGs	Immediate early genes
IRES	Internal ribosome entry site
JNK	C-Jun N-terminal kinase
KO	Knock-out
L-DOPA	Levodopa (L-3,4-dihydroxyphenylalanine)
LRRK2	Leucine-rich repeat kinase 2 (PARK8)
LTD	Long-term depression
LTP	Long-term potentiation
MAPKs	Mitogen-activated protein kinases
MAP2K	MAPK kinase
MAP3K	MAPK kinase kinase
MAP4K	MAPK kinase kinase kinase
MAPKAPK	MAPK-activated protein kinases
MSNs	Medium spiny neurons
MFB	Medial forebrain bundle
mHTT	Mutant Huntingtin protein
MPP	Mitochondrial processing peptidase
MNK1/2	MAPK-interacting kinase 1/2
MPTP	1-methyl-4-phenyl-1,2,3,6-tetrahydropyridine
mRNA	Messenger RNA
MSK1-4	Mitogen- and stress-activated protein kinase 1-4
mtDNA	Mitochondrial DNA
NDP52	Nuclear dot protein 52kDa
NF1	Neurofibromatosis 1
NHPs	Non-human primates
NMDAR	N-terminal-D-aspartate receptor
OPTN	Optineurin
OMM	Outer mitochondrial membrane
P75NTR	P75 neurotrophin receptor

PARIS	Parkin-interacting substrate
PD	Parkinson's disease
P-ERK	Phospho-extracellular signal-regulated kinase
PGC-1α	PPARγ coactivator-1α
PI3K	Phosphoinositide 3-kinase
PINK1	PTEN-induced kinase 1
PLCγ1	Phospholipase C, gamma 1
polyQ	Polyglutamine
PPARγ	Peroxisome proliferator-activated receptor gamma
PARL	Presinilin-associated rhomboid-like protein
Ras-GRF1	Ras protein specific guanine nucleotide releasing factor
RBD	REM behaviour disorder
REM	Rapid eye movement
REST/NRSF	RE1-silencing transcription factor/Neuron-restrictive silencer factor
RBR	RING-in-between-RING
ROS	Reactive oxygen species
RSK1-4	Ribosomal S6 kinase 1 – 4
Ser/Thr	Serine/Threonine
SNCA	Alpha synuclein (PARK1)
Sos1/2	Son of sevenless 1/2
SNc	Substantia nigra pars compacta
SNr	Substantia nigra pars reticularis
STN	Subthalamic nucleus
Syn-1	Synapsin 1
TF	Transcription factor
TH	Tyrosine hydroxylase
TIM	Translocase of the inner membrane
TOM	Translocase of the outer membrane
TrkB	Tropomyosin receptor kinase B
TU	Transducing units
Ubl	Ubiquitin-like
UBS	Ubiquitin-proteasome system

UPDRS	Unified Parkinson's disease rating scale
WPRE	Woodchuck hepatitis post-transcriptional regulatory element
WT	Wild-type
ΔΨm	Mitochondrial membrane potential depolarisation

Table of Contents

Chapter 1: General Introduction

1.1. Background

The term neurodegenerative diseases encompasses a variety of disorders which possess distinct (although sometimes shared) aetiology and pathophysiology and result in disabling symptomology through progressive and inexorable degeneration of neurons. Neurodegenerative diseases fall under the umbrella or brain disorders which include other neurological and neuropsychiatric illnesses and collectively account for 13% of global disease prevalence – higher than cancer (Fineberg *et al.*, 2013). Relatively recent advances in molecular biology enabled identification of the genetic causes of rare familial forms of Alzheimer's disease (AD) (Ertekin-Taner, 2007) and Parkinson's disease (PD) (Deng, Wang and Jankovic, 2018), as well as the cause of Huntington's disease (HD) (MacDonald *et al.*, 1993). However, the cause of other neurodegenerative diseases and non-inherited forms of AD and PD are still currently unknown but have been linked to both genetic and environmental influences, with an increasing body of evidence identifying genetic risk factors which may increase the likelihood of developing a particular disorder (Billingsley *et al.*, 2018). Although all neurodegenerative diseases broadly result in cell death within the nervous system, the exact neuroanatomical target of a disease dictates the symptoms associated with it. For example, degeneration of the hippocampus and cerebral cortex in AD leads to the associated cognitive dysfunction and dementia (Masters *et al.*, 2015). Meanwhile, PD and disease HD patients display degeneration of structures within the basal ganglia, resulting in an overt motor phenotype (although cognitive and psychiatric diseases are often present) (Bates *et al.*, 2015; Obeso *et al.*, 2017).

The complexity of the nervous system and disease processes renders the development of cures or disease-modifying treatments extremely challenging, and as such none are currently available for AD, PD, and HD (Durães, Pinto and Sousa, 2018). However, development of disease-modifying therapies is essential. AD is the most common neurodegenerative disease and the most common cause of dementia, accounting for 50 – 75% of dementia cases (Prince *et al*., 2014) It is estimated that 50 million people are currently suffering with dementia worldwide, with the figure expected to rise to 152 million in 2050 (World Health Organisation, 2017). Although less common, PD affected 6.1 million people globally in 2016 (Feigin *et al.*, 2017) and other neurodegenerative diseases including HD affect many more with only symptomatic treatments typically available (Durães, Pinto and Sousa, 2018). Given that age is

the largest risk factor for development of AD and PD, these diseases represent a growing challenge considering the ageing population. In addition to the disease burden itself, the global cost of dementia alone is estimated to have reached $1 trillion in 2018 and will double to $2 trillion in 2030 (Alzheimer's Society, 2014), emphasising that neurodegenerative diseases represent not just a health crisis but a growing and considerable financial crisis in addition. Understanding the aetiologies and pathophysiologies of neurodegenerative disorders offers the opportunity to understand underlying disease mechanisms which could present novel drug targets and aid in the development of disease-modifying treatments, or even cures (Pangalos, Schechter and Hurko, 2007).

1.2. The Basal Ganglia

The basal ganglia are a collection of evolutionarily-conserved subcortical nuclei embedded deep within the forebrain which interact with the cortex and thalamus to form circuits, or "loops" (Allen and Tsukahara, 1974) (Figure 1.1). The striatum (caudate nucleus and putamen) is the major input nucleus of the basal ganglia, receiving excitatory glutamatergic input from nearly all functional regions of the cerebral cortex, and from certain thalamic nuclei, in addition to modulatory dopaminergic input from neurons of the substantia nigra pars compacta (SNc) ventral tegmental area (VTA) (Moore and Bloom, 1978). 95% of the neuronal population within the striatum is made up by γ-aminobutyric acid (GABA)ergic, inhibitory medium spiny neurons (MSNs) which integrate glutamatergic and dopaminergic inputs and project to downstream basal ganglia nuclei (Reiner *et al.*, 1988). The remainder of striatal neurons are cholinergic and GABAergic interneurons (Grillner and Robertson, 2016). The modulatory glutamatergic subthalamic nucleus (STN), the GABAergic globus pallidus internalis (GPi) and externalis (GPe), and the GABAergic substantia nigra pars reticularis (SNr) complete the basal ganglia (Alexander, 1986). The GPi and SNr are the major output nuclei of the basal ganglia and project to thalamic nuclei and motor centres of the brainstem, keeping these targets under tonic inhibition during resting conditions. MSNs project either directly to the GPi and SNr output nuclei or indirectly by synapsing with the GPe with subsequent synaptic connections between the GPe and STN, and STN and GPi/SNr. Signalling information is then relayed to cortical neurons, through thalamocortical projections. Through this circuitry, cortical information is relayed and refined through the basal ganglia before being returned to the cortex via thalamic nuclei. The basal ganglia are thought to have emerged 560 million years ago, based on similar organisation of the system between mammals and lampreys (Grillner and Robertson, 2016). Due to this similarity, conservation of basal ganglia organisation in mammals is particularly useful from a research perspective as it permits anatomical and functional comparisons between mammalian models and humans.

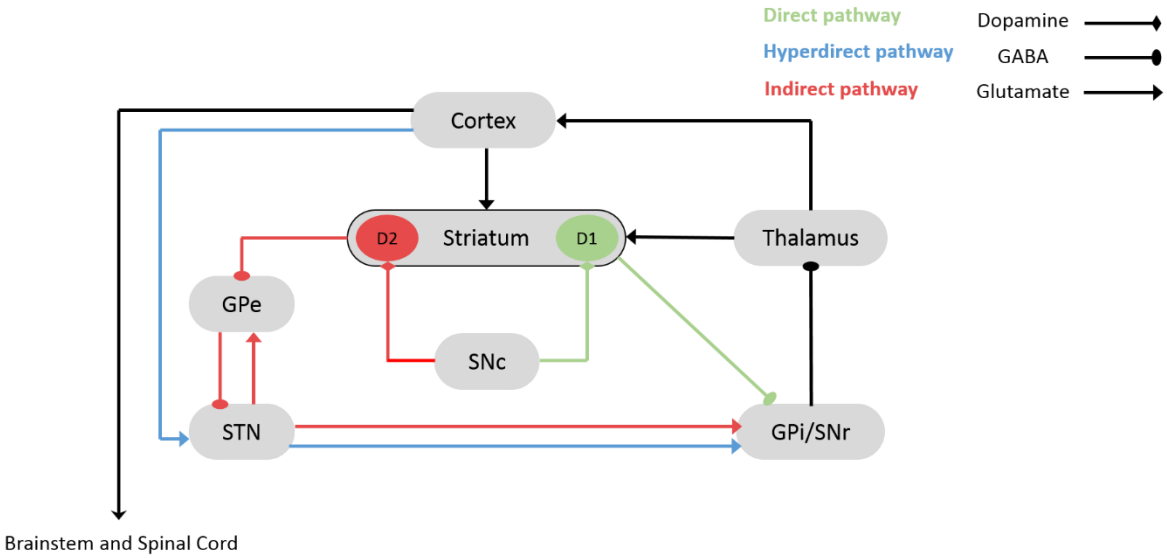

Figure 1.1. Representation of the basal ganglia nuclei and external structures with the direct, hyperdirect, and indirect pathways detailed. Cortical signals are relayed through the basal ganglia before returning the cortex via the thalamus.

1.2.1 Models of the Basal Ganglia

1.2.1.1. The Parallel Circuit Model

One of the original models of basal ganglia function postulated the existence of functionally segregated circuits between the basal ganglia nuclei and cortex (Alexander et al., 1986). According to this model, summarised here, different subdivisions of the striatum receive glutamatergic and dopaminergic innervation from different cortical and midbrain sources which, following relay through the remaining basal ganglia nuclei, leads to the formation of separate, parallel thalamocortical projections. These projections then loop to target the same or closely related cortical regions from which the initial glutamatergic input originated. For instance, the motor circuit is proposed to be formed through glutamatergic and dopaminergic innervation of the putaminal subdivision of the striatum by projections from the sensorimotor cortex and SNc, respectively. The resulting thalamocortical projections then target the premotor cortex. However, it should also be noted that the GPi/SNr nuclei also project to brainstem nuclei (Parent, Smith and Bellefeuille, 1984)). In contrast, the associative circuit (which underlies instrumental learning) is formed through glutamatergic and dopaminergic innervation of the caudate nucleus from the dorsolateral prefrontal cortex and SNc/VTA with thalamocortical projections returning to prefrontal cortex. Although the rodent striatum is not divided into caudate and putamen, functional subdivision is still relatively preserved (Grillner and Robertson, 2016). Associative circuit input is predominantly within the dorsomedial

striatum while motor loop input is predominantly through the dorsolateral striatum. The parallel circuit model hypothesised the existence of at least 5 individual loops and aimed to explain how separate functions, such as motor control and cognition, can be subserved by the same neural circuitry.

1.2.1.2. The Classical Model

The basal ganglia classical model subdivides striatal MSNs into two groups depending on whether they project directly or indirectly to the basal ganglia output nuclei (Albin, Young and Penney, 1989; DeLong, 1990; McGregor and Nelson, 2019). "Direct pathway" MSNs project directly to the GPi/SNr and express dopamine D1-like receptors (D1R) and substance P (Gerfen *et al.*, 1990) (Figure 1.1). In contrast, "indirect pathway" MSNs express dopamine D2-like receptors (D2R) and enkephalin and project to the GPe which, in turn, synapses with STN neurons which project to the GPi/SNr (Gerfen *et al.*, 1990) (Figure 1.1). Importantly, dopamine binding has opposing effects in direct and indirect pathway MSNs. D1R-dopamine binding is stimulatory in direct pathway MSNs due to activation of linked $G_{\alpha olf}$ protein, while dopamine signalling in indirect pathway MSNs is inhibitory due to G_i-coupled D2Rs (Hervé, Rogard and Lévi-Strauss, 1995). As such, at the level of the motor loop, striatal dopamine signalling has opposing effects within the direct and indirect pathways and the extent of signalling within each pathway determines the extent of tonic GPi/SNr-mediated thalamic inhibition (Albin, Young and Penney, 1989). Direct pathway activation inhibits the GPi/SNr, disinhibiting thalamocortical output and promoting movement through signalling between the motor cortex and brainstem and spinal cord (Figure 1.1). Indirect pathway activation has the opposing effect of suppressing movement through elevation of GPi/SNr-mediated thalamocortical inhibition mediated by the glutamatergic STN (Figure 1.1). As such, dopamine exerts a modulatory effect on MSNs with the relative extent of signalling in the direct and indirect pathways regulating control of voluntary movement. The classical model has been extensively studied in the context of neurodegenerative diseases of the basal ganglia, such as PD and HD, as loss of dopamine signalling or MSNs alters the balance of direct and indirect pathway signalling, leading to motor dysfunction (McGregor and Nelson, 2019). Furthermore, the associative loop would also be disrupted under these circumstances, explaining the cognitive symptoms observed in these conditions.

1.4.1.3. The Centre-Surround Model

A centre-surround model of action selection was also developed based on the divergent effects of the direct and indirect pathways at the level of the GPi/SNr (Mink, 1996). In terms of the motor circuit, this model stipulates that in order to execute a voluntary movement, competing motor programmes must be suppressed in to permit the voluntary movement to be properly

carried out. The indirect pathway stimulates the GPi/SNr to inhibit thalamocortical output and suppress competing motor programmes while the direct pathway disinhibits thalamocortical output to select the desired movement. The dynamic model takes into account the hyperdirect pathway, which extends from the cortex to the STN and on to the GPi/SNr with subsequent thalamocortical output, and its role in the timing aspect of basal ganglia signalling (Nambu, 2005). Under this model, following cortical-directed initiation of movement, the hyperdirect pathway output reaches the GPi/SNr first due to low conduction time, acting to suppress both the selected motor programme and competing motor programmes through inhibition of thalamocortical output. Signalling from the direct pathway reaches the GPi/SNr next, disinhibiting a central population of neurons within the GPi to increase thalamocortical signalling, releasing the selected motor programme. The indirect pathway acts in a similar manner to the hyperdirect pathway but reaches the output nuclei following direct pathway stimulation, inhibiting thalamocortical output and suppressing competing motor programmes. Through this model, only the selected motor programme is expressed at the correct time through the coordinated, sequential temporal signalling of the hyperdirect, direct, and indirect pathways. Although both the classical and centre-surround/dynamic models suggest a similar, opposing role of the direct and indirect pathways at the level of the GPi/SNr, the latter emphasises that correct, complementary interaction of both pathways is needed for appropriate initiation of movement and action selection, rather than direct opposition between pathways as suggested by the former (McGregor and Nelson, 2019).

1.4.1.4. The Rate Model

Importantly, many models of basal ganglia are based on the rate model of basal ganglia function (Penney and Young, 1983; Albin, Young and Penney, 1989). Developed in the 1980s and 1990s, the rate model hypothesises that basal ganglia output is determined by the firing rate of neurons within basal ganglia nuclei, with interruption of circuitry through neurodegeneration of these nuclei altering neuronal firing rates and leading to circuit dysregulation and associated motor and cognitive impairment (DeLong, 1990). Although there is a significant amount of evidence to support the rate model based on evidence from humans with HD (Starr *et al.*, 2008) and PD (Benazzouz *et al.*, 2002), as well as animal models of PD (Filion and Tremblay, 1991; Bergman *et al.*, 1994), a number of observations in the same systems diverge from the rate model (reviewed in Nelson and Kreitzer, 2014). This suggests that the rate model is a simplistic, although very useful, model of basal ganglia function and that changes in neuronal firing patterns and synchrony may also play a role in disease-related circuit dysregulation (McGregor and Nelson, 2019). Although additional work must be done to fully characterise the basal ganglia, the models detailed above provide the groundwork for

modelling key aspects of HD and PD symptomology and have contributed a great deal to our understanding of these diseases.

1.3. Parkinson's Disease

1.3.1. General Information

Parkinson's disease (PD), the eponymous neurodegenerative disorder extensively described by James Parkinson in his 1817 seminal work "An Essay on the Shaking Palsy", is the second most common neurodegenerative disease (Obeso *et al.*, 2017). The disease affects 0.3% of the global population with an annual incidence of between 5 and 35 new cases per 100,000 (Pringsheim *et al.*, 2014). Age is the biggest risk factor for PD development, with the disorder rarely presenting in patients under 50 years of age (Twelves, Perkins and Counsell, 2002). 2-3% of the population ≥ 65 years of age suffer with the condition and its incidence is increased 5 – 10 fold between 60 and 90 years of age (Twelves, Perkins and Counsell, 2002). Given that over 65s are projected to account for 22% of the world's population in 2050, the number of people suffering from PD in 2030 will be double that in 2005 (Dorsey *et al.*, 2007). The incidence of PD varies between ethnic groups and is twice more common in men than women in the majority of populations with additional influences such as caffeine consumption and head injury (Dorsey *et al.*, 2018).

1.3.2. Clinical presentation and diagnosis

PD patient symptomology is heterogeneous but four cardinal parkinsonian motor symptoms represent hallmarks of the disease. These motor symptoms are: bradykinesia (characterised by slow initiation of movement with a progressive reduction in the speed and amplitude of repetitive actions), muscular rigidity, resting tremor of 4 – 6 Hz (seen in ~70% of patients over the course of the disease (Helmich *et al.*, 2012)), and postural instability (with no unrelated cause) (Hoehn and Yahr, 1967; Moustafa *et al.*, 2016). For clinical diagnosis of PD, patients must display bradykinesia with one more of the other cardinal signs. Next, other potential neurological causes must be excluded and, finally, supporting prospective positive criteria are required for definite diagnosis (Hayes, 2019). Given the heterogeneity in symptoms, attempts have been made at sub-classification of PD into a relatively slow-progressing tremor-dominant subtype and a non-tremor-dominant subtype (Schiess *et al.*, 2000; Moustafa *et al.*, 2016)

1.3.2.1. Motor symptoms

Despite evidence for alterations in cognition and mood prior to motor onset, patients most often seek medical help upon motor symptom onset and are diagnosed on this basis, as mentioned above. However, patients exhibit secondary motor symptoms in addition to the cardinal signs. Gait deficits are commonly seen in PD, with "shuffling gait" used to describe the classic impairment patients display (Pistacchi *et al.*, 2017). In addition, patients can exhibit

festination and freezing of gait whole mid-step (Bartels *et al.*, 2003). Another common motor symptom, often retrospectively acknowledged during the prodromal stage, is micrographia. This symptom is expressed as a transition in handwriting towards an abnormally small and cramped script which may also display a jagged contour (Rosenblum *et al.*, 2013). In addition, patients may also display deficits in precision grip and speech, with slurred slow speech (dysarthria) a common occurrence (Pinto *et al.*, 2016).

1.3.2.2. Cognitive symptoms

The cognitive burden of PD is often underreported and underappreciated. In fact, cognitive deficits in PD patients were previously attributed to concurrent AD, rather than as a manifestation of PD (Weintraub and Burn, 2011). However, in the long term, up to 80% of PD patients will develop dementia, while 20 – 30% of patients without dementia will display mild cognitive impairment (Hely *et al.*, 2008; Litvan *et al.*, 2012; Pigott *et al.*, 2015). Of the patients displaying mild cognitive impairment, an increased risk of dementia is observed, with 25% developing dementia within 3 years (Pedersen *et al.*, 2013). Moreover, 19% of untreated PD patients display cognitive impairment at the point of diagnosis (Aarsland *et al.*, 1999), suggesting that for many patients cognitive impairment represents an early and progressive concern (Watson and Leverenz, 2010). The cognitive impairment seen in PD patients is heterogeneous but relatively wide-ranging, with patients displaying deficits in attention, executive function, memory, visuospatial skills, and language (reviewed in Watson and Leverenz, 2010). Mild cognitive impairment is often attributed when patients display deficits in more than one cognitive domain (Lawrence, Gasson and Loftus, 2016; Papagno and Trojano, 2018). Amongst the factors associated with development of cognitive decline are: lower education, lower motor scores, being male, and depression (G. Liu *et al.*, 2017).

1.3.2.3. Psychiatric symptoms

Psychiatric symptoms are common in PD patients and were even alluded to by James Parkinson as “melancholy” in An Essay on the Shaking Palsy (Parkinson, 2002). Depression is commonly seen in PD patients throughout the course of the disease, with a systematic review reporting major depression in 17% of PD patients and minor depression in 22% (Reijnders *et al.*, 2008) and antidepressant usage in up to 25% of patients (Weintraub *et al.*, 2003). However, one study reported insufficient recognition and treatment of depression, revealing only 28% of patients with moderate to severe depression were receiving antidepressants (Baig *et al.*, 2015). A further 40% of patients suffer from apathy (den Brok *et al.*, 2015) and anxiety affects 25 – 40% of patients and is not associated with a specific disease stage (Simuni and Fernandez, 2013). Psychosis is also observed in patients (sometimes as a consequence of treatment), with a long-

term cumulative prevalence of 60% and expressed as predominantly visual hallucinations with lower incidences of auditory, tactile and olfactory hallucinations (Fenelon *et al.*, 2010; Forsaa *et al.*, 2010; Weintraub and Burn, 2011). Up to 14% of patients also exhibit poor impulse control, with compulsive gambling and sexual conduct common examples, particularly in patients undergoing treatment (Weintraub *et al.*, 2010).

1.3.2.4. Other non-motor symptoms

Almost all patients suffer with non-motor symptoms, sometimes for decades before diagnosis (Pfeiffer, 2016), and many patients regard these symptoms are more disabling than the motor symptoms of the diseases. However, many non-motor symptoms go unremarked as 68 – 88% of healthy age-matched controls display at least one non-motor symptom as they age, although those with PD tend to exhibit several and at a more severe level (Khoo *et al.*, 2013). Perhaps one of the best-characterised symptoms is hyposmia, a deficit seen in 90% of patients and which has been suggested as a possible screening tool (Doty, Deems and Stellar, 1988; Sui *et al.*, 2019). Pain represents a particularly disabling non-motor symptom of PD, and is most commonly of nociceptive origin although has been ascribed to neuropathic or miscellaneous sources (Blanchet and Brefel-Courbon, 2018). Pain is experienced by the majority of patients and was reported in 76% of patients in one study (Valkovic *et al.*, 2015), negatively impacting on quality of life. Patients also commonly display autonomic disturbances, the symptoms of which are frequently associated with age. Constipation, gastrointestinal dysfunction and urinary abnormalities are seen in PD in addition to erectile dysfunction and diminished sexual desire (Khoo *et al.*, 2013; Pfeiffer, 2016). Furthermore, 90% of patients exhibit sleep disturbances (Kurtis, Rodriguez-Blazquez and Martinez-Martin, 2013), most commonly sleep fragmentation and less commonly as REM sleep behaviour disorder (RBD) which has also been postulated to be a risk factor for PD development (Pfeiffer, 2016).

1.3.3. PD Pathology

1.3.3.1. Basal Ganglia

PD symptomology is predominantly caused by slow and progressive degeneration of dopaminergic neurons within the SNc (particularly the ventrolateral aspect (Fearnley and Lees, 1991)) with cell death in this nucleus representing the classical degenerative hallmark of PD. The consequences of SNc degeneration are reductions in striatal dopamine content and subsequently aberrant signalling within basal ganglia circuitry (Figure 1.2) (McGregor and Nelson, 2019). Reductions in striatal dopamine results in disinhibition of D2R-expressing MSNs and reduced activity of D1R-expressing MSNs which leads to increased activity of the indirect

pathway and reduced activity of the direct pathway, promoting greater stimulation of GPi/SNr output nuclei and a corresponding increase in tonic inhibition of thalamic nuclei and brainstem motor nuclei (Albin, Young and Penney, 1989; DeLong, 1990). Reductions in thalamocortical motor output results in reduced premotor drive and leads to associated PD motor symptoms such as bradykinesia. L-3,4-dihydroxyphenylalanine (L-DOPA), the immediate amino acid precursor of dopamine, is converted to dopamine in the brain and acts to elevate levels of striatal dopamine and normalise signalling, controlling some of the motor deficits associated with the disease (Whitfield, Moore and Daniels, 2014) (See section 1.6.3.1. for more information).

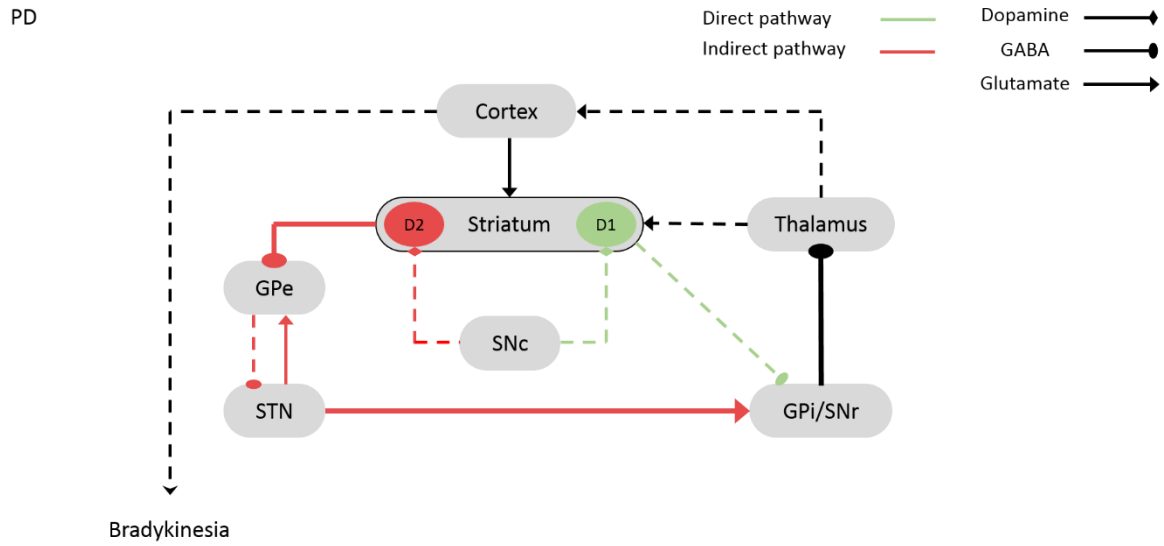

Figure 1.2. The Basal Ganglia in PD. *Degeneration of nigrostriatal projection neurons leads to increased activation of the basal ganglia output nuclei and reduced thalamocortical output, resulting in bradykinesia and other symptoms*

1.3.3.2. Neuronal Vulnerability

Presentation of cardinal symptoms is thought to occur only upon 30 – 50% loss of nigrostriatal neurons and 80% of striatal dopamine (Obeso *et al.*, 2017), meaning that typical diagnosis of the condition occurs many years into the course of the disease. The particular susceptibility of dopamingeric SNc neurons to cell death is still largely unexplained but has been suggested to be due to several intrinsic characteristics of these neurons. Firstly, the extensive arborisation of nigrostriatal neurons exerts considerable metabolic and proteostatic demands on the cell (Matsuda *et al.*, 2009; Sulzer and Surmeier, 2013). Secondly, dopamine oxidation may be harmful to cells (Segura-Aguilar *et al.*, 2014). Thirdly, SNc neurons are autonomic pacemakers that require calcium, the homeostasis of which carries an additional metabolic burden, with metabolic failure and subsequent dysregulation of this process leading to elevated calcium

content and toxicity (reviewed in Sulzer and Surmeier, 2013). Although focus remains on degeneration of the SNc in PD, dopaminergic neurons in the neighbouring VTA also degenerate, albeit to a lesser extent (Alberico, Cassell and Narayanan, 2015). Moreover, degeneration of neurons within brainstem nuclei such as the locus coeruleus and Raphe nuclei are commonly reported in early- and mid-PD, leading to a reduction in the number of noradrenergic and serotonergic cells, respectively (Chan-Palay and Asan, 1989; Halliday *et al.*, 1990). In addition, dopaminergic neurons in the enteric nervous system are degenerated, likely contributing to the constipation commonly reported by PD patients (Li *et al.*, 2011).

1.3.3.3. Lewy Pathology

At the cellular level, PD pathology is also characterised by the presence of cytoplasmic inclusions of aggregated proteins known as Lewy bodies, as well as by Lewy neurites within the axons and dendrites of cells (Braak *et al.*, 2003; Goedert *et al.*, 2013). However, although a key feature of PD, Lewy bodies are also present in normal ageing (Markesbery *et al.*, 2009) and other conditions such as dementia with Lewy bodies and AD (reviewed in Halliday *et al.*, 2011). Lewy bodies and Lewy neurites predominantly consist of aggregated α-synuclein protein (Spillantini *et al.*, 1997) alongside more than 90 other components including ubiquitin (Kuzuhara *et al.*, 1988; Obeso *et al.*, 2017). The α-synuclein aggregates within Lewy bodies are thought to be formed through abnormal oligomerisation of soluble monomeric α-synuclein with subsequent formation of insoluble fibrils (Kim and Lee, 2008). The exact role of different structural configurations of α-synuclein and of Lewy bodies in PD pathophysiology is still disputed, with proponents for both a neuroprotective and pathogenic role for these structures (reviewed in Goedert *et al.*, 2013)

Lewy pathology in PD is extensive within the brain, as well as in the peripheral nervous system. The anatomical order of appearance of Lewy pathology has been proposed to progress in 6 distinct stages according to Braak's hypothesis, with stage correlating to concurrent symptoms (Braak *et al.*, 2003). Braak's hypothesis postulates that idiopathic PD originates in a dual-hit manner through unknown viral or bacterial infection beginning in neurons within the nasal cavity and the gut (Hawkes, Del Tredici and Braak, 2007, 2009). According to Braak's staging system, the pathogenic agent triggers aggregation of α-synuclein within these primary peripheral structures (olfactory neurons and enteric neurons) before spreading to the CNS via the olfactory tract and vagus nerve (Hawkes, Del Tredici and Braak, 2007, 2009; Rietdijk *et al.*, 2017). Under this system, Lewy pathology at Stage 1 is almost entirely confined to the medulla oblongata, spreading to the pontine tegmentum at Stage 2 and continuing to the midbrain (including the SNc) at Stage 3. Next, α-synuclein pathology is observed within the mesocortex at Stage 4 before finally reaching the neocortex at Stages 5 and 6. Lewy pathology is also

observed within the olfactory bulb and enteric nervous system early in PD progression and, in correlating pathology to symptoms, early presentation of anosmia and digestive issues including constipation in the prodromal stage of the disease could be explained by initial pathology and dysfunction within these respective structures (Braak *et al.*, 2003). Following this hypothesis, patients would typically be diagnosed with PD upon presentation of cardinal symptoms at Stage 3 or later, in accordance with nigrostriatal pathology and degeneration. Several lines of evidence point to prion-like transmission of α-synuclein between cells (Luk *et al.*, 2009; Lee *et al.*, 2010) and the Braak hypothesis was recently supported by an animal study in which preformed α-synuclein fibrils were injected into the mouse duodenal and pyloric muscularis layer (Kim *et al.*, 2019). In this study, α-synuclein pathology was shown to spread from the gut into the brain in a vagal-dependent manner with brain pathology staging consistent with that described by Braak. The authors further demonstrated that spread of α-synuclein pathology to the SNc led to death of dopaminergic neurons within this structure and the presentation of both motor and non-motor symptoms in mice. However, although useful in the study of PD, Lewy pathology does not seem to follow Braak staging in a significant number of patients and this system may be best matched to individuals presenting with young onset, long duration PD (Rietdijk *et al.*, 2017).

1.3.4. Causes of PD

PD was initially believed to be an idiopathic disease without a genetic component before monogenic causative mutations were discovered in patients. However, only 5 – 10% of PD patients suffer from monogenic forms of the disease inherited in a Mendelian fashion and 15% of patients exhibit a family history of PD (Kalinderi, Bostantjopoulou and Fidani, 2016; Deng, Wang and Jankovic, 2018; Blauwendraat *et al.*, 2019). Therefore the vast majority of PD cases are idiopathic in origin, stemming from unknown cause but thought to involve both environmental and genetic risk factors (Dorsey *et al.*, 2018; Karimi-Moghadam *et al.*, 2018). Although there is some variation in the symptom profile of different monogenic forms of PD and idiopathic PD, the phenotype of both is typified by nigral degeneration and motor dysfunction with heterogeneous Lewy body pathology, suggesting that genetic and idiopathic PD share common pathophysiological mechanisms (Deng, Wang and Jankovic, 2018). The identification of causative mutations in monogenic PD therefore offers the opportunity to explore pathogenesis and pathophysiology and to generate novel treatments for both forms of the disease.

1.3.4.1. Background

It has become steadily apparent in recent years that PD exists on a genetic spectrum ranging from monogenic, causative mutations at one end to genetic risk factors which increase the

likelihood of developing PD in concert with environmental risk factors at the other (Billingsley *et al.*, 2018). The identification of monogenic mutations has largely been achieved through identification and whole genome/exome sequencing of PD pedigrees while genetic risk factors have been more recently discovered through genome-wide association studies (GWAS) using large samples (Billingsley *et al.*, 2018). Unlike monogenic PD, where the disease typically displays a clear inheritance pattern, mutations associated with genetic risk have been difficult to identify as penetrance and inheritance is more complex and mutations do not always segregate with the disease in the absence of additional necessary modifiers (Hernandez, Reed and Singleton, 2016). The contribution of these risk variants to development of PD is described by two non-mutually exclusive hypotheses (Schork *et al.*, 2009; Billingsley *et al.*, 2018). The common disease, common variant (CDCV) hypothesis states that there are common genetic variants across the general population which have an individually small risk effect but which lead to a cumulatively large amount of risk when present together. In contrast, the common disease, rare variant (CDRV) hypothesis states that increased genetic risk of PD is conferred by rare variants with a large effect on risk.

1.3.4.2. Monogenic Forms of PD

Gene	Protein	Inheritance	Onset	Lewy pathology
***SNCA* (*PARK1-4*)**	α-synuclein	AD	Early	Present
***LRRK2* (*PARK8*)**	LRRK2	AD	Late	Present/variable
***PRKN* (*PARK2*)**	Parkin	AR	Early	Variable
***PINK1* (*PARK6*)**	PINK1	AR	Early	Variable
***VPS35* (*PARK17*)**	Vacuolar protein sorting-associated protein 35	AD	Late	Variable
***DJ-1* (*PARK7*)**	DJ-1	AR	Early	Variable
***ATP13A2* (*PARK9*)**	ATPase 13A2	AR	Early	Variable
***DNAJC6* (*PARK19*)**	Auxilin	AR	Early	Variable
***FBXO7* (*PARK15*)**	F-box only protein 7	AR	Early	Variable

Table 1.3. Monogenic forms of PD. *Mutations in the genes listed are causative in PD and result in autosomal dominant (AD) or autosomal recessive (AR) inheritance with variable onset and Lewy pathology. (Adapted from Deng, Wang and Jankovic, 2018; (Kruger et al., 1998; Papapetropoulos et al., 2001; Hernandez, Reed and Singleton, 2016).*

1.3.4.2.1. *Synuclein Alpha* (*SNCA*)

SNCA, located within the *PARK1* locus on chromosome 4 and encoding α-synuclein protein, was the first gene identified in monogenic familial PD and exhibits autosomal-dominant inheritance (Polymeropoulos *et al.*, 1997) (Table 1.3). Only a year later, α-synuclein was identified as the major component of Lewy bodies (Spillantini *et al.*, 1997) linking monogenic and idiopathic PD and suggesting a common disease mechanism between the two. α-synuclein is a 140 amino acid protein which is evolutionarily conserved in vertebrates (Yuan and Zhao, 2013). Despite

extensive research, the fully resolved structure and normal function of α-synuclein remains elusive, but its presynaptic localisation and membrane-binding region suggest it is involved in neurotransmission through regulation of vesicular trafficking (Maroteaux, Campanelli and Scheller, 1988; Bendor, Logan and Edwards, 2013; Huang *et al.*, 2019; Meade, Fairlie and Mason, 2019). Recent work has implicated α-synuclein in DNA repair (Schaser *et al.*, 2019). The authors demonstrate that α-synuclein undergoes nuclear translocation in response to DNA damage, with knockout of the protein associated with increases in DNA damage. Lewy bodies also appear to sequester α-synuclein in the cytoplasm, preventing the protein from reaching the nucleus to repair damage and suggesting a possible loss of function (LOF) mechanism for α-synuclein in PD pathophysiology.

Mutations in the *SNCA* gene are rare and only a small number of missense mutations within the genes have been identified, alongside whole locus duplications, triplications and quadruplications (Deng and Yuan, 2014; Ferese *et al.*, 2015). In the case of locus multiplications, the extent of gene amplification positively correlates with increased severity of phenotype, demonstrating a gene-dosage effect (Eriksen, Przedborski and Petrucelli, 2005). Missense mutations are localised to the membrane-binding N-terminal region of the protein, with the location of the mutation conferring complete (e.g. p.A53T) or incomplete (e.g. p.A30P) penetrance (Kruger *et al.*, 1998; Papapetropoulos *et al.*, 2001; Hernandez, Reed and Singleton, 2016). Missense mutations lead to altered protein structure and increased oligomeric aggregation, demonstrating that PD can be induced either by elevated α-synuclein production through gene amplification or by altered function of α-synuclein through gain of function (GOF) missense mutations (Reed *et al.*, 2019). Individuals with pathogenic *SNCA* mutations typically present with early-onset, rapidly progressing L-DOPA responsive PD with cognitive dysfunction and dementia, although dementia is more commonly experienced by patients with gene amplification than those with missense mutations (Klein and Westenberger, 2012; Hernandez, Reed and Singleton, 2016).

1.3.4.2.2. *Leucine-Rich Repeat Kinase 2* (*LRRK2*)

Mutations in the *LRRK2* gene, located in the *PARK8* locus of chromosome 12, were first discovered in 2004 (Paisan-Ruiz *et al.*, 2004; Zimprich *et al.*, 2004) (Table 1.3). *LRRK2* mutations are the most common cause of familial PD (Martin *et al.*, 2014), accounting for 4 – 8% of familial cases and a significant number of seemingly sporadic cases (Kang and Marto, 2017). LRRK2 is a large, cytoplasmic protein spanning 2,527 amino acids and (Mata *et al.*, 2006) similar to α-synuclein, its exact function is currently unknown but it appears to protect against oxidative stress and ROS species, regulate α-synuclein propagation and takes part in cellular processes such as autophagy, mitochondrial function and vesicular trafficking (Martin *et al.*, 2014; Bae *et*

al., 2018). Over 100 missense and nonsense mutations have been identified in *LRRK2*, although only 6 mutations which either decrease GTPase activity (which indirectly increases LRRK2 kinase activity) or directly increase kinase activity of the protein have reliably been demonstrated to play a pathogenic role in monogenic PD, with other mutations showing incomplete penetrance (West *et al.*, 2007; Ross *et al.*, 2011). Of the 6 monogenic mutations, G2019S is the most prevalent cause of PD, identified as causative in 42% of familial PD depending on ethnic background (Correia Guedes *et al.*, 2010). The penetrance of the G2019S mutation is incomplete and increases with age from 21% at 59 years of age to 74% at 79 years of age, as well as varying in penetrance between ethnic backgrounds, likely through a founder effect (Healy *et al.*, 2008). In fact, all mutations of *LRRK2* display incomplete penetrance, explaining why mutations within this gene have been identified in a significant number off seemingly idiopathic cases of PD without clear family history (Reed *et al.*, 2019). Clinically, *LRRK2* PD does not differ significantly from idiopathic PD, presenting with mid/late onset, slow-progressing L-DOPA-responsive PD with rare dementia (Klein and Westenberger, 2012; Deng, Wang and Jankovic, 2018). Presence of Lewy body pathology shows variability across mutations, appearing with high frequency in *LRRK2* G2019S patients and less frequently in patients carrying other pathogenic mutations (Poulopoulos *et al.*, 2012).

1.3.4.2.3. *PRKN* (*Parkin*)

Parkin was the first gene to be identified in autosomal-recessive familial PD when a study of 13 Japanese families presenting with juvenile onset PD were discovered to have large-scale deletions in either exon 4 or exons 3-7 of the *Parkin* gene, located in the *PARK2* locus of chromosome 6 (Kitada *et al.*, 1998a) (Table 1.3). The encoded 465 amino acid Parkin protein is a RING-in-between-RING (RBR) E3 ubiquitin ligase which has been reported to play an essential role in mitochondrial quality control, specifically in selective autophagy of damaged mitochondria, commonly referred to as mitophagy (See Section 1.3.5.2.2. for more information). *Parkin* is a large gene spanning 1.3 Mb and is located at a common fragile site within the genome (Smith *et al.*, 2006), giving rise to a diverse range of LOF mutations in all 12 exons of the gene which include point mutations and exonic deletions and duplications (Hedrich *et al.*, 2004; Hernandez, Reed and Singleton, 2016). Of the 147 identified exonic mutations, 33% are SNPs, 13% are minor deletions and the remaining 54% are larger deletions or duplications of more than one exon (Grünewald, Kumar and Sue, 2019). *Parkin* mutations are clinically characterised by juvenile or early onset PD, with mutations in this gene accounting for the disease in 50% of individuals with early onset recessive PD aged between 7 – 58 years of age (Lücking *et al.*, 2000). In addition, *Parkin* mutations have been reported to be present in 77% of apparently idiopathic cases of PD with age of onset below 20 years of age (Lücking *et*

al., 2000). Aside from age at onset, *Parkin* PD is distinguished from idiopathic PD by increased presence of psychiatric disturbances and absence of Lewy pathology, although Lewy bodies are sometimes observed in patients with an older age at onset than is typical (Klein and Westenberger, 2012; Deng, Wang and Jankovic, 2018).

1.3.4.2.4. *PTEN-induced putative kinase 1* (*PINK1*)

Mutations within *PINK1*, an 18Kb gene with eight exons located in the *PARK6* locus on chromosome 1, were discovered in 2004 and have also been shown to be monogenic causes of autosomal-recessive PD (Valente *et al.*, 2004) (Table 1.3). The 581 amino acid protein PINK1 is a Ser/Thr kinase which localises to mitochondria through its N-terminal mitochondrial targeting sequence, playing an important role in mitochondrial function and protection against oxidative stress (Valente *et al.*, 2004). More than 10 mutations have been discovered in the PINK1 gene in PD patients, with these mutations either diminishing the kinase activity of the protein or resulting in truncation and formation of an inactive protein product (Hauser, Primiani and Cookson, 2016). PINK1-induced PD is clinically characterised by early onset, slow-progressing PD with occasional dystonia and psychiatric disturbances (Klein and Westenberger, 2012; Deng, Wang and Jankovic, 2018).

1.3.4.2.5. Other monogenic genes

In addition to the commonly-studied monogenic forms of PD listed above, pathogenic mutations have been identified in additional genes (Table 1.3). Mutations in *VPS35, retromer complex component* (*VPS35*/*PARK17*) lead to autosomal-dominant, late-onset PD (Vilariño-Güell *et al.*, 2011; Zimprich *et al.*, 2011) while mutations in the *parkinsonism associated deglycase* (*DJ-1*/*PARK7*) (Bonifati *et al.*, 2003) and *vacuolar protein sorting 13 homolog c* (*VPS13C*/*PARK23*) (Lesage *et al.*, 2016) genes lead to autosomal-recessive, early-onset PD. In addition, mutations in the *DnaJ heat shock protein family (Hsp40) member C6* (*DNAJC6*/*PARK19*) (Edvardson *et al.*, 2012), *F-box protein 7* (*FBXO7*/*PARK15*) (Shojaee *et al.*, 2008), and *ATPase 13A2* (*ATP13A2*/*PARK9*) (Ramirez *et al.*, 2006) genes lead to autosomal recessive, early-onset PD with atypical features. However, the characterisation of these mutations isn't as clear as those detailed above. These products of these genes have diverse roles but function in PD-related pathways such as endocytosis and protein trafficking, mitochondrial function, and lysosomal function (Deng, Wang and Jankovic, 2018).

1.3.4.3. Genetic Risk

Unlike monogenic forms of PD which typically have mutations segregated with Mendelian disease, risk variants contribute to sporadic PD in a more complex way. The largest GWAS of idiopathic PD to date recently identified genome-wide significant signals for idiopathic PD in 92 loci, 39 of which were novel (Nalls *et al.*, 2018). These signals represent common genetic risk

factors for PD and suggest the genetic component of PD is much more extensive than first realised. Importantly, variants within the *SNCA* and *LRRK2* genes are amongst the risk-associated signals identified in GWAS investigation of idiopathic PD (Chang *et al.*, 2017; Nalls *et al.*, 2018). *SNCA* genetic risk variants are non-coding, with polymorphism in the *Rep1* region within the promoter predisposing individuals to PD through elevated expression of the *SNCA* gene (Maraganore *et al.*, 2006). Meanwhile *LRRK2* has two major risk variants (R1628P and G2385R) which act to increase kinase activity of the encoded enzyme (Ho *et al.*, 2016; Shu *et al.*, 2016). As can be seen, risk variants in the *SNCA* and *LRRK2* gene mimic the effects of monogenic causative mutations in familial PD, with *SNCA* risk variants increasing the amount of α-synuclein similar to gene multiplication, and *LRRK2* risk variants increasing *LRRK2* kinase activity as in monogenic forms. These findings underscore the complex relationship between monogenic and idiopathic PD and the importance of investigating and understanding PD at the genetic level.

1.3.5. PD Pathophysiology

1.3.5.1. α-synuclein and its Degradation

Multiple mechanisms and pathways are believed to contribute to PD pathophysiology. Perhaps unsurprisingly, given the presence of α-synuclein-positive Lewy bodies in idiopathic PD brains and the contribution of mutations in the *SNCA* gene to development of monogenic PD, as well as increased risk of PD, α-synuclein has been extensively investigated for its role in PD pathophysiology. Abnormal aggregation of α-synuclein (a process which is enhanced by overexpression of – or mutations in – the SNCA gene) is believed to be neurotoxic in a GOF manner, as well as perhaps by LOF (Wong and Krainc, 2017; Schaser *et al.*, 2019). Impairments in the ubiquitin-proteasome system (UPS) and lysosomal autophagy system (LAS) could also contribute to α-synuclein-mediated toxicity by permitting aggregation through impaired degradation, leading to a failure of proteostatic homeostasis (Lehtonen *et al.*, 2019). Both of these systems identify proteins targeted for degradation through ubiquitination. Ubiquitin is a small 76 amino acid protein which is covalently conjugated to lysine residues on target proteins through the action of an E3 ubiquitin ligase enzyme (Ciechanover *et al.*, 1980; Hershko *et al.*, 1983). Additional ubiquitin proteins can be joined to one of seven internal lysine residues (or the first methionine) within pre-conjugated ubiquitin proteins (through the coordinated action of E1, E2 and E3 enzymes) to generate poly-ubiquitin chains on the target protein which flag it for removal (Pickart and Eddins, 2004). During UPS-mediated degradation, the proteasome recognises poly-ubiquitin chains and cleaves the target protein to generate short peptides (Ciechanover, 1994).

Proteins, or even whole organelles, can be targeted for removal by the LAS. During this process, target structures are flagged by poly-ubiquitin chains which are, in turn, recognised by autophagy adaptor protein, permitting formation of a double-membrane autophagosome and engulfment of the target (Johansen and Lamark, 2011). The autophagosome then fuses with the lysosome to form an autolysosome, with this structure enabling degradation of the contents by hydrolase action to generate free amino acids (Johansen and Lamark, 2011). In fact, accumulation of α-synuclein has been shown to negatively impact on function of the UPS and autophagy (Winslow *et al.*, 2010; Tanik *et al.*, 2013) potentially generating a feed-forward mechanism impaired clearance of α-synuclein permits aggregation which further impairs the UPS and/or LAS to drive increasing levels of α-synuclein aggregation (Poewe *et al.*, 2017). In support of a role of the LAS in α-synuclein aggregation, overexpression of the familial PD-associated p.E46K and p.A30P α-synuclein variants have been shown to impair autophagy (Yan *et al.*, 2014; Lei, Cao and Wei, 2019). In addition, mutations in *LRRK2* (Volpicelli-Daley *et al.*, 2016), *VPS35* (Tang *et al.*, 2015), and *ATP13A2* (Dehay *et al.*, 2012) have all been linked to increased aggregation of α-synuclein through impairment of the LAS (Poewe *et al.*, 2017). Elevated levels of neuroinflammation have been reported in post-mortem tissue from PD patients (Wilms *et al.*, 2007; Tufekci *et al.*, 2012). α-synuclein aggregates also activate an immune response which could cause dopaminergic neurons express major histocompatibility complex (MHC) class I proteins target them for cell death (Cebrian *et al.*, 2014).

1.3.5.2. The Role of Mitochondria in PD

Mitochondria have been consistently implicated in PD pathophysiology through numerous lines of evidence. These double-membrane organelles serve vital functions in eukaryotic cells – generating adenosine triphosphate (ATP) through oxidative phosphorylation, buffering intracellular calcium levels, and regulating apoptosis with dysregulation of these processes associated with disease (Nunnari and Suomalainen, 2012). Generation of ATP relies on the electron transport chain which consists of a series of mitochondrial protein complexes which mediate the transfer of electrons and pumping of protons to generate the electrochemical gradient necessary to synthesis ATP (Chaban, Boekema and Dudkina, 2014). Normal oxidative phosphorylation and formation of the electrochemical gradient generates a mitochondrial membrane potential (ΔΨm) which is important for normal mitochondrial function and import of proteins from the cytoplasm (Neupert and Herrmann, 2007). The majority of mitochondrial proteins are encoded in the nuclear genome, but a subset are encoded by the 16kB mitochondrial DNA (mtDNA) genome (Andrews *et al.*, 1999). mtDNA contains 13 protein-coding genes which produce proteins needed for oxidative phosphorylation including complexes I, III, IV, and V (Taanman, 1999). Mutation of genes within the mtDNA compromises

oxidative phosphorylation and ATP production and results in a range of mitochondrial diseases such as Charcot-Marie-Tooth 2A which presents with a strong neurodegenerative phenotype (Ryzhkova *et al.*, 2018). Deficits in ATP production negatively impacts on ion transport and subsequently compromises synaptic transmission and calcium buffering, jeopardising neuronal function and health (Nunnari and Suomalainen, 2012). Mitochondria generate reactive oxygen species (ROS), which cause damage to mitochondrial lipids and proteins and induce mtDNA mutations, as a normal by-product of oxidative phosphorylation (Muller, Liu and Van Remmen, 2004; Murphy, 2009). The extent of damage is limited by homeostatic mechanisms which convert ROS to less harmful species (McCord and Fridovich, 1969), degrade damaged proteins and lipids, and repair DNA but mitochondrial impairment can result in excess levels of ROS which can overwhelm the mitochondrion's defences to cause damage and mtDNA mutations which further impede the function of the organelle (Lagouge and Larsson, 2013).

The first indication of a role for mitochondria in PD arose from a clinical characterisation of patients exhibiting acute parkinsonism (Langston *et al.*, 1983). These 4 patients unintentionally self-administered 1-methyl-4-phenyl-1,2,5,6-tetrahydropridine (MPTP) which resulted in almost immediate onset of parkinsonian symptoms including bradykinesia, shuffling gait, stiffness, pill-rolling tremor, and jerking limbs. Parkinsonian symptoms were chronic, although L-DOPA-responsive, and post-mortem analysis distinguished nigrostriatal degeneration to levels comparable to idiopathic PD (Davis *et al.*, 1979). Analysis of MPTP determined that, upon oxidation, this molecule is converted to 1-methyl-4-phenylpyridinium (MPP+) which selectively inhibits mitochondrial complexes I, III, and IV and causes specific degeneration within the SNc due to selective uptake into dopaminergic neurons through the dopamine active transporter (DAT) (Desai *et al.*, 1996; Storch, Ludolph and Schwarz, 2004). Furthermore, exposure to the pesticide rotenone has been demonstrated to lead to selective nigral degeneration, presence of Lewy body-like pathology and associated parkinsonian symptoms through complex I inhibition while the herbicide paraquat also exerts the same degenerative effect and symptomology through production of ROS (Jackson-Lewis, Blesa and Przedborski, 2012; Grünewald, Kumar and Sue, 2019) and both agents have been linked to PD development in humans (Tanner *et al.*, 2011). Aside from these neurotoxins, post-mortem evaluation of idiopathic PD patient SNc, skeletal muscle, and platelets reveal reduced complex I, III, and IV activity in these tissues (Schapira *et al.*, 1990; Grünewald, Kumar and Sue, 2019) further implicating mitochondrial dysfunction and oxidative stress in PD pathogenesis and pathophysiology.

1.5.3.2.1. Mitochondrial Quality Control and Mitochondrial Dynamics

Given the importance of mitochondria for cellular health and function, repair or removal of defective mitochondria represents a crucial homeostatic process. Mitochondrial homeostasis can be seen to occur at the protein level, the organelle level, and the cellular level with the extent of damage determining at which level the homeostatic mechanism will operate (Rub, Wilkening and Voos, 2017). At the protein level, chaperone proteins or proteases can either repair or remove damaged mitochondrial proteins to ensure continued function of the organelle. At the organelle level, minor mitochondrial damage can be alleviated through mitochondrial dynamics. Mitochondrial fusion, facilitated by mitofusins 1 and 2 (Mfn1/2) (Santel and Fuller, 2001), permits the union of two individual mitochondria to form a single mitochondrion through fusion of the membranes, while mitochondrial fission permits the division of a single mitochondrion into two daughter mitochondria (Bereiter-Hahn and Vöth, 1994). In instances where a mitochondrion has a minor impairment, fusion to a more functional mitochondrion could offset any deficits and boost its function (Ni, Williams and Ding, 2015). On the other hand, mitochondrial fission could aid removal of defective mitochondria in cases of more serious damage (Pryde *et al.*, 2016). In cases of more serious damage, defective organelles can be tagged and eliminated through a mitochondria-specific mechanism of autophagy known as mitophagy. At the most severe level of damage, cytochrome c is released from mitochondria into the cell cytoplasm where it initiates apoptosis through caspase signalling (Garrido *et al.*, 2006).

1.3.5.2.2. Mitophagy and PINK1-Parkin

As described in Section 1.3.5.1., defective autophagy is believed to play a role in aggregation of α-synuclein and associated toxicity. If mitophagy were also impaired in PD, dysfunctional mitochondria could accumulate leading to metabolic deficits and oxidative stress, compromising cellular health and leading to apoptosis. Cells with high metabolic activity, such as SNc neurons, would be at particular risk of degeneration in the event of impaired mitophagy. Furthermore, extensive research has demonstrated a seemingly crucial role for PINK1 and Parkin in mitophagy (Jin and Youle, 2012) and mutations in either of the genes encoding these proteins lead to autosomal recessive, early-onset PD (Table 1.3). Thus, these proteins provide an invaluable link between mitochondria, impaired autophagy, and PD. Investigation of mitophagy and the roles of PINK1 and Parkin could offer crucial insight into PD pathophysiology and present new, druggable targets.

1.3.5.2.2.1. Characterisation of PINK1 and Parkin

Knockout (KO) of the *Drosophila PINK1* and *Parkin* orthologues (known as *pink1* and *park*) was demonstrated to produce very similar degenerative phenotypes which produced characteristics which could be reminiscent of PD such as flight muscle degeneration, aberrant mitochondrial morphology and increased sensitivity to cellular stresses, locomotor deficits, mild degeneration of dopaminergic neurons, as well as reduced life-span (Clark *et al.*, 2006; Park *et al.*, 2006). In addition, both groups demonstrated that *park* overexpression in *pink1* KO *Drosophila* could rescue some of the deficits in these flies, but *pink1* overexpression in *parkin* KO Drosophila had no effect on phenotype. Moreover, double KO of *pink1* and *parkin* produced a similar phenotype to single KO (Clark *et al.*, 2006). The lack of increased phenotypic severity in double-mutants and the ability of *parkin* expression to compensate for *pink1* KO led the authors to suggest that PINK1 and Parkin operate within a common pathway, with PINK1 acting upstream of Parkin. Later, cytosolic Parkin was shown to be recruited specifically to damaged mitochondria, leading to their autophagosome-mediated degradation, implicating PD-associated *Parkin* mutations in failure to clear damaged mitochondria (Narendra *et al.*, 2008). Evidence of PINK1-Parkin interaction came in 2012 when a PINK1-dependent mechanism for Parkin mitochondrial recruitment was described (Kondapalli *et al.*, 2012). This paper showed that PINK1 is localised to mitochondria specifically upon depolarisation of the mitochondrial membrane potential (ΔΨm), acting to phosphorylate Parkin specifically at Serine 65 (Ser65) within its ubiquitin-like (Ubl) domain and recruiting the protein to the mitochondria. Furthermore, PINK1-mediated phosphorylation of Parkin was shown to activate Parkin E3 ubiquitin ligase activity, with this activity inhibited by substitution of Parkin Ubl-Ser65 with an alanine (S65A).

However, a subsequent paper detailed ΔΨm-dependent mitochondrial translocation of mutant Parkin S65A in the presence of PINK1 (Kane *et al.*, 2014), raising the question of how Parkin is recruited to the mitochondria despite prevention of PINK1-mediated phosphorylation. Additional work demonstrated that, in addition to Ser65 of the Parkin Ubl domain, PINK1 is able to phosphorylate ubiquitin at a homologous Ser65 to generate phospho-ubiquitin (Kane *et al.*, 2014; Kazlauskaite *et al.*, 2014; Koyano *et al.*, 2014). Phospho-ubiquitin is then able to bind to Parkin and elevate its E3 ubiquitin ligase activity (although not to the same extent as Parkin Ser65 phosphorylation) through allosteric modulation, likely through release of Parkin autoinhibition (Kane *et al.*, 2014; Kazlauskaite *et al.*, 2014; Koyano *et al.*, 2014). Therefore, optimal activation of Parkin E3 ubiquitin ligase activity is dependent upon both direct PINK1-mediated phosphorylation of Parkin Ser65 and indirect PINK1-mediated allosteric modulation of Parkin by phospho-ubiquitin.

1.3.5.2.2.2. PINK1-Parkin-Mediated Mitophagy

The ability of PINK1 to selectively localise to damaged mitochondria and activate Parkin means that the PINK1-Parkin pathway is ideally placed to sense and flag damaged mitochondria for degradation (Figure 1.4). Under normal physiological conditions, PINK1 is synthesised as a 64kDa pre-protein on cytosolic ribosomes and constitutively translocates to mitochondria by merit of its N-terminal mitochondrial targeting motif (Valente *et al.*, 2004; Muqit *et al.*, 2006). In healthy mitochondria, PINK1 is recognised and imported across the outer mitochondrial membrane (OMM) by the translocase of the outer membrane (TOM) complex. Next, the translocase of the inner mitochondrial membrane (TIM) complex begins import of PINK1 across the inner mitochondrial membrane (IMM) but full import of the protein to the matrix is prevented by a hydrophobic domain within PINK1 (Silvestri *et al.*, 2005; Stojanovski *et al.*, 2012; Yamano, Matsuda and Tanaka, 2016). The result is capture of the PINK1 hydrophobic domain by TIM2 and protrusion of the mitochondrial targeting motif into the matrix where it is cleaved by matrix-processing peptidase (MPP) to produce a 60kDa PINK1 intermediate which is itself cleaved by presenilins-associated rhomboid-like protein (PARL) to generate a 52kDa form of PINK1 containing the kinase domain (Jin *et al.*, 2010; Deas *et al.*, 2011; Greene *et al.*, 2012; Yamano, Matsuda and Tanaka, 2016). Processed PINK1 is then released into the cytosol where it is ubiquitinated and degraded by the proteasome (Yamano and Youle, 2013). As such, stable, full-length PINK1 is not co-localised with healthy mitochondria but is instead cleaved and degraded.

However, in the case of mitochondrial damage and subsequent ΔΨm depolarisation, the N-terminal mitochondrial targeting motif of PINK1 associates with the TOM complex but mitochondrial import, and therefore cleavage of PINK1, is prevented resulting in cytosolic presentation of the remainder of the 64kDa PINK1 pre-protein, including the kinase domain (Kondapalli *et al.*, 2012). At least two PINK1 TOMM-associated molecules dimerise, resulting in autophosphorylation and stabilisation on the OMM (Lazarou *et al.*, 2012). Once stabilised at the OMM, PINK1 recruits and activates Parkin in two ways which generate a feedforward mechanism (Ordureau *et al.*, 2015; Wade Harper, Ordureau and Heo, 2018). Firstly, PINK1 is able to phosphorylate pre-existing ubiquitin (at Ser65) on proteins of the OMM. Phospho-ubiquitin chains on the OMM can then allosterically interact with inactive, cytosolic Parkin to partially alleviate its autoinhibition and increase its E3 ubiquitin ligase activity by ~1,000 fold. This interaction retains Parkin at the mitochondria where it increases ubiquitylation of OMM proteins and the resulting poly-ubiquitin chains are phosphorylated by PINK1 after which they recruit and partially activate more cytosolic Parkin, generating a positive feedback loop. Secondly, PINK1 can directly phosphorylate Parkin at Ser65 within the Ubl domain to activate

E3 ubiquitin ligase activity and recruit it to the mitochondria. Activated Parkin can then ubiquitylate locally and the resulting poly-ubiquitin chains can recruit additional cytosolic Parkin following their phosphorylation by PINK1. Both of these mechanisms occur in parallel with the result of the feedforward loop being rapid ubiquitylation of OMM proteins on damaged mitochondria, with diverse targets including Mfn 1 and 2, mitochondrial fission protein 1 (FIS1), mitochondrial Rho GTPase (Miro), and CISD1 (Sarraf *et al.*, 2013; Wade Harper, Ordureau and Heo, 2018). Following the successful actions of Parkin, ubiquitylated substrates recruit autophagy adaptors including nuclear dot protein 52 kDa (NDP52) and optineurin (OPTN) which interact with autophagosomal light chain 3 (LC3) to anchor ubiquitylated mitochondria into autophagosomes which enables their eventual lysosomal degradation (Palikaras, Lionaki and Tavernarakis, 2018). Under this system, PINK1 can be seen to act as a mitochondrial damage sensor, Parkin as a signal amplifier and poly-ubiquitin chains as the signal effector to ensure removal of damaged mitochondria (Wade Harper, Ordureau and Heo, 2018). As such, PD-causing mutations in either PINK1 or Parkin could lead to failure to flag damaged mitochondria for removal, resulting in cellular dysfunction.

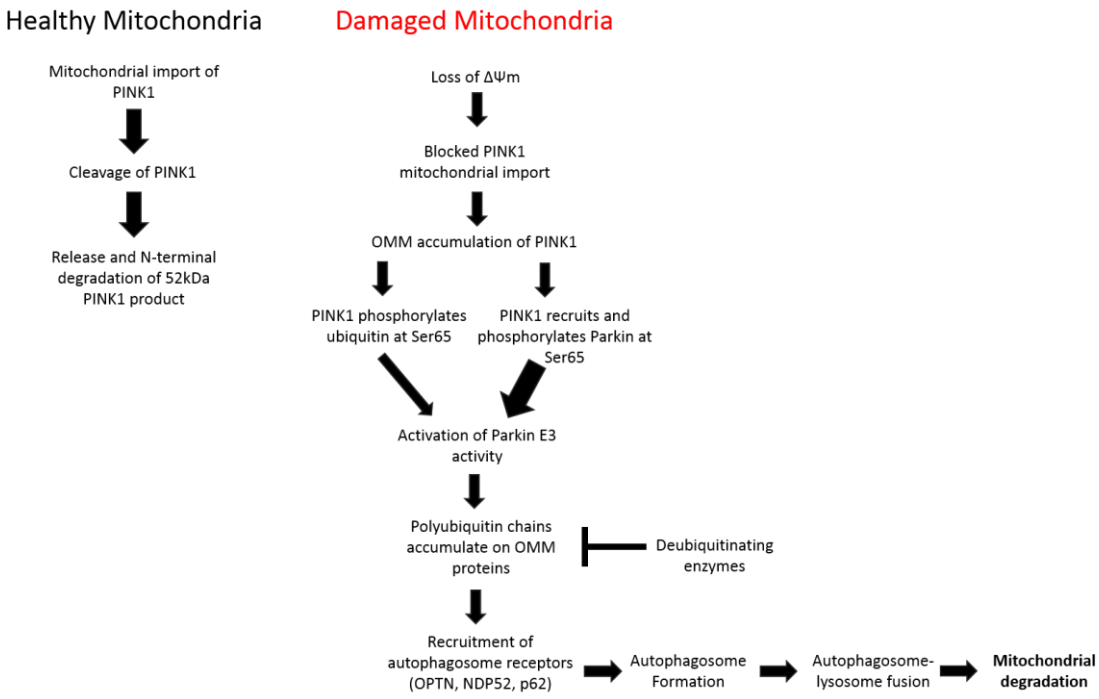

Figure 1.4. PINK1-Parkin-dependent mitophagy. *PINK1 is selectively recruited to damaged mitochondria where it phosphorylates ubiquitin and recruits and phosphorylates cytosolic Parkin to activate its E3 ubiquitin ligase function. Parkin-mediated formation of polyubiquitin chains leads to mitophagy and degradation of mitochondria.*

1.3.5.2.2.3. Roles for PINK1 and Parkin beyond Mitophagy

PINK1 and Parkin also play a role in mito-QC outside of mitophagy (Palikaras, Lionaki and Tavernarakis, 2018). PINK1 phosphorylates Mfn 1 and 2 on the OMM of damaged mitochondria, leading to Parkin association and ubiquitylation which flags Mfn1/2 for proteasomal turnover (Sarraf *et al.*, 2013). Degradation of Mfn1/2 prevents mitochondrial fusion and disrupts endoplasmic reticulum (ER)-mitochondria contacts which have the effect of preventing fusion of the dysfunctional organelle with healthy organelles and isolates dysfunctional mitochondria to facilitate removal (Tanaka *et al.*, 2010; Glauser *et al.*, 2011; McLelland *et al.*, 2018). PINK1 has also been shown to indirectly activate dynamin-related protein 1 (DRP1), promoting mitochondrial fission and aiding mitophagic removal of the damaged organelle (Pryde *et al.*, 2016). In instances of mitochondrial damage, Parkin can ubiquitylate Miro – an OMM membrane which anchors mitochondria to the cytoskeleton – leading to its degradation and prevention of mitochondrial transport which feasibly aids mitophagy by rendering the organelle immobile (Shlevkov *et al.*, 2016). In addition, PINK1 and Parkin have been reported to play a role in mtDNA integrity and immune response (Sliter *et al.*, 2018).

1.4. Huntington's Disease

1.4.1. General Information

Huntington's Disease (HD) is a neurodegenerative disorder characterised by motor, cognitive and psychiatric symptoms with disease onset typically in middle age (Bates *et al.*, 2015). The condition is caused by an expanded CAG trinucleotide repeat within exon 1 of the Huntingtin (*HTT*) gene which results in the production of mutant Huntingtin protein (mHTT) containing an expanded polyglutamine (polyQ) stretch within its N-terminal (MacDonald *et al.*, 1993). Once the CAG length has passed 40 repeats, a HD phenotype with 100% penetrance is observed, although an incomplete penetrance is seen with repeat sizes of between 36 and 39 (Dayalu and Albin, 2015). HD age of onset is negatively correlated with *HTT* CAG repeat length with larger repeat lengths associated with advanced age of onset (Andrew *et al.*, 1993; Duyao *et al.*, 1993; Stine *et al.*, 1993). However, although CAG length is the largest determinant of age of onset, there is still variation between individuals with the same repeat length, implicating additional environmental and genetic influences (Lee *et al.*, 2012). Recent GWAS investigations have determined additional genetic modifiers of age of onset within the *HTT* locus (GeM-HD Consortium, 2019), as well as outside it with DNA repair gene variants particularly implicated (GeM-HD Consortium, 2015; J.-M. Lee *et al.*, 2017; Goold *et al.*, 2019).

HD is caused by aberrant, predominantly gain of function (GOF), activities of mHTT which lead to cellular dysfunction and cell death through a variety of mechanisms such as excitotoxicity, mitochondrial dysfunction, transcriptional dysfunction, autophagy impairment, and loss of trophic support (Zuccato, Valenza and Cattaneo, 2010). Thus, although the causative mutation is highly localised and well-studied, the deleterious effects of mHTT on cellular mechanisms are so wide-ranging that effective therapies may effectively treat one component of the disease but have no impact on others, allowing disease progression to continue. Due to this complexity, currently approved treatments for the disease are still extremely scarce and those that are available are confined to treating disease symptomology (Shannon and Fraint, 2015). However, potential therapeutics which target the mutant *HTT* gene directly are in development and may overcome these issues by directly targeting the root cause (Tabrizi *et al.*, 2019).

1.4.2. HD pathology

1.4.2.1. mHTT Aggregation and Inclusion Bodies

At the microscopic level, HD neuropathology is characterised by the widespread formation of intraneuronal and neuropil inclusion bodies containing ubiquitinated mHTT exon 1 fragment aggregates (DiFiglia *et al.*, 1997; Scherzinger *et al.*, 1999; Sieradzan *et al.*, 1999) with the presence of ubiquitin suggesting impaired protein clearance. The presence of aggregated mHTT fragments and the demonstration that their formation through caspase 6-mediated cleavage significantly contributes to neurotoxicity (Graham *et al.*, 2006) has led to the suggestion that inclusion bodies may be neuroprotective through sequestration of toxic mHTT fragments (Montserrat *et al.*, 2004) but their exact role in HD pathogenesis remains controversial.

1.4.2.2. Cell Death and the Basal Ganglia

HD pathology is characterised selective and progressive degeneration of striatal MSNs with relative sparing of neighbouring cholinergic interneurons, despite ubiquitous expression of the mutant *HTT* gene in neuronal and non-neuronal cell populations (Vonsattel *et al.*, 1985; Strong *et al.*, 1993). Cell death spreads outside of the basal ganglia to cortical regions as the disease progresses (Mann, Oliver and Snowden, 1993; Heinsen *et al.*, 1994). Although MSNs are progressively lost, MSNs of the indirect pathway display an enhanced vulnerability early in the disease in patients and mouse models of HD (Reiner *et al.*, 1988; Xie, Hayden and Xu, 2010). In early/middle-stage PD, motor symptoms of chorea and hyperkinesia predominate while bradykinesia is more prevalent at later stages (Reiner, Dragatsis and Dietrich, 2011). The transition in symptoms can be explained by the relative vulnerabilities of MSN subclasses during disease progression. Early loss of indirect pathway MSNs leads to an imbalance in the relative contribution of direct (movement promoting) and indirect (movement inhibiting) pathway inputs to the basal ganglia output nuclei. As a result, the GPi/SNr are relatively uninhibited, leading to a direct pathway-mediated (thalamocortical) increase in cortical premotor drive which is manifested as choreic involuntary movements (Reiner, Dragatsis and Dietrich, 2011). As the disease progresses, direct pathway neurons also undergo degeneration, resulting in a reduced thalamocortical output and decreased premotor drive, causing bradykinesia and akinesia (Reiner, Dragatsis and Dietrich, 2011). Similar to PD, cognitive and psychiatric disturbances are associated with basal ganglia dysfunction due to altered thalamocortical projections targeting frontal cortices.

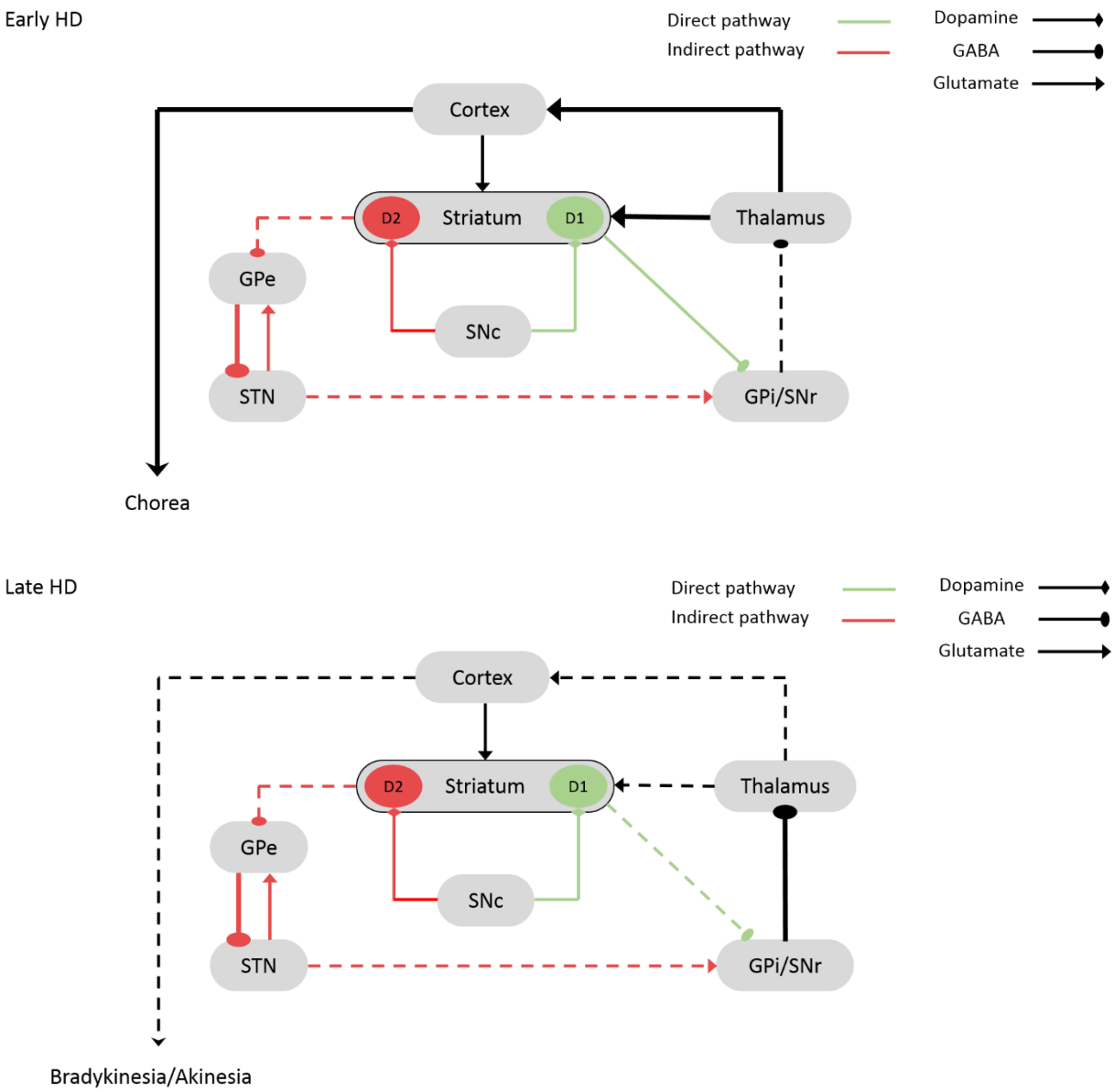

Figure 1.5. The Basal Ganglia in HD. *Preferential degeneration of indirect pathway MSNs early in HD results in elevated thalamocortical output and choreic movements while continued degeneration of both pathways as HD progresses reduces thalamocortical output which presents as bradykinesia/akinesia.*

Several suggestions have been made as to why MSNs display particular vulnerability to mHTT-mediated toxicity. Rhes, a striatal-specific E3 ligase protein has been reported to augment mHTT toxicity (Subramaniam *et al.*, 2009; Mealer *et al.*, 2014) potentially through autophagy dysregulation (Mealer *et al.*, 2014). In addition, the *HTT* CAG repeat is unstable and undergoes somatic expansion throughout the life of patients (Telenius *et al.*, 1994). Somatic expansions is particularly high in striatal neurons and CAG expansions in these cells may render them more vulnerable to cell death (Wheeler *et al.*, 1999; Kennedy *et al.*, 2003; Shelbourne *et al.*, 2007).

The role of brain-derived neurotrophic factor (BDNF) in striatal vulnerability has been particularly well-studied and will be summarised here.

1.4.3. BDNF in HD

1.4.3.1. BDNF Signalling

A reduction in striatal BDNF has been widely investigated as a potential mediator of pathophysiology in HD (reviewed in Zuccato and Cattaneo, 2007). BDNF is a ~14kDa neurotrophic factor which is abundantly expressed within the mammalian brain and was first isolated from pig brain in in the 1980s (Barde, Edgar and Thoenen, 1982; Leibrock *et al.*, 1989). BDNF plays a key role in nervous system development (Huang and Reichardt, 2001), neuroprotection (Zhao *et al.*, 2017), and synaptic function (and therefore cognition) (Lu, Nagappan and Lu, 2014).

BDNF binds to high-affinity tropomyosin receptor kinase B (TrkB) receptors (Glass *et al.*, 1991; Klein *et al.*, 1991) and low-affinity p75 neurotrophin receptors ($p75^{NTR}$) (Rodriguez-Tebar, Dechant and Barde, 1990) on target cells. BDNF-TrkB binding leads to a receptor dimerization and autophosphorylation at tyrosine residues in the cytoplasmic domain which enables recruitment of adaptor proteins to facilitate downstream signalling (Patapoutian and Reichardt, 2001) (Figure 1.6). BDNF-TrkB binding triggers downstream signalling through the Ras-ERK, PI3K-Akt, and PLCγ1 pathways which have the net effect of promoting survival and synaptic plasticity (Chao, 2003). However, BDNF-mediated activation of the $p75^{NTR}$ receptor signals through the c-Jun N-terminal kinase (JNK) pathway and activation of this receptor is associated with cell death when $p75^{NTR}$ is complexed with sortilin (Bhakar *et al.*, 2003). However, the role of the $p75^{NTR}$ receptor is context dependent and it can also interact with TrkB receptors to promote pro-survival function (Wehner *et al.*, 2016).

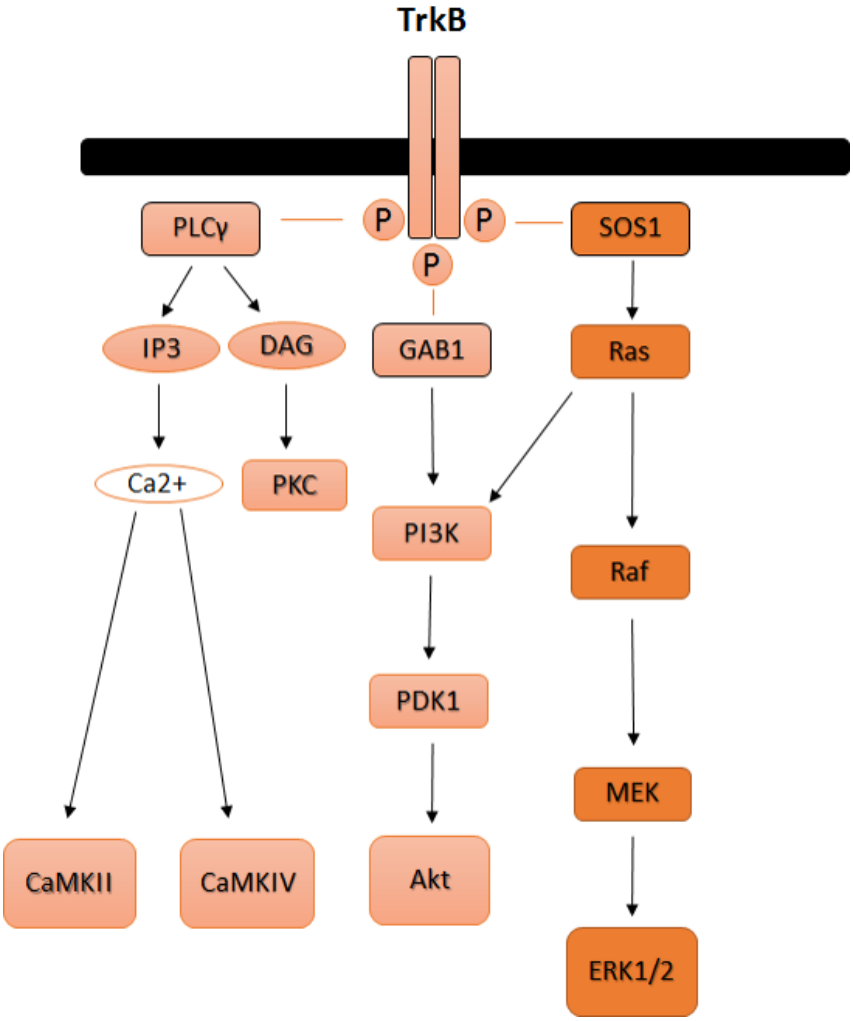

Figure 1.6. BDNF-TrkB signalling. *BDNF binds to TrkB causing dimerization and autophosphorylation of cytoplasmic tyrosine residues. Recruitment of adaptor proteins enables downstream signalling through PLCγ, PI3K-Akt, and Ras-ERK pathways.*

1.4.3.2. Alterations in BDNF in HD

Striatal neurons exhibit low levels of BDNF mRNA, with the majority of striatal BDNF protein thought to be transported from the cortex along corticostriatal afferents (Altar *et al.*, 1997). Several papers have reported decreases in BDNF level in mouse models of HD (Spires *et al.*, 2004) and HD patient post-mortem brain tissue (Ferrer *et al.*, 2000; Zuccato *et al.*, 2008). Two non-mutually exclusive hypotheses for this reduction in striatal BDNF have been presented (Zuccato, Valenza and Cattaneo, 2010). Firstly, presence of wtHTT increases BDNF expression through cytoplasmic sequestration of the transcriptional repressor RE1-silencing transcription factor/neural-restrictive silencer factor (REST/NRSF) by formation of a sequestration complex with additional proteins including Huntingtin-associated protein 1 (HAP1) (Zuccato *et al.*, 2001, 2003). Cytoplasmic sequestration of REST/NRSF prevents it from translocating to the nucleus

where it silences expression of BNDF through binding to the repressor element 1/neuron-restrictive silencer element (RE1/NRSE) site located in *Bdnf* promoter exon II (Zuccato, Valenza and Cattaneo, 2010). In contrast, mHtt interaction with the REST/NRSF sequestration complex is weak, permitting nuclear translocation of REST/NRSF and silencing of *Bdnf* transcription from promoter II.

In addition to expression of BDNF, wtHTT has also been shown to play a positive role in vesicular transport of BDNF through interaction with the dynactin motor complex via HAP1 (Gauthier *et al.*, 2004). Impaired binding of mHTT with the motor complex could disrupt anterograde corticostriatal transport of BDNF and result in reduced striatal BDNF content (Gauthier *et al.*, 2004). A more recent report has described decreased release of BDNF from primary cortical neurons obtained from zQ175 mice at the vesicular level, providing another potential mechanism for a reduction in striatal BDNF levels in HD (Yu *et al.*, 2018).

However, some groups have described normal levels of striatal BDNF but impairment in BDNF signalling at the level of the TrkB receptor in HD models. Normal BDNF levels but decreased phosphorylation of TrkB have been reported in the striata of presymptomatic R6/2 mice and in primary R6/2 striatal culture (Nguyen, Rymar and Sadikot, 2016). Unaltered levels of striatal BDNF have also been described in BACHD and zQ175 mice, although in this case TrkB phosphorylation was normal but signalling through the downstream Akt pathway was weakened due to amplification of $p75^{NTR}$ signalling which acted to inhibit TrkB signalling (Song *et al.*, 2010; Plotkin *et al.*, 2014). A progressive increase in $p75^{NTR}$ expression and a corresponding decrease in TrkB expression has been described in the R6/1 and HdhQ111 striatum and in HD patient striatum, with this imbalance associated with JNK-mediated pro-apoptotic signalling (Brito *et al.*, 2013) suggesting that elevated $p75^{NTR}$ levels could negatively regulate or surpass TrkB-mediated signalling as the disease progresses. However, $p75^{NTR}$-null zQ175 mice display increased striatal degeneration and diminished pro-survival signalling (Wehner *et al.*, 2016), suggesting a protective role for this receptor and further reflecting the context-dependent function of $p75^{NTR}$.

BDNF has key roles in neuronal survival and function (see Section 1.3.3.1.) and striatal BDNF-TrkB signalling has been shown to be decreased in HD, potentially compromising neuronal function and predisposing striatal degeneration (Zuccato and Cattaneo, 2007). Increasing striatal BDNF may therefore represent a promising treatment strategy for HD and will be discussed in more detail in Section 1.6.

1.5. Animal Models of Disease

1.5.1. General Information

Animal models are invaluable tools for identifying and understanding the underlying mechanisms of disease and designing and developing drugs suitable for targeting them (Kreiner, 2018). Disease models cannot be expected to recapitulate the human disease entirely, and choice of model and interpretation of subsequent data must be carefully assessed accordingly if conclusions are to have translational predictivity. Several steps can be taken to ensure that experiments utilising disease models give the best possible results.

Three conditions of validity should be evaluated before beginning a particular experiment using an animal model of disease and will be summarised here from two reviews (Pouladi, Morton and Hayden, 2013; Denayer, Stöhrn and Van Roy, 2014). Firstly, construct validity refers to the extent to which the pathogenic cause of the human disease is recreated in the animal model. For instance, in the case of a genetic disease, the genetic manipulation of the animal should reflect the human genetic circumstances as far as possible. Secondly, face validity refers to the ability of the animal model to accurately reflect the phenotype observed in patients. In the case of neurodegenerative diseases, animals would typically be expected to display progressive, age-dependent degeneration of specific cell populations with associated pathology alongside motor dysfunction (as well as cognitive decline and psychiatric disturbances where appropriate). Finally, predictive validity assesses how well therapeutic benefits in animal models predict corresponding benefit in patients with the same disease. In the case of neurodegenerative diseases where disease-modifying treatments remain elusive, predictive validity cannot be readily reviewed. Although an accurate model of disease would be expected to meet all these conditions of validity as far as possible, there are inherent challenges in doing so due to unknown causes of sporadic disease, complex and poorly understood disease mechanisms, and differences between species such as nervous system anatomy and complexity, lifespan, and variation in the essentiality of proteins and pathways to cellular mechanisms. As such, while animal models may not always meet conditions of validity, they may still be useful if attention is duly paid to the benefits and limitations of using said model.

Experimental work typically begins in cell models of disease which are useful for initial *in vitro* assessment of disease mechanisms and initial screening of potential drug candidates. However, cell models represent a relatively simplistic model of the disease and sometimes rely on gene overexpression, gene knockout, and exposure to toxins or stressors which may not accurately recapitulate the physiological conditions seen in humans, lowering the validity of the model

(Falkenburger and Schulz, 2006). Animal models are therefore essential to understanding the disease *in vivo*, particularly from a systems and behavioural perspective. In the case of genetic diseases, *Drosophila melanogaster* or *Caenorhabditis. elegans* typically represent the first attempts to create animal models of disease owing to the ease of genetic manipulation due to widely available tools and genetic libraries, as well as ease of breeding, low cost, and short lifespan (Jeibmann and Paulus, 2009; Pandey and Nichols, 2011; Grotewiel and Bettinger, 2015). These models are particularly useful to explore dysregulated pathways and processes as well as to conduct rudimentary behavioural testing to explore potential phenotypes. However, *Drosophila* and *C. elegans* are clearly very genetically and behaviourally divergent from humans, lowering construct and face validity (Pouladi, Morton and Hayden, 2013).

If preliminary results are promising, the next step is typically to produce a transgenic, knockout, or knock-in mouse model of the disease which improves construct and face validity owing to increased similarity to humans in terms of genetics and anatomy as well as increased lifespan and capacity for behavioural evaluation. Rat models can also be created and represent an improvement on mouse models due to higher similarity to humans, however creation of genetic rat models of disease is more challenging than mice (Charreau *et al.*, 1996) although methodological improvements have been made with time (Pradhan and Majumdar, 2016). Specific lesions are often created using neurotoxins to generate mouse and rat toxin models of neurodegenerative diseases (Zeng, Geng and Jia, 2018). Although useful in cases of idiopathic diseases and useful for exploring certain disease mechanisms and pathways, these models present with lower validity than genetic models as they do not accurately recapitulate key features of neurodegeneration. Toxin models are acute insults rather than slow-progressing diseases, the pathophysiology of the disease is not completely recreated, and pathology is highly localised to specific brain regions rather than widespread. Generation of large genetic animal models of disease is a desirable next step, particularly with regard to neurodegenerative disorders, as brain size and lifespan increase which allows better potential characterisation of neuropathology and behavioural phenotypes which may be slow-progressing and age-dependent (Pouladi, Morton and Hayden, 2013; Eaton and Wishart, 2017). Non-human primate (NHP) models are considered to be the most comparable to humans and behavioural rating scales used in humans can be used to assess the phenotype in these animals (Pouladi, Morton and Hayden, 2013).

1.5.2. The Importance of Genetic Background

There are a large number of inbred mouse strains (e.g. 129/J, C57BL/6J, CBA/J) and substrains (e.g. 129/J and 129/Sv, C57BL/6J and C57BL/6N, CBA/J and CBA/CaJ) available for use in research (Yoshiki and Moriwaki, 2006). Significant genotypic and phenotypic differences exist between different background strains (Bothe *et al.*, 2004; Brooks, Jones and Dunnett, 2012) and between substrains (Bryant *et al.*, 2008; Matsuo *et al.*, 2010; Fontaine and Davis, 2016; Kang, Hawkins and Kearney, 2019) as the genome and epigenome, as well as environment, determine the suitability of a mouse strain for a particular experiment and must be carefully considered (Crawley *et al.*, 1997). For instance, if animals are being tested on apparatus requiring visual acuity, the choice of an albino mouse strain is ill-advised due to visual deficits. Likewise, an animal with a low level of locomotor activity would not be an advisable choice for experiments exploring motor phenotypes.

The choice of background strain is particularly important in the case of genetically-modified mouse models of disease. Different strains have background-specific genetic elements which can significantly alter the penetrance and/or expressivity of a given mutation through direct suppression/enhancement of gene expression, transcription or translation or through epigenetic variation (Linder, 2006). These strain-specific background modifiers can in turn alter expression of a disease-associated phenotype aligned with the genetic modification. For instance, overexpression of amyloid precursor protein is fatal in some mouse lines but not others (Carlson *et al.*, 1997) and phenotype severity also varies in mouse models of amyotrophic lateral sclerosis (ALS) in a background-dependent manner (Heiman-Patterson *et al.*, 2015).

1.5.3. Generation of Genetically-Modified Mice

The potential confounding effects of generating a mouse model of disease on a mixed genetic background should be carefully considered. Development of genetically-modified mice has often been performed using embryonic stem (ES) cells taken from mice of a 129 substrain due to their robust nature and prevalence in developmental research (Simpson *et al.*, 1997; Limaye, Hall and Kulkarni, 2009). However, C57BL6 mouse substrains are often more desirable for research purposes as they reproduce more reliably than 129 mice, display a superior behavioural profile and were the first mouse line to have their genome sequenced (Bryant, 2011). These experimental considerations have often led to generation of genetically-modified mice on a mixed C57BL6/129 background by the following summarised method (Limaye, Hall and Kulkarni, 2009).

First, 129-derived ES cells are genetically modified to introduce the desired mutation before being inserted into a C57BL6 blastocyst. Next, the blastocyst is implanted into a C57BL6 mouse uterus to produce genetically chimeric offspring with both 129 and C57BL6 DNA. Chimeras carrying the genetic modification in the gonads are selected to be backcrossed with C57BL6 mice to produce offspring with the desired mutation in the germline. However, initial generations of backcrossed mice are on a mixed genetic background as, in addition to the desired mutation, additional 129 donor-derived genes flanking the modified gene are moved to the recipient strain in resulting heterozygotes (HET) or homozygotes (HOM) but not wild-type (WT) animals which do not carry the mutation and therefore have purely recipient (C57BL6) DNA (Eisener-Dorman, Lawrence and Bolivar, 2009). In phenotyping HET/HOM animals against WT animals, researchers can inadvertently introduce genetic confounds into their experiments as the phenotype of mutants may be influenced by extraneous DNA interacting with the mutation of interest, or even by the extraneous DNA alone (Gerlai, 1996; Crusio, 2004).

As such, careful consideration of breeding strategy should be undertaken in order to ensure that the phenotype being explored is limited to the effects of the mutation. One possible method of doing this is to create a coisogenic line by using a DNA library, ES cells, blastocyst and mice of the same inbred genetic background (ie. 129 x 129 cross) (Perez and Palmiter, 2005). However, coisogenic mice are not always fit for experimental purpose (for instance an albino mouse needed for a visual task) and hybrid mice are sometimes required. In this case, the simplest way to minimise the effects of mixed background is through generation of congenic animals. Through backcrossing C57BL6/129 hybrid animals to C57BL6 animals, ~50% of the donor 129 strain DNA is removed each generation, creating congenic animals carrying the mutation of interest and ~99.9% recipient genome after 10 generations (Eisener-Dorman, Lawrence and Bolivar, 2009). However, generation and maintenance of congenic lines is expensive and time-consuming, taking at least 1-2 years. As such, many research groups lack the resources to create these animals which could lead to premature evaluation of phenotype and misleading results. A possible alternative to generation of congenic lines (or an additional control to congenic lines) is to use coisogenic animals (129 X 129) alongside hybrid animals (eg. 129 x C57BL6) within the same experiment in order to establish whether the mutation gives rise to a phenotype in both lines as well as to compare the phenotype of both lines to assess the impact of mixed genetic background. In the event that the phenotype is different between coisogenic and hybrid animals, the genomes of both can be screened for genetic modifiers which may have an impact on disease aetiology (Nadeau, 2001). In a complex genetic disorder such as PD, it is of the utmost importance that production and breeding strategy of genetically-

modified animals is carefully thought out and clearly detailed in publications in order to ensure that the phenotype of a mouse model is attributable to a specific disease-causing mutation rather than due to inherent inter-strain phenotypic differences stemming from a mixed genetic background.

1.5.4. Animal Models of PD

A successful animal model of PD would be expected to recapitulate key features of the disease such as age-dependent, progressive degeneration of dopaminergic neurons within the SNc, presence of Lewy body-like neuropathology (in select cases), and motor dysfunction. Given that the cause of idiopathic PD is still unknown, perhaps unsurprisingly generation of animal models of PD has proven to be very difficult and the resulting models largely disappointing (Beal, 2010). In fact, toxin models of PD are still commonplace as they are more reliable and reproducible than genetic models. However, continued identification of monogenic, causative PD mutations and genetic risk factors could lead to generation of a robust model of PD in the near future. An overview of toxin and genetic models of PD will be given here.

1.5.4.1. Neurotoxin Models of PD

1.5.4.1.1. 6-OHDA

6-hydroxydopamine (6-OHDA) has historically been used to generate rats with a hemi-parkinsonian phenotype (Ungerstedt, 1968) although mouse models also exist (Thiele, Warre and Nash, 2012) (Table 1.7). 6-OHDA is a dopamine analogue which causes selective degeneration of dopaminergic neurons. Upon being taken up by dopamine transporters, 6-OHDA accumulates in the cytosol and results in production of damaging reactive oxygen species (ROS) by either production of hydrogen peroxide (H_2O_2) or inhibition mitochondrial respiratory chain complex I, or a combination of both (Hernandez-Baltazar, Zavala-Flores and Villanueva-Olivo, 2017). By either mechanism, 6-OHDA acts to exploit the enhanced vulnerability of dopaminergic neurons to oxidative stress, resulting in specific lesions with relative sparing of surrounding non-monoaminergic cells, as is observed in human PD. However, administration of 6-OHDA does not cause Lewy body pathology in animal models and there is some off-target damage to noradrenergic neurons (Breese and Traylor, 1971; Jagmag *et al.*, 2016)

6-OHDA is not readily permeable to the blood-brain barrier (BBB), necessitating direct administration to the brain (Kostrzewa and Jacobowitz, 1974). To create a hemi-parkinsonian phenotype, the toxin can be unilaterally administered into the SNc, medial forebrain bundle (MFB), or striatum. SNc and striatal administration result in rapid dopaminergic cell death, while striatal administration leads to slower loss of these neurons (Jagmag *et al*., 2016). Injection at the level of the MFB offers an advantage over striatal administration because resulting degeneration is more specific to the nigrostriatal pathway, sparing the mesolimbic pathway (Perese *et al.*, 1989).

6-OHDA-lesioned animals display a robust hemi-parkinsonian motor phenotype including impaired motor coordination, asymmetrical forelimb akinesia, and rotational behaviour (Ungerstedt, 1968) (Perese *et al*., 1989). Rotational behaviour is of particular note in these animals and amphetamine and apomorphine are commonly injected for behavioural testing. Unilateral 6-OHDA lesioning causes a dopamine imbalance between the intact and denervated striatum, with corresponding supersensitisation of dopamine receptors on the denervated side (Björklund and Dunnett, 2019). Amphetamine and apomorphine can be used to induce opposing rotational behaviour in these animals through presynaptic and postsynaptic mechanisms which each lead to asymmetrical striatal signalling magnitudes and subsequent thalamocortical output from the intact and denervated striatum (Perese *et al*., 1989). Amphetamine induces ipsilateral rotational behaviour in animals through synaptic dopamine release from nigral projections, the extent of which is far greater in the intact striatum than denervated (Ungerstedt, 1971b). Apomorphine acts as a dopamine receptor agonist which, when delivered at a very low dose, can selectively activate supersensitive dopamine receptors on MSNs in the denervated striatum, producing contralateral rotational behaviour in lesioned animals (Ungerstedt, 1971a).

1.5.4.1.2. MPTP

1-methyl-4-phenyl-1,2,3,6-tetrahydropiridine (MPTP) is commonly used to lesion NHPs to generate large animal models of PD (Table 1.7). As described in Section 1.3.5.2., MPTP is oxidised to MPP+ in glia through a reaction catalysed by monoamine oxidase B (MAO-B) (Kupsch *et al.*, 2001). MPP+ is then taken up by neuronal dopamine transporters where it inhibits mitochondrial complexes to stall the electron transport chain and lead to release of ROS and reduce ATP production which leads to cell death (Desai *et al.*, 1996; Storch, Ludolph and Schwarz, 2004). Due to its lipophilic nature, MPTP can be administered systemically as it can readily cross the BBB. MPTP-lesioned NHPs are a good phenocopy of the human condition, displaying bilateral nigral degeneration, Lewy body-like neuropathology and motor dysfunction (Varastet *et al.*, 1994; Porras, Li and Bezard, 2012). However, use of NHPs is expensive and highly restricted, meaning MPTP-lesioned NHPs are only typically utilised when testing promising therapies prior to initiation of clinical trials (Jagmag *et al.*, 2016). Mice are vulnerable to MPTP administration, displaying nigral degeneration and motor dysfunction in the absence of Lewy body-like pathology (Jackson-Lewis and Przedborski, 2007). Interestingly, rats are relatively resistant to the toxin due to differences in MPP+ sequestration (Schmidt and Ferger, 2001).

1.5.4.1.3. Rotenone and Paraquat

Rotenone is an insecticide which inhibits mitochondrial complex I and also inhibits mitosis and proliferation (Jagmag *et al*., 2016) (Table 1.7). Rotenone can be delivered through direct or systemic routes and chronic exposure to the toxin in rats leads to slow nigrostriatal degeneration and Lewy body-like pathology, alongside parkinsonian motor deficits (Fleming *et al.*, 2004). However, rotenone administration is associated with high mortality rate which makes experimental work difficult (Fleming *et al.*, 2004). Paraquat is an herbicide which generates ROS, resulting in nigrostriatal degeneration and Lewy body-like pathology in rodents (McCormack *et al.*, 2002) (Table 1.7). However, administration of this toxin results in significantly variable extents of degeneration between animals, making use of this model difficult for experimental work (Miller, 2007).

Toxin	Primary Species	Mechanism	Route	Lewy Pathology	Cons	Reference
6-OHDA	Rats Mice	Oxidative Stress	Intraparenchymal	No	Kills noradrenergic cells	Ungerstedt, 1968 Thiele, Warre and Nash, 2012
MPTP	NHP	Complex I, III, IV inhibition	Systemic	Yes	Rats are resistant	Varastet et al., 1994
	Mice			No	Doesn't recapitulate PD behaviour in mice	Jackson-Lewis and Przedborski, 2007
Rotenone	Rats Mice	Complex I inhibition	Direct or Systemic	Yes	High mortality rate	Fleming et al., 2004
Paraquat	Rats Mice	Oxidative stress	Systemic	Yes	Large variability	Miller, 2007

Table 1.7. Toxin Models of PD. *Several neurotoxins which act largely at the level of mitochondria are used to generate animal models of PD in mice, rats, and NHPs.*

1.5.4.2. Genetic Mouse Models of PD

The discovery of monogenic genes in PD patients paved the way for the first attempts at creating genetic mouse models of disease in the early 2000's and dozens of different models have been created since that time (Breger and Fuzzati Armentero, 2019). Generation of these mouse models has relied on introduction of mutant transgenes (rodent or human), gene knock-outs, knock-ins or overexpression. PD is typically classified by degeneration of the SNc, motor deficits, and (variable) Lewy pathology. As such, genetic mouse models of PD featured on the EU Joint Programme – Neurodegenerative Disease Research database have been evaluated for presence or absence of these features and tabulated (Fuzzati-Armentero, M. T., & Breger, L. S., & EU JPND, 2018).

1.5.4.2.1. *SNCA* Mutants

Considering the importance of α-synuclein in both monogenic and sporadic PD, many mouse models have been produced which either produce excessive WT α-synuclein or express a mutant form of the *SNCA* gene (Fernagut and Chesselet, 2004). However, results from *SNCA* mouse models have been largely disappointing with phenotypes greatly influenced by the promoter used and whether WT or mutant α-synuclein is produced (Breger and Fuzzati Armentero, 2019).

As can be seen in Table 1.8, the majority of *SNCA* mouse models fail to recapitulate SNc degeneration, motor deficits, or nigral inclusion formation. Moreover, it is apparent that the A53T human mutant is most effective at rendering a parkinsonian phenotype compared with other mutant variants (A30P/E46K) or overexpression of WT *SNCA*. 50% of A53T mutant mice display nigral degeneration, 62.5% of mice demonstrate motor deficits and 50% of mice feature inclusion bodies in the SNc. However, it is apparent that variation in phenotype exists even between studies using the same promoter to drive expression of the same form of the *SNCA* transgene, and that mice frequently exhibit motor deficits in the apparent absence of nigrostriatal cell loss (Table 1.8). In fact, only three models (A53T) display degeneration alongside motor deficits and inclusions (Table 1.8). Furthermore, given the severity and early onset of the *SNCA* phenotype in human PD, the mouse phenotype is surprisingly mild with relatively modest cell loss and motor deficits reported in aged animals. In addition, cell-specific promoters such as rat TH and PITX3 appear to more reliably lead to nigral degeneration but several models utilising the same promoters show no such phenotype. In light of the difficulties in recreating a parkinsonian phenotype, increasing attention has been directed towards generating animal models of PD through targeted transduction of nigral cells using viral vectors containing an *SNCA* transgene.

Viral vector-mediated overexpression of α-synuclein in the SNc has been shown to result in Lewy body-like inclusions and cellular pathology, parkinsonian phenotypes and progressive nigral degeneration in rats (Kirik, Rosenblad, *et al.*, 2002) and NHPs (Kirik *et al.*, 2003). Generation of PD models using overexpression of α-synuclein within the population of SNc neurons lost in PD offers the potential to create a rapid model of PD which may share mechanisms with the human condition. However, overexpression of α-synuclein is rapid and highly-localised in these models, unlike the human condition where α-synuclein accumulation is slow and pathology is widespread.

SNCA	Background Strain	SNCA (species, mutant/WT)	Promoter	Nigral Degeneration	Motor Deficits	SNc Inclusions	References
1	Swiss Webster x C57BL/6J	Human WT	Rat TH	**Mild (19mo)**	No	No	Prasad et al., 2011
2	C57BL/6 /DBA2 line D	Human WT	PDGF	No	**Yes (RR) (3/9mo)**	**Yes**	Masliah et al., 2000
3	C57BL/6 /DBA2 line 61	Human WT	Thy1	No	**Yes (RR, OF 4-14mo)**	**Yes**	Chesselet et al., 2012
4	C57BL/6J X CBA/ca) X Syn-/-CB57BL/6JOla	Human truncated WT	Rat TH	No	**Yes (ACT)**	**Yes**	Tofaris et al., 2006
5	C57BL x B6CH3	Human WT	CaM-tTa	No	**Yes**	No	Nuber et al., 2008
6	Swiss Webster x CB57BL/DAB	Human WT	Rat TH	No	Not reported	No	Richfield et al., 2002
7	C57BL/6J x C57BL/6JOla	Human WT	Rat TH	No	Not reported	No	Prasad et al., 2011
8	C57BL6/CH3	Human WT	PrP	No	No	No	Giasson et al., 2002
9	C57BL/6J	Human truncated WT	ROSA26	No	Not reported	Not reported	Daher et al., 2009
10	FVB/N x 129S6/SvEvTac	Human WT	PAC	No	No	No	Kuo et al., 2010
	Percentage success (n = 10)			**10%**	**40%**	**33.30%**	
11	C57BL6/CH3	Human A30P	Thy1	No	**Yes (6-14mo)**	No	Kahle et al., 2001
12	Swiss Webster x C57BL6/DAB	Human A30P	Rat TH	No	Not reported	No	Matsuoka et al., 2001
13	asyn-/-C57BL/6	Human A30P	BAC	No	No	No	Taylor et al., 2014
14	FVB/N x 129S6/SvEvTac	Human A30P	PAC	No	No	No	Kuo et al., 2010
	Percentage success (n = 4)			**0%**	**33.30%**	**0%**	
15	C3H/C57BL/6J x CB57BL/6J	Human A53T	PrP	**Yes (9 and 12mo)**	**Yes (8-17mo) STR, OF, RR, GA**	Yes	Giasson et al., 2002
16	C57BL/6	Human A53T	Thy1	**Yes (12mo)**	**Yes (2-12mo)**	Yes	Martin et al., 2014
17	C57BL/6J	Human A53T	PITX3-tTa	**Yes (1-12mo)**	**Yes (OF, GA, RR) (1-12mo)**	Yes	Lin et al., 2012
18	C57BL/6J	Human truncated A53T	Rat TH	**Yes (2-12mo)**	**Mild (ACT 2 and 12mo)**	Not reported	Wakamtsu et al., 2008a/b
19	FVB/N x 129S6/SvEvTac	Human A53T	PAC	No	**Yes (RR, OF) (6-18mo)**	No	Kuo et al., 2010
20	C57BL/6 x B6CH3	Human A53T	CaM-tTa	No	Not reported	Yes	Lim et al., 2011
21	Swiss Webster x C57BL6/DAB	Human A53T	Rat TH	No	Not reported	No	Matsuoka et al., 2001
22	C57BL/6J	Human truncated A53T	ROSA26	No	Not reported	Not reported	Daher et al., 2009
	Percentage success (n = 8)			**50%**	**62.50%**	**50%**	
23	CB576J x 129/SvJ	Human truncated E46K	ROSA26	Not reported	Not reported	Not reported	Daher et al., 2009
24	CB57BL/CH3	Human E46K	PrP	No	**Yes**	No	Emmer et al., 2011
	Percentage success not calculated						
25	CB57BL/6J	Human A53T+A30P	Rat TH	No	No	No	Matusoka et al., 2001
	Percentage success not calculated						
	Overall percentage success (n = 25)			**20%**	**44%**	**28%**	

Table 1.8. SNCA genetic mouse models of PD*. Overexpression of WT SNCA and expression of mutant variants produce variable phenotypes as evaluated by nigral degeneration, motor deficits, and SNc inclusions. Percentage success for each approach has been calculated based on the reported presence or absence of these phenotypic features (RR = rotarod; OF = open field; ACT = locomotor activity; STR = startle; GA = gait). Adapted from Fuzzati-Armentero, M. T., & Breger, L. S., & EU JPND, 2018.*

1.5.4.2.2. *LRRK2* Mutants

LRRK2 mutant mice also show variation in phenotype between models (Table 1.9). Models utilise expression of mouse/human WT *LRRK2*, mouse/human G2019S variant *LRRK2*, human R1441C/G variant *LRRK2*, or knockout of endogenous *LRRK2*. Only one model displays nigral degeneration in aged animals (human G2019S under a cytomegalovirus (CMV) promoter) (Table 1.9), although contradictory results were obtained with regard to motor deficits with this model. Despite frequent Lewy pathology in human *LRRK2* PD, particularly in cases of G2019S mutations, inclusions were not reported in any of the mice examined. Interestingly, the majority of models (60%) exhibited motor dysfunction in the apparent absence of neurodegeneration, although motor phenotype was typically mild and limited to locomotor activity with is non-PD-specific.

LRRK2	Background	LRRK2 (species, mutant/WT)	Promoter	Nigral Degeneration	Motor Deficits	SN Inclusions	References
1	C57BL/6J	Mouse WT	BAC	No	**Yes (OF, BB 6 and 12mo)**	No	Li et al., 2010
	Percentage Success not calculated						
2	C57BL/6J	Human WT	BAC	No	**Yes (OF, CYL) >6mo**	Not reported	Beccano-Kelly et al., 2015
3	C57BL/6	Human WT	Pitx3-tTa	No	**Mild (OF 2-18mo)**	Not reported	Liu et al., 2015
4	FVB	Human WT	BAC	No	No	No	Melrose et al., 2010
5	C57BL/6	Human WT	CaM-tTA	No	No	Not reported	Lin et al., 2009
6	FVB/N	Human WT	PDGF (CMV enhancer)	No	No	No	Ramones et al 2011
7	C57BL/6	Human WT	Thy1	No	No	No	Herzig et al., 2012
8	C57BL/6	Human WT	Thy1.2	No	Not reported	No	Garcia-Miralles et al., 2015
	Percentage Success (n = 7)			**0%**	**33.33%**	**0%**	
9	C57BL/6J	Mouse G2019S	Endogenous (knock-in)	No	**Yes (OF 15mo)**	No	Longo et al., 2014
10	C57BL/6J	Mouse FLAG-tagged G2019S	BAC	No	No	No	Li et al., 2010
	Percentage Success (n = 2)			**0%**	**50%**	**0%**	
11	FVB/N	Human G2019S	CMV	**Yes (12-21mo)**	Contradictory	No	Ramones et al., 2011
12	C57BL/6J	Human G2019S	CaM-tTA	No	**Yes (12-22mo)**	No	Lin et al., 2009
13	FVB or FVB-C57BL6	Human G2019S	BAC	No	**Mild (OF 22-24mo)**	No	Melrose et al., 2010, Beccano-Kelly et al.,2015
14	C57BL/6	Human G2019S	Thy1	No	**Mild (OF 7mo)**	No	Herzig et al., 2012
15	C57BL/6	Human G2019S	Pitx3-tTa	No	No	Not reported	Liu et al., 2015
16	C57BL/6	Human G2019S	Thy1.2	No	Not reported	No	Garcia-Miralles et al., 2015
	Percentage Success (n = 6)			**16.67%**	**75%**	**0%**	
17	FVB/N	Human R1441C	PDGF (with CMV enhancer)	Contradictory	**Yes (OF 15-20mo)**	No	Ramones et al., 2011
	Percentage Success not calculated						
18	FVB	Human R1441G	BAC	No	Contradictory	Not reported	Li et al., 2009, Dranka et al., 2013
	Percentage Success not calculated						
19	C57BL/6J	Mouse KO	N/A	No	**Yes (OF 7 and 16mo)**	No	Andres-Mateos et al., 2009
	Percentage Success not calculated						
	Overall Percentage Success (n = 19)			**5.60%**	**60%**	**0%**	

Table 1.9. LRRK2 genetic mouse models of PD*. Overexpression of WT LRRK2 and expression of mutant variants produce variable phenotypes as evaluated by nigral degeneration, motor deficits, and SNc inclusions. Percentage success for each approach has been calculated based on the reported presence or absence of these phenotypic features (OF = open field; CYL = cylinder). Adapted from Fuzzati-Armentero, M. T., & Breger, L. S., & EU JPND, 2018.*

1.5.4.2.3. *PINK1* Mutants

Relatively few *PINK1* mouse models have been created, with manipulation limited to gene knockout (Breger and Fuzzati Armentero, 2019). Motor deficits were not explored in the majority reported and nigral degeneration is typically absent (Breger and Fuzzati Armentero, 2019).

1.5.4.2.4. *Parkin* Mutants

Several *Parkin* mutant mice have been created and evaluation of their success will be discussed in Chapter 2.

1.5.4.2.5. MitoPark Mice

The MitoPark mouse was not modelled on a mutation observed in human PD but was instead created through a reverse genetic approach based on the considerable amount of evidence implicating mitochondrial dysfunction in PD aetiology (Branch *et al.*, 2016). This mouse model displays inactivation of mitochondrial transcription factor A (Tfam) specifically within dopaminergic neurons, leading to reduction in mtDNA expression and associated respiratory chain deficiency (Ekstrand *et al.*, 2007). MitoPark mice display a progressive phenotype characterised by loss of dopaminergic neurons in the SNc (and VTA) beginning at 12 weeks of age, L-DOPA-responsive motor dysfunction beginning at ~14 weeks of age, with small cytoplasmic aggregates appearing at 6 weeks of age (Ekstrand *et al.*, 2007). Although these animals display a phenotype reminiscent of PD, Tfam inactivation is not a genetic cause of human PD. Furthermore, the aggregates observed in these mice are not α-synuclein-positive, unlike Lewy bodies and the age of onset is relatively young. Taken together, these results suggest that MitoPark mice may represent a useful tool for understanding the role of mitochondria in PD but do not necessarily represent an accurate model of the disease and could instead be viewed as a "genetic lesion" model.

1.5.5. Gene-Environment Models

Both rotenone and paraquat have been linked to development of PD and MPTP has been shown to lead to a parkinsonian phenotype in humans following ingestion (Langston *et al.*, 1983; Tanner *et al.*, 2011). Given the ability of these toxins to create a parkinsonian phenotype in humans and animal models of PD, several groups have attempted to combine genetic mouse models with toxin exposure to elicit a robust PD phenotype (Manning-Boġ and Langston, 2007).

Exposure to MPTP has been associated with increased α-synuclein expression in NHP (Purisai *et al.*, 2005) and rodent (Vila *et al.*, 2000) dopaminergic neurons with a corresponding increased sensitivity to MPTP in *SNCA* overexpressing mice compared to controls (Song *et al.*, 2004) and decreased sensitivity to MPTP in *SNCA* KO mice (Dauer *et al.*, 2002). Exposure to

rotenone and paraquat has also been shown to increase expression of α-synuclein in rodents (Betarbet *et al.*, 2000; Manning-Bog *et al.*, 2002) although the relationship between these toxins and α-synuclein is less readily apparent. Although interesting to examine disease mechanisms, and suggesting that mutations within PD-associated genes leads to increased susceptibility to toxin-induced dysfunction, exposure of genetic models to toxins does not appear to create a more accurate phenocopy of PD than exposure to toxin alone.

1.5.5. Animal Models of HD

1.5.5.1. Toxin Models of HD

Similar to PD, the first animal models of HD relied on neurotoxins to approximate HD neuropathology and symptoms. The glutamate receptor agonists ibotenic acid and kainic acid were initially used to selectively ablate MSNs through excitotoxicity Coyle and Schwarcz, 1976; Schwarcz *et al.*, 1984) but were subsequently surplanted by quinolic acid as this toxin spared cholinergic interneurons (Beal *et al.*, 1986; Pouladi, Morton and Hayden, 2013). Peripheral administration of malonate and 3-nitropropionic acid (3-NPA) also leads to striatal lesions predominantly targeting MSNs, in this case through disruption of the electron transport chain (Beal *et al.*, 1993; Brouillet *et al.*, 1993; Pouladi, Morton and Hayden, 2013). Although useful, lesion models are acute and localised meaning they fail to replicate the chronic, widespread nature of HD.

1.5.5.2. Genetic Mouse Models of HD

Identification of the monogenic cause of HD offered the promise of generation of genetically accurate models of disease. Early work on *C. elegans* (Faber *et al.*, 1999; A. L. Lee *et al.*, 2017) and *Drosophila* (Jackson *et al.*, 1998; Lewis and Smith, 2016) demonstrated the ability of the truncated or full-length mutant *HTT* gene to produce neuronal dysfunction and degeneration in these models. Rat models of HD have also been generated and display a motor phenotype (Manfré *et al.*, 2017). However, mouse models of HD predominate and will be discussed briefly here.

An expanded CAG repeat within the *HTT* gene is essential to HD and must therefore be included in animal models of the disease. HD mouse models typically contain either a pathogenic truncated N-terminal fragment of the *HTT* gene containing the CAG expansion, a full-length knock-in of human *HTT* exon 1 (containing the expanded CAG repeat) into the endogenous mouse *HTT* gene, or insertion of a full-length human *mHTT* transgene (Ferrante, 2009) (Table 1.10). Fragment models, such as the R6/1 and R6/2 transgenic mice display an early-onset, rapidly progressing, severe HD phenotype more akin to juvenile HD than the typical form (Mangiarini *et al.*, 1996) (Table 1.10). On the other hand, relative to fragment models, full-length HD models created by knock-in of human *mHTT* exon 1 (such as the HdhQ111 or zQ175) or by expression of the full-length human *mHTT* gene (such as the YAC128 or BACHD) typically present with a late-onset, slow progressing mild phenotype (Wheeler *et al.*, 2002; Slow *et al.*, 2003; Gray *et al.*, 2008; Menalled *et al.*, 2012) (Table 1.10). In addition, the choice of promoter, inclusion of interrupting CAA triplets within the expansion, the use of cDNA or genomic DNA, and the inclusion of upstream and downstream regulatory DNA sequences can all affect the phenotype of mice (Pouladi, Morton and Hayden, 2013). With regard to construct validity, full-

length genomic DNA human *HTT* under the control of the human *HTT* promoter is preferable. However, both fragment and full-length *HTT* models are useful. Fragment models are typically used as screening tools for new therapeutics owing to the fast onset of disease (Ferrante, 2009). However, the severity of the disease prevents longitudinal studies in these animals. Full-length *HTT* models are more representative of the human condition and are used to validate therapeutics and explore pathways and processes dysregulated in the human condition. Interestingly, despite mHTT aggregation and neuronal dysfunction, the majority of mouse models do not display severe neurodegeneration within the striatum (Pouladi, Morton and Hayden, 2013). Significant progress has also been made with regard to large animal models of HD, with NHP, sheep and pig models of HD reported, albeit with less reliable phenotypes than mouse models (Yang *et al.*, 2008, 2010; Jacobsen *et al.*, 2010; Yan, Li and Li, 2019).

Name	HTT	Promoter	CAG length	Striatal Neuropathology	Cognitive	Motor	Reference
R6/1	Fragment 67aa	1kb Human *HTT*	116	Inclusions and Atrophy	Early	Early	Mangiarini et al., 1996
R6/2	Fragment 67aa	1kb Human *HTT*	144	Inclusions and Atrophy	Early	Early	Mangiarini et al., 1996
HdhQ111	Full-length human *HTT* Exon 1 knock-in	Mouse *HTT*	111	Inclusions	Late	Late	Wheeler et al., 2002
zQ175	Full-length human *HTT* Exon 1 knock-in	Mouse *HTT*	188	Inclusions	Late	Late	Menalled et al., 2012
YAC128	Full-length human *HTT*	Human *HTT*	128	Inclusions and Atrophy	Late	Late	Slow et al., 2003
BACHD	Full-length human *HTT*	Human *HTT*	97	Inclusions and Atrophy	Late	Late	Gray et al., 2008

Table 1.10. Genetic mouse models of HD. *Mouse models of HD typically express either an expanded CAG exon 1 fragment, an expanded CAG repeat knock-in, of a full length mutant HTT allele.*

1.5.6. Conclusions

Animal models of neurodegeneration are useful tools for understanding disease mechanisms or screening drug candidates and a great deal of insight can be gained through their careful use. Toxin models, although simplistic, permit exploration of simple mechanisms which are directly related to disease pathophysiology, although degeneration is acute and highly localised. Genetic models are preferable due to higher validity, however the effect of genetic background must be carefully considered. Use of germline genetic animal models of PD remains challenging due to their mild and variable phenotypes but conditional and mixed models could extend their uses. On the other hand, HD mouse models are relatively well-regarded, although they do not recapitulate all aspects of disease such as severe striatal degeneration. Progress in generating large animal models of disease offers the opportunity to

advance research in this field due to higher validity. Generation and characterisation of a successful animal models of neurodegeneration is vital and has the potential to lead to disease-modifying treatments which could revolutionise the treatment of these diseases.

1.6. Therapeutics for Neurodegenerative Diseases

1.6.1. General Information

The classical drug discovery pipeline describes the route a new drug takes between conception and approval and will be summarised here (Mohs and Greig, 2017; Fernández-Ruiz, 2019). The process typically begins with screening multiple compounds for efficacy. Next, the most efficacious compounds are taken forward and modified to improve their desirable structural characteristics for purpose. The drug candidates are further refined and tested in cell and animal models to assess their toxicity and pharmacokinetic/pharmacodynamic profiles. If successful in preclinical development, the drug candidate is entered into clinical trials to evaluate safety and efficacy in humans before being licenced and sold if the appropriate criteria are met. The drug discovery pipeline is a hugely challenging, time-consuming and expensive process, with the cost of development from discovery to FDA approval estimated at an average of $2.6 billion (Han *et al.*, 2018). Furthermore, drug development for diseases of the CNS typically cost more than development of drugs for other systems, and this elevated cost is accompanied by a longer duration of development and marketing (12.6 year average compared to 6.3 years for cardiovascular drug candidates) and higher associated cost as well as, crucially, a lower rate of success in reaching the marketplace (7% vs 15% average across other systems) (Kola and Landis, 2004; Pangalos, Schechter and Hurko, 2007; Han *et al.*, 2018).

1.6.2. The Challenges of Treating Neurodegeneration

The difficulty of drug development for neurodegenerative diseases lies within the complexity of the CNS and the disease process itself. Neurodegeneration can be thought of as the end result of a complex interplay between multiple dysregulated cellular processes and pathways, the relative contributions of which accumulate to surpass a critical threshold for cell-loss (Lang, 2010). Although there are overlaps in the affected processes and pathways between different disorders, their relative contributions to neurodegeneration describe the aetiologies of individual diseases. Identification and assessment of these processes and pathways reflects the best opportunity to develop effective, disease-modifying treatments (Pangalos, Schechter and Hurko, 2007). Drugs which target a single dysregulated cellular process or pathway with a high contribution to neurodegeneration could be used to reduce the overall disease burden below the critical threshold for cell-loss and slow progression. Alternatively, single drugs capable of targeting multiple dysregulated processes or pathways concurrently, or multiple single-target drugs used in combination, could be administered to maximise therapeutic potential and lower the overall disease burden below the critical threshold for cell-loss (Lang, 2010). However, development of drugs targeting specific dysfunctional pathways requires dissection and in-depth understanding of these pathways. Toxin animal models of disease do not accurately

reflect the pathogenesis of neurodegeneration in patients and thus the key challenge in identifying dysregulated pathways and processes in these disease relies on the ability to generate accurate genetic cellular and animal models of disease which display the same dysfunction as is present in the human condition. The advantage of this approach is reflected in an analysis stating that selecting genetically supported targets for drug development could double the success rate in clinical development (Nelson *et al.*, 2015).

An additional complication in successful treatment of neurodegenerative disorders is that they are predominantly idiopathic (with the exception of HD and familial forms of AD and PD) and overt symptom-onset and subsequent diagnosis begins in middle- to old-age, by which point a significant portion of neurons have already degenerated (Sperling *et al.*, 2011). Accordingly, even if drugs are developed which successfully target a particular dysregulated process or pathway, the administration of the drug may be too late to evoke a significant amelioration in the patient's condition. In recognition of this, an increasing amount of work is being carried out to identify easily-screened biomarkers in order to diagnose disease prior to the onset of significant cell-loss and aid evaluation of outcome measures during clinical trials (Jeromin and Bowser, 2017). If treated early, new disease-modifying drugs have a better chance of exerting a meaningful effect by slowing the process of neurodegeneration. In addition, development of neuroprotective or neurorestorative could be presented with a larger therapeutic window.

Taken together, it is apparent that despite a huge increase in research funding, and a corresponding increase in our understanding of the mutations and mechanisms underlying neurodegenerative diseases, development of disease-modifying treatments for neurodegeneration has proven to be extremely challenging (Kola and Landis, 2004; Pangalos, Schechter and Hurko, 2007; Fernández-Ruiz, 2019). The paucity of available therapies which slow or stop disease progression, or indeed reverse the associated damage, suggests that the traditional drug discovery/development process is ill-equipped to meet the demand of neurodegenerative diseases. However, improvement is possible by taking advantage of progress in molecular biology and gene therapy. Firstly, disease processes and pathways can be more effectively and accurately studied through identification of causative mutations and risk factors in patient populations before subsequent modelling in cells and animals. Secondly, owing to the long timescale for drug development, existing therapies effectively targeting disease symptomology can be optimised in order to improve their efficacy and reduce off-target effects. Finally, following identification of dysregulated processes and pathways, novel gene therapy approaches which are site-specific and have the potential to modulate an array of targets can be developed and evaluated.

1.6.3. Current Therapies for PD

1.6.3.1. Pharmacological Therapies

Although used in clinical practice for over 50 years, orally-administered L-DOPA remains the gold standard therapy for controlling motor symptoms of PD during its initial stages and acts to elevate levels of dopamine (Hornykiewicz, 1966; Whitfield, Moore and Daniels, 2014). In healthy cells, dopamine biosynthesis is a two-step process beginning with tyrosine hydroxylase-mediated hydroxylation of L-tyrosine which produces L-DOPA and subsequent decarboxylation of L-DOPA by aromatic l-amino acid decarboxylase (AADC) to produce dopamine (Blaschko, 1942; Juorio *et al.*, 1993; Mura *et al.*, 1995; Meiser, Weindl and Hiller, 2013) (Figure 1.11). The production of L-DOPA by TH is dependent on production of tetrahydrobiopterin (BH4) which is synthesised from guanosine triphosphate (GTP) by GTP cyclohydrolase (GCH1) (Meiser, Weindl and Hiller, 2013) (Figure 1.11) Oral L-DOPA administration therefore provides the immediate precursor to dopamine and relies on activity of endogenous AADC to convert exogenous L-DOPA to dopamine.

L-DOPA, unlike dopamine, can be absorbed through the small intestine and is able to cross the (BBB) via large neutral amino-acid transporters (Wade, Mearrick and Morris, 1973; Stansley and Yamamoto, 2013) making it a much more viable treatment option than direct dopamine replacement. Administration of L-DOPA alongside a peripheral AADC inhibitor such as carbidopa ensures a large amount of L-DOPA is converted to dopamine by centrally-localised AADC, replacing dopamine where needed and reducing peripheral side-effects (Papavasiliou *et al.*, 1972; Whitfield, Moore and Daniels, 2014). However, continued use of L-DOPA is associated with wearing off, on-off phenomena, and dyskinesias in the majority of patients (Thanvi and Lo, 2004; Huot *et al.*, 2013). These adverse motor complications are thought to be caused, at least in part, by the intermittent nature of oral L-DOPA therapy which results in pulsatile increases and decreases in dopamine production and subsequently aberrant cell-signalling (Huot *et al.*, 2013; You *et al.*, 2018). Adjuvant therapy to help control motor fluctuations uses dopamine agonists with half-lives exceeding that of L-DOPA or inhibitors of dopamine-degrading enzymes to prolong the duration of dopaminergic signalling (Alonso Canovas *et al.*, 2014). In addition, L-DOPA formulations are being modified to extend release when ingested or to enable oral disintegration or inhalation which may reduce motor fluctuations (Gupta, Lyons and Pahwa, 2019). An additional intervention is to ensure continuous L-DOPA administration by fitting a jejunal L-DOPA pump, an approach which has been trialled and shown to reduce the motor complications associated with prolonged oral L-DOPA use (Stocchi *et al.*, 2005). However, although effective, the short half-life of L-DOPA makes continuous administration difficult and systemic administration of L-DOPA and additional dopamine-

modulating drugs inevitably leads to off-target effects and is associated with non-motor complications such as impulse control disorders and psychosis (Wu, Politis and Piccini, 2009).

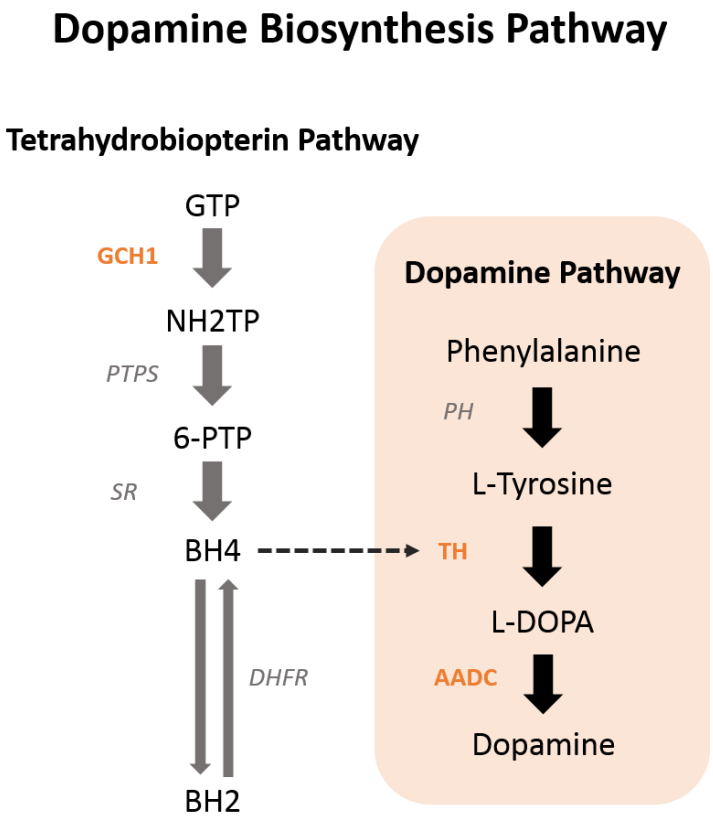

Figure 1.11. The dopamine biosynthesis pathway. *The rate-limiting enzymes for dopamine synthesis are GCH1, TH, and AADC. GCH1 produces BH4, the necessary co-factor for TH to convert L-tyrosine to L-DOPA. L-DOPA is then decarboxylated to form dopamine.*

1.6.3.2. Surgical Interventions

1.6.3.2.1. Deep Brain Stimulation

Deep brain stimulation (DBS) was developed for PD in the 1990s and has been used to ease motor symptoms of the disease ever since (Pollak *et al.*, 1993). Typically, electrodes are implanted within the brain to deliver high frequency current to the STN (Eisinger *et al.*, 2019) although the GPi has also been targeted (Volkmann *et al.*, 2004). Although the mechanism of action of DBS is not fully understood, the intervention is based on predications made by the rate model of basal ganglia dysfunction in PD and stimulation of the STN is postulated to alter signalling through the basal ganglia circuitry with the eventual result of ameliorating the dysregulated cortical motor output observed in PD (Eisinger *et al.*, 2019) (Section 1.3.3.1.). Although considered safe and effective, DBS is associated with speech, cognitive and motor side-effects, improves only a subset of symptoms, and the degree of stimulation cannot be readily altered without the specialist intervention (Cyron, 2016).

1.6.3.2.2. Cell Therapies

The history of cell therapies has been reviewed previously (Parmar, Torper and Drouin-Ouellet, 2019) and will be summarised here. The first attempt at cell replacement therapy in PD patients was conducted in 1987, with subsequent addition of patients over the course of several subsequent years (Lindvall *et al.*, 1989). Building upon evidence of functional recovery in treated 6-OHDA-lesioned rats (Björklund, Schmidt and Stenevi, 1980), patients received striatal transplants of foetal ventral midbrain dopaminergic cells into the striatum to release dopamine locally (Lindvall *et al.*, 1989). Although overall successful at eliciting clinical improvement in treated patients, the extent of improvement varied widely between patients. Progression into double-blind placebo-controlled trials followed in the 1990s but was met with disappointing results, with seemingly no therapeutic benefit and the occurrence of graft-induced dyskinesia in the majority of patients (Freed *et al.*, 2001; Olanow *et al.*, 2003). However, evaluation of patients 3-5 years post-graft revealed a clinical improvement (albeit with high inter-subject variability) in treated patients (Barker *et al.*, 2013). These data also provided a set of criteria for optimal clinical outcomes with include selection of young patients with no dyskinesias as well as a strict regimen of immunosuppression to prevent graft reduction following transplantation. Taken together, these trials suggest that, although cell replacement can be highly effective, a high variability in the extent of recovery exists between patients, with treatment accordingly targeted towards only a select proportion of individuals who meet the criteria for optimal clinical outcomes. In addition, graft-induced dyskinesia represents a significant potential side-effect, as does the danger posed by immunosuppression. The production of human embryonic stem cells (hESCs) and induced pluripotent stem cells (iPSCs)

fit for the sole purpose of cell replacement is ongoing and may reduce the risks and complications of cell replacement therapy, potentially representing a significant leap forward in the treatment of PD (Barker *et al.*, 2019; Parmar, Torper and Drouin-Ouellet, 2019).

1.6.4. Current Therapies for HD

HD represents a prime candidate for development of therapies targeting neurodegeneration as it is typically inherited and has an identified monogenic cause and toxic species. However, in spite of these features, development of disease-modifying therapies for HD has proven challenging. This difficulty is due to the wide array of cellular pathways dysregulated by the mHTT protein which lead to motor, cognitive and psychiatric symptoms (Bates *et al.*, 2015). Therefore, HD presents with a wide-range of therapeutic targets which influence pathophysiology and symptomology to varying extents. The complexity and challenge of HD drug development is best appreciated by looking at the success of clinical trials. In a comprehensive review of 99 HD clinical trial outcomes spanning from 1999 to May 2017, the overall success rate (i.e. receiving licencing) was calculated as 3.5% which is lower than the overall success rate for neurological diseases (9%) (Travessa *et al.*, 2017). Furthermore, the authors demonstrated that phase-specific success rates were low at early trial phases and were even lower in later phases, reflecting early promise but subsequent difficulty in bringing HD therapeutics through the drug development pipeline (Travessa *et al*., 2017). This lack of sustained success may be due to issues such as overinterpretation of early data or enhancement of placebo effect (Caron, Dorsey and Hayden, 2018).

1.6.4.1. Pharmacological Therapies

At present, only two drugs are currently FDA approved for the treatment of HD, both of which treat chorea. Tetrabenazene, a reversible inhibitor of vesicular amine transporter 2 (VMAT2), has been used since 2008 and acts to reduce monoamine release which reduces initiation of involuntary movements by attenuating activation of indirect pathway MSNs (Huntington's Study Group, 2006). The second drug, deutetrabenazine, was approved in 2017 and is a chemically-modified analogue of tetrabenazine which works through the same mechanism but is more resistant to metabolism, lengthening the half-life and increasing systemic availability (Frank *et al.*, 2016; Caron, Dorsey and Hayden, 2018). Although effective, both of these drugs cause significant side-effects in other aspects of motor function, as well as in cognitive function and psychiatric state (Caron, Dorsey and Hayden, 2018). Aside from HD-specific drugs, anti-psychotics such as olanzapine are commonly prescribed off-label, acting to antagonise D2Rs which reduces indirect pathway over-activation (Unti *et al.*, 2017). Psychiatric symptoms are

commonplace in HD patients are predominantly treated with pre-existing antidepressants and antipsychotics (Adam and Jankovic, 2008). HD-related cognitive dysfunction has been targeted with cholinesterase inhibitors but results have been disappointing (Vattakatuchery and Kurien, 2013).

1.6.4.2. Cell Therapies

The majority of studies attempting to use cell therapy in HD have transplanted neural stem cells (NSCs) from human foetal ganglionic eminence (GE) into the diseased adult striatum with the intention of these cells forming an integrated graft of MSNs capable of restoring neural circuitry and improving functional deficits (Bachoud-Lévi, 2017). Preclinical work has demonstrated that this approach shows promise in animal models of HD (McBride *et al.*, 2004; Ryu *et al.*, 2004), however considerable variability exists in the outcomes of such studies (Choi, Choi and Hong, 2018). In the clinical setting, the majority of cell replacement therapy trials have utilised foetal GE tissue in open-label pilots with few patients with generally disappointing results (reviewed in (Bachoud-Lévi, 2017)). Safety of cell replacement therapy in was first established in patients in the 1990's (Kopyov *et al.*, 1998) with the first report of long-term functional recovery in treated patients reported by Bachoud-Levi and colleagues in 2000 (Bachoud-Lévi *et al.*, 2000). However, subsequent open-label trials have largely failed to reproduce functional improvements with only 4 of 30 patients with available data demonstrating long-term improvements or stabilisation following treatment (Bachoud-Lévi, 2017). Despite these results, a multicentre trial is currently ongoing (Schramm *et al.*, 2015; Bachoud-Lévi, 2017).

Attention has recently turned to the potential of pluripotent stem cells for cell transplantation therapy in order to minimise the ethical and logistical issues associated with use of foetal tissue (reviewed in (Li and Rosser, 2017)). The use of pluripotent stem cells could generate large single-source banks of cells established under standardised differentiation and quality control protocols with the additional potential of generating iPSCs from the patient's own somatic cells to minimise risk of graft rejection (Liu *et al.*, 2016; Li and Rosser, 2017). A non-neuronal approach to cell-therapy seeks to transplant adipose-derived stem cells (ASCs) or mesenchymal stem cells (MSCs) to release trophic factors in order to enhance function, survival and compensatory neurogenesis of neighbouring diseased MSNs in a paracrine fashion (Lee *et al.*, 2009; Snyder *et al.*, 2010; Connor, 2018). Transplantation of MSCs overexpressing BDNF showed preclinical promise and a phase I clinical trial utilising these cells is currently in the planning stages (Deng *et al.*, 2016; Pollock *et al.*, 2016).

At present, foetal cell transplantation has demonstrated variable efficacy in HD patients although trials are still ongoing and advances in the iPSC field may improve this strategy and

reduce limitations associated with foetal tissue. Furthermore, the use of non-neuronal stem cells is a promising alternative to cell-replacement and could represent a neuroprotective disease-modifying strategy.

1.6.4.3. Treatment of HD with BDNF

As discussed in Section 1.4.3., reductions in striatal BDNF have been implicated in HD pathophysiology and its replacement represents a possible disease-modifying strategy. Direct administration of BDNF is not a plausible treatment strategy in patients. Although not attempted in HD, direct recombinant BDNF administration has been conducted via subcutaneous and intrathecal routes in ALS patients during phase I/II and phase III clinical trials (The BDNF Study Group, 1999; Ochs *et al.*, 2000). In both cases, BDNF administration induced significant side-effects at high doses did not have a beneficial effect in patients, most likely due to failure to reach vulnerable neurons (Deng *et al.*, 2016). A considerable amount of preclinical work has shown promise in elevating BDNF through other routes in animal models of HD (including through MSC transplantation mentioned above) and several efforts have been made to increase levels in patients. A summary of these efforts and their outcomes will be discussed here.

1.6.4.3.1. Genetic BDNF Modulation and Artificial Ligands

Genetic modulation of BDNF expression has been explored in several HD mouse models. Knockdown of BDNF expression results in advanced onset and greater severity of cognitive and motor deficits in the R6/1 mouse (Canals *et al.*, 2004; Giralt *et al.*, 2009) with administration of exogenous BDNF improving neuronal dysfunction (Canals *et al.*, 2004). Furthermore, overexpression of BDNF is able to ameliorate motor dysfunction and HD pathology in R6/1 and YAC128 mice (Gharami *et al.*, 2008; Xie, Hayden and Xu, 2010; Giralt *et al.*, 2011). However, the polar nature and short half-life of BDNF presents difficulties associated with administration and bioavailability (Zuccato and Cattaneo, 2007). As a result, preclinical focus has turned to a variety of pharmacological interventions which have been demonstrated to increase BDNF expression and result in a reduction in HD-related pathology and behavioural deficits in a variety of mouse models. In addition, at the BDNF receptor level, a specific small molecule TrkB ligand was shown to increase striatal TrkB activation and associated signalling in R6/2 and BACHD mice with resulting improvements in motor deficits and reductions in pathology (Simmons *et al.*, 2013). Interestingly, a small molecule $p75^{NTR}$ receptor ligand has also been shown to ameliorate HD-related pathology and behavioural deficits in the same mouse model (Simmons *et al.*, 2016). Aside from pharmacological interventions, environmental enrichment has been shown to slow disease progression in R6/1 mice and increase BDNF levels in the

striatum and hippocampus of R6/1 mice relative to controls (Spires *et al.*, 2004), suggesting a neuroprotective effect.

1.6.4.3.2. Pharmacological Modulation of BDNF by Antidepressants

The antidepressants sertraline and amitryptaline have been shown to increase BDNF expression and exhibit therapeutic efficacy in HD models (Table 1.12) (Peng *et al.*, 2008; Cong *et al.*, 2015). Additionally, paroxetine administration mediates improvements in motor dysfunction and reduction in neuropathology in the HD-N171-82Q mouse, although the effect on BDNF was not quantified (Duan *et al.*, 2004). The beneficial effects of antidepressants in depressed patients is thought, in part, to be due to increased expression of BDNF and subsequent synaptic plasticity (Castrén and Antila, 2017). In support of this, chronic administration of several different antidepressants was shown to cause an elevation in BDNF mRNA (Nibuya, Morinobu and Duman, 1995), and BDNF-induced plasticity-associated genes in the rat hippocampus (Sairanen *et al.*, 2007). Furthermore, chronic antidepressant usage has also been reported to increase BDNF expression in the hippocampi of depressed patients (Chen *et al.*, 2001). However, several antidepressants have been trialled in HD patients, with disappointing results. Bupropion had no effect on apathy or secondary outcomes (Gelderblom *et al.*, 2017); citalopram had no effect on executive function but did elevate mood in the absence of clinical depression (Beglinger *et al.*, 2014); and fluoxetine had no effect on total functional capacity, neurological, or cognitive ratings (Como *et al.*, 1997). In addition, the mood stabiliser lithium carbonate was unsuccessful in alleviating symptoms in HD patients (Leonard *et al.*, 1975; Vestergaard, Baastrup and Petersson, 1977) (Leonard et al., 1975) despite evidence that chronic administration of this drug can elevate BDNF levels in the rat brain (Fukumoto *et al.*, 2001) and alleviate behavioural symptoms in HD mice (Chiu *et al.*, 2011).

As can be observed from both the preclinical and clinical data, a range of antidepressants have been investigated, complicating the picture of the efficacy for antidepressants in HD. In fact, a recent meta-analysis of 6 papers investigating BDNF levels in depressed patients following antidepressant treatment reported that not all antidepressants result in an increase in BDNF levels, suggesting that more focussed research should be conducted to identify the most promising drug candidates (Arumugam *et al.*, 2017). One potential reason for the discrepancy between preclinical and clinical data could be that the ability of antidepressants to increase BDNF in the clinical setting has predominantly been validated in the hippocampus, rather than in the striatum which is the main site of dysfunction in HD. Another potential reason for the discrepancy could be due to the stage at which antidepressants were administered. Sertraline was administered to R6/2 mice at 6 weeks of age (Peng *et al*., 2008) while amitriptyline and paroxetine were administered to N171-82Q mice at 8 week of age (Cong *et al*., 2015; Duan *et*

al., 2004). In these cases, treatment was begun at an intermediate or early stage in the progression of the disease, whereas clinical studies were conducted in symptomatic patients following diagnosis. In this way, antidepressants may be exerting a neuroprotective effect in animal models in the earlier stages of disease, while HD patients have already progressed beyond the point where antidepressants would be effective. Given that around one in five prodromal HD patients take antidepressants (Rowe *et al.*, 2012), the influence of these drugs on disease progression has the potential to be investigated in large numbers of patients. However at present the use of antidepressants as a disease-modifying treatment remains to be validated.

1.6.4.3.3. Additional BDNF Modulating Drugs

The phosphodiesterase inhibitors rolipram and TP-10 have been shown to increase BDNF expression and exert an improvement in motor function and reduction in HD-associated pathology in R6/2 mice (DeMarch *et al.*, 2008; Giampà *et al.*, 2010) (Table 1.12). In addition, the mixed lineage kinase (MLK) inhibitor CEP-1347 and the ampakine CX929 have also conferred behavioural improvement through elevated BDNF expression in HD mouse models (Apostol *et al.*, 2008; Simmons *et al.*, 2009, 2011) (Table 1.12). Cysteamine, a licenced aminothiol, has been shown increase BDNF expression and ameliorate pathology and cognitive function in R6/1 mice (Borrell-Pagès *et al.*, 2006) (Table 1.12). However, randomised, double-blind, placebo controlled clinical trial found no benefit of cysteamine relative to placebo in HD patients (Verny *et al.*, 2017).

Fingolimod is an approved immunomodulatory drug used for relapsing-remitting multiple sclerosis (Calabresi *et al.*, 2014). The drug acts as a sphingosine-1 phosphate (S1P) receptor modulator and has been shown to increase BDNF in the mouse striatum through activation of ERK signalling (Deogracias *et al.*, 2012). When administered to R6/2 and R6/1 mice, fingolimod was shown to reduce motor and cognitive deficits as well as improve synaptic plasticity (Di Pardo *et al.*, 2014; Miguez *et al.*, 2015) (Table 1.12). In addition, sphingosine-1 phosphate metabolism has shown to be dysregulated in post-mortem tissue of HD patients (Di Pardo *et al.*, 2017), suggesting that although fingolimod is being evaluated for use in other diseases such as ALS it could represent an attractive candidate for use in HD. Pridopidine, an immunomodulator, has been shown to increase striatal BDNF levels in R6/2 mice and confer neuroprotection and improved motor function (Squitieri *et al.*, 2015) (Table 1.12). However, a recent multicentre phase II, randomised, placebo-controlled clinical trial showed no improvement in motor score in HD patients receiving the drug at doses higher than those used in previous trials with negative outcomes (Reilmann *et al.*, 2019). Another immunomodulatory, laquinimod, has been reported to increase striatal BDNF as well as improve motor function and

MSN survival (but not animal lifespan) in R6/2 mice (Ellrichmann *et al.*, 2017) (Table 1.12). However, in a large phase II placebo-controlled trial, laquinimod failed to improve motor score but did however result in reduced volume loss in the caudate (Reilmann *et al.*, 2018) suggesting that it could represent a potential neuroprotective strategy in HD.

Drug	Action	Mouse Model	BDNF Expression	Pathology	Behaviour	Reference
Sertraline	SSRI	R6/2	Increased	Reduced	Improved motor	Peng et al., 2008
Amitriptyline	Tricyclic antidepressant	N171-82Q	Increased	Reduced	Improved motor	Cong et al., 2015
Rolipram	Phosphodiesterase type IV inhibitor	R6/2	Increased	Reduced	Improved motor	DeMarch et al., 2008
TP-10	Phosphodiesterase PDE10A inhibitor	R6/2	Increased	Reduced	Improved motor	Giampa et al.,2010
CEP-1347	Mixed lineage kinases (MLKs) inhibitor	R6/2	Increased	NA	Improved motor	Apostol et al., 2008
CX929	Ampakine	CAG140	Increased	NA	Improved cognition	Simmons et al., 2009
		R6/2	Increased	Reduced	Improved motor	Simmons et al., 2011
Cysteamine	Aminothiol	R6/1	Increased	Reduced	NA	Borrell-Pages et al., 2006
Fingolimod	Sphingosine-1-phosphate receptor modulator	R6/2	Increased	Reduced	Improved motor	Di Pardo et al., 2014
		R6/1	Increased	Reduced	Improved cognition	Miguez et al., 2015
Pridopidine	Immunomodulator	R6/2	Increased	Reduced	Improved motor	Squitieri et al., 2015
Laquinimod	Immunomodulator	R6/2	Increased	Reduced	Improved motor	Ellrichmann et al., 2017

Table 1.12. BDNF modulating drugs in mouse models of HD. *A variety of drugs modulate BDNF through various mechanisms and have been shown to ameliorate the pathological and behavioural burdens of the HD.*

1.6.4.3.4. Conclusions

Taken together, it appears that the preclinical promise of BDNF-modulating therapeutics has not yet translated into the clinical setting. Direct administration of BDNF is not a plausible solution and drugs which increase levels of BDNF have been unsuccessful at clinical trial. This suggests that either elevating BDNF does not confer therapeutic benefit in HD patients or that the drugs are not potent enough to mediate a therapeutic effect. However, the reductions in striatal BDNF in HD mice and the improvement in these animals following genetic and pharmacological increases in BDNF implicate this pathway in HD pathophysiology and suggest it represents a prime candidate for therapeutics.

These results suggest that strategies outside of increasing BDNF directly should be considered. This is particularly important given the reported imbalance in striatal TrkB/$p75^{NTR}$ as HD progresses and reduced activation and/or signalling through the TrkB receptor (Song *et al.*, 2010; Brito *et al.*, 2013; Plotkin *et al.*, 2014), as discussed in Section 1.4.3., because increasing BDNF may favour signalling through the $p75^{NTR}$ receptor which could lead to cell-death and worsening of the condition. Development of specific TrkB ligands (Simmons *et al*., 2013) could prevent off-target signalling through $p75^{NTR}$ but reduced BDNF-mediated TrkB phosphorylation

may limit any benefit of this approach (Plotkin *et al.*, 2014). Although a $p75^{NTR}$ receptor ligand improved the phenotype of HD mice (Simmons *et al.*, 2016) the highly context-dependent function of the $p75^{NTR}$ receptor and its role in cell death may preclude clinical development of this approach. A potential refinement toward modulating BDNF signalling could be to bypass receptors and instead directly influence the downstream signalling pathways. By increasing signalling specifically downstream of TrkB, off-target $p75^{NTR}$ receptor signalling could be avoided and this approach could also overcome issues associated with impaired TrkB phosphorylation. The Ras-ERK signalling pathway represents a promising candidate for such an approach its function in neurons and specific role in HD will be discussed in Chapter 4.

1.6.5. Gene Therapy

1.6.5.1. General Information

With the continued development and refinement of molecular biology, gene therapy approaches for treating, or even curing, diseases have become promising alternatives to conventional medicine. The aim of gene therapy is to introduce nucleic acid sequences into diseased cells which, when expressed, will be beneficial to the cell and ameliorate the condition (Kumar *et al.*, 2016). Although termed gene therapy, the therapeutic nucleic acid used could encode a conventional WT protein, a zinc finger, a reverse oligonucleotide, a small interfering RNA, or a peptide (Choudhury *et al.*, 2017). The choice of one of these agents can lead to production of healthy protein, repression of endogenous pathogenic gene expression, repression of pathogenic protein translation, or production of a therapeutic peptide. One of the most effective and commonly-used methodologies to deliver gene therapy is through use of viral vectors. Certain viruses, such as lentivirus (LV) and adeno-associated virus (AAV) have evolved over millions of years to infect human cells, depositing their genome within the host and utilising the molecular machinery present to continue their life-cycle (Samulski and Muzyczka, 2014; Milone and O'Doherty, 2018). Owing to their ability to introduce and express nucleic acids within host human cells, over the course of several decades scientists have endeavoured to modify LVs and AAVs to eliminate non-essential components of the viral genome and instead incorporate genes of interest. In this way, recombinant viral vectors capable of delivering engineered stretches of nucleic acids with minimal risk of virus replication have been produced and tested.

Gene therapy has clear advantages over typical medications (Choudhury *et al.*, 2017). Firstly, in cases of disease with known genetic cause, nucleic acids can be rationally designed to directly address the aetiology of the disease being targeted. Secondly, a single administration

of gene therapy is sufficient for long-term or even permanent benefit, eliminating the need for repeated dosing. Finally, when appropriate, the genetic construct can be administered directly at high concentrations within a highly localised area, overcoming design and distribution challenges associated with conventional medicines such as crossing of the blood-brain barrier, peripheral metabolism of drug molecules, and unwanted off-target drug effects.

Several key considerations must be made before utilising gene therapy in order to maximise clinical efficacy (Summarised from Naso *et al.*, 2017). Firstly, the cell or tissue to be targeted must be characterised in order to tailor the viral vector to best meet the specific requirements of that cell/tissue. Secondly, the safety profile of the nucleic acid to be used must be assessed and the titre at which the viral vector is given carefully considered. Thirdly, the choice of systemic or local delivery must be made on the basis of whether the disease is localised or widespread, if the viral vector can cross the BBB in the case of neurological disorders, if sufficient viral vector can reach the target when factoring in peripheral uptake, and whether transduction of certain cell-types could lead to side-effects. Additionally, the design of the nucleic acid construct can be designed with a tissue-specific promoter to limit expression to restricted cell-types despite off-target transduction, or to be under a constitutive promoter such as CMV which will lead to expression in all transduced cells. Furthermore, additional genetic components such as a woodchuck hepatitis virus post-transcriptional regulatory element (WPRE) can be placed downstream of a transgene to increase its expression at the post-transcriptional level (Zufferey *et al.*, 1999). As can be seen, rational viral vector design permits the generation of therapeutic agents which can be tailored to specific diseases and specific cell-types, conferring potential for disease modification in currently incurable diseases such as HD and PD. LV and AAV vectors are the most commonly utilised viral vectors and their key features and current status as therapeutic agents in the field of neurodegeneration will be discussed here.

1.6.5.2. Lentiviral Vectors (LVs)

1.6.5.2.1. General Information

Over the last 2 decades, many preclinical explorations of gene therapy have revolved around the use LVs. LVs are commonly derived from wild-type human immunodeficiency virus 1 (HIV-1). A wild-type LV (wtLV), such as HIV-1, has an encapsidated viral particle which contains a relatively large single-stranded RNA genome ~9kb in length flanked by regulatory long-terminal repeats (LTRs) (Sakuma, Barry and Ikeda, 2012). The viral genome contains nine genes including *gag* (encoding structural proteins), *pol* (encoding the enzymes necessary for reverse transcription of viral RNA to DNA and subsequent integration into the host genome), *rev* (which enables nuclear export of viral RNA out the nucleus) and *env* (encoding the envelope glycoproteins which are present on the viral particle surface) (Milone and O'Doherty, 2018). HIV-1 transduces cluster of differentiation 4-positive (CD4+) T cells in humans, leading to development of HIV and, if left untreated acquired immune deficiency syndrome (AIDS) (Deeks *et al.*, 2015).

1.6.5.2.2. Safety Considerations

A series of modifications have been made to the wtHIV-1 genome to generate three "generations" of successively safer LVs with improved safety profiles predominantly through rendering the virus replication-deficient (Milone and O'Doherty, 2018). First generation LVs were modified to remove some non-essential viral genomic elements, with the essential genes for viral particle formation, transduction and DNA integration retained (Naldini *et al.*, 1996; Ramezani and Hawley, 2002). LVs were produced as a four plasmid system consisting of three separate helper plasmids containing essential viral genes (*gag-pol, rev*, *env*) and one gene transfer plasmid which are used to transiently transfect packaging cells such as HEK293 (Milone and O'Doherty, 2018). The gene transfer plasmid contains the transgene expression cassette flanked by cis-regulatory sequences and is the only plasmid to contain a packaging signal, ensuring that only this plasmid (and therefore the transgene) encapsidated and subsequently integrated into the host genome (Merten, Hebben and Bovolenta, 2016). The use of separate plasmids reduces the risk of homologous recombination events and the likelihood of generating a replication-competent viral particle. A further functional modification created a pseudotype by replacing the viral *env* gene with a sequence to instead produce vesicular stomatitis virus (VSV-G) glycoproteins in order to expand the tropism of the viral particle beyond CD4+ T-cells through interaction with low-density lipoprotein (LDL) receptors (Akkina *et al.*, 1996). Second generation LVs were further refined through additional removal of non-essential viral sequences (Zufferey *et al.*, 1997). Third generation LVs were engineered to incorporate a constitutively active promoter within the upstream LTR which enabled deletion

of the *tat* sequence which is crucial for viral replication (Dull *et al.*, 1998). Third generation LVs were also rendered self-inactivating through disruption of endogenous promoter/enhancer function via deletions within the 3'LTR (Dull *et al.*, 1998; Zufferey *et al.*, 1998).

1.6.5.2.3. Cell Entry and Integration

One of the main attractions of using LVs is their capacity to integrate genes into the host genome which enables potentially permanent expression of the transgene even in dividing cells (Sakuma, Barry and Ikeda, 2012). LVs achieve this through the following mechanism. The viral glycoproteins interact with host receptors, enabling entry into host cells through membrane fusion of endocytosis (Milone and O'Doherty, 2018). Next, LVs undergo uncoating which releases viral proteins and the RNA genome (collectively known as the reverse transcription complex (RTC)) into the cytoplasm (Bukrinsky *et al.*, 1993; Hulme, Perez and Hope, 2011). Viral RNA is then reverse transcribed by the viral reverse transcriptase enzyme to produce double-stranded proviral DNA which enters the cell nucleus complexed with viral proteins (collectively known as the pre-integration complex (PIC)) (De Rijck *et al.*, 2007). Integration of proviral DNA is catalysed by the viral integrase enzyme as well as host enzymes with full integration completed by host-mediated DNA repair (Milone and O'Doherty, 2018). Although integration is an attractive prospect, it represents a potential safety risk as HIV-1-based LVs show preference for integration in transcriptional units which could lead to insertional mutagenesis and development of cancer (Bokhoven *et al.*, 2009; Ranzani *et al.*, 2013).

1.6.5.3. Adeno-Associated Viral Vectors

1.6.5.3.1. General Information

First characterised in the 1960s, wild-type adeno-associated viruses (wtAAVs) are small (25nm) members of the Parvoviridae family which commonly infect humans (Atchison, Casto and Hammon, 1965; Srivastava, Lusby and Berns, 1983). Although infectious, wtAAVs are not thought to cause disease and require an adenovirus or herpes simplex virus 1 (HSV-1) helper-virus to replicate (Samulski and Muzyczka, 2014). wtAAVs are encapsidated but non-enveloped and contain a ~4.7kb linear, single-stranded DNA genome flanked by 145bp palindromic inverted terminal repeats (ITRs) which are essential for genome replication and packaging (Srivastava, Lusby and Berns, 1983; Naso *et al.*, 2017). The genome contains three genes which, through three promoters and alternative splicing and translational start sites, give rise to at least 9 gene products (Naso *et al.*, 2017). The *rep* (replication) gene is required for viral genome replication and packaging, the *cap* (capsid) gene is required for production of viral capsid proteins, and the *aap* (assembly) gene is required for production of assembly-activating protein

(AAP) which is a nuclear protein thought to participate in capsid assembly through scaffolding function (Naso *et al.*, 2017). Recombinant adeno-associated viral vectors (AAVs) are produced by genetically engineering wtAAVs to remove the viral genes and instead replace them with an expression cassette (typically a promoter followed by the gene of interest and subsequent terminator) flanked by the viral ITRs (Drouin and Agbandje-McKenna, 2013). This process renders the AAV replication-deficient but still able to enter the host cell and deliver the engineered DNA.

1.6.5.3.2. AAV Serotypes

One of the major attractions of using AAVs for gene therapy lies in the variety of serotypes, determined by differences in the capsid, which, in turn determine the tropism (the preference for a particular serotype to transduce a given cell-type) of the AAV (Srivastava, 2016). The viral *cap* gene encodes three capsid proteins VP1 (87kDa), VP2 (73kDa), and VP3 (62kDa) through alternative splicing and an alternative start codon. 60 viral capsid proteins interact in a VP1:VP2:VP3 ratio of 1:1:10 to form the icosahedral capsid shell which protects the DNA genome (Samulski and Muzyczka, 2014). The capsid proteins interact with primary proteoglycan carbohydrates (namely sialic acid, galactose, and heparin sulfate) as well as secondary receptors on the target cell-surface (Srivastava, 2016). Variation in the sequence of the *cap* gene alters the preference of the encoded capsid proteins for host cell carbohydrates, meaning that different serotypes of AAV interact with different cell-types (which vary in terms of carbohydrate and secondary receptor properties) to differing degrees (Srivastava, 2016). Through selection of a particular serotype, the therapeutic potential of AAV-mediated gene therapy can be maximised by selecting an AAV serotype which efficiently transduces the cells most affected in the disorder in question (Naso *et al.*, 2017). AAV2 is the best-studied serotype and is commonly-used for research purposes as it displays a broad tropism (Srivastava, 2016). In addition, many AAVs are produced as pseudotypes with AAV2 ITRs but coding sequence for a capsid of another serotype (Srivastava, 2016).

1.6.5.3.3. AAV Cell Entry and Expression

Following interaction with cell-surface receptors, the AAV is internalised via clathrin-mediated endocytosis and is subsequently trafficked within the endosomal pathway before escape from the endosome and nuclear entry (Uhrig *et al.*, 2012). Within the nucleus, the viral particle is uncoated and second strand synthesis occurs to convert the ssDNA genome to dsDNA (Nash, Chen and Muzyczka, 2008). Importantly, unlike LVs, the AAV dsDNA ITR-flanked transgene is not integrated into the host genome, but exists as an episome within the nucleus where it is able to undergo sustained, long-term transcription (Samulski and Muzyczka, 2014). Episomes are at risk of gradual elimination in dividing cell populations but have been demonstrated to

undergo stable, long-term expression in skeletal muscle and non-dividing cells such as neurons (Kaplitt *et al.*, 1994; Kessler *et al.*, 1996). Although episomal, it must be noted that there are rare reports of AAV-mediated integration events which could potentially be mutagenic (Russell, 2007; Chandler, Sands and Venditti, 2017) Although the risk of insertional mutagenesis is extremely low, administration of AAV is still immunogenic, albeit to a lesser degree than other viruses (Mingozzi and Buning, 2015; Mingozzi and High, 2017). Both the capsid and DNA elicit an immune response, a process which is of particular note in the case of AAVs as a large proportion of the population have been exposed to wtAAV and will therefore have an adaptive immune response to therapeutic AAV administration (Boutin *et al.*, 2010). In the case of clinical trials, patients are often pre-screened to determine whether they have been pre-exposed and are more resistant to the AAV serotype which is to be administered as the clinical efficacy of such a treatment could be attenuated by the patient's immune reaction (Mingozzi and High, 2017). Although a compromise is possible by using a serotype to which the patient has not been pre-exposed, this substitution may not be possible due cost implications of manufacturing AAVs of multiple serotypes as well as due to considerations regarding optimal tropism for the disease in question. In addition, an immune response against the transgene product could be experienced as the protein could be recognised as foreign if patients lack the endogenous protein or the protein has been engineered to deviate from the endogenous form (Naso *et al.*, 2017).

1.6.5.3.4. AAV Design and Production

AAVs are most commonly produced through triple transient transfection of a packaging cell line (often HEK293) with separate plasmids containing the cassette of interest, the AAV *rep*/*cap* genes, and necessary helper genes (Samulski and Muzyczka, 2014). Viral particles containing the gene of interest are then produced within these cells and they are extracted and purified before quality control and titration. By transfecting selected *cap* genes to determine AAV serotype, AAVs can be produced with the optimal tropism for a target cell-type (Srivastava, 2016). In addition to natural serotypes, novel AAV serotype variants have been produced through *in vivo*-directed evolution to further specify tropism for certain tissues (Yang, Li and Xiao, 2011; Büning *et al.*, 2015). Similar to LVs, cell-specific promoters such as human synapsin-1 (hSYN1) and regulatory elements like WPRE can be introduced to limit gene expression to neurons or increase transgene expression. However, there are drawbacks to use of AAVs. A key limitation of AAV production is that the product yield is restricted to a ceiling of 10^5 genome copies (GC)/cell which is equivalent to 10^{14} GC/L (Naso *et al.*, 2017). Although additional manufacturing platforms have been created by transforming mammalian or insect cell-lines with key components for AAV production such as helper genes or the *rep* gene, as opposed to

transient transfection, these platforms do not increase the yield above the conventional method (Naso *et al.*, 2017). These production limits mean that AAVs should be generated to be as potent as possible in order to maximise their use when required at large volumes.

1.6.5.3.5. Monocistronic AAVs

The major limitation of AAV use is the cassette packaging limit of ~4.7kb (including ITR sequences). Attempts to manufacture an AAV carrying a packaging cassette above 5kb results in a significant reduction in yield or truncations, limiting their use as therapeutic agents in diseases requiring large stretches of DNA or multiple genes (Wu, Yang and Colosi, 2010). One obvious strategy to overcome this issue is through use of multiple monocistronic AAVs (carrying a single transgene < 4.7kb) to separately transduce cells, resulting in expression of multiple transgenes without exceeding packaging limitations. While this strategy may be effective, it has several drawbacks. Firstly, production of GMP-quality viral vectors is an expensive process (Naso *et al.*, 2017). Therefore, the cost of manufacturing several viral vectors would be considerably more expensive than manufacturing one. Secondly, transducing cells with multiple separate AAVs typically means that cells require co-expression of each separate transgene to elicit therapeutic benefit. Using multiple separate viral vectors, it is not possible to ensure that cells are transduced by each viral vector administered, meaning that therapeutic benefit may not be conferred in cases where cells do not express all transgenes. Finally, host immunogenic response to AAVs has been shown to correlate with capsid number (Colella, Ronzitti and Mingozzi, 2018). When gene therapy is administered using separate monocistronic AAVs at high titres, the host immune system encounters a high number of viral particles and therefore capsids. Thus, the immune response to multiple separate AAVs will potentially be much higher than that of a single multicistronic AAV despite potential delivery of transgenes at equimolar amounts. In fact, from an experimental standpoint, it would be advisable to use an elevated titre of multiple monocistronic AAVs to increase the probability of transgene co-expression.

1.6.5.3.6. Multicistronic AAVs

Multicistronic AAVs carry multiple transgenes within the same viral particle. In addition to reduced immunogenicity, multicistronic AAVs would reduce cost by requiring production of a single viral vector and ensure co-expression of transgenes within transduced cells. However, design of multicistronic AAVs must be carefully considered before use. Expression of multiple transgenes can theoretically be achieved from a monocistronic viral vector by placing each transgene under a separate promoter to generate multiple transcriptional units within a single expression cassette. However, the use of multiple tandem promoters can lead to interference between transcriptional units which can suppress expression of transcriptional units and lead

to an unpredictable suppression of transgene expression (Allera-Moreau *et al.*, 2006; Curtin *et al.*, 2008). This can occur through multiple mechanisms of promoter interference including impediment of transcriptional machinery between promoters and epigenetic silencing of one promoter through expression of the other (Shearwin, Callen and Egan, 2005). As such, promoter interference could potentially prevent sufficient expression of one of the transcriptional units below the threshold required for therapeutic benefit. Promoter interference is particularly important to consider in cases where co-expression of both transcriptional units is essential. Another consideration regarding use of multiple promoters relates to the packaging constraints of AAVs. The commonly used CMV promoter is relatively large at 800bp (Gray *et al.*, 2011). A bicistronic viral vector utilising two CMV promoters would therefore have 1.6kb of the 4.7kb packaging capacity occupied before inclusion of the gene of interest and any regulatory elements. It would therefore be preferable to be able to stoichiometrically express multiple transcriptional units under a single promoter to prevent promoter interference and retain sufficient packaging capacity. This aim can be achieved using linkers.

1.6.5.3.6.1. Internal Ribosome Entry Site (IRES) Linkers

IRES sequences are naturally occurring and are found in the 5' untranslated regions (5'UTR) of certain picornavirus mRNAs (Renaud-Gabardos *et al*., 2015). IRES sequences are endogenously translational enhancers, permitting cap-independent internal initiation of translation (Renaud-Gabardos *et al*., 2015). This feature permits production of bicistronic AAVs whereby 2 transgenes are placed under the control of a single promoter but separated by an IRES sequence. In this way, transcription of the expression cassette will generate a single transcript but presence of the IRES will allow translation of both transgenes to produce separate proteins. This is achieved as the first transgene can be translated by the canonical cap-dependent mechanism through 5' UTR recognition, while the second transgene can be translated through the 40S ribosomal subunit binding to the IRES sequence prior to the start of the transcript (Komar and Hatzoglou, 2011). Therefore, IRES sequences permit translation of multiple proteins from a single transcriptional unit under the control of a single promoter. Importantly, multicistronic vectors containing IRES sequences have been reported to result in better long-term gene expression than multiple monocistronic vectors in mouse skeletal muscle ((Allera-Moreau *et al.*, 2007). In addition, use of multicistronic-IRES-containing vectors have been shown to be better than multicistronic vectors with tandem promoters, with the IRES alleviating the promoter interference/silencing and failure to co-express both transgenes sometimes observed with multiple transcriptional units (Allera-Moreau *et al*., 2006). However, cap-independent IRES-mediated expression of the second transgene has been reported to be

significantly lower than that of the upstream transcript (Mizuguchi *et al.*, 2000) potentially limiting efficacy in cases that require equivalent co-expression.

1.6.5.3.6.2. Foot and Mouth Disease Virus (FMDV) 2A Linkers

2A linkers are also useful tools for protein co-expression from multicistronic vectors. 2A linkers are "self-cleaving" and result in translation of multiple proteins from a single transcript by inducing ribosome skipping at the C-terminal (Liu *et al.*, 2017) In this way, if successful, the same ribosome can translate each transcript in a continuous fashion, with the 2A sequence between each transcript promoting production of independent "cleaved" proteins. 2A linkers present several benefits when compared with IRES linkers. Firstly, 2A linkers are ~20 amino acids in length while IRESs are considerably larger (Furler *et al.*, 2001). Given the ~4.7 kB packaging capacity of AAVs, the 2A sequence represents a more attractive insert. In addition, IRES sequences display cell-type specific efficiencies in translation while 2A-mediated translation is comparable across cell-types due to ribosomal conservation (Minskaia and Ryan, 2013). Furthermore, due to consistency in translation mechanism between reading frames, both proteins from a bicistronic vector will be produced at equimolar amounts, with demonstrated higher second gene expression from 2A-vectors than IRES-vectors demonstrated (Furler *et al*., 2001).

1.6.5.4. Gene Therapies in Neurodegeneration

1.6.5.4.1. General Information

Several gene therapies are already on the market, predominantly for treatment of cancers and retinal disorders (Shahryari *et al.*, 2019). Luxturna™ - an AAV2-based therapy for treatment of choroideremia – has recently been approved after displaying remarkable efficacy in clinical trials (Russell *et al.*, 2017). Due to the paucity of drugs and the attractive therapeutic platform offered by modern viral vectors, attention is now increasingly turning toward the use of gene therapy for treatment of neurodegeneration (Sudhakar and Richardson, 2019).

1.6.5.4.2. Gene Therapy for PD

1.6.5.4.2.1. Neuroprotection

The two main gene therapy approaches for PD which have been brought to clinical trial are aimed at either preserving vulnerable neurons or replacing intrastriatal dopamine (Sudhakar and Richardson, 2019). The first strategy may represent a disease-modifying approach to treating PD, slowing degeneration of nigrostriatal cells and therefore slowing progression of disease. This approach is predominantly mediated through administration of viral vectors which express transgenic glial cell line-derived neurotrophic factor (GDNF) or its gene homolog neuritin within the putamen or substantia nigra. Although met with preclinical success (Choi-Lundberg *et al.*, 1998), this approach has translated poorly to double-label randomised control clinical trials, demonstrating no clinical efficacy when compared to sham (Lang *et al.*, 2006).

1.6.5.4.2.2. Dopamine Replacement

The second strategy aims to use viral vectors to ectopically express transgenic TH, GCH1, and AADC enzymes of the dopamine biosynthesis pathway (See Section 1.6.3.1.) within striatal cells in order to increase the amount of intrastriatal dopamine despite ongoing of nigrostriatal neuron degeneration (Björklund, Cederfjäll and Kirik, 2010; Sudhakar and Richardson, 2019). Several independent groups have attempted this intervention, utilising different viral vectors expressing single or combined dopamine biosynthesis enzymes in order to do so.

1.6.5.4.2.2.1. Single Enzyme Approach

The single enzyme approach is mediated through ectopic expression of AADC, the enzyme responsible for converting L-DOPA to dopamine, within cells of the striatum. AADC is normally localised to serotonergic and dopaminergic terminals within the striatum and is responsible for the conversion of orally-administered L-DOPA in this brain region (Arai *et al.*, 1994; Björklund, Cederfjäll and Kirik, 2010), with the majority of AADC localised to serotonergic terminals in the rat striatum (Arai *et al.*, 1994). However, over the course of the disease, progressive nigral degeneration results in fewer nigrostriatal terminals (and thus less AADC) within the striatum

which, in turn, leads to a reduced capacity to catalyse the production of dopamine and a reduced benefit of oral L-DOPA (Nagatsu and Sawada, 2007; Christine *et al.*, 2009). The aim of inducing striatal AADC expression is to produce a sustained enhancement in the efficiency of oral L-DOPA conversion within the striatum, producing sufficient dopamine for symptomatic relief despite disease progression.

Three independent clinical trials using an AAV2 to transduce either striatal or putaminal-only cells with AADC have been conducted (Table 1.13). The outcomes of these trials showed this approach was safe and well-tolerated with an improvement in UPDRS III motor score and an increase in uptake of AADC tracer as assessed by PET scan (Christine *et al.*, 2009, 2019; Muramatsu *et al.*, 2010). These results suggest that AADC is active and effective in enhancing striatal dopamine production from oral L-DOPA. An optimisation of this approach was recently published as part of a phase I trial using MRI-guided infusion of AAV2-AADC to track putaminal spread of the infusate during surgery (Christine *et al*., 2019). Patients were administered with one of three ascending doses with the outcomes reporting dose-dependent improvement in anatomical spread, motor score, and PET activity. Although results of AADC gene therapy are promising thus far, like any phase I clinical trial, they are small studies without control groups and the outcomes should therefore be interpreted with caution. Two of the phase I clinical trials described are progressing to phase I/II (Table 1.13) which will give more information on the efficacy of this approach. From these initial results it appears that AADC therapy can increase efficiency of striatal conversion of oral L-DOPA to dopamine, resulting in functional improvement as assessed by motor score. Treated patients could conceivably receive a lower dose of oral L-DOPA in light of the action of AADC. However, AADC therapy is only effective in combination with exogenously-administered L-DOPA and as such patients will remain dependent on administration of oral L-DOPA, retaining the associated risks of dyskinesia and off-target effects (See Section 1.6.3.1.).

Vector	Injection Site	Phase	Safety	UPDRS III	PET	Reference
AAV2-CMV-hAADC-2	Caudate and Putamen	I	Safe	Improved (6 months)	Increased activity (6 months)	Christine et al., 2009 Eberling et al., 2008
AAV2-CMV-hAADC-2	Putamen	I (I/II ongoing)	Safe	Improved (6 months)	Increased activity (6 months)	Muramatsu et al., 2010
AAV2-CMV-hAADC	Putamen	I (I/II ongoing)	Safe	Improved (12 months)	Increased activity (6 months)	Christine et al., 2019

Table 1.13. Clinical trials for AADC expression. *Clinical trials have displayed a good safety profile and suggestions of clinical benefit at their early stages.*

1.6.5.4.2.2.2. Multiple Enzyme Approach

The multiple enzyme approach aims to either ectopically express TH, GCH1, and AADC within in striatal cells in order to produce a continuous, localised supply of dopamine (triple combination therapy) or to ectopically express TH and GCH1 to produce a continuous, localised supply of L-DOPA with subsequent conversion of L-DOPA to dopamine by endogenous AADC (double combination therapy) (Björklund, Cederfjäll and Kirik, 2010; Sudhakar and Richardson, 2019). The advantages to such an approach are that the need for oral L-DOPA could be drastically reduced or even eliminated, continuous dopamine production could lead to a reduction in motor fluctuations and dyskinesia associated with pulsatile oral L-DOPA-mediated dopamine signalling, and production of dopamine would be restricted to the striatum, thereby reducing the risk of off-target effects (Björklund, Cederfjäll and Kirik, 2010; Cederfjäll *et al.*, 2012).

Previous work has demonstrated that triple transduction of rat 6-OHDA-denervated striatum with three separate monocistronic AAVs expressing TH, GCH1, and AADC elevated dopamine production and led to long-term functional recovery (Shen *et al.*, 2000) while an extension of this approach in MPTP-lesioned NHPs had similar successful outcomes (Muramatsu *et al.*, 2002). Although effective, production of three separate monocistric viral vectors is expensive (particularly at GMP-grade) and successful dopamine production is dependent on co-expression of the three enzymes within the same cells – something which cannot be guaranteed with separate viral vectors amongst other reason stated in Section 1.6.6.3.5.).

A clinical exploration of triple combination therapy using a lentiviral tricistronic equine infectious anaemia virus (EIAV) known as ProSavin was brought to phase 1/2 open-label clinical trial (Palfi *et al.*, 2014). At the preclinical stage, ProSavin-induced elevation in dopamine production and associated functional recovery was reported in 6-OHDA-lesioned rats and MPTP-lesioned NHPs (Jarraya *et al.*, 2009). During the ProSavin trial, which is still ongoing, 15 patients received one of three ProSavin doses: a low dose of $1.9x10^7$ transducing units (TU/ml, a medium dose of $4.0x10^7$ TU/ml, and a high dose of $1x10^8$ TU/ml. Importantly, a significant improvement in motor function (UPDRS part III) from baseline was recorded in all patients at 6 months post-LV and no adverse effects of treatment were recorded. Although promising, the motor improvements recorded fall into the placebo range for surgical interventions and no difference in efficacy was reported between doses despite a more than 5-fold difference between the lowest and highest doses. These modest effects have been reported to be sustained for up to eight years of follow-up despite continued progression of PD, lending support to ProSavin-mediated functional improvement (Palfi *et al.*, 2018). Thus, although

ProSavin may be efficacious, and certainly displays tolerability, disappointingly the magnitude of therapeutic benefit does not approach that seen in rodent and non-human primate studies.

Given the success of this approach in animal models, and taking into consideration that ProSavin should express each rate-limiting enzyme required for dopamine synthesis, the lack of robust improvement in patient outcomes suggests that the methodology was flawed, rather than the logic of the approach itself. Delivery of an insufficient titre of ProSavin or insufficient spread of ProSavin within the brain could have led to inadequate transduction of cells and inadequate production of dopamine as a consequence. A second non-mutually exclusive reason for the disappointing results reported could be that one or more of the transgenes delivered were expressed at insufficient amounts to produce dopamine at the necessary levels for robust functional recovery. In recognition of the need to increase levels of LV-mediated dopamine replacement, the ProSavin expression cassette has recently been optimised by altering transgene order and inserting a GS15 flexible linker between TH and GCH1 (Stewart *et al.*, 2016). The optimised LV has been demonstrated to produce a significantly higher yield of dopamine than ProSavin following putaminal administration in MPTP-lesioned NHPs (Badin *et al.*, 2019) and plans are in place to progress the optimised viral vector to clinical trial. Co-expression of TH and GCH1 in the absence of AADC has also been trialled and will form the basis of Chapter 3.

1.6.5.4.3. Gene Therapy for HD

1.6.5.4.3.1. BDNF Gene Therapy

Intraparenchymal infusion of viral vectors to produce a striatally-localised, continuous supply of BDNF could eliminate the issues associated with administration, short half-life and side-effects described in Section 1.6.4.3. Although not tested in HD patients, viral vector-mediated expression of BDNF has been shown to be protective in R6/2 mice (Arregui *et al.*, 2011) and quinolinic acid-lesioned rats (Bemelmans *et al.*, 1999; Kells, Henry and Connor, 2008). However, sustained increases in BDNF concentration are associated with downregulation of TrkB receptors (Osborne *et al.*, 2018), potentially precluding gene therapy approaches continuously increasing BDNF directly. In addition, intraparenchymal viral vector approaches result in highly-localised expression of the transgene, preventing potential widespread benefit.

1.6.5.4.3.2. HTT Lowering Strategies

Gene therapy for HD remains relatively undeveloped with no licenced treatments currently available (Sudhakar and Richardson, 2019). However, Given that HD is a monogenic condition, the mutant allele, RNA and protein are easily identifiable and targetable, paving the way for implementation of HTT-lowering strategies (Wild and Tabrizi, 2017). Recent advances in molecular biology now offer the opportunity of targeting the root cause of HD, either through direct manipulation of the mutant allele, or by targeting the mRNA transcript to reduce production of mHTT protein. In this way, the extent of dysregulation of each downstream pathway affected by mHTT could, in principle, be ameliorated through administration of a single therapeutic agent with a single target, overcoming the main issue of designing and developing drugs for HD. Furthermore, genetic testing and/or development of HD biomarkers could ensure that HTT-lowering therapies are begun as early as possible in the presymptomatic stages of HD in order to maximise therapeutic benefit and to delay disease onset as far as possible (Caron, Dorsey and Hayden, 2018).

At the DNA level, the mutant *HTT* allele can be targeted using zinc-finger nucleases to repress transcription and prevent mHTT production or alternatively by using transcription activator-like effector nucleases (TALENs) or CRISPR/Cas9 to edit the gene (Tabrizi, Ghosh and Leavitt, 2019). At the mRNA level, the mutant transcript can be targeted using RNA interference (RNAi) approaches or antisense oligonucleotides (ASOs) (Tabrizi, Ghosh and Leavitt, 2019). Both RNAi and ASOs are engineered to recognise motifs within the target mRNA, allowing them to bind and cleave it through nuclease activity, resulting in mRNA degradation and prevention of translation (Watts and Corey, 2012). Both DNA- and RNA-targeting strategies have been met with success in preclinical studies and two ASOs have been brought to clinical trial for HD (Mestre, 2019). Although more of a genetic therapy, rather than conventional gene therapy, an ASO known as IONIS-HTT_{RX} has received a great deal of recent attention. IONIS-HTT_{RX} has been demonstrated to be safe and well-tolerated in a randomised, double-blind, multiple-ascending-dose phase 1-2a clinical trial, with a dose-dependent reduction in cerebrospinal fluid (CSF) mHTT concentrations following repeated intrathecal administration in adults with early-stage HD (Tabrizi *et al.*, 2019). Although encouraging, the functional effects of lowering mHTT have yet to be fully evaluated and it remains to be seen whether IONIS-HTT_{RX} significantly lowers mHTT in deep brain structures like the striatum which are relatively distal from CSF. In addition, IONIS-HTT_{RX} is non-*HTT* allele-specific and possible detrimental effects associated with reductions in wtHTT must be monitored for (Skotte *et al.*, 2014)s. Twin randomised, double-blind placebo-controlled clinical trials are also underway to assess the safety and

tolerability of two mutant allele-specific ASOs known as WVE-120101 and WVE-120102 (Hersch *et al.*, 2017).

The potential benefits of ASOs for treatment of HD is emphasised by the recent licencing of Nusinersen, an ASO designed for treatment of infantile-onset spinal muscular atrophy which displayed excellent results (Finkel *et al.*, 2017), emphasising the potential for ASOs in HD. However, treatment with ASOs will require repeated intrathecal dosing over the course of the patient's life which is intrusive and will require specialist services. Gene therapy could be used to improve HTT-lowering strategies by using viral vectors to produce the therapeutic agent following a one-time treatment. UniQure are currently bringing such a therapy to the clinical setting. AMT-130 is an AAV expressing a micro RNA (miRNA) which binds to HTT RNA, silencing translation and production of mHTT protein (Potkin and Potkin, 2018).

1.6.6.5. Conclusions

Design and development of traditional therapies have generally not been met with success in the clinical setting despite preclinical promise, suggesting that the predictivity of current animal models of PD and HD is low. Development of better animal models could improve translation of such therapies and drive progress in this field. In addition, the development of gene therapies for neurodegeneration is receiving increasing attention and could lead to effective therapies for PD and HD, with several clinical trials for treatment of PD and two clinical trials using ASOs for HD ongoing. Although progress has been slow, these advancement are encouraging and represent significant progress in treating these disorders.

Chapter 2: Motor Characterisation of the Parkin$^{S65A/S65A}$ Mouse

Data generated for this thesis were independently analysed using linear interpolation and published (**McWilliams et al. (2018): Phosphorylation of Parkin at serine 65 is essential for its activation *in vivo).*** However, different conclusions were reached and my analysis found no motor phenotype on the balance beam, in contrast to the paper.

2.1. Introduction

Mutations within the *PRKN* gene are responsible for the majority of cases of early onset autosomal-recessive PD and juvenile onset sporadic PD (Kitada *et al.*, 1998b; Lücking *et al.*, 2000). The encoded Parkin protein has been reported to play a key role in mitophagy alongside its upstream kinase PINK1, which phosphorylates Parkin at Ser65 to recruit it to damaged mitochondria and activate its E3 ubiquitin ligase activity (See Section 1.3.5.2.). Understanding the role of the PINK1-Parkin pathway and its potential dysfunction in PD could elucidate disease mechanisms and generate new treatments for both familial and sporadic PD. Accordingly, a range of models with Parkin knockout or mutations have been produced in an attempt to model PD.

2.1.1. Cellular Models

The majority of work characterising the PINK1-Parkin pathway utilised cellular models in which mitochondrial membrane potential was artificially depolarised using mitochondria uncoupling agents such as Carbonyl cyanide m-chlorophenyl hydrazone (CCCP) or antimycin/oligomycin A (Narendra *et al.*, 2008; Kondapalli *et al.*, 2012; Kane *et al.*, 2014; Kazlauskaite *et al.*, 2014; Koyano *et al.*, 2014; Lazarou *et al.*, 2015). Although useful for identifying components pathway components and substrates, relating the results from these cellular models to the conditions in nigral neurons *in vivo* is not straightforward. The use of proliferative cell models does not reflect the terminally-differentiated nature of neurons, most cellular models rely on overexpressesion of PINK1 or Parkin to levels which do not accurately reflect signalling under normal physiological conditions, and mitochondrial uncoupling agents administered to induce mitophagy do not have a comparable biological correlate (McWilliams and Muqit, 2017). Thus, in order to fully understand how mutant forms of PINK1 and Parkin lead to PD, *in vivo* models must be generated and characterised.

2.1.2. *Drosophila* Models

The first *Drosophila* models with *Parkin* orthologue knockout (*park* KO) were generated around the same time as the first mouse models and helped to identify that PINK1 and Parkin share a common pathway (Clark *et al.*, 2006; Park *et al.*, 2006). Parkin null *Drosophila* are infertile and display locomotor deficits through flight muscle degeneration as well as reduced lifespan (Greene *et al.*, 2003; Pesah *et al.*, 2004; Cha *et al.*, 2005). Furthermore, non-motor symptoms including defects in learning and memory and weakened circadian rhythms have been reported (Julienne *et al.*, 2017). In addition, cells within these models have been shown to have altered number and morphology and to be more sensitive to oxidative stress (Cha *et al*., 2005; Pesah *et al*., 2004; Whitworth *et al*., 2005). Degeneration of dopaminergic neurons has been reported to be present in some models (Whitworth and Pallanck, 2017; Cackovic *et al.*, 2018) but absent in others (Greene *et al*., 2003; Pesah *et al*., 2004; Cackovic *et al*., 2018), demonstrating variability in the key PD pathological feature in *Drosophila* models. At the cellular level, Parkin has previously been described as essential for mitophagy and to have a role in promotion of respiratory chain protein turnover in *Drosophila* (Vincow *et al.*, 2013). Collectively, it appears that Parkin null *Drosophila* display a range of phenotypic traits which may be related to human PD, albeit with variable reports of dopaminergic neuron degeneration.

However, two recent papers have reported relatively conflicting results with regard to the role of Parkin in *Drosophil*a basal mitophagy. Using the same *park* knockout line crossed with mitophagy reporter lines (in which mitochondria are fluorescently tagged to visualise mitophagy), one group reported reduced initiation of mitophagy accompanied by dopaminergic neuron degeneration, advanced mitochondrial ageing, and abnormal mitochondrial morphology (Cackovic *et al.*, 2018) while another group reported no change in basal mitophagy in dopaminergic neurons as well as lack of evidence of mitophagy in flight muscle cells (Lee *et al.*, 2018). These contrasting results are hard to reconcile but could feasibly be due to methodological differences. The report of absent mitophagy in flight muscle cells suggests that the commonly-reported flight muscle degeneration in Parkin null flies is due to a mitophagy-independent role of Parkin (Green *et al*., 2003; Pesah *et al*., 2004; Cha *et al*., 2005.

Taken together, these results demonstrate a consistency in reports of a locomotor phenotype and reduced lifespan in Parkin null *Drosophila* but mixed reports of dopaminergic cell death in regions analogous to the mammalian substantia nigra pars compacta - a crucial feature of PD. Furthermore, conflicting roles for Parkin in mitophagy have been reported Cackovic *et al.*, 2018; Lee *et al.*, 2018) and the role of Parkin in flight muscle degeneration has been suggested to be mitophagy-independent (Lee *et al.*, 2018). Although useful for pathway characterisation,

the role of Parkin may be better characterised in mammalian models due to higher model validity.

2.1.3. Mouse *Parkin* Knockout Models

2.1.3.1. Germline Mutations

The first mouse models with deletions of *Parkin* exons 2, 3, or 7 were produced and phenotyped by independent labs between 2003 and 2005 in an attempt to model PD (Table 2.1). The deleted exons have been shown to be important for Parkin function and mutations and deletions within each of these regions have been shown to cause autosomal recessive juvenile-onset PD (Lücking *et al*., 2000). *Parkin* exon 3, which encodes the Ubl domain containing Ser65, was deleted by two groups (Goldberg *et al.*, 2003; Itier *et al.*, 2003), with the majority of the exon being replaced by an enhanced green fluorescent protein (EGFP) sequence in the case of the former. Both papers report a motor phenotype in the mice generated (Table 2.1). Goldberg and colleagues report deficits in balance beam performance of mutant animals between 2 and 18 months of age, but normal performance on the rotarod over the same timeframe. However, while Goldberg reports normal locomotor activity in the open field even in advanced age, Itier and colleagues show decreased exploration of a novel environment and decreased locomotor activity at 6 months in their mutant animals.

Animals with *Parkin* exon 7 (encoding a RING domain) deletion have been reported to display normal performance on the rotarod and balance beam up to 24 months of age (Von Coelln *et al.*, 2004) (Table 2.1), supporting the data obtained by Goldberg and colleagues using exon 3 deletion *Parkin* animals. Interestingly, non-motor deficits are reported in all models described so far, with impaired somatosensory abilities on the adhesive removal test (Goldberg *et al*., 2003), cognitive deficits on the T-maze (Itier *et al*., 2003), and decreased startle (von Coelln *et al*., 2004) reported. Later work on *Parkin* exon 3 deletion mice also reported deficits in procedural and short-term spatial memory, due to deficiency in hippocampal LTP, but no deficits in motor function (Rial *et al.*, 2014) (Table 2.1). Taken together, the motor phenotype of Parkin knockouts is unclear from these papers, with conflicting results, even between models with the same exon deletion. Heterogeneous results are also reported at the cellular level. Both Goldberg and Itier report increased extracellular striatal dopamine in their animals, while von Coelln reports no change. Interestingly 30% of exon 7 mutants display cell loss within the locus coeruleus, a site of degeneration in PD, from 2 months of age (von Coelln *et al*., 2004).

The most extensive characterisation of germline *Parkin* mutant mice was conducted in *Parkin* exon 2 deletion mice (Perez and Palmiter, 2005) (Table 2.1). The authors tested mice on an extensive battery of 25 tests of neurological function, motor ability, emotionality, and

cognition from 3 – 22 months. Amongst the motor tests used were rotarod, balance beam, open field, 48-hour locomotor activity, and footprint gait analysis. Significant differences between *Parkin* mutants and WT mice were reported for rotarod at 6 months of age and 48-hour locomotor activity at 3 and 12 months of age. Motor differences between genotypes were also reported for the hanging-wire-grip test and pole test, both at 6 and 18 months of age. Importantly, differences between mutant and WT animals were not reported for exploratory locomotor behaviour or on balance beam, mirroring results from Goldberg and von Coelln. Perez and Palmiter (2004) also replicated *Parkin* mutation-related changes in acoustic-startle and reported additional differences in the tail-suspension test and decreased body weight. However, preliminary studies by Perez and Palmiter were conducted on F2 generation mice on mixed genetic background (B6:129S4), as were the studies by Goldberg and Itier. When Perez and Palmiter repeated tests using *Parkin* mutants on a 129S4:129S4 coisogenic background, they failed to replicate the majority of the differences observed in chimeric mice. Crucially, the remaining significant differences relative to WT mice fell within the range of expected false positives.

Although there is considerable variability in the behavioural phenotype of these mice, one significant consistency is the lack of degeneration of dopaminergic SNc neurons observed in all the models reported here (Goldberg *et al.*, 2003; Itier *et al.*, 2003; von Coelln *et al.*, 2004; Perez and Palmiter, 2005) (Table 2.1). The variability in motor deficits, lack of SNc neurodegeneration and disappearance of phenotype when controlling for genetic background (Perez and Palmiter, 2005) raise the question of whether the parkinsonian phenotypes reported may be due to genetic effects due to mixed background rather than due to Parkin knockout (See Section 1.5.2.) These issues relating to phenotypic variability and lack of neurodegeneration (and phenotype in coisogenic animals) call into question the suitability of germline *Parkin* exon deletions for modelling PD.

Reference	Animal (Background)	Parkin Exon Manipulation	Dopamine Changes	Nigral Degeneration	Motor Deficits	Non-Motor Deficits	Mitochondrial Deficits	Additional Information
Germline Mutations								
Perez and Palmiter 2005	Mouse (C57BL6;129S4)	Exon 2 deletion	Absent	Absent	Rotarod Locomotor activity Hanging wire grip test Pole test	Acoustic startle Tail suspension Weight	Unknown	
	Mouse (129S4;129S4)				Absent/False positive	Absent/False positive	Unknown	
Goldberg et al., 2003	Mouse (C57BL6;129SV)	Exon 3 deletion; replaced with EGFP	Increased striatal dopamine	Absent	Balance beam	Adhesive removal	Unknown	
Itier et al., 2003	Mouse (C57BL6;129SV)	Exon 3 deletion	Increased striatal dopamine	Absent	Locomotor activity	Cognitive deficits	Unknown	
Rial et al., 2014	Mouse (C57BL6;129SV)	Exon 3 deletion	Increased basal striatal dopamine	Absent	Absent	Cognitive deficits	Unknown	Impaired hippocampal LTP
von Coelln et al., 2003	Mouse (C57BL6;129SV)	Exon 7 deletion	Absent	Absent	Absent	Acoustic startle	Unknown	Cell loss in locus coeruleus
Inducible/Stressor								
Shin et al., 2011; Stevens et al., 2015	Mouse (not stated)	Cre/lox Exon 7 deletion	Unknown	Present	Unknown	Unknown	Fewer and larger mitochondria	
Pickrell et al., 2015	Mouse (congenic C57BL6J;129S4)	Mutator x Exon 3 deletion; replaced with GFP	Reduced striatal dopamine	Present	Pole test	Unknown	Decreased Complex I/III activty	
Pinto, Nissanka and Moraes., 2018	Mouse (congenic C57BL6J;129S4)	PD-mito-PstI x Exon 3 deletion	Altered turnover	Anticipation but equivalent to PD-mito-PstI	Anticipation but equivalent to PD-mito-PstI	Unknown	Fewer and larger mitochondria	Hybrid mouse shows anticipation

Table 2.1. Parkin knockout models*. Germline Parkin null mice display variable but mild phenotypes and are typically on mixed genetic backgrounds. Inducible or stressor crossed Parkin null mice display more robust phenotypes and mitochondrial dysfunction*

2.1.3.2. Inducible/Stressor Models

In contrast to earlier germline models with Parkin deletions, more recent models have been able to demonstrate Parkin-related degeneration of the SNc and have helped to shed light upon mitophagy-independent Parkin functions *in vivo* (Table 2.1). Conditional *Parkin* exon 7 deletion mice have been created through lentiviral-mediated expression of Cre in the forebrain of exon 7 floxed *Parkin* mice aged 6-8 weeks old (Shin *et al.*, 2011). Unlike germline exon 7 deletion mice (von Coelln *et al*., 2004), conditional exon 7 deletion mice exhibit a progressive and selective degeneration of dopaminergic neurons within the SNc (Shin *et al.*, 2011) (Table 2.1). Nigral degeneration was the direct result of Parkin Interacting Substrate, PARIS (ZNF746) accumulation due to loss of Parkin-mediated ubiquitylation and subsequent degradation (Shin *et al.*, 2011). This resulted in transcriptional repression of peroxisome proliferator-activated receptor gamma (PPARγ) coactivator-1α (PGC-1α), leading to impaired mitochondrial biogenesis and associated decline in mitochondrial mass and respiration (Shin *et al.*, 2011; Stevens *et al.*, 2015).

A separate approach crossed Parkin knockout mice with homozygous Mutator mice (Pickrell *et al.*, 2015). Mutator mice accumulate mutations within mtDNA at an accelerated rate due to expression of a mutant DNA polymerase G with impaired proofreading function but do not display motor deficits or SNc degeneration (Trifunovic *et al.*, 2004). However, when *Parkin* exon 3 deletion mice (as used in Goldberg *et al*., 2003) were crossed with Mutator mice, the resulting offspring exhibited L-DOPA-responsive impairments in motor coordination and selective degeneration of doapmingeric neurons and an associated reduction in striatal dopamine (Pickrell *et al*., 2015) (Table 2.1). This phenotype was dependent on Parkin inactivation and was not associated with an increased number of mtDNA mutations, but was associated with mitochondrial dysfunction as assessed by reduced Complex I and III activity (Pickrell *et al*., 2015). In addition, crossing of the same exon 3 Parkin deletion mice described above with PD-mito-*Pst*I mice (which present with double-stranded mtDNA breaks specifically within dopaminergic neurons) resulted in impaired mitochondrial morphology and anticipation of motor deficits and nigral neurodegeneration usually observed in PD-mito-*Pst*I mice, but did not exacerbate the severity of these symptoms (Pinto, Nissanka and Moraes, 2018) (Table 2.1). From these data it appears that conditional knockout or exacerbation of mtDNA damage can produce a parkinsonian phenotype in Parkin null mice which is not observed in germline mutants. This discrepancy could suggest that compensatory mechanisms exist which reduce the impact of germline mutations. The expression of a parkinsonian phenotype in Parkin null animals crossed with mutant lines which experience mtDNA is very interesting when

considering that PD patients have a higher number of mtDNA mutations compared to age-matched healthy controls (Bender *et al.*, 2006).

2.2. Aims

Unlike α-synuclein and LRRK2, a wealth of data has been generated demonstrating PINK1-Parkin-dependent mitophagy *in vitro*, and the essentiality of PINK1-mediated activation of Parkin through phosphorylation at Ser65. However, the physiological importance of this phosphorylation and pathway have not been explored *in vivo*. In addition, past germline deletions within the *Parkin* gene have produced heterogeneous behavioural and pathological results when introduced into animal models. Through introduction of a serine to alanine substitution at Parkin residue 65, an alteration similar to that identified in 2 patients with autosomal recessive PD, the aim of this chapter was to establish whether novel *Parkin*$^{S65A/S65A}$ knock-in mice presented with a parkinsonian motor phenotype. Secondly, through collaborator-led investigation of mitophagy in these animals, we aimed to directly assess the effect of Parkin Ser65 inactivation on mitophagy *in vivo* for the first time, offering the opportunity to potentially link cellular dysfunction with behavioural dysfunction and bring valuable new insights into PD pathogenesis.

2.3. Materials and Methods

2.3.1. Generation of Parkin$^{S65A/S65A}$ Mice

Full details of the generation protocol can be found in McWilliams et al. (2018). Briefly, homozygous *Parkin*$^{S65A/S65A}$ (C57BL/6-*Prkn*$^{tm1.1Muqit}$/J) knock-in mice were generated by TaconicArtemis GmbH through homologous recombination-mediated introduction of a knock-in point mutation into the *Park2* gene in mouse ES cells. BAC clones from the C57BL/6J RPCIB-731 library were used to generate the targeting vector, before this vector was transfected into the TaconicArtemis C57BL/6N Tac ES cell line. Homologous recombinant clones were isolated and the knock-in allele obtained. Knock-in mice were crossed and maintained on the C57BL/6J inbred background strain.

2.3.1.2. Animal Husbandry and Legislation

Mice used in this study were maintained and tested in accordance with the 2013 European Union Directive 2010/63/EU and the UK Animals (Scientific Procedures) Act of 1986. Male and female animals were housed by sex (and littermate for male mice) in mixed genotype-cages containing 2 – 5 animals per cage. Animals were maintained under controlled conditions, with frequent monitoring, within holding rooms under a 06:00 – 18:00 light-dark cycle and a temperature of 21°C ± 1°C. Animals had *ad libitum* access to food and water throughout their lives and minimum environmental enrichment (tunnel, chew stick and bedding). Mice were health-checked and weighed weekly according to institutional guidelines.

An experimental group of homozygous *Parkin*$^{S65A/S65A}$ (HOM) mice and a control group of wild-type (WT) littermates were used in this study and further subdivided by sex. Mice were received from the MRC Protein Phosphorylation and Ubiquitylation Unit at the University of Dundee at the beginning of the study. 51 Parkin$^{S65A/S65A}$ (HOM) and wild-type (WT) littermate mice of approximately 12 months of age were received at the beginning of the study. The cohort consisted of the following sexes and genotypes: 25 WT mice (14 males and 11 females) and 26 HOM mice (11 males and 15 females). Mice were removed from their holding room and taken to a procedure room to undergo two rounds of motor testing on the same apparatus at 12- and 18 months of age. Behavioural testing was carried out during the light cycle and was designed to detect presence of a motor phenotype. In the time between testing, animals were confined to their cages outside of being removed for weighing and health checks. Mice were pre-allocated to group by collaborators in Dundee and the behavioural testing was conducted in a blinded fashion at 12 months. Data analysis required knowledge of genotype, preventing true blinding at the 18 month testing time-point. However, care was taken to limit knowledge of genotypes to limit subjective bias. Between arrival and the experimental end-point, 16

animals were either culled (WT total = 5: 3 males, 2 females; HOM total = 7: 1 male, 6 females) or found dead (WT total = 4: 3 males, 1 female; 0 HOM) leaving a total of 38 mice. Animals were culled when the humane end-point was reached. In this experiment, animals were culled due to non-genotype-specific over-grooming or severe and sustained weight loss.

If animals were culled or died before being tested at 18 months of age, they were excluded from analysis. In the case of balance beam testing, 2 animals failed to complete the task and were excluded from analysis but included in analysis for other tests due to successful completion (Table 2.2). 3 animals completed the rotarod, balance beam and gait tasks but were deemed too unwell to undergo testing in the activity boxes so were excluded from locomotor activity analysis.

Total = 38	**WT**		**HOM**		**Total**	
	Male	Female	Male	Female	WT	HOM
Rotarod	10	7	9	12	17	21
Balance Beam	10	**6F**	9	**11F**	16	20
Locomotor Activity	**9C**	7	9	**10C**	16	19
Gait	10	7	9	12	17	21
C: Animals culled before testing						
F: Animals failed test and were excluded						

Table 2.2. Representation of the number of animals in each test and reasons for exclusions*. The total number of animals possible were included in rotarod and gait but 2 animals were excluded from balance beam analysis due to failure to complete the task and 3 animals were excluded from locomotor activity as humane end-points were reach and they had to be culled.*

2.3.3. Behavioural Testing

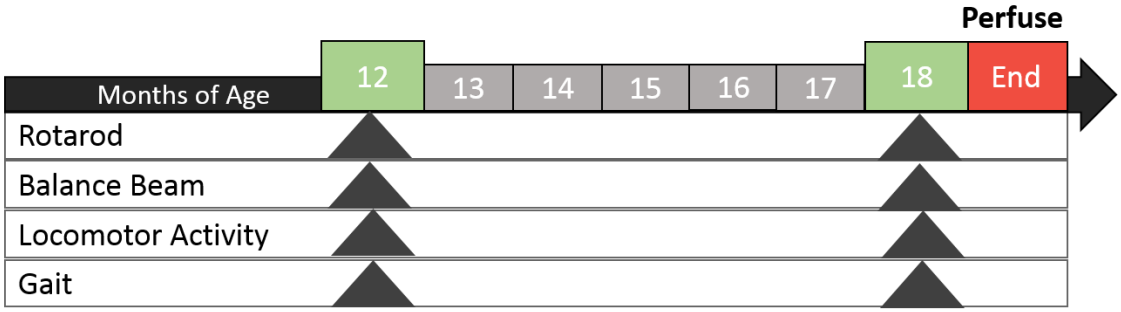

***Figure 2.3. Experimental Timeline**. Animals were tested at 12 and 18 months of age. Grey triangles indicate at which time-points tests were carried out.*

2.3.3.1. Rotarod

Mice were trained and tested on the rotarod (Ugo Basile, model number 47600, Varese, Italy) over the course of 5 days in order to assess motor coordination and balance. On day 1, mice were slowly habituated to the apparatus by increasing the acceleration from 4rpm, to 8rpm, to 12rpm and finally allowing the rotarod to accelerate from 12rpm to its maximum setting of 44rpm. Acceleration was halted and speed kept constant for 2 minutes at each interval. Day 2 consisted of first training the mouse at 12rpm for 2 minutes before allowing a 1 hour recovery period followed by training on the full acceleration protocol of 4-44rpm over 300 seconds. On training days 1 and 2, mice were put back on to the rotarod upon falling. On days 3, 4 and 5 mice were tested on the 4-44rpm rotarod accelerating protocol, with a maximum testing time of 300 seconds allowed. The latency of the mice to fall from the rotarod on the last 2 trials was recorded and averaged to give the score. When mice fell, they were returned to their home cage. If mice stayed on the apparatus for the full 300 seconds, they were removed from the rotarod and their score recorded as 300 seconds.

2.3.3.2. Balance Beam

Mice were tested on the balance beam in order to assess motor coordination and balance. The balance beam apparatus consists of a wooden beam, 1 metre in length, tapered in width from 1.5cm to 0.5cm from start to end and positioned at a 17° angle of ascent, with the beam leading to a house box.

On day 1, mice were placed within the house box at the end of the beam, before being placed at increasing distances away from the house box until the animal learned to walk from the start of the beam to the house box. On day 2, animals were tested over two successive trials and the results combined to give average scores on scores on 3 parameters. At the beginning of the task, animals were placed at the beginning of the beam facing 180° from the home box at the

end of the beam. Latency to turn was recorded as the length of time between placing the mouse on the beam and the mouse turning 180° to face the house box. Latency to traverse the beam was recorded as the length of time between the mouse crossing the start line with a forepaw and the second hindlimb crossing the finish line. Forepaw and hindpaw slips were counted between the start and end lines, with a score of 1 being given every time a paw slipped from the main beam platform. The number of paw slips made with the left limbs were live-scored while the number of paw slips made with the right limbs, the latency to turn, and the latency to traverse the beam were scored from video footage taken of the trials.

2.3.3.3. Spontaneous Automated Locomotor Activity

Locomotor activity was recorded by housing mice in Perspex cages measuring 40cm x 24cm x 18cm for 32 hours and counting the number of non-perseverative breaks mice made through 3 infrared beams traversing the cage. Mice were given *ad-libitum* access to powdered food and a water bottle and were kept under their usual 6:00 – 18:00 12-hour light/dark cycle, using lamps set to a timer. Data were recorded using MED-PC® (version 4) software (Vermont, USA). Mice were placed in the cages at 12:00 and the trial begun. When analysing the data, a 24-hour time period was extracted from 15:00 on the day the trial began to 15:00 the next day in order to exclude the increased number of beam breaks mice would typically produce when first exploring a novel environment. The 24-hour time period was assessed as a whole and further divided into a light phase (when mice are least active) and dark phase (when mice are most active). The light phase represents the 12-hour non-contiguous period when mice were exposed to light between the hours of 15:00 – 18:00 and 06:00 – 15:00 the next day. The dark phase represents the 12-hour contiguous period between the hour of 18:00 and 06:00 when the lamp was turned off. The first 30 minutes of beam breaks were taken to assess exploratory behaviour and habituation.

2.3.3.4. Gait analysis

The presence of disease-related gait abnormalities was investigated by conducting measurements of animals' strides. Gait analysis was conducted in an apparatus consisting of a narrow Perspex corridor (measuring 65cm x 5cm x 15cm) leading to a darkened house box. Animals were first placed in the house box for 1 minute, before being removed and placed at the start of the corridor, with encouragement to move toward the house box given if needed. Upon successfully traversing the corridor once, mice were removed from the apparatus and the floor of the corridor lined with tight-fitting white paper. The animal was then scruffed and its forepaws painted with non-toxic red paint and its hindpaws with non-toxic blue paint. The mouse was then slowly lowered into the start of the corridor, after which it was free to traverse the corridor, moving towards the house box, leaving clearly distinguishable fore- and hind-paw

prints along the paper. Following completion of the task, mice were placed in a blue roll-lined cage containing a small amount of lukewarm water to aid in washing away the paint, before being returned to their home cage. In order to conduct gait analysis, 4 clear paw prints were required to be recorded from each side of the animal. 3 parameters were measured from these prints. First, stride-length was recorded as the average distance (in mm) between the preceding and proceeding hindpaw on each side. Next, hind- and fore-paw base widths were recorded as the average distance (in mm) between the corresponding contralateral hind- and fore-paws. Finally, overlap was recorded as the average distance (in mm) between the ipsilateral hind- and fore-paws within a stride. In the case of the hindpaw landing in front of the forepaw, a positive overlap value was assigned. When the hindpaw landed behind the forepaw, a negative overlap value was assigned.

2.3.4. Perfusion-Fixation

Animals were killed via intraperitoneal injection of 0.2 ml Euthatal (Merial, Essex, UK) before being transcardially perfused with PBS (pH 7.4) for 1 minute, followed by 4% PFA (pH 7.4) for 6 minutes to fix tissue. Following fixation, animals were decapitated and their brains removed. Brains were then post-fixed in 4% PFA at 4°C for 24 hours, after which they were cryopreserved in 25% sucrose at 4°C. Brains were kept in sucrose for no more than 48 hours, after which they were sectioned coronally into a 1 in 6 series of 35µm slices using a sliding sledge freezing microtome (Leitz, Wetzlar). Brain slices were then transferred into a 48 well plate where they were stored in antifreeze at -20°C. Brains were then sent to collaborators where they were processed.

2.3.5. Statistics

All statistical tests were conducted in SPSS. When data were not normal or did not display equal variances, they were transformed accordingly before an ANOVA was performed. The test used for each analysis is displayed in Table 2.4.

When analysing the data, sex was always initially included as a between-subjects variable within the statistical analysis. Data from each motor test was first evaluated using a three-way mixed ANOVA with Bonferroni pairwise-comparisons (within-subjects variable: age; between-subjects variables: genotype and sex). If a main effect of sex was found it was reported and the statistical values for age and genotype and any interactions were taken from this ANOVA, and male and female animals were not combined and statistically evaluated. In cases where a main effect of sex or an interaction between sex and another variable were not reported, data from male and female animals were combined according to genotype and a two-way mixed ANOVA with Bonferroni pairwise-comparisons conducted (within-subjects variable: age; between-

subjects variable: genotype) to generate the statistical values stated in the results. For consistency, figures for each test include male and female data representation, as well as a combined representation. Significance bars and asterisks are present only on the relevant representations according to the sex criterion described above.

Behavioural Test	Figure	Statistical Test	Independent Variables	Dependent Variables
Rotarod	2.5	Three-way mixed ANOVA	Genotype x Age x Sex	Latency to Fall
Balance Beam	Slips (2.6A)	Two-way mixed ANOVA	Genotype x Age	Paw Slips
	Turn (2.6B)	Three-way mixed ANOVA	Genotype x Age x Sex	Latency to Turn
	Traverse (2.6C)	Two-way mixed ANOVA	Genotype x Age	Latency to Traverse
Locomotor Activity	Light (2.7A)	Two-way mixed ANOVA	Genotype x Age	Beam Breaks
	Dark (2.7B)	Two-way mixed ANOVA	Genotype x Age	Beam Breaks
	24hr (2.7C)	Three-way mixed ANOVA	Genotype x Age x Hour	Beam Breaks
	30min Total (2.7D)	Two-way mixed ANOVA	Genotype x Age	Beam Breaks
	30min/bin (2.7E)	Three-way mixed ANOVA	Genotype x Age x Bin	Beam Breaks
Gait	Stride-length (2.8A)	Two-way mixed ANOVA	Genotype x Age	Distance (mm)
	Forepaw BW (2.8B)	Two-way mixed ANOVA	Genotype x Age	Distance (mm)
	Hindpaw BW (2.8C)	Three-way mixed ANOVA	Genotype x Age x Sex	Distance (mm)
	Overlap (2.8D)	Two-way mixed ANOVA	Genotype x Age	Distance (mm)

***Table 2.4. Statistical details**. The statistical test and variables used for each behavioural test are listed.*

2.4. Results

2.4.1. Rotarod

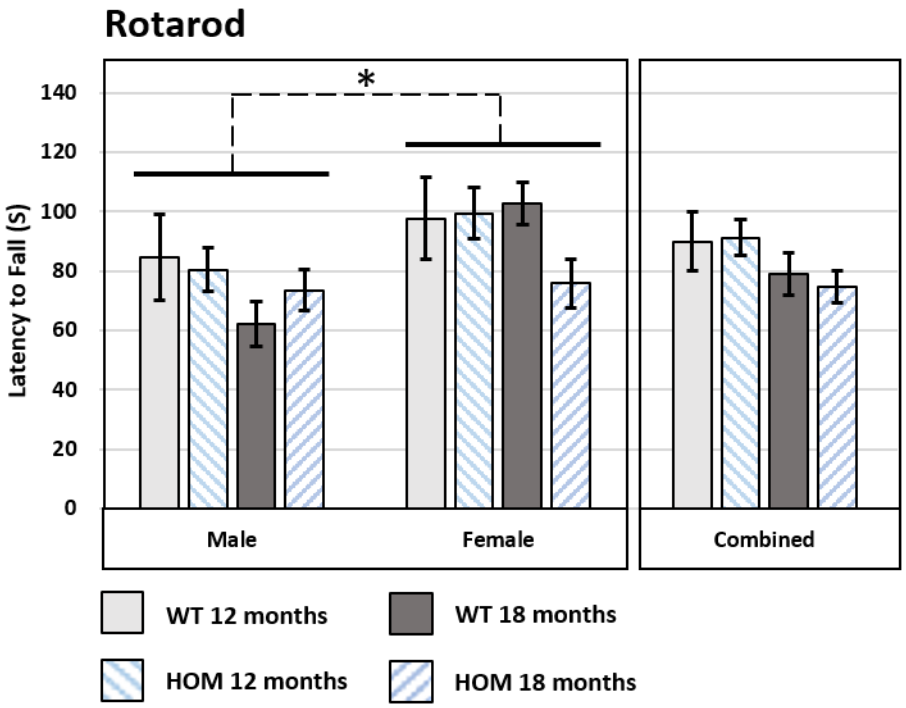

Figure 2.5. Rotarod performance of WT and HOM mice at 12 and 18 months. *Males were significantly more impaired on the rotarod than females. The latencies to fall from the rotarod of male and female WT/HOM animals at 12 and 18 months of age (left pane) and male and female combined WT/HOM animals at the equivalent time-points (right pane). Significant differences between sexes are indicated by bars with dashed lines, with significance level represented by p ≤ 0.05*, p ≤ 0.01**, and p ≤ 0.001***. Values are expressed as means ± SEM. WT n = 17 (10 ♂, 7 ♀); Parkin$^{S65A/S65A}$ n = 21 (9 ♂, 12 ♀).*

Animals were trained and tested on the rotarod task in order to compare motor coordination between WT and *Parkin*$^{S65A/S65A}$ animals (Figure 2.5). Male mice were significantly more impaired on the rotarod than female mice as evidenced by a shorter latency to fall ($F(1, 34) = 6.891$, $p = 0.013$). WT and HOM mice exhibited comparable latencies to fall, demonstrating that HOM animals do not display impaired motor coordination on the rotarod task ($F(1, 34) = 0.413$, p = n.s.). More advanced age was not associated with impairment on the rotarod, with comparable latencies to fall at 12 and 18 months ($F(1, 34) = 3.091$, p = n.s.). There were no significant interactions between age and genotype ($F(1, 34) = 0.236$, p = n.s.). Taken together, these results show that females performed better on the rotarod than males, but genetic background and age do not significantly affect the motor coordination.

2.4.2. Balance Beam

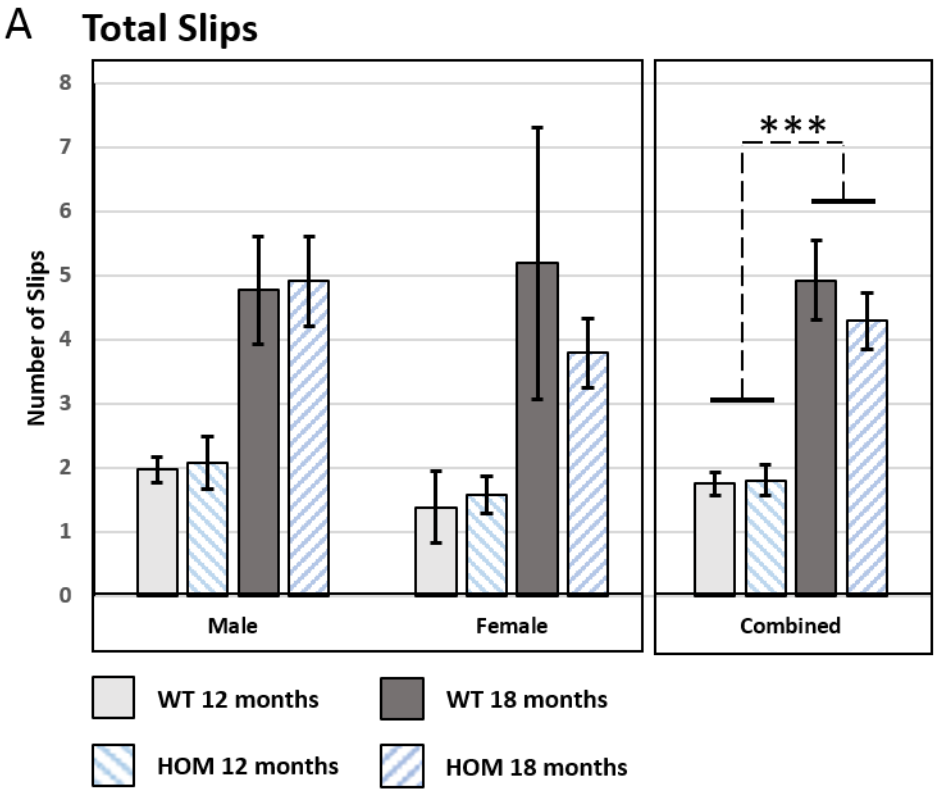

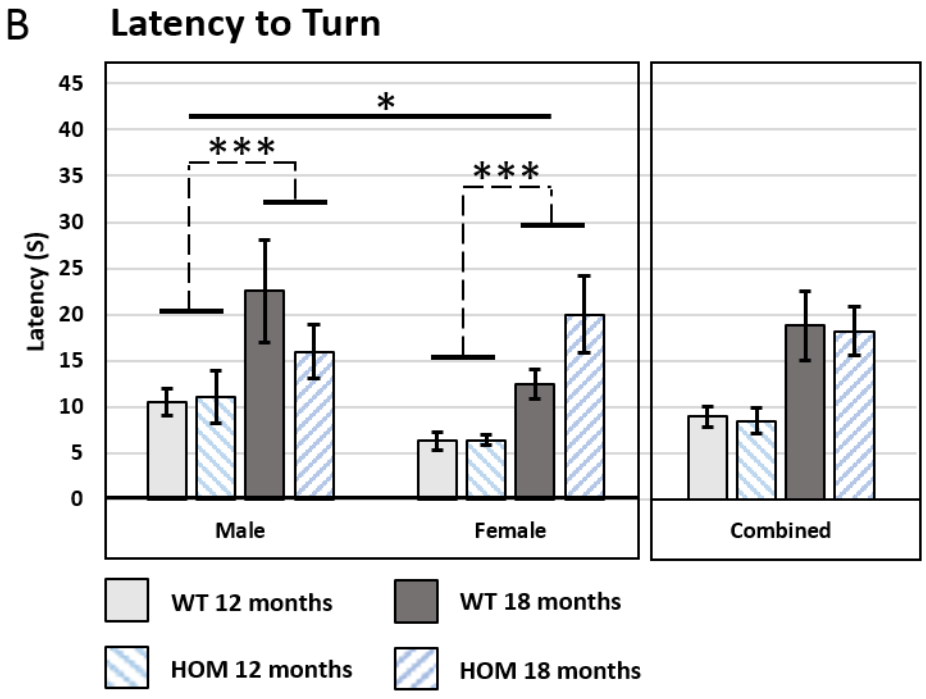

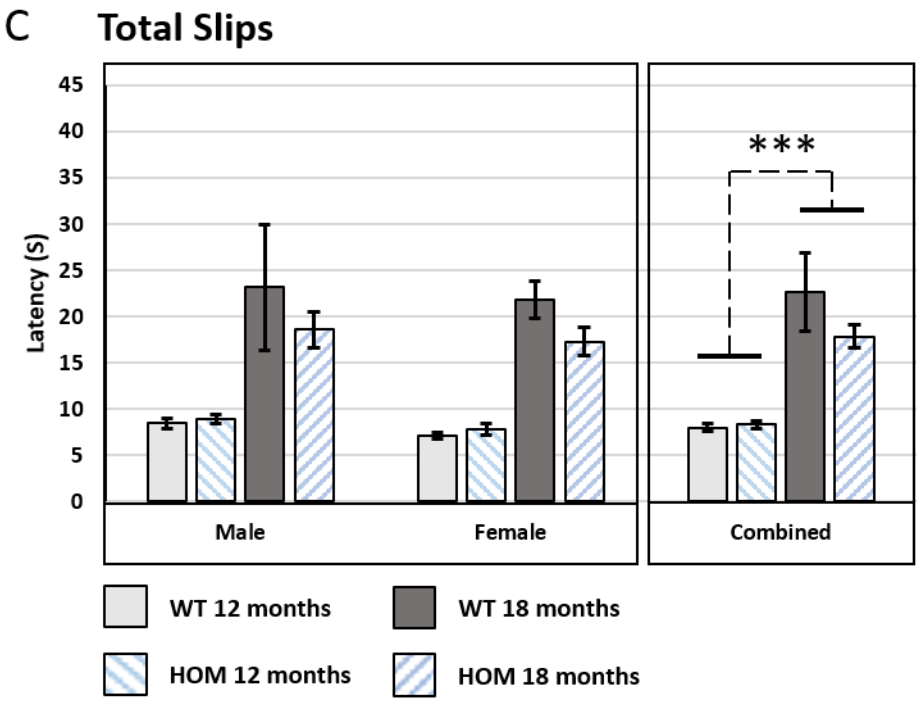

Figure 2.6. Balance beam performance of WT and Parkin$^{S65A/S65A}$ mice at 12 and 18 months. *Animals displayed a more impaired performance on the balance beam at an increased age. These figures show the total number of paw slips (hind- and fore-paw slips combined) made while animals traversed the balance beam (A), the latency to turn at the end of the beam (B), and the latency to traverse the beam (C). Significant differences between sex are indicated by a long bar while significant differences between age are indicated by smaller bars with dashed connecting lines with significant level represented by p ≤ 0.05*, p ≤ 0.01**, and p ≤ 0.001***. Values are expressed as means ± SEM. (A) WT n = 16 (10 ♂, 6 ♀); HOM n = 20 (9 ♂, 11 ♀), (B) WT n = 16 (10 ♂, 6 ♀); HOM n = 20 (9 ♂, 11 ♀), (C) WT n = 16 (10 ♂, 6 ♀); HOM n = 20 (9 ♂, 11 ♀).*

2.4.2.1. Paw slips

Male and female animals did not differ in the number of paw slips made as they traversed the beam (F (1, 32) = 2.063, p = n.s.) (Figure 2.6A). In addition, there was no difference in the number of paw slips made by WT and HOM mice (F (1, 34) = 0.401, p = n.s.), suggesting that balance and motor coordination on the balance beam is not impaired in HOM animals. In contrast, 18 month old mice made more paw slips at 18 months than 12 months (F (1, 34) = 52.768), p = < 0.001) reflecting a decline in balance and motor coordination with advanced age. There were no significant interactions between age and genotype (F (1, 34) = 0.452, p = n.s.).

2.4.2.2. Latency to turn

Female mice exhibited a significantly shorter latency to turn than male mice ($F(1, 32) = 4.674$, $p = 0.038$), with their smaller size likely conferring increased mobility (Figure 2.6B). WT and HOM mice did not differ in their latency to turn ($F(1, 32) = 0.026$, p = n.s.). However, an age-related deficit in performance was again seen on this metric, with mice taking longer to turn at 18 months compared to 12 months ($F(1, 32) = 37.685$, $p = < 0.001$). There were no significant interactions between age and genotype ($F(1, 32) = 0.074$, p = n.s.).

2.4.2.3. Latency to Traverse

Male and female mice did not differ in their latency to traverse the beam ($F(1, 32) = 0.495$, p = n.s.) (Figure 2.6C). There was also no difference in latency to traverse between WT and HOM animals ($F(1, 34) = 0.300$, p = n.s.) which, when viewed alongside the paw slip and latency to turn data, suggests that genotype has no impact on balance and motor coordination on the balance beam. In contrast, age negatively affected the latency to traverse, with mice taking longer to traverse the beam at 18 months than 12 months ($F(1, 34) = 90.832$, $p < 0.001$). No significant interactions between age and genotype were reported ($F(1, 34) = 0.850$, p = n.s.).

2.4.3. Locomotor Activity

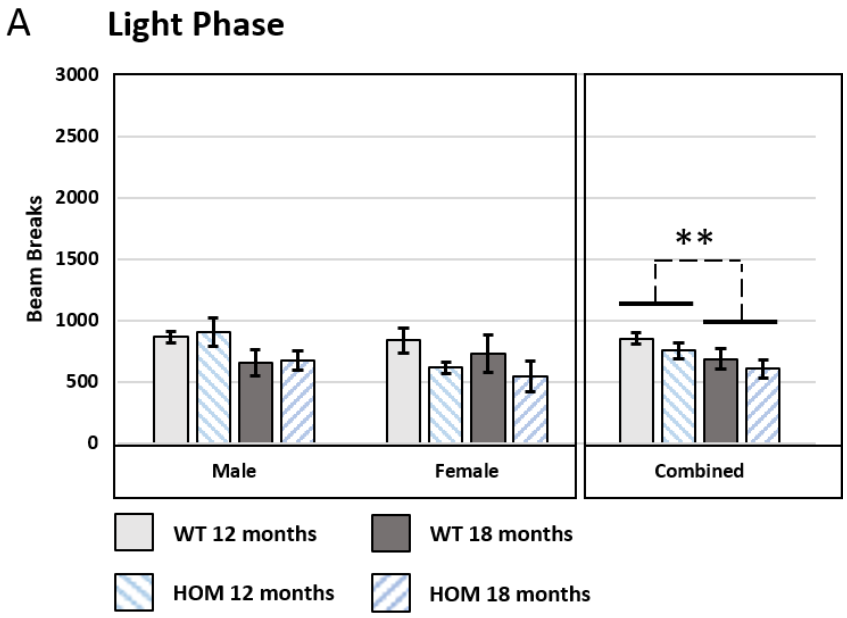

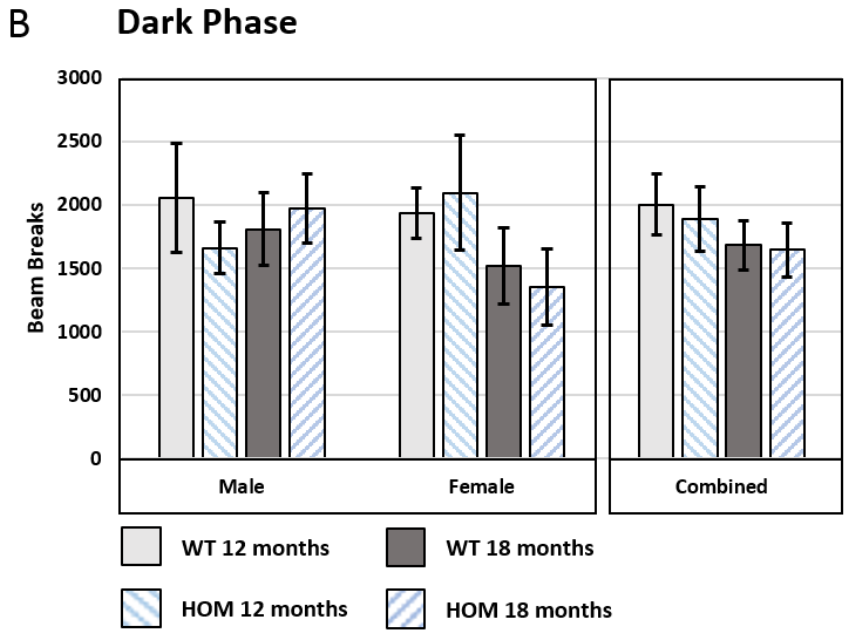

C

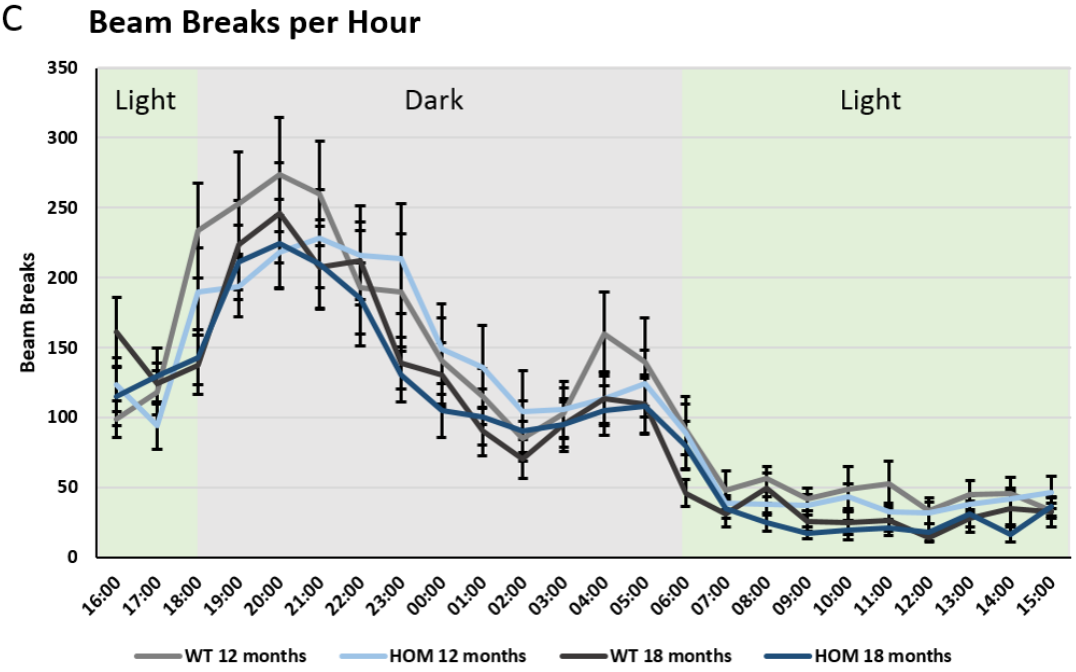
Beam Breaks per Hour
Light
Dark
Light
Beam Breaks
350
300
250
200
150
100
50
0
16:00
17:00
18:00
19:00
20:00
21:00
22:00
23:00
00:00
01:00
02:00
03:00
04:00
05:00
06:00
07:00
08:00
09:00
10:00
11:00
12:00
13:00
14:00
15:00
WT 12 months
HOM 12 months
WT 18 months
HOM 18 months

D

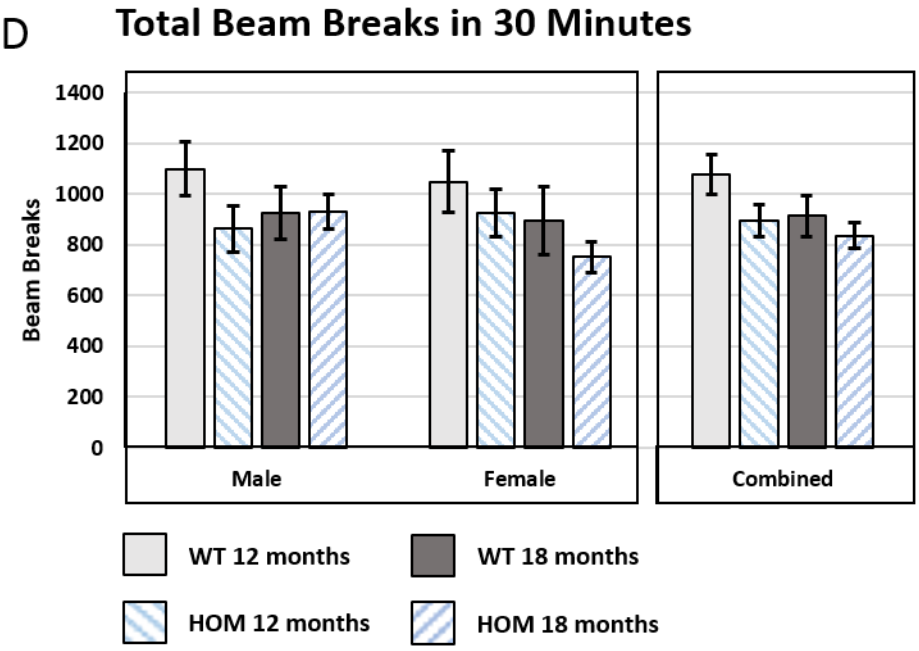
Total Beam Breaks in 30 Minutes
Beam Breaks
1400
1200
1000
800
600
400
200
0
Male
Female
Combined
WT 12 months
WT 18 months
HOM 12 months
HOM 18 months

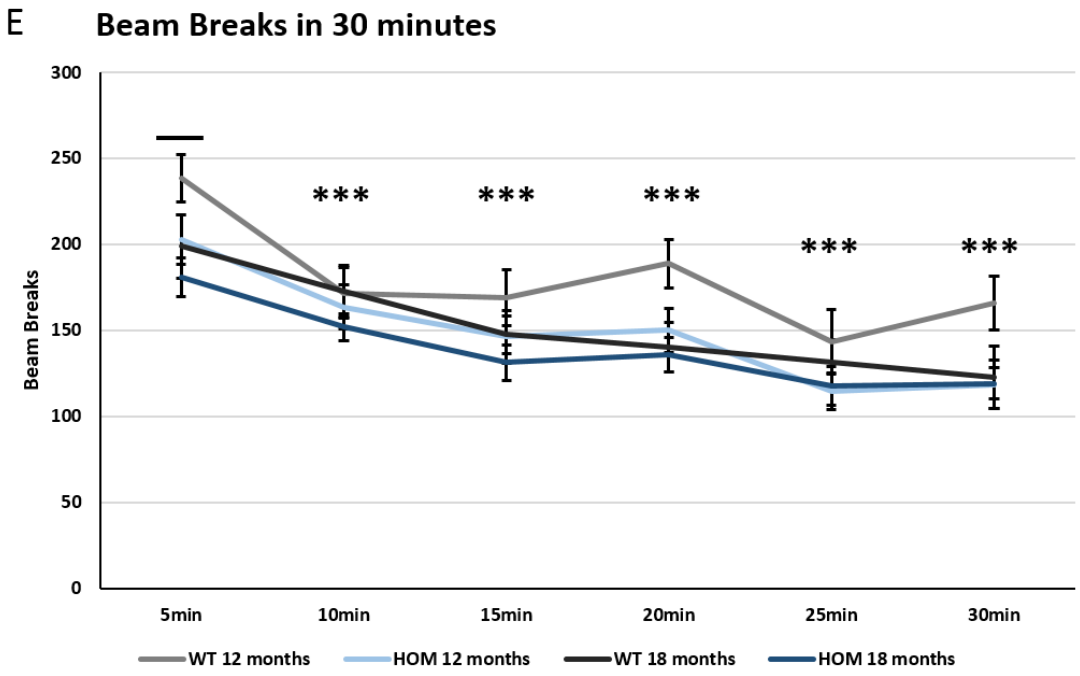

Figure 2.7. 24-hour and 30-minute locomotor activity of WT and Parkin$^{S65A/S65A}$ mice at 12 and 18 months. *Animals were significantly less active during the light phase at 18 months compared to 12 months, but both WT and HOM animals display normal habituation. The number of beam breaks mice made during the 6am – 6pm light phase of testing (A), the number of beam breaks mice made during the 6pm – 6am dark phase of testing (B) and the number of beam breaks mice made during the entire 24 hour period of testing (light and dark phases combined) (C). The total number of beam breaks during the first 30 minutes of animals being inside the activity boxes is shown in (D) while the number of beam breaks made during each 5 minute time bin of the first 30 minutes of activity is displayed in (E). Significant differences between ages and times are indicated by small bars with dashed connecting lines with significance level represented by p ≤ 0.05*, p ≤ 0.01**, and p ≤ 0.001***. Values are expressed as means ± SEM. All WT n = 16 (9 ♂, 7 ♀); HOM n = 19 (9 ♂, 10 ♀).*

2.3.4.1. Light phase

Comparison of number of beam breaks showed that male and female animals did not differ in activity during the light phase of testing (F (1, 31) = 1.340, p = n.s.) (Figure 2.7A). Genotype did not affect the number of beam breaks performed in the light phase (F (1, 33) = 1.197, p = n.s.) but advanced age was associated with a decline in activity during this phase (F (1, 33) = 7.766, p = 0.009). There were no significant interactions between age and genotype (F (1, 33) = 0.022, p = n.s.).

2.3.4.2. Dark phase

Sex (F (1, 31) = 0.361, p = n.s.), and genotype (F (1, 33) = 0.602, p = n.s.). also had no effect on activity during the dark phase of testing when animals are at their most active (Figure 2.7B). Unlike during the light phase of testing, mice did not display a decline in activity levels at 18 months compared to 12 months, suggesting that age does not influence activity during this phase of testing (F (1, 33) = 0.009, p = n.s.). There were no significant interactions between age and genotype (F (1, 33) = 2.761, p = n.s.).

2.3.4.3. 24-hour period

No effect on overall activity levels across the 24-hour testing period was observed when mice were compared by sex (F (1, 31) = 0.508, p = n.s.) or genotype (F (1, 33) = 0.250, p = n.s.) suggesting that there are no locomotor activity deficits in HOM animals (Figure 2.7C). There was however a decrease in activity levels at 18 months compared to 12 months (F (1, 33) = 4.524, p = 0.041), reflecting an age-related decline in activity. A significant effect of hour was reported (F (23, 759) = 50.820, p < 0.001), reflecting the normal elevation of activity level in the dark phase compared to the light phase. There were no significant interactions between age and genotype (F (1, 33) = 0.050, p = n.s.).

2.3.4.4. Initial 30 minutes

The first 30 minutes of testing across the 24-hour testing period was taken to determine whether animals differed in their activity levels in response to placement within a novel environment (Figure 2.7D). Male and female animals did not differ in activity over this period, suggesting normal exploration (F (1, 31) = 0.738, p = n.s.). Likewise, WT and HOM animals explored to an equivalent extent (F (1, 33) = 3.022, p = n.s.) with age having no effect (F (1, 33) = 3.104, p = n.s.). No significant interactions between age and genotype were reported (F (1, 33) = 0.877, p = n.s.).

In order to determine whether mutant animals habituated normally the novel environment, the number of beam breaks in each 5-minute time-bin across the initial 30-minute testing period were compared (Figure 2.7E). As expected, animals displayed a decrease in activity over time (F (5, 165) = 46.240, p < 0.001), reflecting habituation. Male and female animals habituated to equivalent degrees (F (1, 31) = 0.510, p = n.s.) while no effect of genotype was observed (F (1, 33) = 3.670, p = n.s.), suggesting HOM animals display normal habituation as well as exploration of a novel environment. Advanced age did not affect habituation over this time period (F (1, 165) = 2.706, p = n.s.). There were no interactions between age and genotype (F (1, 33) = 0.601, p = n.s.).

2.4.4. Gait


A
Stride Length
Distance (mm)
100
90
80
70
60
50
40
30
20
10
0
***
Male
Female
Combined
WT 12 months
WT 18 months
HOM 12 months
HOM 18 months

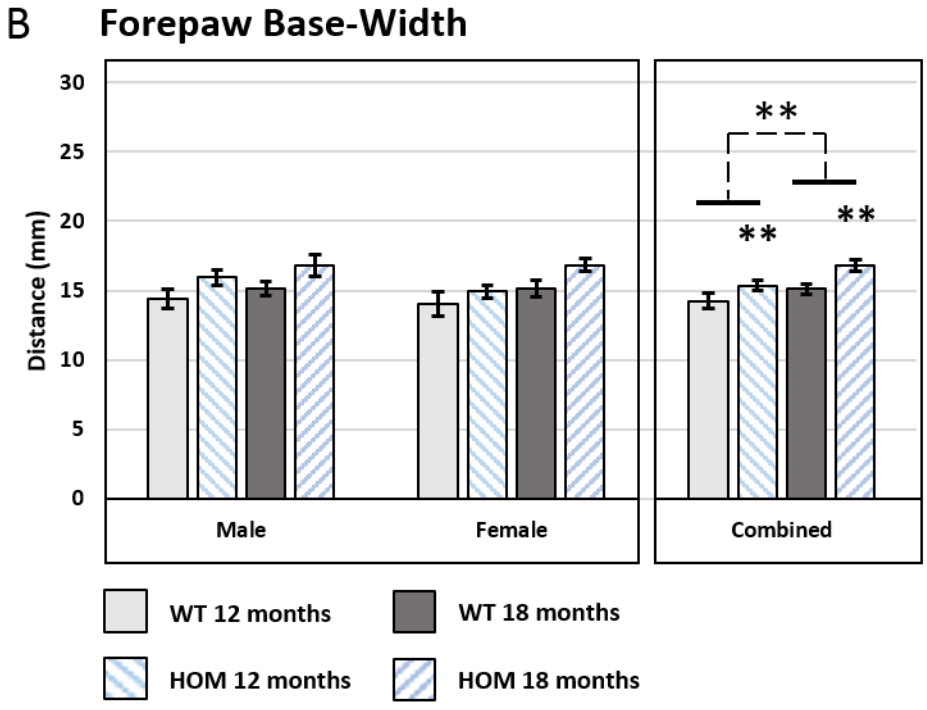
B
Forepaw Base-Width
Distance (mm)
30
25
20
15
10
5
0
**
**
**
Male
Female
Combined
WT 12 months
WT 18 months
HOM 12 months
HOM 18 months

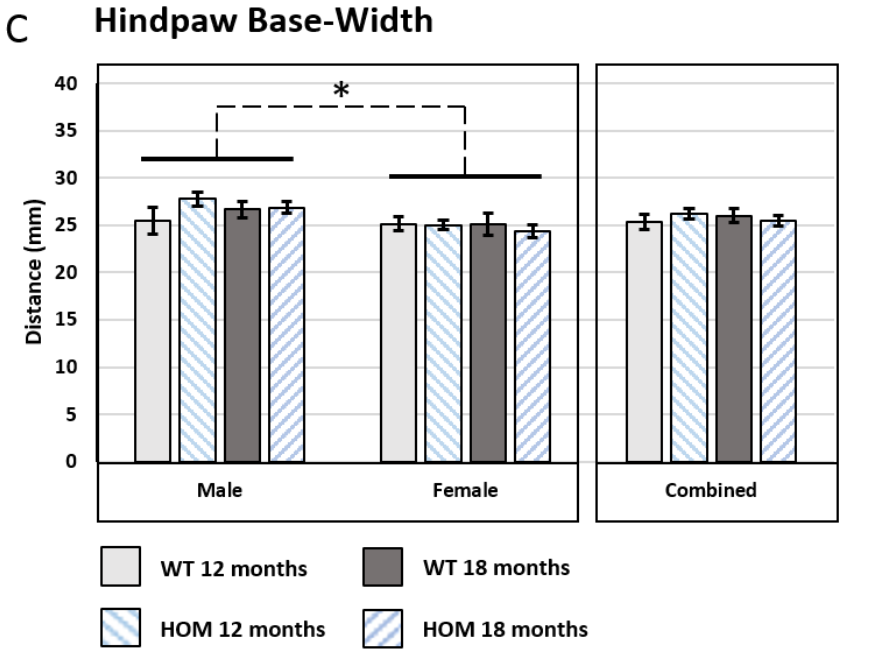

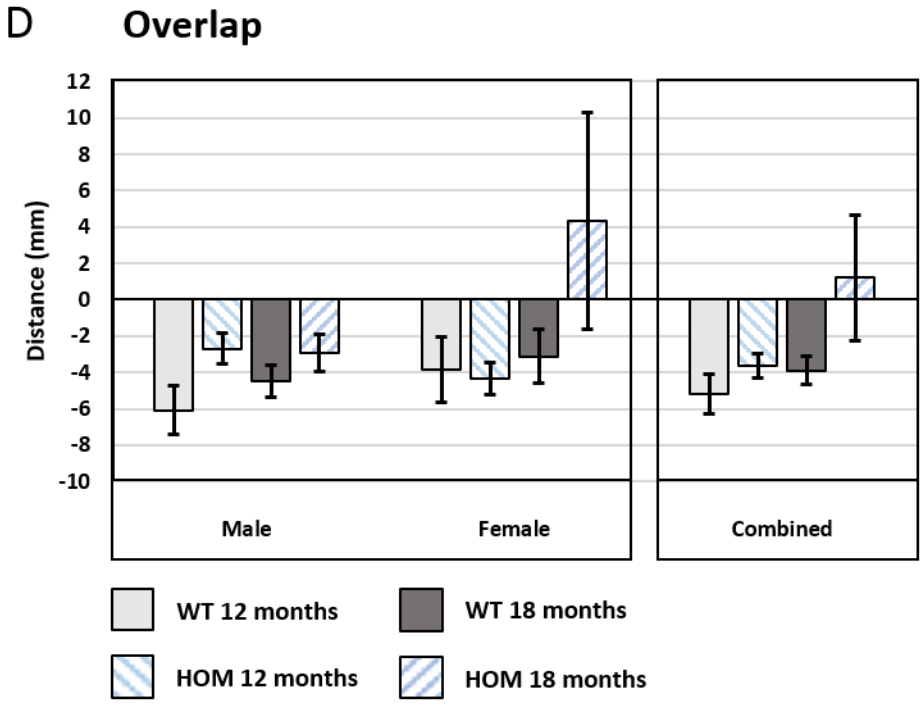

Figure 2.8. Gait analysis of WT and Parkin$^{S65A/S65A}$ mice at 12 and 18 months. *Animals displayed significantly altered stride-length and forepaw base-width at greater age, with HOM animals displaying significantly increased forepaw base-widths at both time-points compared to WT mice. Displaying measures obtained from gait analysis of mice at 12 and 18 months of age, including stride-length (A), forepaw base-width (B), hindpaw base-width (C), and overlap (D). Significant differences between ages are denoted by small bars with dashed connecting lines, significant differences between genotypes are indicated by asterisks above HOM bars, while significant differences between sexes are displayed by long bars with significance level represented by p ≤ 0.05*, p ≤ 0.01**, and p ≤ 0.001***. Values are expressed as means ± SEM. All WT n = 17 (10 ♂, 7 ♀); HOM n = 21 (9 ♂, 12 ♀).*

2.4.4.1. Stride-length

Male and female animals did not differ in their stride-length ($F(1, 34) = 3.654$, p = n.s.) (Figure 2.8A) and nor did WT and HOMs ($F(1, 36) = 1.601$, p = n.s.). Aged animals did however display a shortened stride-length at 18 months ($F(1, 36) = 20.795$, $p < 0.001$) suggesting that age negatively impacts on stride-length but genotype does not. No significant interactions between age and genotype were reported ($F(1, 36) = 0.281$, p = n.s.).

2.4.4.2. Forepaw base-width

Forepaw base-width did not differ by sex ($F(1, 34) = 0.510$, p = n.s.) (Figure 2.8B). However, HOM animals presented with a significantly increased forepaw base-width animals compared to WT animals ($F(1, 36) = 9.706$, $p = 0.004$), indicative of a more splayed forepaw stature. An age-related increase in this measurement was also seen in older animals ($F(1, 36) = 9.308$, $p = 0.004$) suggesting that both genotype and increased age alter this aspect of gait in a similar way. There were not interactions between age and genotype ($F(1, 36) = 0.591$, p = n.s.).

2.4.4.3. Hindpaw base-width

Male mice exhibited a larger hindpaw base-width than female mice ($F(1, 34) = 6.046$, $p = 0.019$), likely reflecting their larger size (Figure 2.8C). Unlike the forepaws, hindpaw base-width did not differ between the two genotypes ($F(1, 34) = 0.328$, p = n.s.) or between 12 and 18 month old animals ($F(1, 34) = 0.037$, p = n.s.) suggesting that genotype and age determine limb-dependent base-width alterations. No interactions between age and genotype were seen ($F(1, 34) = 0.241$, p = n.s.).

2.4.4.4. Overlap

The extent of overlap between fore- and hind-paws (Figure 2.8D) did not differ by sex ($F(1, 34) = 1.028$, p = n.s.), genotype ($F(1, 36) = 2.262$, p = n.s.), or age ($F(1, 36) = 2.632$ p = n.s.) with no interaction between age and genotype ($F(1, 36) = 0.897$, p = n.s.). However, it should be noted that this measurement shows a high degree of variability between animals.

2.4.5. Additional Results

The following results are taken from (**McWilliams et al. (2018): Phosphorylation of Parkin at serine 65 is essential for its activation *in vivo)*** and were obtained by collaborators. They are included here to provide context to the behavioural results detailed here.

2.4.5.1. *Parkin*$^{S65A/S65A}$ Expression and Activity

The expression of the Parkin$^{S65A/S65A}$ mutant protein was comparable to the levels of WT Parkin protein in control animals across several regions of the brain (including the striatum and ventral midbrain) as well as in peripheral tissue. In primary neuronal cultures from *Parkin*$^{S65A/S65A}$ mice, PINK1-mediated phosphorylation of Parkin at Ser65 and Parkin-mediated ubiquitylation of its substrate CISD1 were undetectable following application of antimycin and oligomycin to cultured cells. In addition, PINK1-mediated phosphorylation of Ub at Ser65 was also undetectable in mutant cultures. These data demonstrate that the *Parkin*$^{S65A/S65A}$ mutant is successfully expressed at normal levels and that the substitution of serine to alanine at residue 65 was successful in preventing protein phosphorylation. Moreover, the mutant protein displayed undetectable E3 ubiquitin ligase activity following mitochondrial depolarisation, with the lack of P-Ub supporting the essential role of Parkin activity in the feedforward mechanism of PINK1-Parkin pathway-mediated phospho-Ub accumulation (Ordureau *et al.*, 2015).

2.4.5.2. *Parkin*$^{S65A/S65A}$ Histology

IHC analysis revealed comparable TH-positive dopaminergic cells within the SNc and nigrostriatal terminals in the dorsal striatum between 18 month old WT and mutant animals, as well as no difference in striatal anatomy or volume. Furthermore, the number of iDISCO+-resolved nigrostriatal projections did not differ between genotypes and neither did the extent of ionized calcium-binding adapter molecule 1 (IBA1) and glial fibrillary acidic protein (GFAP) staining which labels microglia and astrocytes. The levels of striatal dopamine and dopamine turnover also did not differ between genotypes. These data strongly suggest that *Parkin*$^{S65A/S65A}$ mice displayed no overt PD-related neurodegenerative phenotype, or presence of neuroinflammation, even at advanced age.

2.4.5.3. *Parkin*$^{S65A/S65A}$ Mitochondrial Function and Basal Mitophagy

Parkin$^{S65A/S65A}$ mice displayed deficits in mitochondrial respiration specifically within the striatum at 12 months of age, but not 3 months. To assess basal mitophagy, the *Parkin*$^{S65A/S65A}$ mouse was crossed with the *mito*-QC mitophagy reporter line. Basal mitophagy within nigrostriatal cell bodies and projections was found to be equivalent between *Parkin*$^{S65A/S65}$/*mito*-QC animals and WT/*mito*-QC animals. These data demonstrate that inactivation of Parkin results in age-related deficits in mitochondrial respiration specifically

within the striatum but does not lead to deficits in basal mitophagy within SNc neurons, suggesting that Parkin is dispensable for this process in mice *in vivo*.

2.4.5.4. Patient Case Studies and Primary Culture Investigations

Two patients with homozygous mutations in the *PARK2* locus, which caused an S65N substitution in the Parkin protein, were identified. However, one of these patients was also shown to carry three PD-associated gene variants in addition to the *PARK2* mutation. Preliminary assessment of transformed HeLa cells expressing S65A, S65N, or WT forms of Parkin revealed that both mutant forms of Parkin resulted in loss of E3 ubiquitin ligase activity and phospho-ubiquitin accumulation to a comparable degree. Furthermore, primary fibroblast cultures obtained from one of the homozygous *Parkin* S65N patients (without additional risk variants) revealed lack of Parkin phosphorylation at residue 65 and reductions in E3 ubiquitin ligase activity and phospho-ubiquitin accumulation following mitochondrial depolarisation compared to WT controls. Furthermore, levels of mitophagy following mitochondrial depolarisation were indistinguishable between mutant and control fibroblasts. These data suggest that although Parkin phosphorylation and activity in mutant primary fibroblasts is compromised, Parkin activity is dispensable for mitophagy in these cells.

2.5. Discussion

2.5.1. Summary

Over the course of this study, aged *Parkin*$^{S65A/S65A}$ knock-in mice and WT littermates were assessed for the presence of a parkinsonian motor phenotype at two time-points of 12 and 18 months of age. Mutant mice did not display a robust parkinsonian phenotype with the only difference relative to WT controls being a wider forepaw base-width at both time-points (Figure 2.8B). Furthermore, collaborator-led investigation determined unaltered basal mitophagy in the nigral neurons of mutant animals in addition to lack of nigrostriatal degeneration or reduction in striatal dopamine (Section 2.4.5.). However, age-dependent reduction in mitochondrial function was reported in mutant mice.

2.5.2. Motor Dysfunction

Previous germline Parkin mutants have displayed variable deficits in motor coordination (Table 2.1). However, in our hands *Parkin*$^{S65A/S65A}$ mice displayed no impairment in motor coordination or balance on the rotarod (Figure 2.5) and balance beam (Figure 2.6), relative to WT mice, at 12 and 18 months of age. Both tests are commonly used to phenotype PD models and have been shown to be sensitive to nigral dysfunction (Drucker-Colín and García-Hernández, 1991). The reported balance beam deficits beginning at 2 months of age are surprising as the mice are relatively young and appear to make fewer slips as they age, rather than progressively more as might be expected with age (Goldberg *et al.*, 2003). In addition, the same animals do not display a deficit on the rotarod at any of the equivalent time-points up to 18 months (Goldberg *et al.*, 2003) although both WT and *Parkin*$^{S65A/S65A}$ mice displayed age-dependent deficits on the balance beam but not the rotarod, highlighting differences in sensitivity between the two tests and suggesting the motor deficits observed are relatively subtle. An impaired motor performance was reported by Perez and Palmiter and mixed background mice, but this was not sustained when controlling for background (Perez and Palmiter, 2005). Thus, impaired motor coordination in Parkin null animals appears to be subtle or altogether absent in the models previously described.

Parkin$^{S65A/S65A}$ mice did not display deficits in locomotor activity over the course of 24 hours or first 30 minutes of testing (Figure 2.7) suggesting a lack of hypolocomotor phenotype and normal exploration and habituation to a novel environment. Reductions in activity have been reported in Parkin null mice (Itier *et al.*, 2003; Perez and Palmiter, 2005), however no deficits were observed in coisogenic mutants in the case of the latter and the former used a very short 3 minute trial time in the open field which could allow environmental stressors to predominate and confound the data. Reductions in exploratory behaviour over the course of 30 minutes

were also reported (Itier *et al.*, 2003) but were not described in other studies (Goldberg *et al.*, 2003; Von Coelln *et al.*, 2004) Alterations in locomotor activity are not PD-specific and can be due to non-motor factors. The lack of reductions in activity over the 24-hour period in *Parkin*$^{S65A/S65A}$ mice and the reductions in activity in both WT and *Parkin*$^{S65A/S65A}$ mice with age suggest that the test is relatively sensitive and a hypolocomotor phenotype is not present in these mutant animals.

Gait disturbances are commonly observed in PD patients and would be expected in an animal model of the disease. A short stride-length could be comparable to a shuffling gait, an enlarged base-width suggests a more splayed stature and could indicate difficulty in supporting the torso, while a reduction in overlap could suggest reduced extension of the hindlimbs. At both 12 and 18 months, *Parkin*$^{S65A/S65A}$ mice displayed a larger forepaw base-width than WT controls (Figure 2.8B) but did not display any additional deficits on the metrics measured (Figure 2.8). While a wider forepaw base-width may indicate gait abnormalities in *Parkin*$^{S65A/S65A}$ mice, the lack deficits in other measurements between genotypes makes interpretation of this single change difficult. This is especially true as the gait test showed age-related reductions in both WT and knock-in animals, highlighting the sensitivity of the test. Gait was investigated by Perez and Palmiter (2005) and no difference was reported between genotypes, supporting these results.

Non-motor phenotypes were reported in all Parkin null mice (Table 2.1) but were not explored here. Although interesting, a robust model of PD would be expected to display clear motor symptoms, in addition to non-motor symptoms, and while these non-motor differences are suggestive of a phenotype, they are not necessarily representative of a parkinsonian phenotype and a motor phenotype is mild or absent. While cognitive ability is impaired in PD and has been reported to be altered in Parkin null animals (Itier *et al.*, 2003), deficits in other metrics such as startle are generalised and more difficult to relate directly PD. These results must therefore be treated with caution before stating that Parkin null animals described here are truly models of PD.

The variability in results between Parkin null mice is difficult to explain, with animals displaying different results on the same test. Although *Parkin* exons 2, 3 or 7 were deleted by different groups, all of these deletions are found in humans and are sufficient to cause PD and all cause truncation of the Parkin protein. While the possibility that some of these mutations were hypomorphic and some were complete loss of function cannot be ruled out, this seems unlikely given the understanding of Parkin structure and when considering that deletion of the same exon also produced differing results (Goldberg *et al.*, 2003; Itier *et al.*, 2003). In the case of

Parkin$^{S65A/S65A}$ mice, the amino acid substitution was designed to specifically prevent PINK1-mediated phosphorylation of Parkin. However, Parkin could still theoretically be recruited to mitochondria and allosterically partially activated by phospho-ubiquitin (See Section 1.3.5.2.2.2), thus retaining some function. However, substitution of Ser65 substitution was shown to prevent Parkin activity in primary cultures from mice and PD patients (Section 2.4.5.) but it is not possible to say whether this lack of activity is seen *in vivo*. In addition, these primary cultures were not neuronal, and so underlying mitophagy pathways may vary between tissue types.

One possible reason for the variability in phenotype could be the mixed genetic backgrounds of the animals tested (Perez and Palmiter, 2005). Flanking donor DNA is retained even after several crosses and can significantly influence the phenotype, as discussed in Section 1.5.2., 129 and C57BL6 animals display significant behavioural differences (Brooks, Jones and Dunnett, 2012) and the disappearance of phenotype when using coisogenic animals and false-positive calculations compared to mixed background animals suggests that background effects could be responsible for the mild behavioural differences observed rather than Parkin knockout (Perez and Palmiter, 2005). *Parkin*$^{S65A/S65A}$ mice were generated on a mixed C57BL/6J;C57BL/6N background (Mcwilliams *et al.*, 2018). While there are differences in behavioural profile between these substrains, they are more genotypically and phenotypically similar than 129 and C57BL/6 strains, and this similarity could potentially explain the lack of phenotype seen in these animals compared to Parkin null mice. Later inducible/stressor crosses with Parkin null mice were congenic and therefore background variation is not as much of a concern in interpreting these data (Table 2.1).

2.5.3. Mitochondria and Neurodegeneration

The most significant consistency between germline Parkin mutants, including *Parkin*$^{S65A/S65A}$, is the lack of neurodegeneration in the SNc (Table 2.1). The lack of neuronal death in this region is striking given that these models are designed to emulate PD and behavioural dysfunction is reported. Furthermore, some authors report an increase in extracellular striatal dopamine in mutant animals (Goldberg *et al*., 2003) (Itier *et al*., 2003) while others do (von Coelln *et al*., 2004) (Perez and Palmiter, 2004) adding to the variation in findings between models. Our own results from *Parkin*$^{S65A/S65A}$ mice demonstrate comparable levels of striatal dopamine between genotypes in addition to comparable nigrostriatal innervation (Section 2.4.5.). These data suggest that the nigrostriatal system is intact in these animals and can explain the lack of phenotype in *Parkin*$^{S65A/S65A}$ mice. In contrast to germline mutants, conditional Parkin null mice or Parkin null mice crossed with mtDNA stressor models display robust neurodegeneration in the SNc (Table 2.1). The presence of neurodegeneration in these

models suggests the existence of compensatory mechanisms which, in the case of germline mutations, can compensate for lack of Parkin activity but which are overwhelmed in the presence of acute loss of function or additional stressors. This conclusion is supported by comparable levels of mitophagy in WT and *Parkin*$^{S65A/S65A}$ SNc (Section 2.4.5.). Several other E3 ubiquitin ligases have been shown to function in mitophagy (Palikaras, Lionaki and Tavernarakis, 2018) and basal mitophagy can occur in a PINK1-independent manner in mouse SNc neurons (McWilliams *et al.*, 2018). Although mitophagy was not measured in previous germline models, it would be surprising if it were altered in light of these recent findings. These lack of effect of the Parkin S65A mutation on mitophagy in the present study and the discrepancy between absence/mild phenotype in germline models and robust parkinsonian phenotypes in inducible/stressor parkin null models suggests that either Parkin mutations result in PD through mitophagy-independent mechanisms or that Parkin is dispensable for basal mitophagy but plays an important role in mitophagy under stress conditions. It would be interesting to evaluate changes in mitophagy in Parkin null/stressor models.

Mitochondrial dysfunction was not assessed in previous germline models, but inducible/stressor models have demonstrated changes in mitochondrial number and morphology (Stevens *et al.*, 2015; Pinto, Nissanka and Moraes, 2017) and reduced mitochondrial complex function (Pickrell *et al.*, 2015) (Table 2.1). *Parkin*$^{S65A/S65A}$ mice exhibited striatal-specific reductions in mitochondrial respiration in an age-dependent manner (Section 2.4.5.). These data point to additional roles of Parkin in mitochondrial quality control (Section 1.3.5.2.2.3.) and suggest that mutations in Parkin could result in mitochondrial deficits which could lead to associated cellular dysfunction and presence of motor symptoms in the absence of largescale defects in mitophagy.

2.5.4. Conclusions

Parkin$^{S65A/S65A}$ mice exhibited a widened forepaw base-width (Figure 2.8B) compared to WT animals in the absence of any other deficits. In addition, no alteration in SNc number or striatal projections was discovered and basal mitophagy in the SNc was unaffected by the mutation. However, mitochondrial respiration was affected in the striatum with advanced age. These results suggest that *Parkin*$^{S65A/S65A}$ mice are not a robust model of PD. Although two patients carrying a *PRKN* S65N mutation have been identified, this number is clearly very small and one of these patients also carried additional genetic risk factors for PD (Section 2.4.5.) making interpretation of this mutation in humans difficult. The disparity in phenotype between germline Parkin null mutants and inducible/stressor crossed Parkin null animals suggests the existence of compensatory mechanisms and imply that loss of Parkin activity alone may not be sufficient for expression of a parkinsonian phenotype in mice. This may be

because, by merit of a relatively short lifespan, mice do not age to a sufficient degree to place additional stresses on cells, through accumulation of mtDNA mutations for instance. Models which accumulate mtDNA mutations to cause expression of a parkinsonian phenotype and suggest an additional "push" is needed for Parkin-mediated pathogenesis. However, *PRKN* mutations typically result in early onset PD in humans, raising the question of where additional stresses (if any are required for human PD) arise. Our increasing knowledge of PD risk variants may help to identify other factors which influence the disease. The results contained in this chapter and results from others summarised here suggest that the essentiality of the PINK1-Parkin mitophagy pathway should be reconsidered and that increasing work should be done to understand the additional roles of the pathway. Given that both *PINK1* and *PRKN* mutations are causative in PD, this pathway represents a promising target for identification of pathophysiological mechanisms and therapeutics research.

Chapter 3: Optimisation of Continuous L-DOPA Synthesis in the 6-OHDA Rat Model of PD

3.1. Introduction

3.1.1. General Information

Oral L-DOPA remains the gold-standard treatment for controlling PD motor symptoms in the initial stages but is associated with off-target effects as well as wearing-off, motor fluctuations, and dyskinesia with continued use (Section 1.6.3.1.). Neuroprotective gene therapy strategies have largely failed (Section 1.6.5.4.2.1.) but gene therapy strategies aiming to replace dopamine through ectopic expression of AADC or AADC in combination with TH and GCH1 (Palfi *et al.*, 2014) have been met with modest success in the clinical setting, albeit at lower levels than would be predicted by preclinical outcomes (Section 1.6.5.4.2.2.). These initial results encourage continued exploration of the approach but emphasis the need for optimisation. The production of a bicistronic AAV containing the *TH* and *GCH1* transgenes separated by a linker could represent such an optimisation.

3.1.2. Double Enzyme Approach for Gene Therapy

The rate-limiting enzymes for L-DOPA production are TH and GCH1 with AADC required for conversion to dopamine (Figure 1.11). Progressive nigrostriatal degeneration leads to progressive reductions in TH, GCH1, and AADC over the course of PD. However, serotonergic neurons are relatively spared from degeneration and AADC is still localised to the terminals of these cells within the striatum, in addition to spared nigrostriatal terminals. AADC activity has been reported to be reduced by 73.5% in 6-OHDA rat striatum, 92% in NHP putamen, and 87% in post-mortem putaminal tissue from PD patients (Ciesielska *et al.*, 2017). From these data it is apparent that although AADC activity is significantly lowered, some activity is still retained within the striatum/putamen even after severe nigrostriatal degeneration in experimental models and patients. Furthermore, non-dopaminergic cells such as fibroblasts can be induced to spontaneously produce L-DOPA *in vitro* via double transduction with *TH* and *GCH1* alone with grafting of transduced fibroblasts in the 6-OHDA-deneravated striatum resulting in production of dopamine (Bencsics *et al.*, 1996). Additional studies have demonstrated that monocistronic AAV-mediated ectopic expression of TH and GCH1 within the denervated striatum of 6-OHDA-lesioned rats is sufficient for dopamine production and associated

functional recovery in the absence of AADC (Kirik *et al.*, 2002; Björklund *et al.*, 2010). Thus, at the preclinical level, although AADC is needed for L-DOPA conversion spared dopaminergic and serotonergic neuronal processes within the lesioned striatum appear to be an adequate enough source of AADC for dopamine synthesis, removing the need for inclusion of AADC in gene therapy approaches.

3.1.3. Bicistronic Viral Vectors for L-DOPA Production

The first bicistronic viral vector used for dopamine replacement therapy was an AAV2/AAV5 pseudotype with *TH* and *GCH1* each under the control of separate human synapsin 1 (hSYN1) promoter (Cederfjäll *et al.*, 2012). The pseudotype was selected based on an experiment demonstrating that AAV1 and AAV5 serotypes transduced neurons to an equivalent degree and that both displayed superior transduction profiles to AAV2 (Dodiya *et al.*, 2010). A *WPRE* element was positioned downstream of *TH* to ensure a TH:GCH1 expression ratio of 5:1 as this ratio previously shown to result in optimal L-DOPA production in 6-OHDA-lesion rat striatum (Björklund *et al.*, 2009). The authors demonstrated that administration of AAV-*TH-GCH1* (*TH-GCH1*) at a titre of 9.7E13 gc/ml into the denervated striatum of hemi-parkinsonian 6-OHDA rats led to widespread expression of both transgenes across the striatum, overlying cortex and globus pallidus with associated increases in striatal L-DOPA and dopamine relative to lesion-only controls (Cederfjäll *et al.*, 2012) . Animals underwent extensive behavioural testing across a period of 40 weeks post-infusion and displayed complete functional recovery as assessed by the cylinder, adjusting steps, corridor and staircase tasks with a marked 50% reduction in apomorphine- and amphetamine-induced rotational behaviour. These results demonstrate that AAV-*TH-GCH1* is capable of significantly increasing striatal dopamine production in the denervated striatum and of producing a sustained and substantial in motor function. Worryingly however, treated animals displayed cell loss and increased microglial activation specifically within the ipsilateral globus pallidus, indicating an off-target adverse response to transfection within this neuronal subpopulation.

Following proof of concept, the researchers conducted a dose-response study using 4 separate titres of AAV-*TH-GCH1* at 1E11 gc/ml, 1E10 gc/ml, 5E9 gc/ml, and 9E8 gc/ml with a *GCH1-GCH1* control AAV at a titre of 2E11 gc/ml (Cederfjäll *et al.*, 2013). All animals infused with A*AV-TH-GCH1* displayed dose-dependent transgene expression within the denervated striatum. At the behavioural level, infusion of the TH-GCH1 at 1E11 gc/ml and 1E10 gc/ml mirrored previous results in 6-OHDA rats (Cederfjäll *et al.*, 2012) with widespread TH and GCH1 expression observed in the denervated striatum and complete and sustained functional recovery on the cylinder, adjusting steps, and corridor tests. No difference was seen in the extent of functional recovery using these two high titre AAVs despite a 10 times difference in dilution. In

comparison, delivery of TH-GCH1 at 5E9 gc/ml elicited only partial behavioural recovery on the corridor test at 12 weeks post-infusion despite only a two times dilution between 1E10 gc/ml and 5E9 gc/ml. Administration of AAV-*TH-GCH1* at 9E8 gc/ml and AAV-*GCH1-GCH1* produced no functional recovery. Pallidal cell loss was also observed in this experiment, although only at the highest dose of AAV-*TH-GCH1* and not in animals administered with an equivalent dose of AAV-*GCH1-GCH1*, suggesting that cell death within the globus pallidus is both titre-related and dependent upon TH expression. Following the success of high titre AAV-*TH-GCH1* in 6-OHDA-lesion rats, the same AAV was administered to the putamen MPTP-lesioned NHPs at a titre of 2.6E12 gc/ml. However, delivery of AAV-*TH-GCH1* was not associated with improvement in motor score up to 6 months post-infusion and transgenic TH expression and production of L-DOPA were undetectable.

In a follow-up study, MPTP-lesioned NHPs pre-treated with peripheral L-DOPA were administered with the same AAV-*TH-GCH1* AAV as in previous studies at doses of 9E9 gc/ml, 9E10 gc/ml or 9E11 gc/ml (Rosenblad *et al.*, 2019). In this study, treated NHPs displayed dose-dependent, sustained improvement in motor scores in the absence of peripherally-administered L-DOPA (off-L-DOPA) when AAV-*TH-GCH1* was delivered at titres of 9E10 gc/ml and 9E11 gc/ml. Both of these doses elicited equivalent motor improvement at levels directly comparable to that evoked by an optimal dose of peripheral L-DOPA in the absence of any adverse dyskinetic effects. However, putaminal expression of the *TH* transgene was found to be unexpectedly lower than that of *GCH1* despite placement of a *WPRE* downstream of *TH* to increase its expression above that of *GCH1* at a 5:1 ratio. Furthermore, TH was not co-expressed in all GCH1-positive cells suggesting differential transcription of transgenes despite successful transduction of cells. However, TH and GCH1 showed expected relative expression levels when human neuroblast cells were transduced with AAV-*TH-GCH1*, suggesting that the reduced TH expression level in NHPs is an unexplained *in vivo* effect.

Rosenblad and colleagues did not speculate as to how infusion of the same AAV-*TH-GCH1* in the same animal model evoked functional recovery and detectable TH expression in their study but no functional recovery and undetectable TH expression in the prior study (Cederfjäll *et al.*, 2013). The more recent study delivered 40µl of 2.6E12 gc/ml AAV-*TH-GCH1* per hemisphere to the caudate and putamen while Cederfjäll delivered 90µl per hemisphere of a maximum dose of 9E11 gc/ml to the putamen only. The deviations in outcomes are difficult to assess based on these experimental differences, particularly as a higher titre of AAV would typically be expected to result in more robust transgene expression. Despite these discrepancies, the behavioural recovery observed in NHPs treated with AAV-*TH-GCH1* is encouraging and suggests that this strategy has translational potential (Rosenblad *et al.*, 2019).

3.1.4. Review of the Literature and Optimisation of Approach

In reviewing the current literature detailing gene therapy-mediated dopamine replacement, several conclusions can be drawn which should direct future research. Firstly, therapeutic benefit of this approach lies within a narrow "Goldilocks zone". Functional recovery requires a high-titre AAV but an excessively high titre confers no additional therapeutic benefit but instead risks off-target cell loss and inflammation (Cederfjäll *et al.*, 2012, 2013). In contrast, reducing the titre outside of the Goldilocks zone confers little-to-no functional recovery. Secondly, functional improvement has been shown to be possible through expression of TH and GCH1 in the absence of AADC (Cederfjäll *et al.*, 2012, 2013; Rosenblad *et al.*, 2019). The latest study in NHPs suggests that residual AADC activity within the denervated putamen is sufficient for AAV-*TH-GCH1*-mediated functional improvement to a degree comparable to an optimal peripheral dose of L-DOPA but with significantly reduced risk of associated off-target effects, motor fluctuations and dyskinesia (Rosenblad *et al*., 2019). Therapeutic benefit in an MPTP-lesioned NHP is particularly encouraging given that AADC activity in this model has been reported to be reduced to a greater extent than in human tissue (Ciesielka *et al*., 2017). In fact, exclusion of AADC from viral vectors may improve the safety profile of this approach by limiting excessive production of dopamine (and preventing dopamine-induced toxicity) by imposing a ceiling on L-DOPA decarboxylation determined by the endogenous level of AADC (Björklund, Cederfjäll and Kirik, 2010). However, it must be noted that the efficacy of AAV-*TH-GCH1* therapy may be reduced as PD progresses and AADC activity falls due to ongoing neurodegeneration. However, MPTP-lesioned NHPs are considered a model of end-stage PD (Rosenblad *et al*., 2019), suggesting that patients could benefit from treatment even at late stages of the disease. Finally, problems with scaling-up therapy have been consistently reported. Despite excellent outcomes in 6-OHDA-lesioned rats, administration of AAV-*TH-GCH1* to NHPs has led to lack of functional improvement of TH expression (Cederfjäll *et al*., 2013) or functional improvement but unexpectedly low TH expression/co-expression with GCH1 despite a downstream *WPRE* (Rosenblad *et al*., 2019). Similarly, ProSavin produced only modest improvements in motor scores in PD patients (Palfi *et al.*, 2014) despite excellent outcomes at the preclinical level (Jarraya *et al.*, 2009). Recognition of the need to increase dopamine production led to optimisation of the ProSavin expression cassette which improved outcomes in MPTP NHPs (Badin *et al.*, 2019). The expression cassette used by Cederfjäll and Rosenblad and colleagues contains *TH* and *GCH1* under separate promoters, the use of which has been associated with promoter interference and suppression of transgene expression (See Section 1.6.5.3.6.) which could explain lack of TH expression as reported in the aforementioned experiments (Cederfjäll *et al.*, 2012, 2013; Rosenblad *et al.*, 2019).

Modification of the AAV-*TH-GCH1* expression cassette to drive expression of both transgenes from a single promoter may minimise the risk of transcriptional interference, improve transgene expression and represent a significant optimisation of this approach. Linkers could be introduced between transgenes to enable this (See Section 1.6.5.3.6.). Furthermore, although ProSavin has been shown to be safe in patients, clinical use of an optimised AAV would be preferable. AAVs have a superior safety profile and are considered non-pathogenic in humans, have very low risk of replication due to genetic engineering and need for a helper virus, have low immunogenicity due to absence of viral proteins, and carry very low risk of insertional mutagenesis (See Section 1.6.5.3.) In addition, the expanded tropism of AAVs allows flexible tailoring of gene therapy to a particular application or cell-type (See Section 1.6.5.3.2.). This proclivity for use of AAVs over LV is reflected in their higher usage in gene therapy clinical trials (Annoni *et al.*, 2018).

3.2. Aims

The primary aim of this study was to establish whether multicistronic AAVs containing *TH* and *GCH1* transgenes separated by linkers, but within a single transcriptional unit, led to improved transgene expression, dopamine production and associated behavioural recovery in 6-OHDA lesioned rats than AAVs with the same transgenes under tandem promoters. The secondary aim was to investigate whether usage of either an IRES or 2A linker led to better outcomes. To investigate these aims, 3 bicistronic *TH-GCH1* AAV2/AAV1-pseudotyped viral vectors were produced:

- GPT002 was designed to resemble the AAV used by Cederfjäll and colleagues (Cederfjäll *et al*., 2012, 2013; Rosenblad *et al*., 2019) and was used as a reference vector to allow indirect comparison with these previous experiments. This AAV contained the *TH* and *GCH1* transgenes under separate, tandem *CMV* promoters with a *WPRE* downstream of *TH*.
- MRX001 contained *TH* and *GCH1* transgenes separated by an IRES linker with both transgenes driven by a single CMV promoter with a *WPRE* downstream of *TH*.
- MRX002 resembled MRX001 except a 2A linker was positioned between the two transgenes instead of an IRES

To explore the primary and secondary aims, AAVs were administered into the denervated striatum of 6-OHDA-lesioned rats at one of two doses based on previous AAV-*TH-GCH1* dose-response experiments in rats demonstrating complete functional recovery with a dose of ≥1E10 gc/ml but only partial recovery with 5E9 gc/ml (Cederfjäll *et al*., 2013). Therefore 5E9 gc/ml was chosen as the highest dose in the current study based on evidence that this dose

represented the minimal threshold for any functional recovery in the previous experiment. By halving the higher dose, 2.5E9 gc/ml was selected as the lower dose in the current study based on the observation that administration of 1E10 gc/ml produced complete functional recovery in lesioned rats while halving the dose to 5E9 gc/ml led to incomplete functional recovery (Cederfjäll *et al*., 2013). Using GPT002 as a reference vector predicted to display similar efficacy to Cederfjäll's AAV-*TH-GCH1*, the primary and secondary aims of this experiment were explored through evaluation of functional improvement and transgene expression in the following way:

- Can administration of MRX001 and/or MRX002 improve transgene expression functional recovery at a dose of 5E9 gc/ml (the reported minimal threshold for partial functional recovery) compared to administration of an equivalent dose of GPT002?
  - Do MRX001 and MRX002 differ in efficacy?
- Can administration of MRX001 lead to sufficient transgene expression to evoke associated functional recovery at a dose of 2.5E9 gc/ml (below the reported minimal threshold for partial functional recovery) compared to administration of an equivalent dose of GPT002?

In this way, we aimed to establish whether expression of *TH-GCH1* from a single transcriptional unit and driven by a single promoter represented an optimisation of approach and also sought to evaluate whether inclusion of an IRES or 2A linker represented a further optimisation.

3.3. Materials and Methods

3.3.1. Generation of AAVs

AAVs were designed by Dr Mike McDonald and produced and titrated by Vigene Biosciences. Briefly, AAVs were produced through triple transfection of HEK293 cells, with the resulting viral particles purified by gradient ultracentrifugation. Next, titre was calculated as viral genome copy number per ml (gc/ml) by quantitative real-time PCR against the AAV2 ITR sequence. Three distinct AAVs were produced: GPT002, MRX001, and MRX002. GPT002 was constructed to be similar to the biscistronic vector used in Cederfjäll et al., (2012, 2013) while MRX001 and MRX002 were constructed on the same basis but contained either an IRES or 2A linker between TH and GCH1 transgenes (Table 3.1; Figure 3.2). Importantly, all vectors used in the current study featured the same TH and GCH1 transgenes under the control of the CMV promoter with a woodchuck hepatitis virus posttranscriptional regulatory element (WPRE) downstream of TH to enhance transcription of this transgene above that of GCH1 in a 5:1 ratio.

Study	Vector name	AAV serotype	Genes	Promoter	WPRE, downstream TH	Linker	Titres
Cederfjall	TH-GCH1	AAV2/AAV5	TH, GCH1	hSyn-1	Yes	None	Range
Current	GTP002	AAV2/AAV1	TH, GCH1	CMV	Yes	None	2.5E9, 5E9
Current	MRX001	AAV2/AAV1	TH, GCH1	CMV	Yes	IRES	2.5E9, 5E9
Current	MRX002	AAV2/AAV1	TH, GCH1	CMV	Yes	2A	5E9

Table 3.1. Differences and similarities between Cederfjall AAV and current study AAVs. *Current AAVs have the same serotype, transgenes and promoters with a WPRE downstream of TH. Current AAVs differ in the presence or absence of linker and type of linker, as well as titre.*

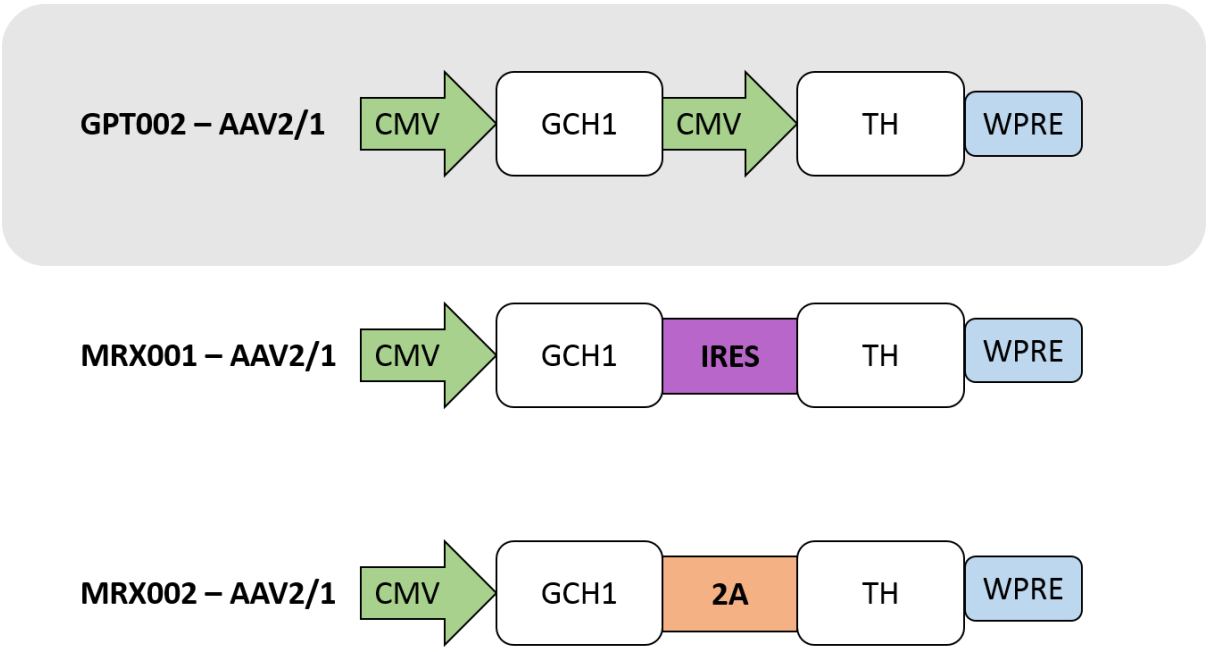

***Figure 3.2. Diagrammatic representation of the major components of AAVs used in the present study**. GPT002 has a tandem promoter configuration while MRX001 and MRX002 contain an IRES or 2A linker, respectively. A WPRE is downstream of TH in each case and all AAVs are an AAV2/1 pseudotype.*

3.3.2. Animal Husbandry and Legislation

Rats used in this study were maintained and tested in accordance with the 2013 European Union Directive 2010/63/EU and the UK Animals (Scientific Procedures) Act of 1986. Rats were housed in cages containing 4 rats per cage and were maintained under controlled conditions, with frequent monitoring, within holding rooms under a 06:00 – 20:00 light-dark cycle and a temperature of 21°C ± 1°C. Animals had *ad libitum* access to food and water throughout their lives and minimal environmental enrichment (tunnel, chew sticks, and bedding). Rats were health-checked and weighed weekly according to institutional guidelines.

An experimental cohort of 52 adult female Sprague Dawley (Crl:CD(SD)) rats of an average weight of 250g were received from Charles River at the beginning of this study. 6 animals were removed at the start of the study due to incomplete 6-OHDA lesioning and the experiment continued with 46 animals divided into 5 groups based on AAV type and titre. One animal from the lesion control group was retroactively removed from analysis at the end of the study due to discovery of an incomplete lesion during histological analysis, leaving a total of 45 experimental animals in the study. 3 rats (See Table 3.3.) were excluded from cylinder analysis due to making a very low number of touches during testing. Rats were removed from their holding room and taken to a procedure room to undergo motor testing. In the time between testing, animals were confined to their cages outside of being removed for weighing and health

checks. Rats were allocated to groups by a collaborator following 6-OHDA surgery in order to balance the extent of baseline amphetamine-induced rotations between groups. Behavioural testing and data analysis during the experiment were done blind to group.

Total = 45	Groups						
	Lesion	GPT002 2.5E9	GPT002 5E9	MRX001 2.5E9	MRX001 5E9	MRX002 5E9	Total
Adjusting Steps	6	7	8	8	8	8	45
Vibrissae	6	7	8	8	8	8	45
Cylinder	6	7	**7F**	**6F**	8	8	42
Amphetamine Rotations	6	7	8	8	8	8	45
Apomorphine Rotations	6	7	8	8	8	8	45
Optical Density	6	7	8	8	8	8	45
F: Animals failed test and were excluded							

Table 3.3. Representation of the number of animals in each test and reasons for exclusions*. The total number of animals possible were included in each test and optical density analysis with the exception of the cylinder task where 3 animals failed to complete sufficient touches.*

3.3.3. Stereotaxic Surgery

3.3.3.1 6-OHDA Lesions (Assisted by Rachel Hills)

12µg freebase 6-OHDA solution was pre-mixed with 0.001% ascorbate saline and kept frozen. Just prior to surgery, 6-OHDA solution was defrosted and kept on ice. Anaesthesia was induced by placing animals in a Perspex induction chamber which was slowly filled with a rising concentration of isoflurane (Teva, UK), reaching 4% total volume in 1L/min oxygen. Following induction to surgical plane anaesthesia, the animal was removed from the induction chamber and the fur overlying the scalp shaved with clippers. The animal was then placed on a heated mat within the sterile surgical area, and mounted to the stereotaxic frame (Kopf) with the toothbar set to -2.4. Rats were maintained under surgical plane anaesthesia using 1 - 3% isoflurane in carrier oxygen at 0.8L/min. Prior to surgery the animal was subcutaneously injected with Metacam (Boheringer Ingelheim, 5mg/ml at 1mg/kg) for post-surgical analgesia and Viscotears solution was applied to the eyes to prevent drying and irritation during the surgery. Dilute Videne solution was next spread across the shaved scalp area using a sterile cotton bud. A midline incision through the scalp was made using a sterile scalpel blade, and the tissue overlying the skull cleared using the blunt side of the scalpel blade and cotton buds. Bregma was located and its coordinates taken. Next, holes were drilled through the skull overlying the injection sites and 3µl of 6-OHDA at 4µg/µl was administered at 1µl/min using the following coordinates: AP: -4.0, ML: - 1.3, DV: -7.0 from dura to target the MFB. To inject 6-OHDA, a 5ml Hamilton syringe was fitted to a Harvard micro-drive infusion pump and

connected via polyethylene tubing to a stainless steel cannula. Following successful infusion, the cannula was slowly withdrawn after 2 minutes of diffusion time and cleaned with 70% ethanol and dH_2O between animals. The scalp was sutured with Vicryl Rapide (Ethicon) and a subcutaenous injection of 5ml glucose-saline (5% w/v and 0.9% w/v respectively) was administered. Rats were next placed in a recovery box heated to 30°C and left until fully conscious and mobile, before being returned to their home cage. Animals were monitored and weighed for 3 days post-surgery and cages were supplemented with additional food to aid recovery.

3.3.3.2. Infusion of AAV

Surgery was conducted using the same method as above except for the following differences. Prior to surgery, AAV solution was made up to the correct dose of either 5E9 gc/ml or 2.5E9gc/ml by dilution with Dulbecco's PBS with $MgCl_2$ and $CaCl_2$ (Sigma-Aldrich, UK). Dilution was carried out inside a tissue culture hood using sterile equipment. Working AAV solutions were placed on ice until needed and were not kept longer than 6 hours. All AAV waste was treated with Virkon for 24 hours before disposal. The following coordinates were used to target the dorsal striatum via 2 injection sites, each with 2 depths: AP: +1.0, ML: -2.8, DV_1: -4.5, DV_2: -3.5 and AP: 0.0, ML: -4.0, DV_1: -5.0, DV_2: -4.0. Each animal received 1.5µl of AAV solution at the ventral site and 1.0µl of AAV solution at the dorsal site, both delivered at a speed of 6.67nl/sec. A 1 minute diffusion time was observed after the ventral infusion, followed by a 3 minute diffusion time after the dorsal infusion before the cannula was slowly removed.

3.3.4. Behavioural Testing

A behavioural baseline was taken 4 weeks post-lesion and behavioural testing was resumed from 3 weeks post-AAV infusion onwards (See Figure 3.4). The baseline result was compared with the final time-point for each test.

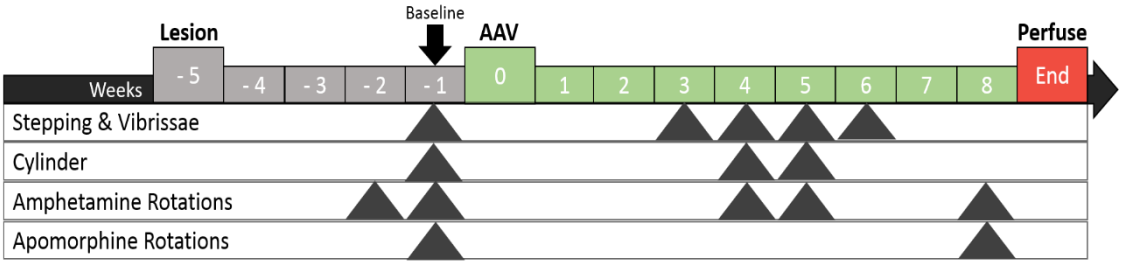

***Figure 3.4. Experimental Timeline**. A baseline was taken at 4 weeks post-lesion. Grey triangles indicate the week at which each test was administered over the course of the study.*

3.3.4.1. Adjusting Steps Test

Rats were assessed for forelimb akinesia using the adjusting steps test. Rats were held horizontally within forelimb-reaching distance of the bench top. The ipsilateral or contralateral forelimb was restrained while the unrestrained limb was left free and placed on the bench to permit a weight-bearing touch. The animal was then slowly moved horizontally across a 100cm section of bench with its paw making contact and the number of adjusting steps made were counted. The ipsilateral and contralateral limbs were tested 3 times each in forwards and backwards directions and averages taken. After each individual test, the animal was returned to its home cage and the remaining animals in the cohort tested before being tested again. If an animal struggled against restraint and stepping was disrupted, it was returned the start of the testing area and the assessment repeated.

3.3.4.2. Vibrissae-Evoked Forepaw Placing Test

Spontaneous sensorimotor function was tested using the vibrissae-evoked forepaw placing test. Rats were held and restrained in the same way as in the adjusting steps test but positioned slightly below the bench surface and with the vibrissae parallel to the bench edge. In order to test function, the animal was raised upwards from below the bench surface so that the vibrissae ipsilateral to the forelimb to be tested brushed against the edge of the bench. Care was taken to ensure only the vibrissae made contact with the bench. Healthy animals display a tendency to abduct the forelimb and place the forepaw on to the bench surface in response to whisker stimulation on the ipsilateral side. Lesioned animals will display normal forepaw placing in response to whisker stimulation on the intact side, but few to no forepaw placements

on the lesioned side. Both the intact and impaired forelimbs were tested in this manner for 10 consecutive runs each and the number of successful forepaw placements counted.

3.3.4.3. Cylinder Test

Animals were tested for forelimb locomotor asymmetry using the cylinder test. Animals were tested in a Pyrex® glass beaker (300mm x 180mm) with a three-sided mirror placed directly behind the beaker to allow a 360° view of the animal within the apparatus. When placed inside a novel environment, animals tend to rear onto their hind legs and explore the arena, placing their forepaws against the inside walls of the cylinder as they do so. Healthy animals will show a roughly equal distribution of left and right forepaw touches during the task, while impaired animals will show a noted preference for intact (ipsilateral) forepaw touches. Rats were placed into the cylinder and video recorded. The number of forepaw touches (irrespective of side) was live-scored and, upon reaching 30, the trial terminated. Post-hoc scoring of the first 20 weight-bearing touches was conducted from video footage and the number of touches made with the impaired forepaw (contralateral touches) was calculated as a percentage of the 20 total touches. Animals were tested once per time-point, but where animals showed little activity in the trial and did not reach 30 touches within 15 minutes of being placed inside the cylinder, the number of touches was recorded and the animals removed from the apparatus. Animals were then retested later the same day or the next day and the number of touches between trials combined. If an animal performed no touches it was removed from the analysis for the cylinder test (See Table 3.3).

3.3.4.3. Amphetamine-Induced Rotations

The frequency of ipsilateral amphetamine-induced rotations animals performed over 90 minutes was recorded following i.p. injection with 2.5 mg/kg of methamphetamine hydrochloride (Sigma-Aldrich, UK) in sterile saline. Following injection, animals were fitted with an elastic band around their abdomen and placed in one of a bank of 16 automated rotometer bowls (Rotorat, Med Associates, VT) with the elastic band attached to the recording arm of the apparatus. Animals were left undisturbed in a dark room for the duration of the trial and were tested once per time-point. Amphetamine rotations were used as an exclusionary criterion for experimental inclusion at 4 weeks post-lesion. Six of the 52 rats lesioned with 6-OHDA performed fewer than 6 amphetamine-induced rotations per minute, suggesting an incomplete lesion of < 95% SNc cell loss. These animals were thus removed from the experiment and received no further intervention or testing.

3.3.4.4. Apomorphine-Induced Rotations

The frequency of contralateral apomorphine-induced rotations animals performed over 60 minutes was recorded following subcutaneous injection with 0.05mg/kg apomorphine hydrochloride hemihydrate (Sigma-Aldrich, UK) in sterile saline. Animals were fitted to rotomoters and the trial conducted as above.

3.3.5. Histology

3.3.5.1. Perfusion-Fixation

Animals were killed via intraperitoneal injection of Euthatal (Merial, Essex, UK) before being transcardially perfused with PBS (pH 7.4) for 2 minutes, followed by 4% PFA (pH 7.4) for 6 minutes to fix tissue. Following fixation, animals were decapitated and their brains removed. Brains were then post-fixed in 4% PFA for 4 hours at room temperature, after which they were cryopreserved in 25% sucrose at room temperature until they sank. Brains were then sliced into 40µm sections using a sliding sledge freezing microtome (Leitz, Wetzlar) in a 1:12 series, after which the sections were transferred into an antifreeze-filled 48 well plate and stored at -20°C.

3.3.5.2. Immunohistochemistry

Sections from each animal were placed in individual pots filled with TBS. Sections were quenched to limit endogenous peroxidase activity before blocking with 5% normal goat serum in TXTBS. Next, an anti-TH monoclonal primary antibody (Fisher, MA1-24654) was applied (at a concentration of 1:400 with 5% normal goat serum in TXTBS) and brains were incubated at room temperature overnight. The TH antibody was chosen to detect both endogenous TH and the transgenic TH. Following washing, an anti-mouse biotinylated secondary antibody was applied and sections incubated for 3 hours before ABC kit was applied and DAB staining completed. Sections were removed from DAB solution and thoroughly washed in TBS before being mounted onto double subbed 1% gelatinised slides (Thermo Scientific, Menzel Gläser) and allowed to dry overnight. The next day, sections were dehydrated and cleared *in situ* on slides by placing in the following solutions, successively, for 10 minutes each: 70%, 95% and 100% alcohol solutions, followed by xylene. Slides were then cover-slipped using DPX mountant and allowed to dry.

3.3.5.3. Optical Density (Assisted by Rachel Sellick)

Photographs of 3 successive TH-stained sections with clearly visible dorsal striatum were taken at 4X magnification under the microscope (Leica). The anatomical position of the sections were kept as consistent as possible between animals and microscope setting were also kept consistent throughout. Optical density analysis was carried out using ImageJ software. For each

brain section used, an area of interest was drawn around the dorsal striatum on the ipsilateral (denervated) and contralateral (intact) side as well as over a piece of overlying (unstained) cortex on each side. Using the pre-set calibration settings in ImageJ, the optical density of the ipsilateral and contralateral striata and cortices was separately measured. Next, the striatal value was subtracted from the cortical value for each side in order to control for variation in background staining. An average optical density value for the ipsilateral and contralateral dorsal striatum was then taken from the 3 sections measured and compared.

3.3.6. Statistics

All statistical tests were conducted in SPSS. When data were not normal or did not display equal variances, they were transformed accordingly before an ANOVA was performed.

Test	Figure	Statistical Test	Independent Variables	Dependent Variables
Stepping	Ipsi Forward (3.5A) Contra Forward (3.5B) Ipsi Backward (3.5C) Contra Backward (3.5D)	Two-way mixed ANOVA	Group x Time	Number of Steps
Vibrissae	Ipsilateral (3.6A) Contralateral (3.6B)	Two-way mixed ANOVA	Group x Time	Number of Responses
Cylinder	3.7	Two-way mixed ANOVA One Sample T-Test	Group x Time 50%	% contralateral touches % contralateral touches
Amphetamine	3.8	Two-way mixed ANOVA	Group x Time	Rotations/minute
Apomorphine	3.9	Two-way mixed ANOVA	Group x Time	Rotations/minute
Optical Density	3.1	One-way ANOVA	Group	Optical Density

***Figure 3.5. Statistical details**. The statistical test and variables used for each behavioural test are listed.*

3.4. Results

3.4.1. Adjusting Steps Task

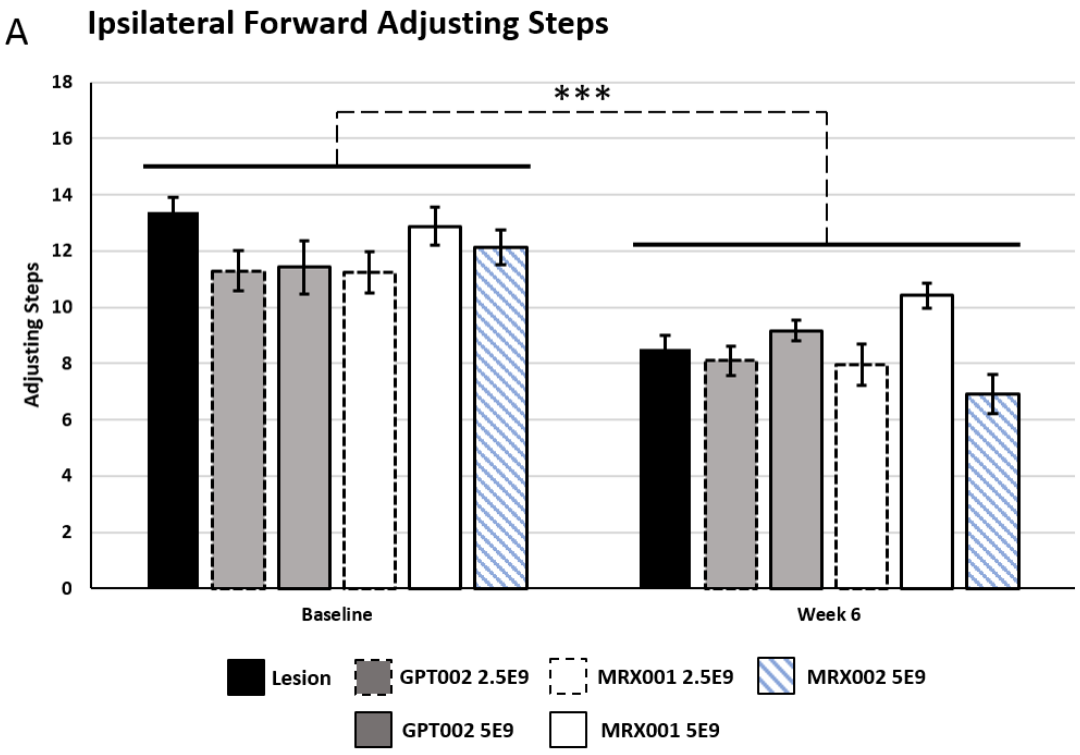

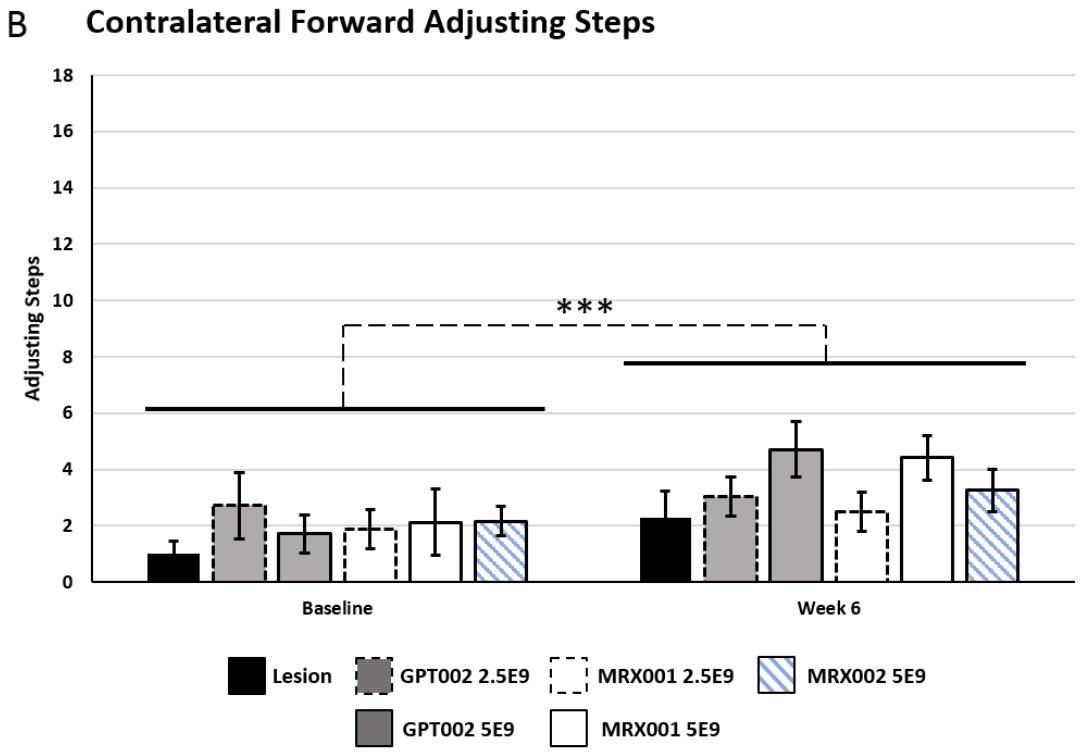

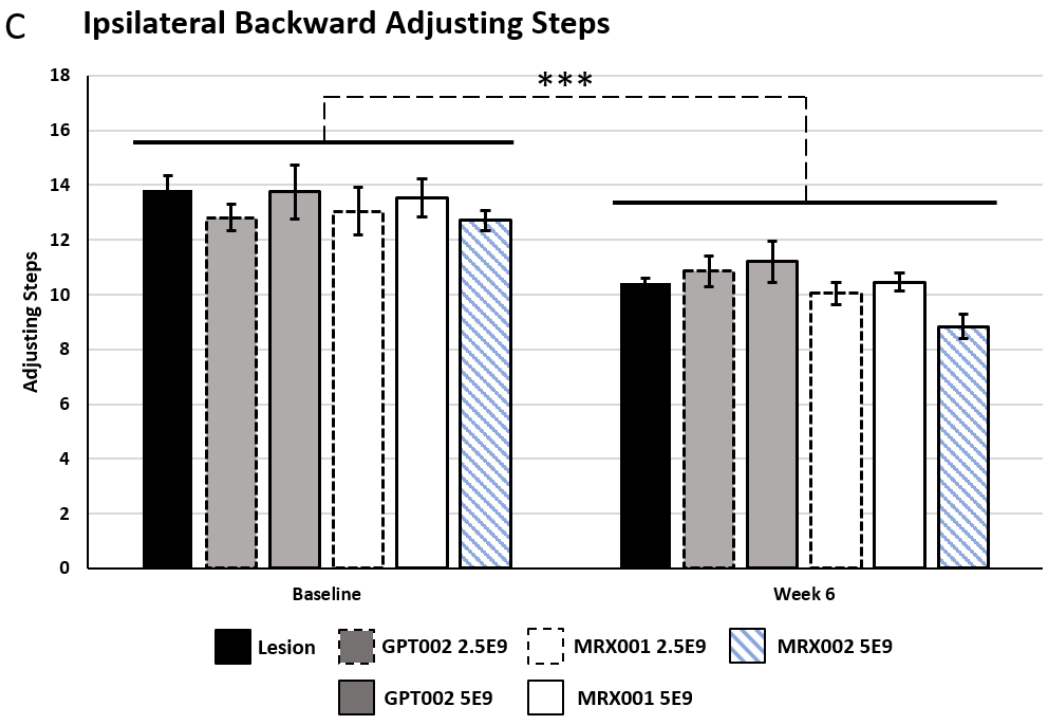

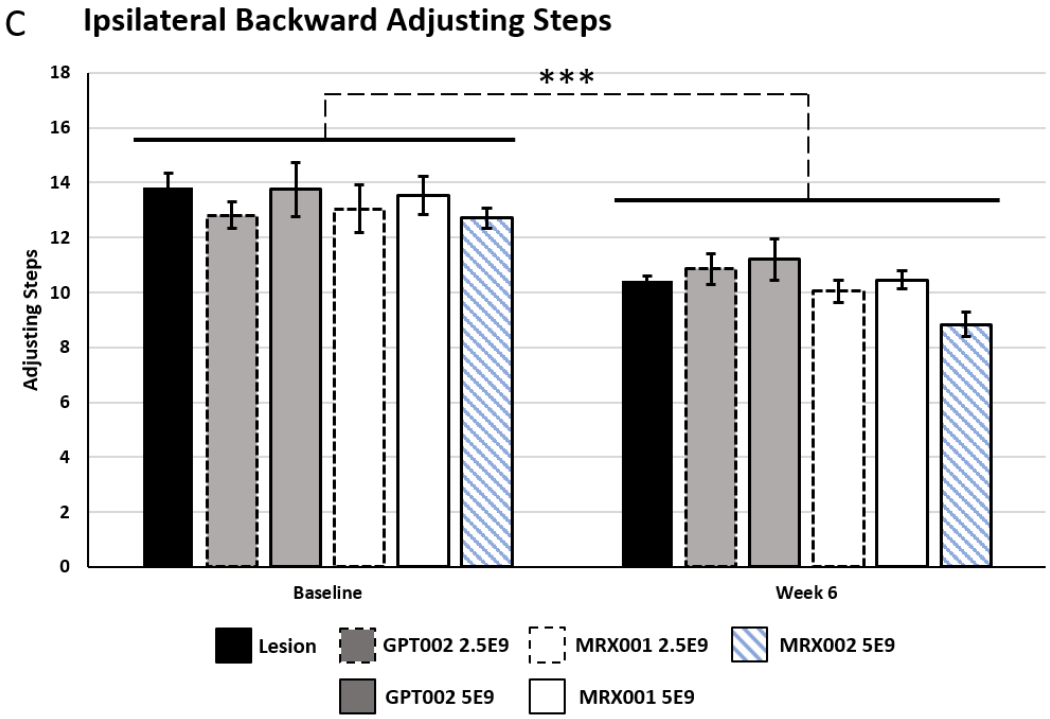

Figure 3.6. The performance of animals on the adjusting steps task. *Animals made significantly fewer adjusting steps with the ipsilateral paw, and significantly more adjusting steps with the contralateral paw at 6 weeks compared to baseline. The average number of ipsilateral forward adjusting steps (A), contralateral forward adjusting steps (B), ipsilateral backward adjusting steps (C) and contralateral backward adjusting steps (D) made during 3 non-consecutive trials are shown at baseline and week 6 of testing. Significant differences in the number of adjusting steps between time-points are indicated by significance bars and dashed connecting lines with asterisks ($p \leq 0.05$*, $p \leq 0.01$**, and $p \leq 0.001$***). Values are expressed as means ± SEM. All: Lesion n = 6, GPT002 2.5E9 n = 7, GPT002 5E9 n = 8, MRX001 2.5E9 n = 8, MRX001 5E9 n = 8, MRX002 5E9 n = 8.*

The number of adjusting steps made between baseline and week 6 of testing were compared (Fig 3.3). Rats made fewer ipsilateral forward (Figure 3.6A) and ipsilateral backward (Figure 3.6C) adjusting steps at 6 weeks compared to baseline ($F(1, 39) = 87.907$, $p < 0.001$) and ($F(1, 39) = 83.801$, $p < 0.001$) respectively, an effect which likely reflects the tendency of Sprague-Dawley rats to become habituated to the task due to repeated exposure. Animals in the MRX001 5E9 group made significantly more ipsilateral forward steps (Figure 3.6A) than those in the MRX001 2.E9 and MRX002 groups but there were no interactions between group and week ($F(5, 39) = 1.794$, p = n.s.) suggesting these differences stem from natural variation between animals rather than an effect of treatment. The number of ipsilateral backward steps did not differ between groups ($F(5, 39) = 1.639$, p = n.s.) and there were no interactions between group and week ($F(5, 39) = 0.700$, p = n.s.) (Figure 3.6C).

In contrast to the ipsilateral paw, rats made significantly more contralateral forward (Figure 3.6B) and contralateral backward (Figure 3.6D) adjusting steps ($F(1, 39) = 15.963$, $p < 0.001$) and ($F(1, 39) = 177.632$, $p < 0.001$) respectively. However, no difference was seen in the number of contralateral steps made in the forward ($F(5, 39) = 0.733$, p = n.s.) or backward ($F(5, 39) = 0.624$, p = n.s.) directions and there were no interactions between group and week ($F(5, 39) = 0.700$, p = n.s.) and ($F(5, 39) = 1.405$, p = n.s.). These data reveal that administration of AAVs were unsuccessful in improving impaired paw performance above lesion-only control level and that the increase in the number of steps observed at week 6 is not associated with treatment. Instead, the elevation in contralateral steps may be due to repeated exposure to the task or other factors independent of treatment.

To minimise inter-subject variation, data were normalised by calculating the change (as integers) in the number of steps between baseline and week 6 (Figures not shown). No significant changes in the number of ipsilateral or contralateral steps in either direction between baseline and week 6 were noted (data not shown) further supporting the lack of AAV-induced functional improvement on this task.

3.4.2. Vibrissae-Evoked Forepaw Placement

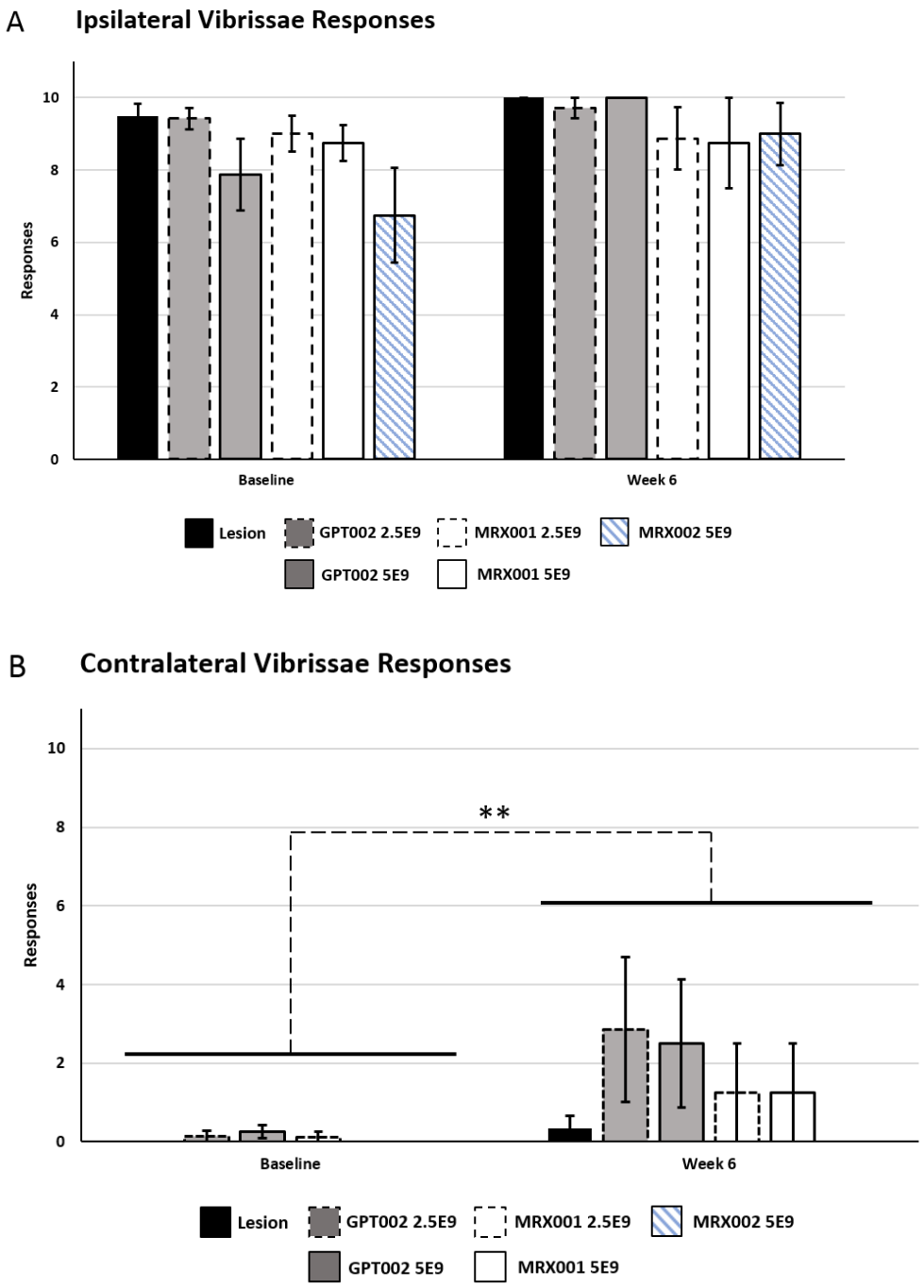

Figure 3.7. The performance of animals on the vibrissae-evoked forepaw placement task. *The number of responses animals made to ipsilateral vibrissae stimulation did not differ between baseline and week 6, while the number of responses made in response to stimulation of the contralateral vibrissae increased significantly over the same period. The average number of responses to 10 consecutive trials of ipsilateral vibrissae stimulation (A) and contralateral vibrissae stimulation (B) are shown for baseline and week 6 of testing. Significant differences in the number of responses between time-points are indicated by significance bars and dashed connecting lines with asterisks ($p \leq 0.05$*, $p \leq 0.01$**, and $p \leq 0.001$***). Values are expressed as means ± SEM. Lesion n = 6, GPT002 2.5E9 n = 7, GPT002 5E9 n = 8, MRX001 2.5E9 n = 8, MRX001 5E9 n = 8, MRX002 5E9 n = 8.*

The number of forepaw placements performed in response to vibrissae stimulation was compared between baseline and week 6 of testing. The number of ipsilateral forepaw placements (Figure 3.7A) did not differ between baseline and week 6 ($F(1, 39) = 3.792$, p = n.s.) or between treatment groups ($F(5, 39) = 1.255$, p = n.s.). In contrast, the number of contralateral forepaw placements (Figure 3.7B) increased between baseline and week 6 ($F(1, 39) = 5.757$, $p = 0.021$) although there was no effect of treatment $F(5, 39) = 8.008$, p = n.s.) and no significant interactions between treatment and week ($F(5, 39) = 0.643$, p = n.s.) suggesting that the increase in responses placements was independent of a treatment effect. Notably, a large amount of variability in the number of responses at week 6 was observed which could indicate that a small number of animals improved on this task.

3.4.3. Cylinder

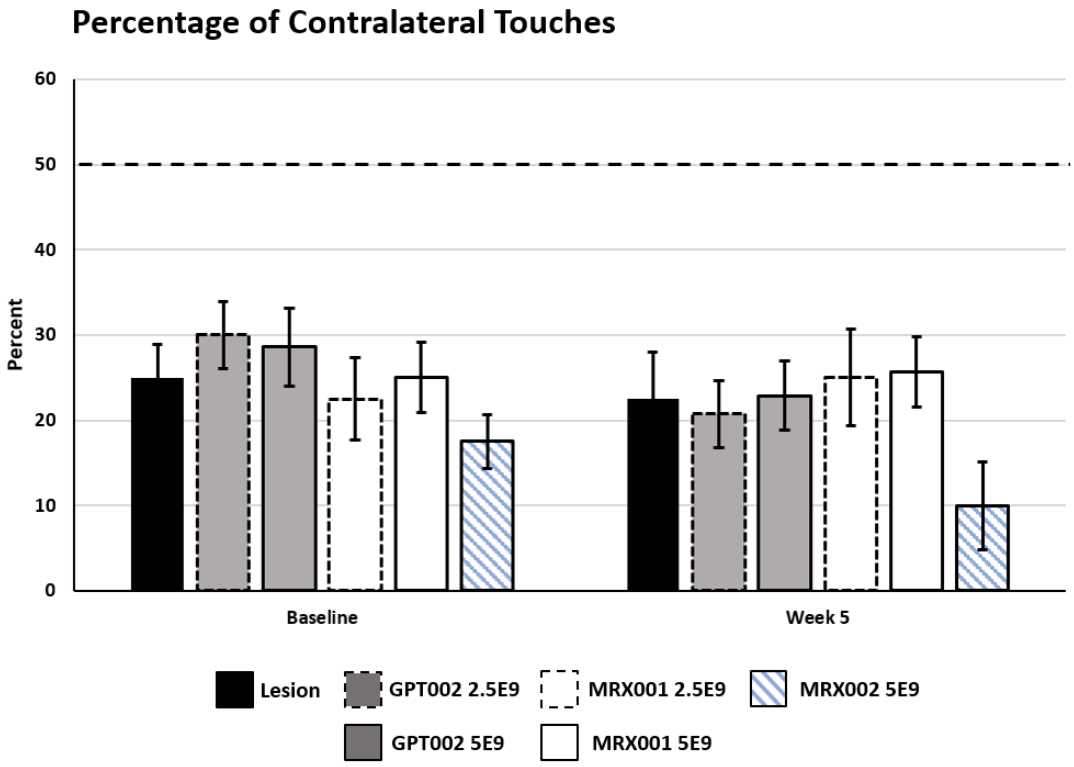

Figure 3.8. Performance of animals on the cylinder task. *Animals showed no significant improvement on the cylinder task between baseline and week 5. The percentage of touches animals made with their contralateral paw (from 20 total touches) while inside the cylinder is plotted with a dashed line at 50% indicating the expected amount of touches healthy animals would make with the left paw. Values are expressed as means ± SEM. Lesion n = 6, GPT002 2.5E9 n = 7, GPT002 5E9 n = 7, MRX001 2.5E9 n = 6, MRX001 5E9 n = 8, MRX002 5E9 n = 8.*

The percentage of touches animals made with their ipsi- and contra-lateral forepaws within the cylinder were compared between baseline and week 5 (Figure 3.8). The percentage of contralateral forepaw touches did not increase between baseline and week 5 ($F(1, 36) = 3.127$, p = n.s.) and there was no effect of treatment ($F(5, 36) = 1.785$, p = n.s.) which indicates that treatment had no beneficial effect on this test. Lack of therapeutic benefit was confirmed with one-sample T-tests which showed the mean percentage of contralateral touches were significantly different from 50% for each group at both time-points (data not shown), demonstrating that treatment did not elevate usage of the impaired forelimb to expected healthy levels.

3.4.4. Amphetamine-induced Rotations

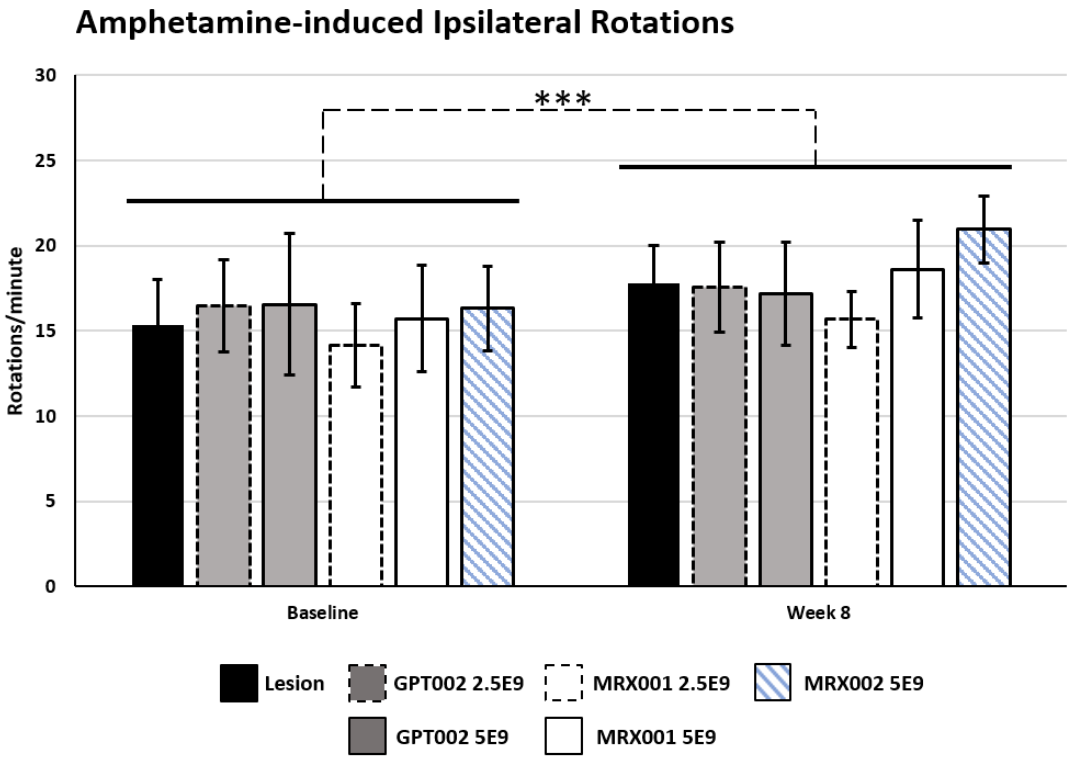

Figure 3.9. Amphetamine-induced rotational behaviour. *Animals showed a slight but significant increase in the number of amphetamine-induced rotations they performed at week 8 compared to baseline. The average number of amphetamine-induced rotations animals performed at baseline and week 8 are shown. Significant differences in the number of rotations/minute between time-points are indicated by significance bars and dashed connecting lines with asterisks ($p \leq 0.05$*, $p \leq 0.01$**, and $p \leq 0.001$***). Values are expressed as means ± SEM. Lesion n = 6, GPT002 2.5E9 n = 7, GPT002 5E9 n = 8, MRX001 2.5E9 n = 8, MRX001 5E9 n = 8, MRX002 5E9 n = 8*

The average number of amphetamine-induced ipsilateral rotations per minute were compared between baseline and week 8 (Figure 3.9). Rats exhibited an increase in ipsilateral rotational behaviour at week 8 compared to baseline ($F(1, 39) = 14.021$, $p = 0.001$) in the absence of an effect of treatment ($F(5, 39) = 0.313$, p = n.s.) or interactions between treatment group and week ($F(5, 39) = 0.561$, p = n.s.). Elevation in dopamine within the denervated striatum would be expected to decrease the number of amphetamine-induced rotations. The modest increase in rotational behaviour over time coupled with the statistical readouts suggest that AAVs had no therapeutic benefit on this task.

3.4.5. Apomorphine-Induced Rotations

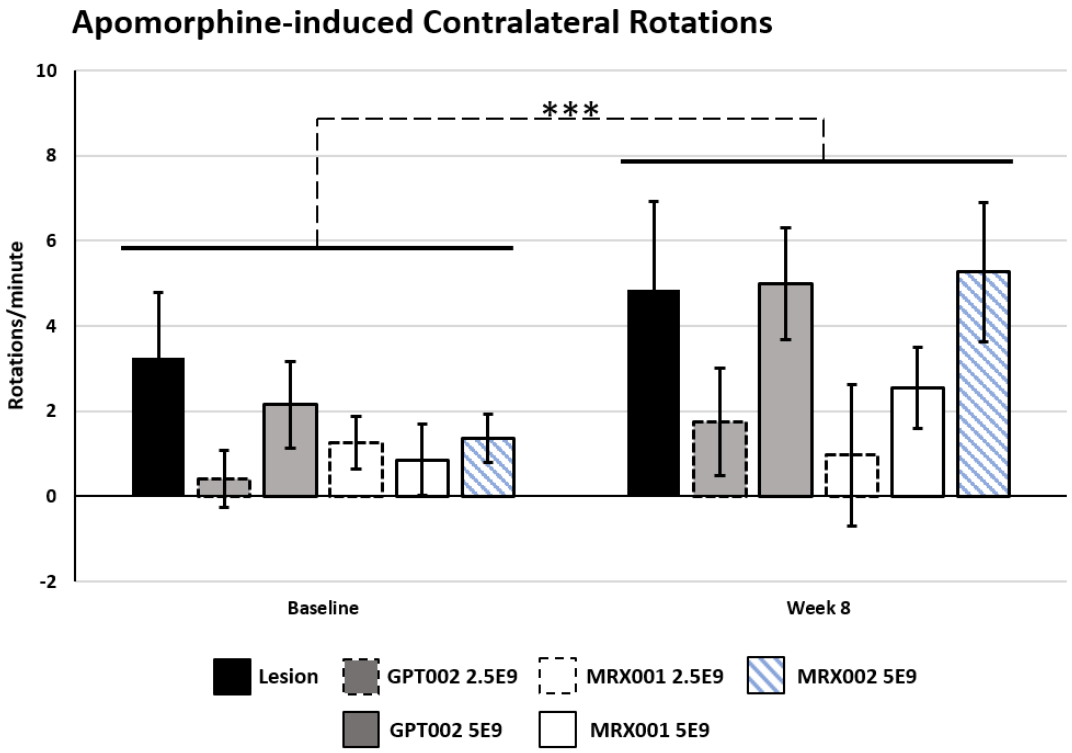

Figure 3.10. Apomorphine-induced rotational behaviour. *Animals showed a slight but significant increase in the number of apomorphine-induced rotations they performed at week 8 compared to baseline. The average number of apomorphine-induced rotations animals performed at baseline and week 8 are shown. Significant differences in the number of rotations/minute between time-points are indicated by significance bars and dashed connecting lines with asterisks ($p \leq 0.05$*, $p \leq 0.01$**, and $p \leq 0.001$***). Values are expressed as means ± SEM. Lesion n = 6, GPT002 2.5E9 n = 7, GPT002 5E9 n = 8, MRX001 2.5E9 n = 8, MRX001 5E9 n = 8, MRX002 5E9 n = 8.*

The average number of apomorphine-induced contralateral rotations per minute were compared between baseline and week 8 (Figure 3.10). Similar to amphetamine-induced rotation results, animals displayed an increase in apomorphine-induced rotational behaviour over time ($F(1, 39) = 13.510$, $p = 0.001$) with no effect of treatment ($F(5, 39) = 1.524$, p = n.s.) and no interactions between treatment group and week ($F(5, 39) = 1.434$, p = n.s.). As such, AAV treatment does improve behaviour on this task. However, as in the vibrissae-evoked forepaw placement task, a high degree of variability between responses was observed at week 8 which could suggest that AAVs affected apomorphine-induced rotational behaviour in some animals.

3.4.6. Optical Density (Assisted by Rachel Sellick)

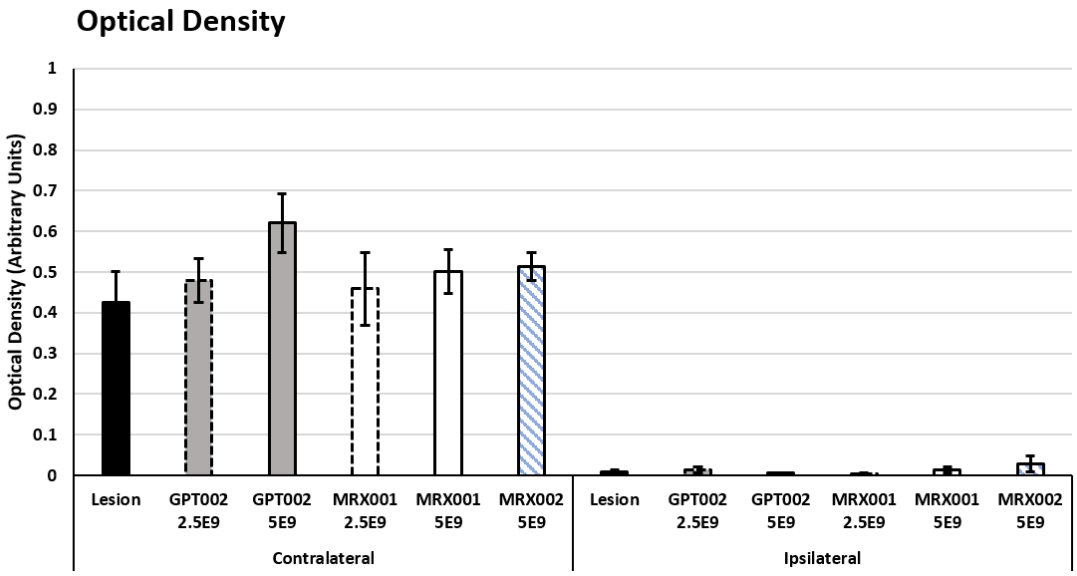

Figure 3.11. Optical Density of TH-staining in the intact (contralateral) and denervated (ipsilateral) dorsal striatum. *TH was significantly more highly expressed in the contralateral striatum than the ipsilateral striatum, and all AAVs failed to increase the level of truncated TH above control levels in the ipsilateral striatum. The optical density of TH-positive staining is shown. Values are expressed as means ± SEM. Lesion n = 6, GPT002 2.5E9 n = 7. GPT002 5E9 n = 8, MRX001 2.5E9 n = 8, MRX002 5E9 n = 8.*

Optical density values were obtained for the contralateral (intact) and ipsilateral (lesioned) animals in brains stained for TH (Figure 3.11). Optical density of the ipsilateral striatum did not differ between groups ($F(5, 44) = 1.032$, p = n.s.), indicating that none of the AAVs were able to increase TH immunoreactivity above lesion-only controls. This suggests that expression of TH was very low in the striatum and could indicate that AAVs were administered at an insufficient titre for measurable TH expression. Representative brains are displayed in Figure 3.12.

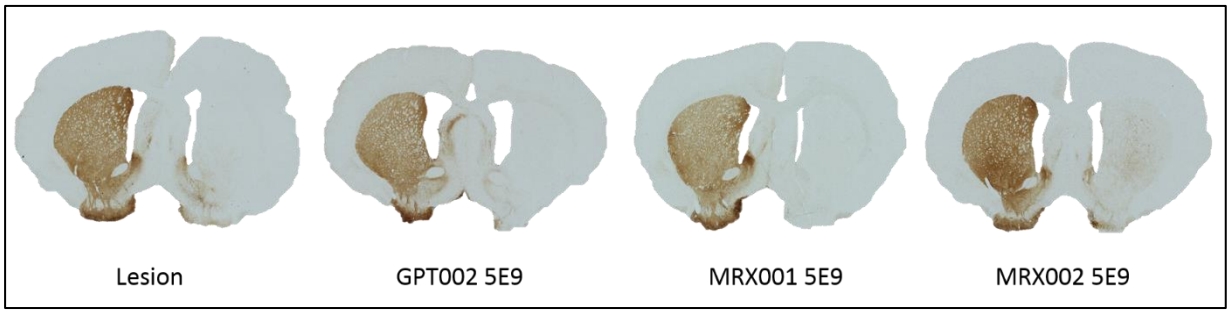

Figure 3.12. Coronal sections of brains stained for TH. *TH-positive staining is clearly discernible in the intact striatum with a profound reduction in immunoreactivity on the denervated side despite administration of the highest dose of AAV.*

3.4.7. Re-evaluation of Viral Titre

Given the lack of functional recovery and TH expression, the stock solution titre of the AAVs was reassessed (Table 3.13). When titrated against the viral *ITR* sequence, the titre of GPT002 and MRX001 was largely unchanged from the original values. However, when AAVs were titrated against the *TH* and *GCH1* transgenes, the titre was much lower than that measured against the *ITR*.

	Sequence Titrated Against			
AAV	**ITR (Original)**	**ITR (Re-evaluation)**	**TH**	**GCH1**
GPT002	1.95E13 gc/ml	1.97E13 gc/ml	1.09E13 gc/ml	3.00E12 gc/ml
MRX001	1.45E13 gc/ml	1.24E13 gc/ml	8.98E12 gc/ml	7.81E12 gc/ml
MRX002	NA	NA	NA	NA

Figure 3.13. Titration of AAVs against the ITR, TH, and GCH1 sequence. *TH-positive staining is clearly discernible in the intact striatum with a profound reduction in immunoreactivity on the denervated side despite administration of the highest dose of AAV.*

3.5. Discussion

3.5.1. Summary

Over the course of this study, Sprague Dawley rats were unilaterally lesioned with 6-OHDA to generate animals with hemi-parkinsonian motor deficits which were measured and validated 4 weeks post-lesion using amphetamine and apomorphine-induced rotations, adjusting steps test, vibrissae-evoked forelimb placement test, and cylinder test. After generating this behavioural baseline, animals were divided into a lesion-only control and 5 treatment groups. Animals in each treatment group received a unilateral striatal (ipsilateral to lesion) infusion of the following AAVs carrying *TH* and *GCH1*: GPT002 (at a dose of 5E9 gc/ml or 2.5E9 gc/ml), MRX001 (at a dose of 5E9 gc/ml or 2.5E9 gc/ml), and MRX002 at a dose of 5E9 gc/ml. From 3 weeks post-AAV, animals were tested over the course of 5 weeks on the tests listed above with varying frequency (See Figure 3.4). No improvement in motor function relative to lesion-only controls was observed for any treatment group over the duration of testing, suggesting that AAVs were not an effective therapy.

3.5.2. Behavioural Evaluation

Animals performed significant more adjusting steps with their contralateral paw at week 6 compared to baseline (Figure 3.6B, D). However, lesion-only control animals also performed significantly more steps with time, indicating that this effect is independent of AAV administration. The elevation in the number of steps is difficult to explain but may be due to a change in operator handling between baseline and testing which artificially inflated the results. Although there may be a possibility that animals showed a partial recovery of function due to repeated exposure to the task, the number of adjusting steps was higher than baseline at 3 weeks post-AAV (data not shown) suggesting that increased exposure was not responsible for this change. In addition, Cederfjäll and colleagues did not report a comparable effect in control animals in their experiment (Cederfjäll *et al.*, 2013). The reduction in number of ipsilateral steps (Figure 3.6A, C) is likely due to reduced response of rats due to familiarity with the task.

Although there was an increase in the number of responses to contralateral vibrissae stimulation between baseline and week 6, there was no significant difference between groups (Figure 3.7B). In addition there was a large amount of variability in the number of contralateral responses between individuals within groups. 10 contralateral responses at week 6 were recorded for two animals in both GPT002 groups, and one animal in both MRX001 groups while 2 contralateral responses were recorded for one animal in the lesion groups. Remaining animals within the above groups, and all animals in the MRX002 group, made zero responses at week 6. Thus, a minority of animals scoring highly within groups is responsible for the

increase from baseline, making evaluation difficult. Only a small minority of animals appear to recover, and recovery appears to be all-or-nothing on this task. Cederfjäll and colleagues did not validate behavioural recovery on this task, making comparison difficult.

Animals did not display recover of forelimb symmetry in the cylinder task (Figure 3.8) and performance was unchanged between baseline and week 5 of testing in contrast to the complete recovery shown by Cederfjäll and colleagues (Cederfjäll *et al.*, 2013). The number of amphetamine- and apomorphine-induced rotations increased between baseline and week 8 of testing (Figures 3.9 & 3.10). Previous work has displayed a floor effect of around 50% reduction in rotational behaviour in treated animals displaying complete behavioural recovery on other measures due to the ectopic nature of dopamine release from transduced striatal cells (Björklund, Cederfjäll and Kirik, 2010; Cederfjäll *et al.*, 2012). The increase in rotational behaviour in response to amphetamine and apormorphine reported here suggest that insufficient dopamine was produced and released to reduce lateralisation of dopamine release in or affect dopamine receptor sensitivity, respectively.

3.5.3. Optical Density and Viral Titres

The TH primary antibody used to stain tissue was selected to detect both endogenous TH and transgenic TH protein to permit a direct comparison of optical density between TH-positive tissue in the ipsilateral and contralateral striatum. Administration of AAVs failed to increase levels of TH in the ipsilateral striatum above lesion-only control levels (Figure 3.11), indicating that AAVs were unsuccessful in mediating ectopic TH expression to a significant degree. These results are in stark contrast to those obtained by Cederfjäll and colleagues who reported detectable transgenic TH expression at a dose of 9E8 gc/ml which is significantly lower than the highest dose of 5E9 gc/ml administered in the present study (Cederfjäll *et al*., 2013). Thus it appears that the lack of behavioural recovery in treated animals is due to insufficient production of dopamine due to insufficient expression of transgenic TH. The lack of ectopic TH expression suggests that either AAVs were not administered at a sufficient titre or that transgene expression was compromised following transduction.

In re-evaluating the viral titres (Table 3.13), the most obvious reason for lack of efficacy is that AAVs were administered at an insufficient titres. AAVs were diluted to working concentrations of 5E9 gc/ml or 2.5E9 gc/ml based on a stock solution titration calculated by qPCR against the viral *ITR* sequence. However, this method of titration has been reported to lead to artifical inflation of viral titre due to comparison against a standard calibration curve based on a linearised plasmid (D'Costa *et al.*, 2016). When conducting qPCR against the *TH* or *GCH1* trasngenes, the viral titre was shown to be up to 6 times lower than that calculated through

use of the *ITR* (Table 3.13). Therefore, working solutions were diluted to a significantly greater extent than realised and were below 5E9 and 2.5E9 gc/ml. This is highly significant as the high dose of 5E9 gc/ml used in this study was selected to be at the minimum threshold for behavioural recovery. A large reduction in dose below this threshold would be expected to result in no efficacy upon administration due to insufficient transgene expression and thus dopamine production. Cederfjäll and colleagues titrated their AAV against the *WPRE* sequence which is located internally to the *ITR*, meaning that their titration is likely to be more representative of the actual value.

3.5.4. Conclusions

In conclusion, no behavioural recovery was observed on any task in any of the treatment groups over the duration of testing. Animals in all groups displayed increased stepping with their contralateral paw post-AAV, but the presence of this characteristic in the lesion-only group suggests this is a treatment-independent feature potentially stemming from operator conduct. The lack of behavioural rescue in this study makes it impossible to compare the efficacy of GPT002, MRX001, and MRX002 and so we cannot conclude whether inserting linkers results in more efficient transgene expression and behavioural amelioration at lower titres *in vivo*. The apparent lack of efficacy of all AAVs is most likely explained by inflated titration of stock solutions leading to administration of a sub-therapeutic dose of AAV a dose-response experiment should be conducted to confirm this.

Chapter 4: An *in vivo* Characterisation of the Potential ERK-Modulating Peptide RB5

4.1. Introduction

HD represents a difficult target for treatment. Despite being caused by a single mutation, HD is characterised by wide-ranging dysfunction stemming from multiple dysregulated pathways. As such, instead of a conventional single-target approach, therapies could be designed to target multiple pathways at once. Therapeutic modulation of the Ras-ERK signalling pathway may present the opportunity for such widespread regulation. However, due to the complexity of the pathways involved, any potential ERK-modulating compound should first be characterised in healthy WT animals.

4.1.1. Mitogen-Activated Protein Kinases (MAPKs) Cascades

Mitogen-activated protein kinases (MAPKs) are a group of 14 highly-conserved protein serine/threonine (Ser/Thr) kinases (in mammals) subdivided into conventional and atypical MAPKs (Cargnello and Roux, 2011). The conventional MAPKs are the best-studied members of this group of proteins and contain the extracellular signal-regulated kinases 1/2 (ERK1/2), c-Jun amino-terminal kinases 1-3 (JNK1-3) and p38 (α, β, γ, δ) families (Cuenda and Rousseau, 2007; Cargnello and Roux, 2011; Zeke *et al.*, 2016). The members of these families form key components in some of the most ancient signal transduction pathways present in all eukaryotic cells, phosphorylating downstream substrates in response to receptor activation and thus converting extracellular signals into a wide array of intracellular responses (Cargnello and Roux, 2011). The existence of multiple MAPK transduction pathways within the same cell allows for coordinated signalling in response to an array of distinct inputs (Krishna and Narang, 2008). Each cascade consists of at least 3 tiers of enzymes (Roskoski, 2012). Upon extracellular stimulation, a GTP-binding protein or adaptor protein activates the first tier of the cascade – the MAPK kinase kinase (MAP3K) – which when activated is able to phosphorylate MAP2K which in turn phosphorylates the MAPK. Following MAPK activation, specific downstream substrates (known as MAPK-activated protein kinases (MAPKAPK) are phosphorylated and continue the phosphorylation cascade. By responding to distinct extracellular stimuli and effectively transducing the signal to appropriate intracellular targets, individual MAPK cascades

act to regulate key cellular processes such as proliferation, differentiation, development, stress response, and apoptosis (Rubinfeld and Seger, 2005).

4.1.1.2. The Ras-ERK Signalling Cascade

The first and best characterised MAPK cascade is the Ras-ERK signalling pathway, which is activated in response to multiple signalling events and has hugely wide-ranging regulatory roles in processes such as cell adhesion, cell cycle progression, cell migration, cell survival, differentiation, metabolism, proliferation, and transcription and translation (Roskoski, 2012). The Ras-ERK pathway contains 4 tiers before the subsequent MAPKAPK tier. The MAP4K tier of this pathway is the membrane-bound protein Ras, which is a small GTPase consisting of 3 isoforms: H-Ras, K-Ras, N-Ras (Hobbs, Der and Rossman, 2016). In its inactive form, Ras is bound to GDP but, upon activation, is converted to Ras-GTP – its active form. Upon BDNF-TrkB binding, conversion of GDP to GTP is mediated by the guanine nucleotide exchange factor son of sevenless (Sos1/2), which is recruited to the plasma membrane upon receptor stimulation (Bonfini *et al.*, 1992; Pierre, Bats and Coumoul, 2011) (Figure 4.1). In the case of N-methyl-D-aspartate (NMDA) receptor activation, Ras is activated by the Ras protein-specific guanine nucleotide-releasing factor 1 (Ras-GRF1) (Krapivinsky *et al.*, 2003) (Figure 4.1). Active Ras is then able phosphorylate, and recruit to the plasma membrane, the next MAP3K tier in the cascade, Raf (A-Raf, B-Raf, C-Raf), through a multistage process involving dimerisation (Wan *et al.*, 2004). Raf is a serine/threonine kinase which activates the MAP2K MEK (MEK 1/2) through phosphorylation of Ser218 and Ser222 within the activation loop of human MEK (Zheng and Guan, 1994). MEK1/2 are dual-specificity protein kinases which phosphorylate the MAPK tier proteins ERK 1/2 at Tyr204/187 and Thr202/188 in the activation loop of the human protein (Akinleye *et al.*, 2013) to generate active phospho-ERK (P-ERK) (Figure 4.1). ERK1/2 are the only identified substrates of MEK, denoting high signalling specificity at this level of the cascade. Multiple scaffold proteins also regulate the function of the pathway, acting to co-localise individual proteins to increase efficiency of the cascade (Casar and Crespo, 2016).

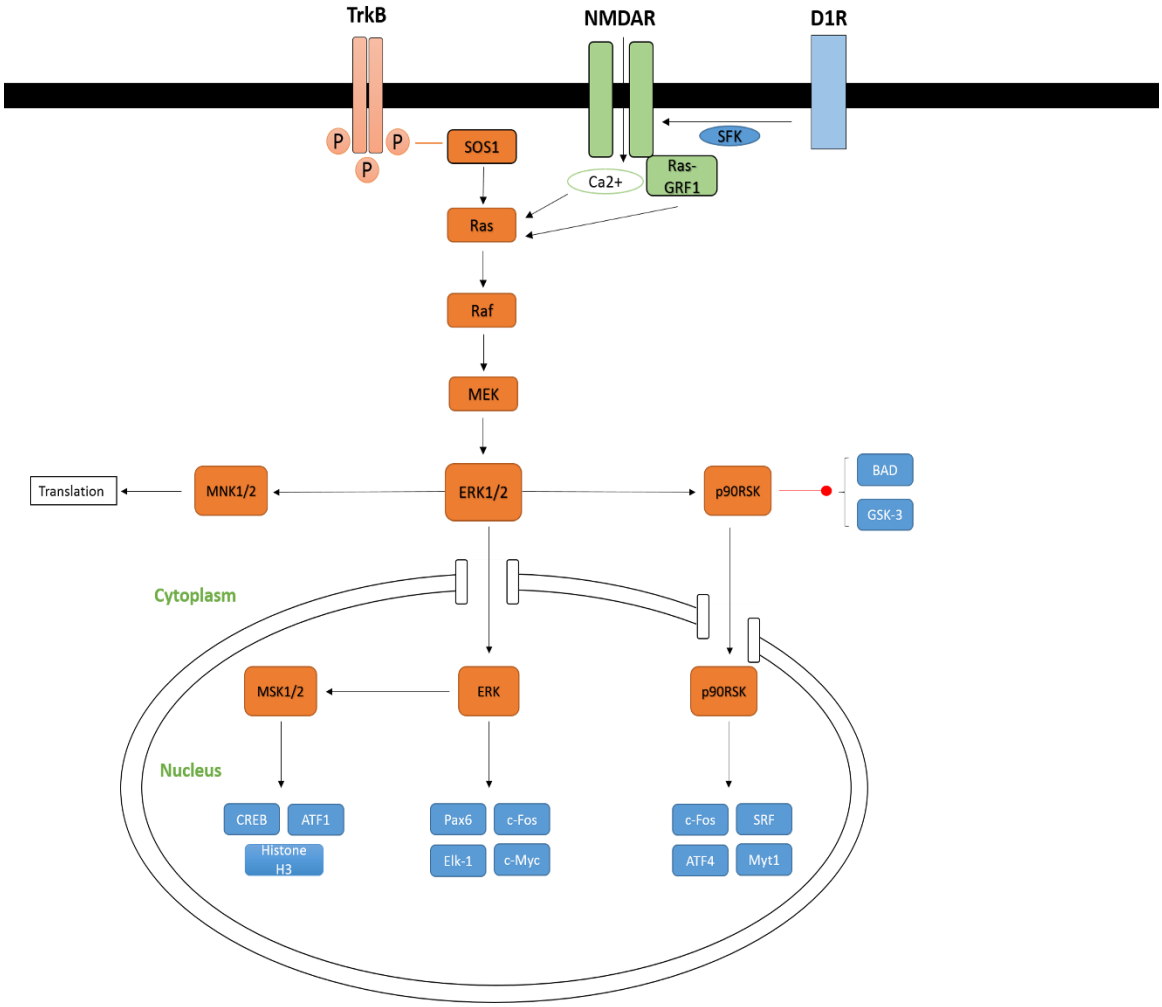

Figure 4.1. ERK activation in response to TrkB and NMDA receptor signalling. *ERK1/2 are activated by MEK as a result of signalling through the Ras-ERK cascade. ERK/2 phosphorylates multiple cytoplasmic and nuclear substrates to generate a widespread signalling response.*

4.1.1.3. ERK1/2

ERK1/2 (collectively referred to as ERK in this thesis) are the prototypical MAPKs. ERK1 and ERK2 are encoded by *MAPK3* and *MAPK1* genes, respectively. The ERK isoforms arose around 400 million years ago as a result of a whole genome duplication event early in the vertebrate phylum (Buscà *et al.*, 2015). When measured between initiation and stop codons, the *MAPK1* gene (located at chromosome 16p11.2) is around 15 times larger than the *MAPK3* gene (located at 22q11.22), with the first intron of MAPK1 spanning 59kb (Buscà *et al.*, 2015). ERK1/2 are ubiquitously expressed but are particularly enriched in the brain, skeletal muscle, thymus and heart (Cargnello and Roux, 2011). ERK1 and ERK2 cDNA was first cloned in the 1990s (Blank *et al.*, 1996) and the protein sequences of each isoform share an 84% sequence homology (Buscà, Pouysségur and Lenormand, 2016). The ERK1 protein is larger than ERK2, consisting of a 44 kDa protein made up of 379 amino acids, while ERK2 is a 42 kDA protein of 360 residues

in humans (Roskoski *et al*., 2012). The difference in size between ERK1 and ERK2 is accounted for by a 17 amino acid insertion and a 2 amino acid insertion within the N-terminal and C-terminal of ERK1, respectively (Buscà, Pouysségur and Lenormand, 2016). ERK is a proline-directed protein kinase with many intracellular targets, phosphorylating substrates at Ser/Thr residues and displaying preferences for substrates containing a Pro-Xxx-Ser/Thr-Pro sequence (Roux and Blenis, 2004). Upon appropriate receptor activation, ERK1 and ERK2 are activated in parallel and have been reported to exhibit identical substrate specificity (Von Kriegsheim *et al.*, 2009). P-ERK1/2 phosphorylate cytoplasmic, cytoskeletal, and nuclear substrates directly and, by phosphorylating downstream MAPAPKs, also result in indirect phosphorylation of cytoplasmic and nuclear targets, propagating the ERK signal (Ünal, Uhlitz and Blüthgen, 2017). The number of ERK substrates is vast, consisting of 659 direct targets and 1,848 indirect targets (Ünal, Uhlitz and Blüthgen, 2017). Amongst the best characterised cytoplasmic MAPKAPKs directly activated by P-ERK are: ribosomal S6 kinase 1-4 (RSK1-4), mitogen- and stress-activated protein kinase 1/2 (MSK1/2), and MAPK-interacting kinase 1/2 (MNK1/2) (Hauge and Frödin, 2006; Carriere *et al.*, 2008; Dreas *et al.*, 2017). In the nucleus, P-ERK1/2 directly phosphorylate a number of transcription factors (TFs) and TF regulators and plays a crucial role in inducting the expression of immediate early genes (IEGs) (Sgambato *et al.*, 1998; Whitmarsh, 2007). Termination of the ERK signal requires dephosphorylation of either one of tyrosine or threonine motifs and is mediated by tyrosine-specific, threonine-specific or dual-specificity phosphatases (Kondoh and Nishida, 2007).

4.1.1.4. The Neuronal Roles of ERK

As mentioned, *MAPK3/MAPK1* gene expression is particularly high in the brain. ERK signalling has been shown to be integral to synaptic plasticity and learning and memory (reviewed extensively (Adams and Sweatt, 2002; Thomas and Huganir, 2004). Briefly, ERK signalling has been shown to be important in induction and maintenance of long-term potentiation (LTP) (English and Sweatt, 1997), induction of long-term depression (LTD) (Kawasaki *et al.*, 1999), AMPA receptor trafficking (Zhu *et al.*, 2002), neuronal excitability (Morozov *et al.*, 2003), and structural plasticity of dendritic spines (Wu, Deisseroth and Tsien, 2001). These cellular processes are associated with learning and memory and it should be therefore unsurprising that ERK signalling has been demonstrated to be crucial for long-term memory formation on multiple tasks (Atkins *et al.*, 1998; Blum *et al.*, 1999; Shiflett and Balleine, 2011). Deficits in amygdala synaptic plasticity and long-term memory of avoidance tasks, with intact short-term memory and learning, was demonstrated in a Ras-GRF1 knockout mouse exhibiting reduced ERK activation, signifying the specificity of ERK-related deficits (Brambilla *et al.*, 1997).

At the level of the striatum, ERK has been shown to be critically important for instrumental learning and performance through induction of corticostriatal LTP (Calabresi *et al.*, 2000; Valjent *et al.*, 2005; Shiflett and Balleine, 2011). Coordinated activation of dopamine D1Rs and glutamatergic NMDA receptors within striatal MSNs is required for robust ERK activation (Figure 4.1) and induction of corticostriatal LTP, with LTP likely enabled by P-ERK-mediated $K_v4.2$ potassium channel downregulation and associated enhanced cellular responsiveness (Varga *et al.*, 2000). For example, during striatal-dependent instrumental learning, animals undergo action-outcome association learning. Upon making a correct response to a particular stimulus, animals are rewarded. Reward is associated with dopamine release and D1R activation on MSNs in the dorsal striatum which, when activated concurrently with NMDARs, results in a robust increase in ERK signalling within these cells (Shiflett, Brown and Balleine, 2010). In this way, increases in ERK signalling are phased with periods of learning, resulting in corticostriatal LTP induction and association encoding (Shiflett and Balleine, 2012). Furthermore, striatal ERK signalling has been shown to be involved in affect and arousal (Todorovic *et al.*, 2009), as well as in adaptations and behaviours in response to repeated exposure to drugs of abuse (Girault *et al.*, 2007) and is potentially implicated in habitual behaviour due to excessive training (Shiflett, Brown and Balleine, 2010). ERK signalling has also been demonstrated to be essential for the learning of striatal-dependent motor tasks (Hutton *et al.*, 2017). Global or intrastriatal inhibition of ERK signalling in mice being trained on the rotarod task resulted in normal early acquisition motor skill but impaired consolidation of the motor skill, demonstrating the importance of striatal ERK signalling in motor learning and performance as well as instrumental learning and performance (Bureau *et al.*, 2010). In addition, striatal ERK signalling has been demonstrated to play a key role in regulation of locomotor activity (Besusso *et al.*, 2013) with deletion of ERK from either direct or indirect pathway MSNs resulting in a hypo- or hyper-locomotor phenotype respectively (Hutton *et al.*, 2017). Thus, inhibition of striatal ERK signalling results in marked impairment in learning and memory as well as basal locomotion.

All descriptions of ERK-mediated impairments listed in this section thus far have been caused by a deficiency in ERK through inhibition or genetic manipulation. However, a group of developmental conditions, known as RASopathies which commonly exhibit elevated Ras-ERK signalling, offer insight into the importance of correct regulation of the ERK cascade. Neurofibromatosis 1 (NF1) is the most common RASopathy and is caused by loss of function mutations within the *NF1* gene which encodes neurofibromin (Rauen, 2013). Neurofibromin is a GTPase-activating protein which functions to catalyse the conversion of active Ras-GTP to inactive Ras-GDP, thus terminating downstream signalling through ERK (Cichowski *et al.*, 2003).

NF1 is characterised by developmental defects such as craniofacial abnormalities, heart defects and delayed growth (Ryu and Lee, 2016) as well as learning difficulties and attentional deficits in 30 – 45% of patients (Silva *et al.*, 1997). A mouse model of NF1 displayed impaired long-term spatial memory, which could be overcome by extensive training, without deficits in cued fear conditioning (Silva *et al.*, 1997). Crucially, impaired spatial memory was shown to be caused by deficits in hippocampal LTP (Costa *et al.*, 2002) and cognitive impairments could be rescued through genetic and pharmacological attenuation of aberrant increased Ras-ERK signalling in these mice (Costa *et al.*, 2002; Li *et al.*, 2005). In addition, NF1 mice have been shown to display motor impairments (Kim *et al.*, 2014). Although most published work has focused on the role of the cerebellum, (van der Vaart *et al.*, 2011) report no cerebellar component to motor dysfunction in their hands. However, when tested on the rotarod, mice displayed normal early acquisition of the task but fail to consolidate the motor skill later on, a pattern reminiscent to that previously reported following ERK inhibition (Bureau *et al*., 2010).

From these data it is clear that Ras-ERK signalling plays a crucial role in synaptic plasticity underlying behaviour. In addition, both attenuation and enhancement of ERK signalling lead to cognitive and motor deficits in mice. However, rescue of cognitive impairments in a mouse model of NF1 strongly suggests that ERK-modulating therapies can overcome such deficits, and that ERK represents a promising therapeutic target for disorders characterised by cognitive and motor dysfunction.

4.1.1.5. ERK in Huntington's Disease

The Ras-ERK pathway has been shown to be heavily involved in cell survival, synaptic plasticity, and striatal-mediated behaviours (see Section 1.5.), all of which are negatively affected in HD. However, despite a general agreement on impaired neurotrophic signalling in HD patients and models, the evidence for alterations in ERK activity in HD is conflicted, even within the same model (reviewed extensively in (Bowles and Jones, 2014). However, StHdhQ111 cell models, HdhQ111 mice, and HD patient fibroblasts all demonstrate a reduction in basal ERK activation while exon 1 models show variation with increases as well as decreases reported (Table 4.2). Considering the acute toxicity of mHTT fragments and severe phenotype of exon 1 models, elevated ERK activation may not be comparable with that seen in the human condition or may in fact be a beneficial compensatory mechanism. Therefore, given the evidence of impaired BDNF signalling and the importance of the ERK pathway in TrkB-mediated signalling, as well as decreased ERK activation in the more representative HdhQ111 mouse and patient fibroblasts, increasing ERK signalling could represent a therapeutic approach for HD. This assertion is supported by evidence of ERK-mediated neuroprotection in HD-associated pathogenic processes. Firstly, ERK activation is stimulated in response to mHTT *in vitro*, with ERK signalling

resulting in a corresponding decrease in pro-apoptotic caspase-3 and 7 activation (Apostol *et al.*, 2006). Furthermore, ERK signalling has been implicated in processes thought to result in MSN cell death. Ginés and colleagues reported a specific reduction in TrkB-mediated ERK activation and corresponding hypersensitisation of mHTT-expressing cells to oxidative stress compared to controls, a characteristic which was rescued by pharmacological activation of the ERK pathway (Ginés, Paoletti and Alberch, 2010). Furthermore, dysregulated ERK signalling has been extensively implicated in glutamate-induced excitotoxicity (Bodai, Laszlo; Marsh, 2013). In addition, existing drugs which enhance Ras-ERK signalling have been demonstrated to be neuroprotective in HD models. Polyphenols are naturally occurring compounds which activate ERK signalling. Two of these compounds, fisetin and resveratrol, were found to be neuroprotective *in vitro* and *in vivo*, reducing pathology in HD *Drosophila* and improving rotarod performance and lifespan in R6/2 mice (Maher *et al.*, 2011). In addition, the drug pizotifen which is typically used to treat migraine was shown to increase ERK signalling which exerted a corresponding increase in the viability of StHdhQ111 cells and protected against neuropathology and motor impairment on the rotarod in the R6/2 mouse (Sarantos *et al.*, 2013).

Model	ERK alteration	Brain Region	Age	Reference
StHdhQ111 Cells	Decreased	NA	NA	Gines et al., 2010; Baksi et al., 2013
R6/1	Increased	Striatum	20 - 30 weeks	Saavedra et al., 2011
R6/2	Increased	Striatum	8 - 12 weeks	Lievens et al., 2002
	Unchanged	Striatum	10 - 11 weeks	Gianfriddo et al., 2004
	Decreased	Striatum	10 weeks	Simmons et al., 2013
HdhQ111	Decreased	Striatum	E15	Liot et al., 2013
Human fibroblasts	Decreased	NA	NA	Melone et al., 2013

Table 4.2. Alternations in ERK in HD models*. Variable changes in ERK are seen in different cell and animal models of PD. Adapted from Bowles and Jones, 2014.*

4.1.1.6. ERK1/2 Functional Redundancy or Isoform-Specific Functions?

The retention of functionally redundant genes across evolutionary time is unusual, and duplicate genes are typically progressively eliminated (Buscà, Pouysségur and Lenormand, 2016). At the protein level, the two ERK isoforms appear to be very similar, displaying an extremely close protein sequence identity within substrate-binding domains (Lee *et al.*, 2004), parallel activation upon receptor signalling (von Kriegsheim *et al*., 2009) similar half-lives (68 hours and 53 hours respectively) (Schwanhausser *et al.*, 2011), and substrate phosphorylation

with equivalent efficiency (Lefloch, Pouyssegur and Lenormand, 2008). Furthermore, although mammals express both ERK1 and ERK2, cartilaginous fish, birds, and frogs do not have *MAPK3* genes and therefore do not express ERK1 (Buscà, Pouysségur and Lenormand, 2016). On the other hand, snakes, lizards and geckos do not express ERK2 (Buscà, Pouysségur and Lenormand, 2016). The similarity in function between ERK isoforms and the presence of only a single isoform in certain animals would appear to suggest that ERK1 and ERK2 are functionally redundant. However, several studies have reported isoform-specific functions of these proteins.

Among the first reports of isoform functional specificity came from (Pagès *et al.*, 1999; Saba-El-Leil *et al.*, 2003) who demonstrated that germline knockout of *Mapk3* in embryos produced viable, fertile mice while knockout of *Mapk1* was embryonic lethal. These papers suggested that ERK isoforms have different roles in development, and that ERK2 is able to compensate for ERK1 but not *vice versa*. In addition, ERK1 knockdown has been described to promote proliferation and tumorigenesis *in vitro*, while ERK2 knockdown exerted the opposite effect (Vantaggiato *et al.*, 2006). These results suggest functional differences between isoforms, with only ERK2 driving proliferation and ERK1 limiting ERK2 activity. Differences in nuclear shuttling velocity of activated ERK isoforms have been described and suggested to be responsible for limitation of ERK2 activity (Marchi *et al.*, 2008). In this model, P-ERK1 shuttles through the nuclear envelope more slowly than P-ERK2, rendering P-ERK1 more susceptible than P-ERK2 to dephosphorylation and subsequent inactivation. As such, P-ERK2 would be expected to be accountable for the majority of ERK signalling as P-ERK1 exhibits little efficacy. In this way, P-ERK1 activation could restrict ERK nuclear signalling output by competing for upstream MEK phosphorylation, limiting the amount of ERK2 that can be activated and attenuating signalling. The difference in shuttling velocity was reported to be due to residues 8 – 39 located within the N-terminal of ERK1, as excising this region from ERK1 produced comparable protein shuttling kinetics to P-ERK2 while fusion of the N-terminal region to P-ERK2 brought its kinetics down to the level of P-ERK1.

At the behavioural level, conditional hypomorphic mice expressing 20 – 40% less ERK2 than normal displayed deficits in long-term memory in classic fear conditioning as well as task-dependent learning, spatial, and reference memory deficits (Satoh *et al.*, 2007). In addition, Mazzucchelli *et al*. reported that ERK1 knockout mice display a hyperlocomotor phenotype with absence of habituation and enhanced long-term memory on the passive avoidance task (Mazzucchelli *et al.*, 2002). These behavioural changes were associated with increased ERK2 signalling and enhanced synaptic plasticity in the nucleus accumbens. These 2 papers suggest

that ERK2, but not ERK1, play a key role in learning and memory and that increasing ERK2 signalling may result in cognitive enhancement.

However, recent reports have called for re-evaluation of the literature to take into account the tissue-specific relative expressions of ERK1 and ERK2 (Frémin *et al.*, 2015; Buscà, Pouysségur and Lenormand, 2016). The ratio of ERK isoform activation has been reported to be directly proportional to the ratio of ERK isoform expression, with both isoforms phosphorylated and activated by the same upstream kinase MEK (Lefloch, Pouyssegur and Lenormand, 2008). Furthermore, knockout of one ERK isoform leads to an increase in activation of the other isoform due to reduced competition for activation by MEK (Lefloch, Pouyssegur and Lenormand, 2008). If both activated P-ERK isoforms exhibit functional redundancy then they would be expected to contribute to global ERK signalling equally when expressed (and therefore activated) at equimolar amounts. However, ERK2 is more highly expressed than ERK1 in most mammalian tissues (Buscà *et al.*, 2015) and so it follows that levels of activated P-ERK2 will be higher than activated P-ERK1 in these tissues. Under these conditions, P-ERK2 would contribute to global ERK signalling to a greater degree than P-ERK1. In fact, in mice, ERK2 has been reported to contribute to 80% of steady-state global ERK signalling, with ERK1 accounting for only 20% (Lefloch, Pouyssegur and Lenormand, 2008). Therefore, despite an expected corresponding increase in ERK1 activation, the murine embryonic lethality of ERK2 knockout could be explained by a catastrophic decrease in global ERK signalling due to the inability of ERK1 to compensate as a result of an insufficient expression. In support of this, a gene-dosage effect of ERK signalling has been reported whereby mice are viable despite germline ERK knockout or knockdown, irrespective of isoform, so long as a critical threshold of ERK signalling is surpassed (Frémin *et al.*, 2015) which further supports a functionally redundant role of the ERK isoforms in normal development. In addition, the report of opposing roles of ERK1 and ERK2 in cell proliferation (Vantaggiato *et al*., 2006) has been challenged by an opposing study which suggests normal proliferation upon ERK2 knockout due to compensation by ERK1 (Sanjo *et al.*, 2007). With regard to ERK1 partial agonism, no mechanism for slower shuttling is immediately apparent with regard to protein structure (Buscà, Pouysségur and Lenormand, 2016). However, slower shuttling of ERK1 could potentially be due to slower phosphorylation of ERK1 due to higher ERK2 expression, and therefore activation, or even due to size differences. Furthermore, ERK1 null animals have been reported to display no change in performance on the passive avoidance task (amongst other measures) or changes in baseline synaptic transmission with no change in ERK2 expression or activation (Selcher *et al.*, 2001). These findings are in direct opposition to a separate study using ERK1 knockout mice (Mazzucchelli *et al*., 2002).

In light of this evidence, it appears that ERK1 and ERK2 are most likely functionally redundant, and that the majority of reports of isoform specificity in the past are due to changes in expression levels. Retention of both functionally redundant ERK isoforms could be explained by the fact that duplicate genes are retained longer if they are highly-expressed and the products function in signalling cascades (Brunet *et al.*, 2006; Buscà, Pouysségur and Lenormand, 2016)as the ERK proteins do. Furthermore, differential expression of both ERK isoforms may allow regulation of overall ERK signalling output which could allow fine-tuning of ERK output.

4.1.1.1.7. RB5 – Work Leading to the Present Study

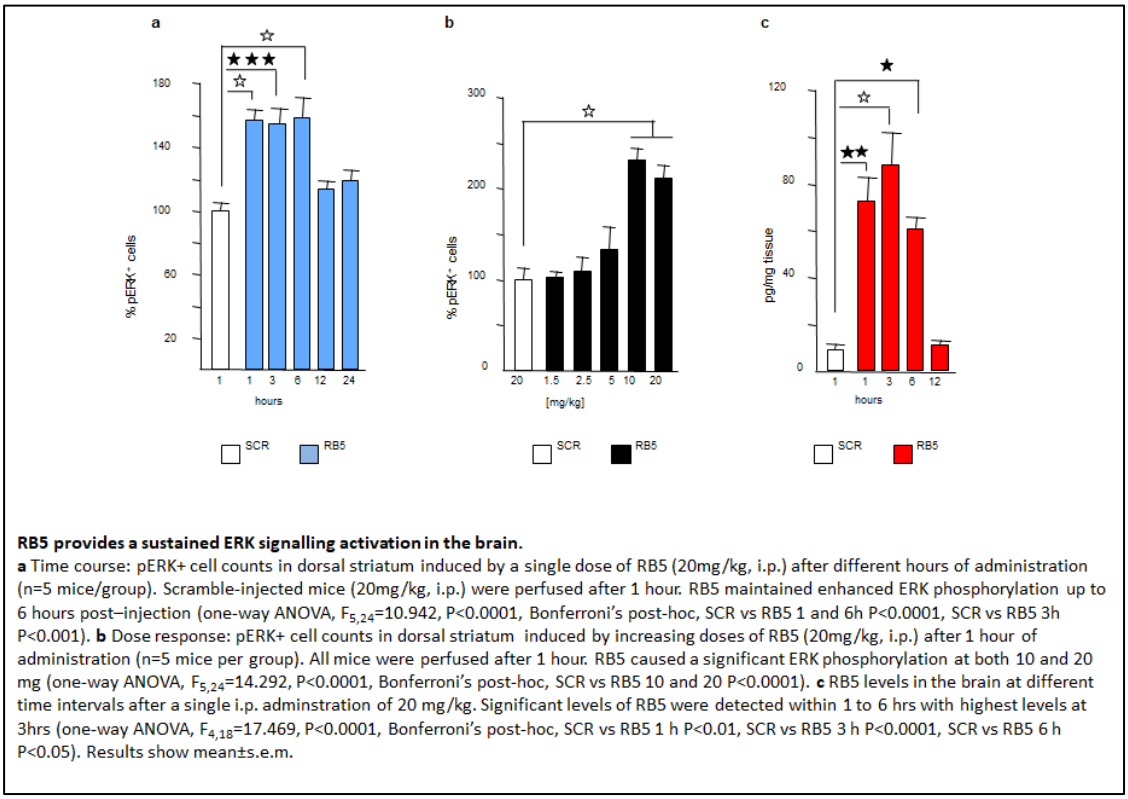

RB5 provides a sustained ERK signalling activation in the brain.
a Time course: pERK+ cell counts in dorsal striatum induced by a single dose of RB5 (20mg/kg, i.p.) after different hours of administration (n=5 mice/group). Scramble-injected mice (20mg/kg, i.p.) were perfused after 1 hour. RB5 maintained enhanced ERK phosphorylation up to 6 hours post–injection (one-way ANOVA, $F_{5,24}$=10.942, P<0.0001, Bonferroni's post-hoc, SCR vs RB5 1 and 6h P<0.0001, SCR vs RB5 3h P<0.001). **b** Dose response: pERK+ cell counts in dorsal striatum induced by increasing doses of RB5 (20mg/kg, i.p.) after 1 hour of administration (n=5 mice per group). All mice were perfused after 1 hour. RB5 caused a significant ERK phosphorylation at both 10 and 20 mg (one-way ANOVA, $F_{5,24}$=14.292, P<0.0001, Bonferroni's post-hoc, SCR vs RB5 10 and 20 P<0.0001). **c** RB5 levels in the brain at different time intervals after a single i.p. adminstration of 20 mg/kg. Significant levels of RB5 were detected within 1 to 6 hrs with highest levels at 3hrs (one-way ANOVA, $F_{4,18}$=17.469, P<0.0001, Bonferroni's post-hoc, SCR vs RB5 1 h P<0.01, SCR vs RB5 3 h P<0.0001, SCR vs RB5 6 h P<0.05). Results show mean±s.e.m.

Figure 4.3. Provided by Riccardo Brambilla/Ilaria Morella. *Evidence for sustained striatal ERK activation (A) in response to 10-20 mg/kg systemic injection of RB5 (B), with evidence for sustained bioavailability of RB5 peptide in the brain (C). Results compared to administration of scrambled (SCR) control peptide.*

The RB5 sequence is analogous to amino acids 7 – 38 of human ERK1 and the peptide is conjugated to Tat to endow it with cell-penetrating properties. A scrambled (SCR) version of the peptide is typically used as a control.

Previous work from the Brambilla lab demonstrated a significant and sustained increase in striatal ERK signalling (as measured by immunohistochemistry and cell-counts for P-ERK-positive cells in the dorsal striatum) (Figure 4.3A) in response to systemic administration of the cell-penetrating peptide RB5 systemically administered at a dose of 10 or 20 mg/kg (Figure 4.3B). Furthermore, RB5 peptide was still present in the brain up to 6 hours after injection (Figure 4.3C). These data suggest that a sustained increase in basal striatal ERK signalling can be achieved following a single systemic injection of RB5 peptide.

4.2. Aims

BDNF has been shown to be neuroprotective in HD, but difficulties in administration make it a challenging strategy for therapy (Section 1.6.4.3.). Building upon the substantial evidence for a neuroprotective role of Ras-ERK signalling in HD, the aim of this study was to establish whether lentiviral vectors (LVs) at a titre of 1E11 viral particles/ml could be used to constitutively express the RB5 peptide (LV-RB5) within the dorsal striatum of WT mice to produce a long-term, striatal-specific enhancement in ERK signalling relative to LV-GFP controls. Considering the novelty of the approach, the variability in reports of ERK signalling alterations in HD models (Section 4.1.1.5.), and the reported pleiotropic roles of ERK signalling in behaving animals, (Section 4.1.1.4.) it was first important to extensively characterise RB5 in wild-type animals to establish efficacy and to screen for side-effects prior to its introduction to HD models. In addition, gene therapy approaches are designed to be long-term interventions. As such, the effects of RB5 expression over the course of several months were investigated during this study. As the eventual aim was to administer RB5 to animal models of HD, which are commonly tested for cognitive and motor dysfunction, it was important to investigate whether administration of LV-RB5 altered the performance of WT mice on these tasks. This is particularly important given that enhanced ERK signalling in animal models of NF1 is associated with cognitive deficits as well as impaired motor performance (Silva *et al.,* 1997) (Section 4.1.1.4) which could confound studies investigating RB5 in HD models. Failure of NF1 mice to consolidate the rotarod task (van der Vaart *et al.*, 2011) particularly implicates dysregulated striatal ERK signalling in impairment on this task.

Finally, a more thorough time-course of RB5 administration at a dose of 10 mg/kg was conducted than that shown in Figure 4.3 in order to confirm whether RB5 increases striatal ERK activation and, if so, over what time frame.

4.3. Materials and Methods

4.3.1. Production of Lentiviral Vectors (Conducted by Dr Ilaria Morella)

4.3.1.1. Molecular Cloning

The translated RB5 sequence without TAT sequence is: GGGGGEPRRTEGVGPGVPGEVEMVKGQPFDV

The following oligonucleotides were obtained from Sigma Aldrich.

RB5 Forward: 5'GGGGCGGCGGCGGCGGCGAGCCCCGTAGAACCGAGGGCGTCGGCCCGGGCGTCCCGGGCGAGG TGGAGATGGTGAAGGGCCAGCCGTTCGACGTG3'

RB5 Reverse: 5'TCGAGCACGTCGAACGGCTGGCCCTTCACCATCTCCACCTCGCCCGGGACGCCCGGGCCGACGCCC TCGGTTCTACGGGGCTCGCCGCCGCCGCCGCCC3'

The oligonucleotides were dissolved in water to a final concentration of 100ng/µl. Next, 50µl each of RB5 forward and reverse oligonucleotides were mixed and annealed at 98°C for 5 minutes, before cooling to room temperature.

The annealed oligonucleotides were then amplified by PCR and Hindiii and Xhoi restriction sites introduced through addition of the following primers:

Forward: 5'CCCAAGCTTGGGGCGGCGGCGGCGGCGA 3'

Reverse: 5' CCGCTCGAGCCCACGTCGAACGGCTG 3'

PCR was conducted in 20 tubes using the following reagents:

- 0.5µl Tag Phusion (NEB)
- 2µl annealed RB5 sequence
- 0.5µl dNTPs (25nM)
- 2.5µl of forward primer (10µM)
- 2.5µl of backward primer (10µM)
- 1.5µl DMSO
- 10µl GC buffer
- 30.8µl H_2O

RB5 amplification was conducted through PCR using the following cycle:

1. 98°C - 30 seconds
2. 98°C – 10 seconds
3. 72°C – 30 seconds
4. 72°C – 30 seconds

5. 72°C – 5 minutes

NB. 2 – 4 were run for 35 cycles

Following amplification, RB5 DNA was precipitated with 2 volumes of ethanol 100%+ 1/10 sodium oxaloacetate, incubated for 30 minutes at -80°C and centrifuged at 13,000 RPM for 10 minutes. The DNA pellet was washed in 70% ethanol, allowed to dry and resuspended in 20µl of DNase-free water. Around 40ng/µl of DNA was recovered.

The amplified insert was ligated (at an insert:vector ratio of 10:1) to 25ng of Zero Blunt TOPO vector (Invitrogen) using 1µl of T4 ligase. The ligation mix was incubated overnight at 16°. On the next day, One Shot® TOP10 Chemically Competent E. coli cells were transformed with the ligated insert using the following methodology: One vial of One Shot® TOP10 cells was thawed on ice. Next, 2µl of the ligated insert was pipetted into the vial of cells and the resulting solution mixed gently. The vial was then incubated on ice for 30 minutes. Next, the cells were heat-shocked for 45 minutes at 42°C without shaking. The vial was then placed on ice for 2 minutes before 250µl of room temperature S.O.C. medium was added. The vials were then shaken for 1 hour at 37°C and 225 RPM.

250µl of solution was taken from each vial and was plated onto LB plates containing 50µg/ml kanamycin, with the plate incubated at 37°C overnight. On the following day, single colonies were picked and shaken overnight at 37°C in Luria Broth medium containing 50µg/ml kanamycin.

Plasmid DNA was then extracted from this solution using a Qiagen Miniprep kit. Next, RB5 insertion was validated by restriction analysis and subsequent sequencing.

30µg of Zero Blunt TOPO vector-RB5 was digested with BamHI/Xbal and run on agarose gel. The RB5 insert was then purified from the agarose gel. RB5 was subsequently ligated into p305 GFP LV DNA previously digested with BamHI/Xbal in the presence of 1µl of T4 ligase at a insert:vector ratio of 3:1. Competent One Shot Stbl3 E. coli cells were next transformed with the ligation product as described above. Transformed cells were plated onto Luria Broth agar medium in the presence of ampicillin (100µg/ml) and incubated overnight at 37°C. The following day, single colonies were picked and incubated and shaken in Luria Broth media containing ampicillin (100µg/ml) overnight at 37°C. Plasmid DNA was extracted using a Qiagen Miniprep kit and RB5 insertion validated by restriction analysis. Plasmid maps for LV-GFP (4.2A) and LV-RB5 (4.2B) are displayed below.

4.3.1.2. Lentiviral Production

$9x10^6$ HEK293 cells were seeded into 150mm dishes in the presence of DMEM High Glucose GlutaMax (Thermofisher Scientific) supplemented with 10% Fetal Bovine Serum (FBS, Euroclone) and 100 U/ml penicillin/streptomycin (Thermofisher Scientific).

22 hours later, culture media was replaced with Iscove's Modified Dulbecco's Medium (IMDM, Sigma Aldrich) supplemented with 10% FBS, 100 U/ml penicillin/streptomycin, and 2mM L-glutamine (Thermofisher Scientific).

2 hours later, transfection was carried out using the calcium phosphate method. The lentiviral plasmid DNA solution was prepared with the following DNA: 9µg of pENV (VSVG), 12.5µg pMDLg/pRRE, 6.25µg pRSV-REV and 30µg. The solution was made up to a final volume of 1.125ml using 0.1X TE buffer (stock 1X TE buffer: 10mM Tris pH 8.0, 1mM EDTA pH 9.0). 125µl of 2.5M $CaCl_2$ was added to the plasmid mix and the solution incubated for 20 minutes at room temperature.

A $CaPO_4$ precipitate was formed by dropwise addition of 1.25ml of 2X HBS (281mM NaCl, 100mM HEPES, 1.5mM Na_2PO_4 at pH 7.09) to the DNA-TE-$CaCl_2$ solution during vortexing. Cells were then incubated with the completed solution for approximately 16 hours. Next, culture media was replaced with fresh IMDM supplemented with 10% FBS, 100 U/ml penicillin/streptomycin, 2mM L-glutamine and 1mM sodium butyrate (Sigma Aldrich). After 24 hours, culture media was collected and filtered through a syringe filter unit (Millex-GP 0.22µm, Millipore) and centrifuged at 20,000 RPM for 2 hours at 20°C. The resulting pellet containing the LV was resuspended in PBS 1X (20µl per dish) and stored at -80°C).

4.3.1.3. Titration of LVs

Six 35mm dishes were each seeded with $5x10^4$ HEK293 cells. The next day, serial dilutions of the LV were made to generate LV solutions ranging from 10^{-3} to 10^{-7}. A negative control solution was created from pure media with no LV. Each plate of HEK293 cells was then incubated in 1ml of one of the dilutions or the negative control. After 5 days of incubation, cells were detached using 500µl of trypsin per dish. An equal volume of PBS/FBS 1% was added to each of the resulting cell solutions, before centrifugation at 12,000 RPM for 5 minutes at 20 °C. The supernatants were discarded and the remaining pellets resuspended in 400 µl of 2% PDFA for 5 minutes. FACS analysis was used to count the number of GFP-positive cells in each suspension and the titration was then calculated as such: (% of GFP-positive cells) x ($5x10^4$) / dilution factor. For the LV-RB5, the titer was calculated as 10^{10} viral particles/ml.

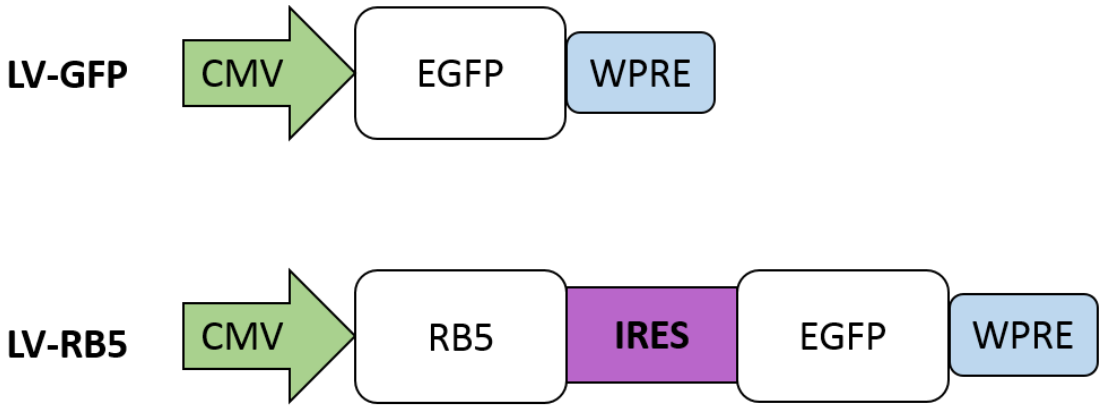

Figure 4.4 Diagrammatic representation of the major components of LV-GFP and LV-RB5. *Both LVs contain an EGFP reporter and transgene expression is driven by a CMV promoter in both cases, with a WPRE positioned downstream of EGFP. RB5 and EGFP are separated by an IRES linker in the case of RB5. Components are not drawn to scale.*

4.3.2. Animal Husbandry and Legislation

Mice used in this study were maintained and tested in accordance with the 2013 European Union Directive 2010/63/EU and the UK Animals (Scientific Procedures) Act of 1986. Animals were maintained under controlled conditions, with frequent monitoring, within holding rooms under a 06:00 – 18:00 light-dark cycle and a temperature of 21°C ± 1°C. Animals received minimal environmental enrichment (tunnel, chew stick and bedding) and were health-checked and at least weighed weekly according to institutional guidelines.

4.3.2.1. LV-GFP and LV-RB5 Characterisation

40 adult male C57BL/6J mice were obtained from JAX and housed in cages containing 5 mice each. Animals had *ad libitum* access to food and water throughout their lives (except when under water restriction (See Section 4.3.4.6.1.) Mice were health-checked and weighed three times per week when under water restriction.

Animals were divided equally to create two experimental groups of 10 animals each (LV-GFP or LV-RB5) prior to surgery. One animal from the LV-RB5 cohort died during surgery. 20 LV-GFP and 19 LV-RB5 animals received LV infusion at one month of age and were tested at 5-6 months of age (Figure 4.5) Mice were removed from their holding room and taken to a procedure room to undergo motor testing. Behavioural testing was carried out during the light cycle and was designed to detect presence of a motor phenotype. In the time between testing, animals were confined to their cages outside of being removed for weighing and health checks. Behavioural analysis was conducted blind to group. During histological analysis it became apparent that a

proportion of the animals in both experimental groups had undergone significant neurodegeneration (8 LV-GFP animals, 9 LV-RB5 animals). As such, these animals were retroactively excluded from behavioural analyses in an attempt to limit confounding effects. For stereological assessment of P-ERK-positive cells, 5 LV-GFP and 5 LV-RB5 animals were selected based on high GFP expression.

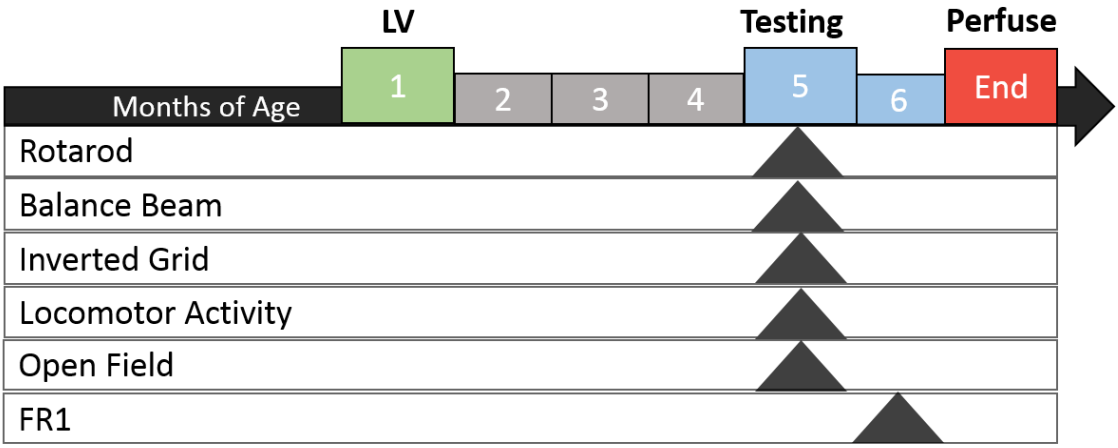

Figure 4.5. Experimental Timeline. *Animals were injected with LV at 1 month of age before behavioural testing began at 5 months of age. The grey triangles indicate when each test was conducted.*

Total = 22	Groups		
	LV-GFP	**LV-RB5**	**Total**
Rotarod	12	10	22
Balance Beam	12	10	22
Inverted Grid	12	10	22
Locomotor Activity	12	10	22
Open Field	12	10	22
FR1	12	10	22
Fluorescence	12	10	22
Stereology	**5***	**5***	10
*Only selected brains were stained for P-ERK			

Table 4.6. Representation of the number of animals in each test and reasons for exclusions*. The total number of animals possible were included in each behavioural test. Only 5 selected animals per group were included in stereological analysis.*

4.3.2.2. RB5 Pharmacokinetics

80 CD1 Crl:CD1(ICR) mice were obtained from Charles River and housed in cages containing 5 mice each. Animals were equally divided into two treatment groups (SCR control or RB5) with 5 mice per time-point prior at the beginning of the study. Mice were removed from their holding room and taken to a procedure room for injection. Following injection, animals were returned to their home cage.

4.3.3. Stereotaxic Surgery

Anaesthesia was induced by placing animals in a Perspex induction chamber which was slowly filled with a rising concentration of isoflurane (Teva, UK), reaching 4% total volume in 1 L/min oxygen. Following induction to surgical plane anaesthesia, the animal was removed from the induction chamber and the fur overlying the scalp shaved with clippers. The animal was then placed on a heated mat within the sterile surgical area and mounted to the stereotaxic frame (Kopf). Mice were maintained under surgical plane anaesthesia using 1 - 3% isoflurane in carrier oxygen at 0.8 L/min. Prior to surgery the animal was subcutaneously injected with Metacam (Boheringer Ingelheim, 2 mg/ml at 1 mg/kg) for post-surgical analgesia and Viscotears solution was applied to the eyes to prevent drying and irritation during the surgery. Dilute Videne solution was next spread across the shaved scalp area using a sterile cotton bud. A midline incision through the scalp was made using a sterile scalpel blade, and the tissue overlying the skull cleared using the blunt side of the scalpel blade and cotton buds. Bregma was located and its coordinates taken. Next, holes were drilled through the skull overlying the injection sites using the following coordinates: Lateral site AP = 1.2, ML = ±1.4, DV = -3; Medial site AP = 0.3, ML = ±2.3, DV = -2.4. Next, 1 µl of LV was injected at ~0.2 µl/minute at each site. 5 minutes of diffusion time was allowed after completion of each infusion, before the cannula was slowly retracted over ~2 minutes and cleaned with 70% ethanol and dH_2O between animals. The scalp was sutured with Vicryl Rapide (Ethicon) and a subcutaenous injection of 1 ml glucose-saline (5% w/v and 0.9% w/v respectively) was administered. Mice were next placed in a recovery box heated to 30°C and left until fully conscious and mobile, before being returned to their home cage. Animals were monitored and weighed for 3 days post-surgery and cages were supplemented with additional food to aid recovery.

4.3.4. Behavioural Testing

4.3.4.1. Rotarod

Mice were trained and tested on the rotarod (Ugo Basile, model number 47600, Varese, Italy) in order to assess motor coordination and balance. Mice were tested on the 4-44 RPM accelerating protocol 3 times per day over 3 days with a maximum trial time of 300 seconds. Animals were allowed 20 minutes recovery time between runs and were returned to their

home cages upon falling. Any animals staying on the apparatus for the full 300 seconds were removed from the rotarod and their score recorded as 300 seconds.

4.3.4.2. Balance Beam

Mice were tested on the balance beam in order to assess motor coordination and balance. The balance beam apparatus consists of a wooden beam, 1 metre in length, tapered in width from 1.5cm to 0.5cm from start to end and positioned at a 17° angle of ascent, with the beam leading to a house box. On day 1, mice were placed within the house box at the end of the beam, before being placed at increasing distances away from the house box until the animal learned to walk from the start of the beam to the house box. On day 2, mice were placed at the start of the beam, facing away from the house box and the following parameters were recorded and averaged over 2 trials: Turn Time was the amount time it took the mouse to turn from its starting position facing away from the house box to facing towards the house box, Run Time was the amount of time it took for the mouse to traverse the beam from its first step over the start line to its first step over the finish line, and Paw Slips were the total number of hind- and fore-paw slips the mouse made as the animal traversed the beam between the start and finish lines, with the left paw slips recorded in person and the right paw slips recorded and scored post-testing.

4.3.4.3. Inverted Grid

The inverted grid test was used to assess grip strength and coordination of the animals. Animals were placed on a mesh grid measuring 30cm x 30cm which was then raised 30cm above a towel-cushioned worktop and inverted so that the mouse was upside-down, clinging to the underside of the grid. Latency of the mouse to fall from the grid was recorded, with a maximum session time of 60 seconds implemented. Mice underwent 2 non-consecutive tests on the same day.

4.3.4.5. Open Field

Animals were placed in an open-topped, walled arena (40 cm x 20 cm x 40 cm) made of opaque white plastic. The arena was positioned beneath an infrared camera, and mice were filmed and tracked by Ethovision software as they explored for the 20-minute testing session, after which mice were removed and returned to their home cage. Mice were tested in two sessions separated by 24-hours and the arena was cleaned with ethanol between mice. Data was then extracted and analysed to give measures of distance travelled, velocity and the cumulative durations spent in the wall zone (defined within the Ethovision programme as the zone around the entire periphery of the box, extending 4 cm from the walls of the arena towards the centre) and centre zone (defined in the programme as the remainder of the arena). Distance-travelled

and velocity give an indication of the activity of the animals and the amount of exploration, while the relative durations spent in the wall and centre zones give a measure of thigmotaxis and a suggestion of anxiety-related behaviour.

4.3.4.6. Operant Testing

4.3.4.6.1. Water Restriction

Mice were water-restricted in a gradual fashion across the course of 1 week until they received 3 hours of *ad libitum* access to water per day. Concurrently, mice were introduced to small volumes Yazoo strawberry milk in their home cages to prevent an aversive reaction during testing.

4.3.4.6.2. Acclimatisation

Mice were first acclimatised to operant boxes over the course of 2 days. On the first day, a large volume of strawberry milk was delivered through the magazine to build association between magazine and reward. The next day, mice were rewarded if they entered the magazine, further strengthening the association.

4.3.4.6.3. Fixed Ratio (FR1) Schedule

Mice were trained on the Skinner operant set-up. Two 11 mm holes containing infrared beams were located in close proximity on either side of the reward magazine (left hole and right hole). Prior to the start of the first trial, strawberry milk was painted around the left and right hole to encourage exploration. At the beginning of a 20-minute FR1 trial, the main light turned off and the left and right holes lit up. Mice learned to associate a single nose-poke within the left or right hole with receiving a reward of strawberry milk. Mice were trained for one trial per day over the course of 14 days and were limited to 50 rewards per day in an effort to prevent overtraining and habit formation. At the end of each trial, animals were removed from boxes and returned to their home cage. If an animal made < 10 responses in 10 minutes, the box was opened and the holes painted during the trial. Painting-induced pokes were removed from daily totals. If an animal made < 20 responses over the course of a trial, the holes were painted with milkshake before the start of the trial next day.

4.3.5. Production of RB5 and SCR Peptides

RB5 and SCR peptides were synthesised by Genecust Europe (Luxembourg). Both peptides were fused to the TAT sequence of HMV-1 to confer cell-penetrating ability. The RB5 sequence is analogous to amino acids 7 – 38 of human ERK1.

RB5 sequence: GRKKRRQRRRP**PQ**GGGGGEP**RR**TEGVGPGVPG**E**V**E**MVKGQPFD**V**

SCR sequence: GRKKRRQRRRPPRVGPGVPEGVGVAVFGVKEPGQTGDVGPVG**E**

Amino acids in bold in the sequences above were in D-form and the first N-terminal amino acid acetylated. Batches of 200 mg, highly purified by high-performance liquid chromatography (HPLC) (purity>95%) were produced. The lyophilised peptides were dissolved in acetic acid 10% (2 µl of acetic acid 10% per mg of peptide). Once dissolved, deionised water was added to obtain a final solution 10 mg/ml. For *in vivo* experiments the peptides were further diluted in PBS 1X.

4.3.6. Histology

4.3.6.1. Perfusion-Fixation

Animals were killed via intraperitoneal injection of 0.2 ml Euthatal (Merial, Essex, UK) before being transcardially perfused with PBS (pH 7.4) for 1 minute, followed by 5% PFA (pH 7.4) for 6 minutes to fix tissue. Following fixation, animals were decapitated and their brains removed. Brains were then post-fixed in 4% PFA at 4°C for 24 hours, after which they were cryopreserved in 30% sucrose at 4°C. Brains were kept in sucrose for no more than 48 hours, after which they were sectioned coronally into a 1 in 6 series of 35 µm slices using a sliding sledge freezing microtome (Leitz, Wetzlar). Brain slices were then transferred into a 48 well plate where they were stored in antifreeze at -20°C until required.

4.3.6.2. Area of Fluorescence

Area of fluorescence was calculated in Image J using images taken under fluorescent microscopy at 1.6 X magnification. For each brain, 4 equivalent successive sections with dorsal striatum present were measured. The area of the left and right dorsal striata was recorded and the area of fluorescence within these defined areas was also measured. The percentage area of fluorescence out of total dorsal striatal area was then calculated.

4.3.6.3. P-ERK Immunohistochemistry on Free-Floating Sections

Striatal sections from each animal were sorted into a 24 well plate and washed in TBS to remove residual antifreeze, before quench consisting of 3% hydrogen peroxide and 10% methanol in TBS was applied to limit endogenous peroxidase activity. Sections then underwent further washes in TBS before block consisting of 5% normal goat serum (NGS) in Triton-X-Tris-Buffered-Saline (TXTBS) was applied for 1 hour at room temperature to prevent non-specific binding of the primary antibody. Following blocking, rabbit anti-P-ERK primary antibody (Cell Signaling, cod. 4370) in 5% NGS-TXTBS (with an antibody ratio of 1:1000) was applied and the slices shaken overnight at 4°C. The following day, the sections were washed in TBS to remove unbound primary antibody, and the secondary biotinylated goat anti-rabbit antibody (BA1000, Vector) at a 1:200 ratio with NGS-TXTBS was added for 1 hour at room temperature. Afterwards, unbound secondary antibody was washed off in TBS before application of ABC kit (1 drop of solution A and 1 drop of solution B for every 5ml of TBS needed to cover the sections, made up 30 minutes before use) for 1 hour at room temperature. Sections were then washed in TBS. Next, a solution of 200 µl DAB in 10 ml TBS was made up and each well containing sections received 1 ml of this DAB solution, incubated for 1 minute. Following this, 13 µl of 3% hydrogen peroxide in TBS was added to the well in order to initiate the DAB reaction. After 40 seconds, the active DAB solution was removed and the sections washed in TBS to stop the reaction. After washing, sections were removed and mounted onto double subbed 1% gelatinised slides (Thermo Scientific, Menzel Gläser) and allowed to dry overnight. The next day, sections were dehydrated and cleared *in situ* on slides by placing in the following solutions, successively, for 10 minutes each: 70%, 95%, and 100% denatured ethanol and xylene. Slides were then cover-slipped using DPX mountant and allowed to dry.

4.3.6.4. Stereology

Stereological cell counts of striatal P-ERK-positive cells were conducted using Visiopharm Integrator System (VIS) software. Firstly, whole brain sections were photographed under 1.2 X magnification and the dorsal striatum mapped as a region of interest. Next, counting frames (285 μm^2) were generated in an unbiased fashion across the region of interest and cells within the frames were counted at 100 X magnification. The number of cells in each section using the formula: **$C = \Sigma c\ (\Sigma A \times (\Sigma n \times a)) \times f$.**

C = estimated number of cells

Σc = number of cells counted

ΣA = sum of regions of interest area

Σn = number of frames allocated to the regions of interest

f = frequency of sectioning

Next, an Abercrombie-corrected cell count was calculated from the above value by using the formula: **$aC = C \times (ST/(ST+D))$**

aC = Abercrombie-corrected cell count

C = estimated number of cells

ST = section thickness

D = cell diameter

4.3.7. Statistics

All statistical tests were conducted in SPSS. When data were not normal or did not display equal variances, they were transformed accordingly before an ANOVA was performed.

4.4. Results

4.4.1. Area of Fluorescence

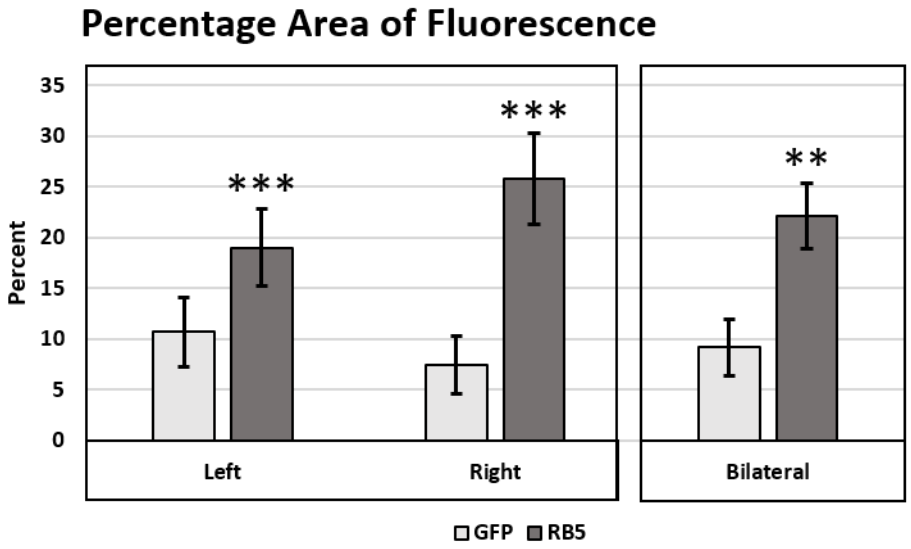

Figure 4.8. Percentage area of fluorescence within the dorsal striatum. *Treatment with LV-RB5 results in a significantly higher percentage area of fluorescence than LV-GFP. Percentage striatal area of fluorescence for LV-GFP- and LV-RB5-treated animals in the left and right striata (left pane) and as a total bilateral percentage area (right pane). Significant differences in percentage area of fluorescence between LVs are indicated by asterisks ($p \leq 0.05$*, $p \leq 0.01$**, and $p \leq 0.001$***). Values are expressed as means ± SEM. LV-GFP n = 12, LV-RB5 n = 10.*

Both the control viral vector (LV-GFP) and experimental viral vector (LV-RB5) express an EGFP reporter (referred to as GFP). The presence of fluorescent GFP-positive tissue shows that both LV-GFP an LV-RB5 successfully transduced striatal cells. In order to evaluate the spread of transduction, the area of GFP-positive tissue within the left and right dorsal striatum was measured and divided by the total area of left or right dorsal striatum to generate left and right percentage areas of fluorescence (Figure 4.8; 4.9). Left and right areas were also summed and divided by total dorsal striatum area to give a bilateral percentage area of fluorescence (Figure 4.8). LV-GFP and LV-RB5 transduced the left and right hemispheres comparably as evidenced by the equivalent area of fluorescence in each hemisphere ($F(1, 40) = 0.062$, p = n.s.), demonstrating that there was no lateralisation of expression resulting from methodological issues which could affect behaviour. However, LV-RB5 administration resulted in a greater bilateral area of fluorescence than LV-GFP (($t(20) = -3.042$, $p = 0.006$) (Figure 4.8) which suggests that LV-RB5 transduced cells more effectively than LV-GFP.

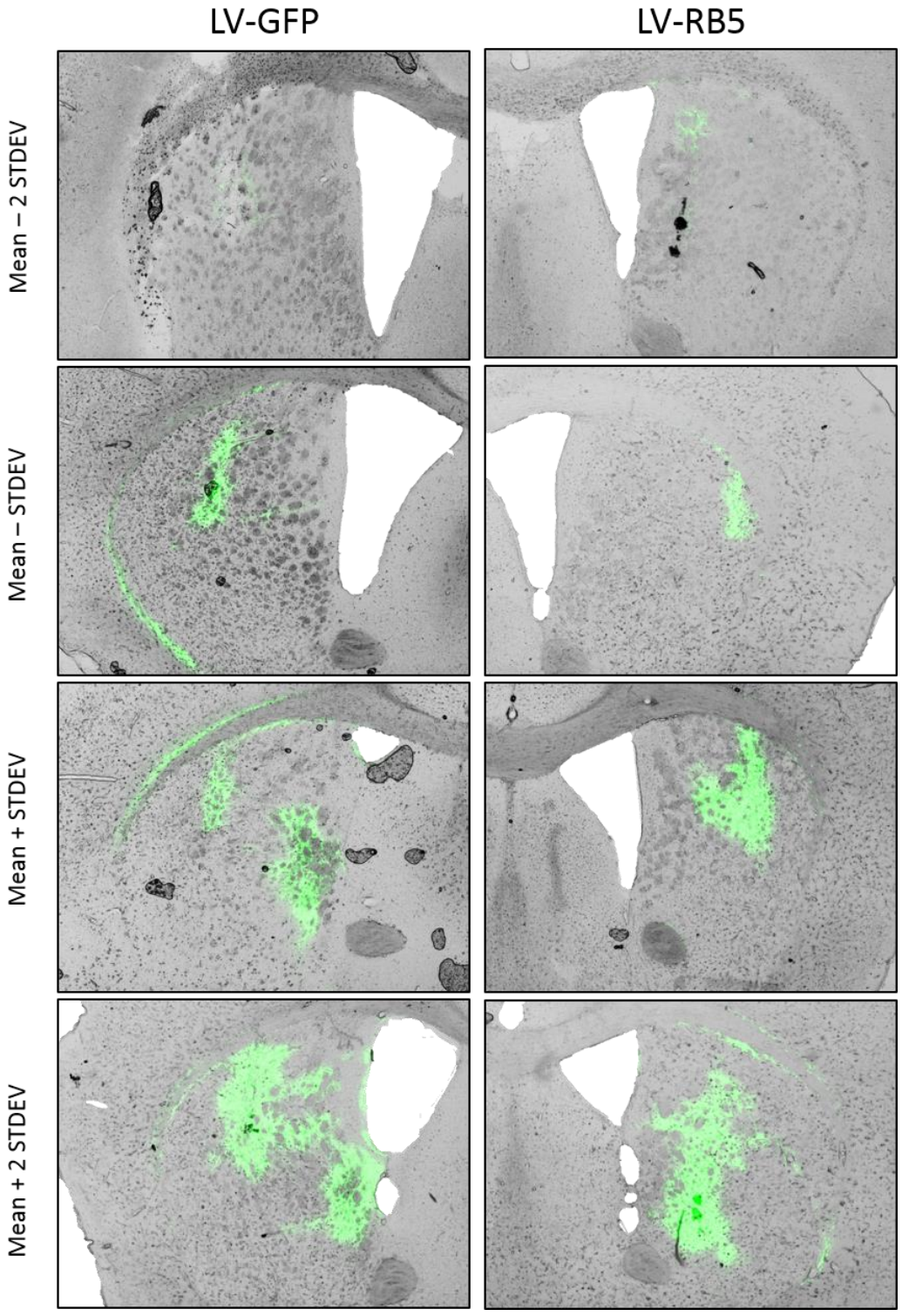

Figure 4.9. Areas of fluorescence within the dorsal striatum. *Representation of GFP-positive tissue overlaid onto brightfield images of the dorsal striatum. Images are arranged vertically in order of ascending area of fluorescence for LV-GFP and LV-RB5.*

4.4.2. Behavioural Testing

4.4.2.1 Rotarod

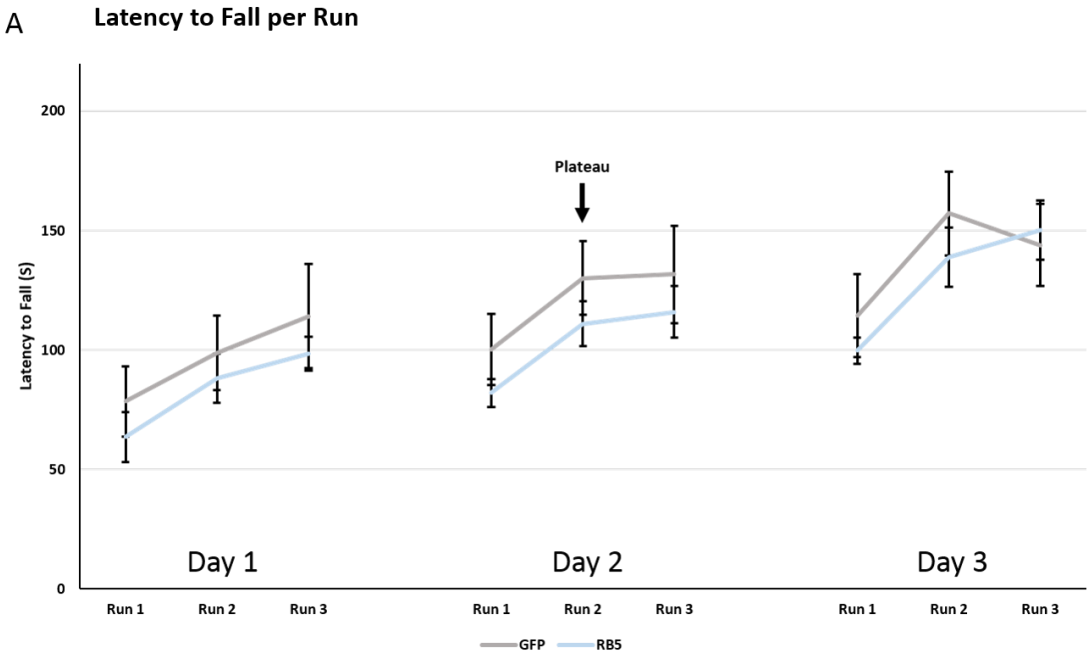

Figure 4.10. LV-GFP and LV-RB5 performance on the rotarod. *LV-GFP and LV-RB5 mice displayed comparable motor coordination and motor learning on the rotarod. Average latencies of LV-GFP and LV-RB5 mice to fall from the rotarod on each of the three non-consecutive trials performed on each of the three consecutive days. Values are expressed as means ± SEM. LV-GFP n = 12, LV-RB5 n = 10.*

Animals were tested on the commonly used rotarod to determine whether motor learning or coordination were affected by expression of GFP or RB5 (Figure 4.10). Animals displayed a normal learning profile with improvement in performance over time ($F(8, 160) = 13.819$, $p < 0.001$) with improvement reaching a plateau at Run 2 on Day 2. Performance on the rotarod did not differ between LV-GFP and LV-RB5 animals ($F(1, 20) = 0.658$, p = n.s.) demonstrating that motor coordination was comparable between groups. Furthermore, there was no interaction between group and run ($F(8, 160) = 0.316$, p = n.s.) showing that performance was comparable at each time-point and suggesting that motor learning was equivalent.

4.4.2.2. Balance Beam

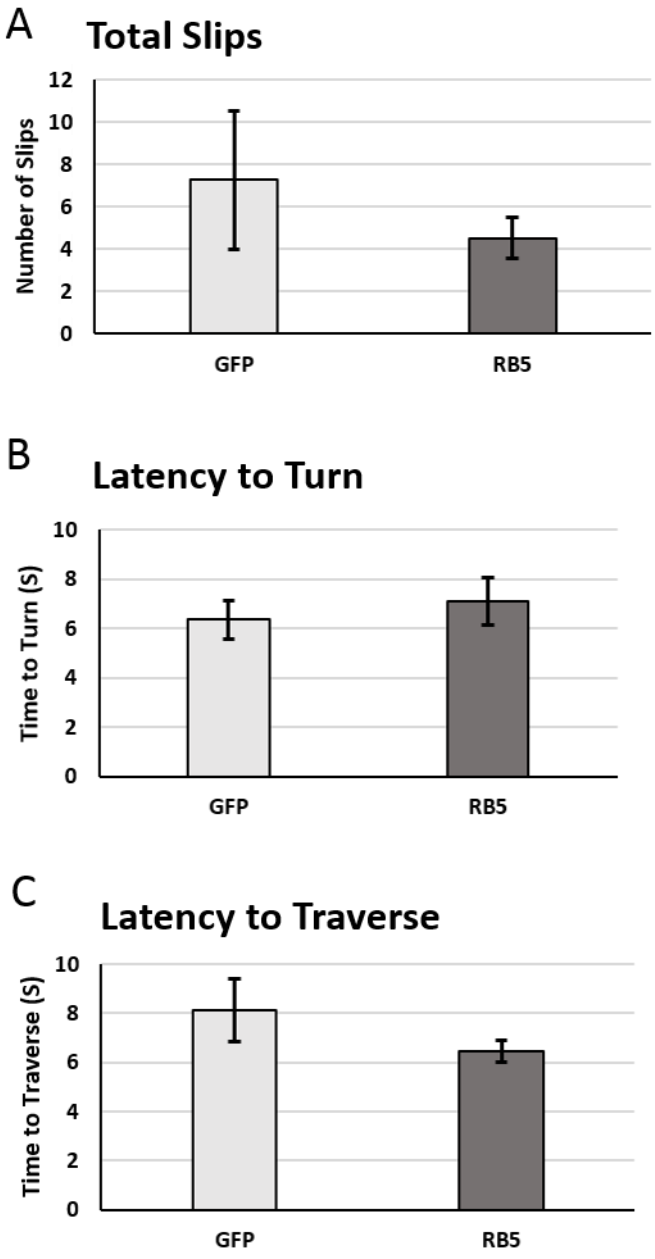

Figure 4.11. Performance of LV-GFP and LV-RB5 on the balance beam. *LV-GFP and LV-RB5 mice displayed comparable performance on the balance beam. LV-GFP and LV-RB5 mice were assessed on three parameters on the balance beam: total number of paw slips (A), the latency to turn (B), and the latency to traverse the beam (C). Values are expressed as means ± SEM. All LV-GFP n = 12, LV-RB5 n = 10.*

Animals were tested on the balance beam to assess motor coordination and balance (Figure 4.11). The performance of LV-GFP and LV-RB5 was comparable with regard to paw slips ($t(20) = 0.744$, p = n.s.) (Figure 4.11A), latency to turn ($t(20) = -0.600$, p = n.s.) (Figure 4.11B) or latency to traverse the beam ($t(20) = 1.111$, p =n.s.) (Figure 4.11C), suggesting that balance and motor coordination did not differ between groups on the balance beam.

4.4.2.3. Inverted Grid

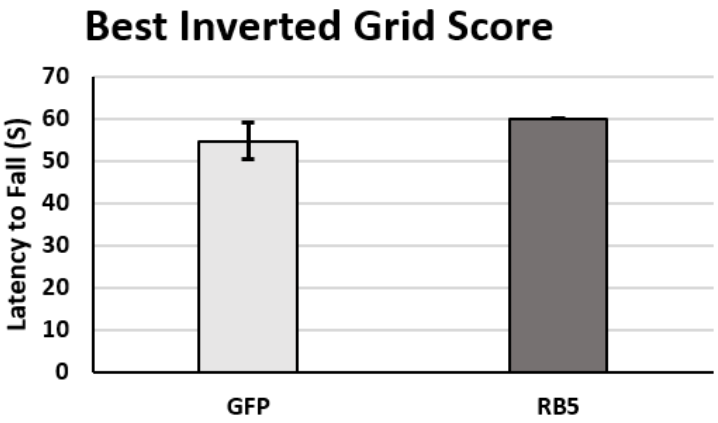

Figure 4.12. Performance of LV-GFP and LV-RB5 on the inverted grid test. *LV-GFP and LV-RB5 did not differ significantly in their performance on the inverted grid test. Mice were tested on their ability to hold on to an inverted grid over a 60 second maximum testing period, with the best latency to fall out of two tests taken as the test value. Values are expressed as means ± SEM. LV-GFP n = 12, LV-RB5 n = 10.*

In order to gain a non-neuronal correlate of motor ability, the fore- and hind-limb muscle strength of animals was assessed using the inverted grid task (Figure 4.12). Both groups of animals displayed equivalent latencies to fall from the grid ($t(11) = -1.122$, p = n.s.), suggesting that limb muscle strength did not differ between LV groups and thus should not have affected performance on other motor tasks.

4.4.2.4. Locomotor Activity

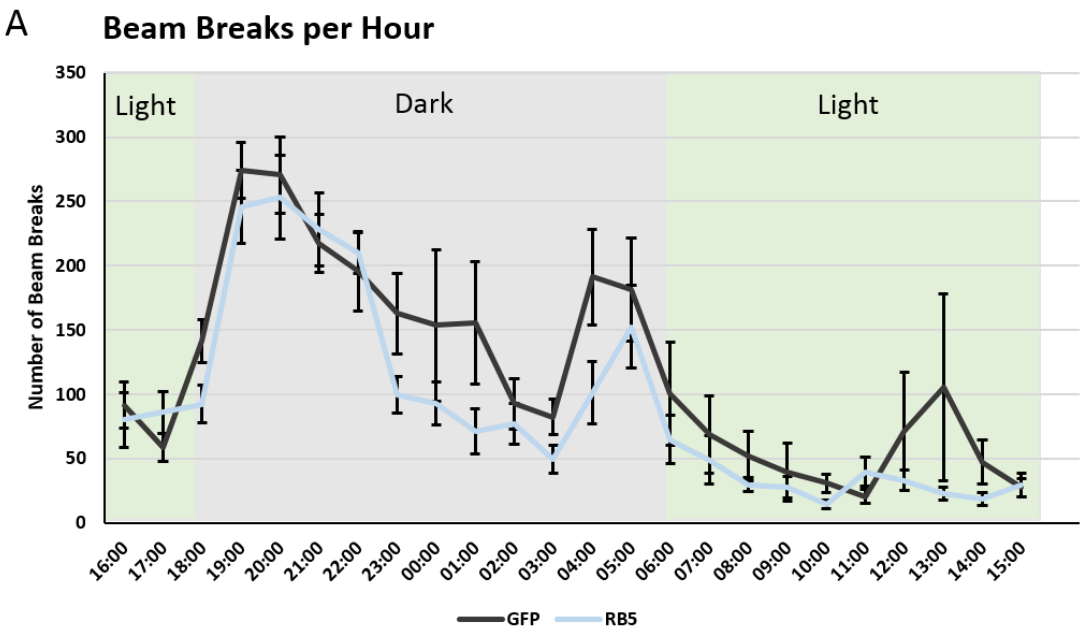

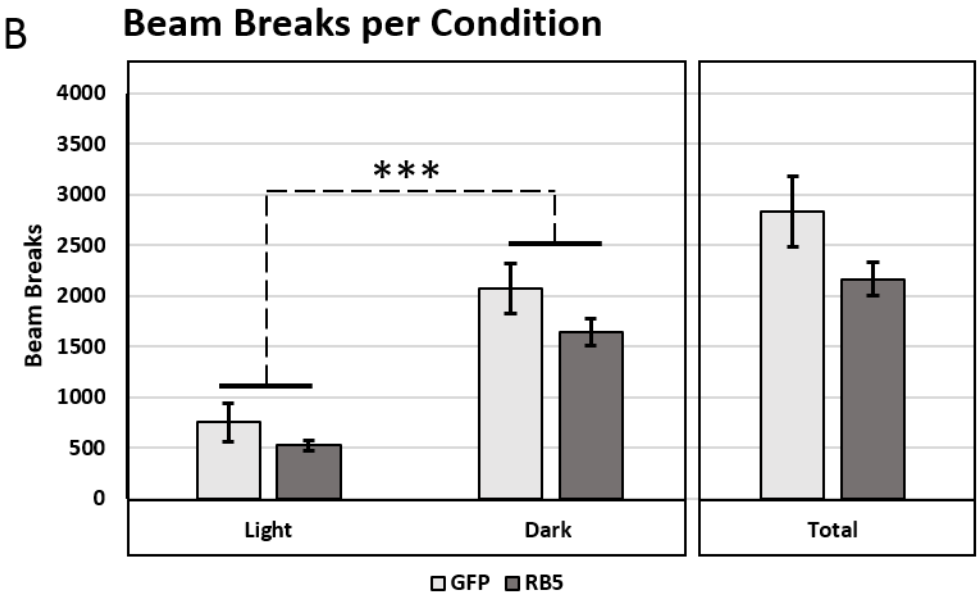

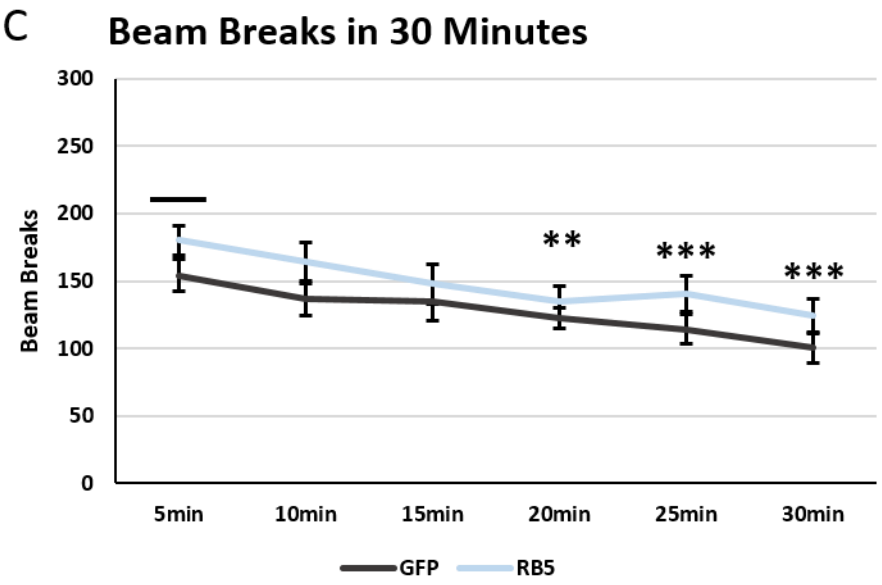

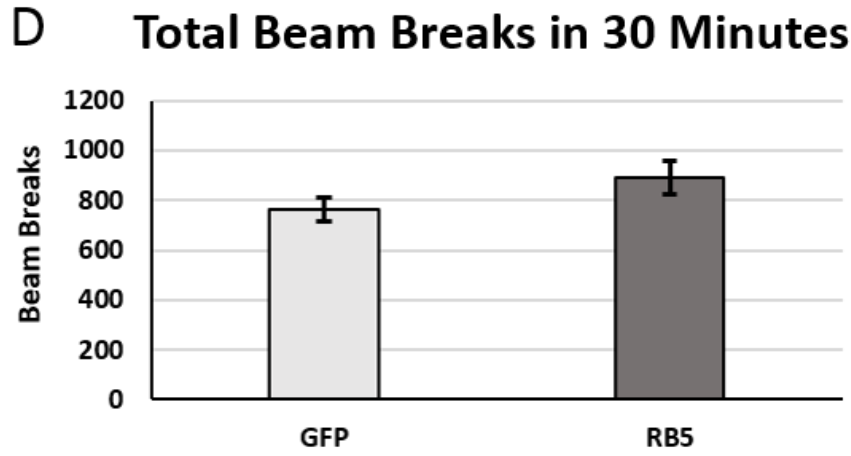

Figure 4.13. Locomotor activity of LV-GFP and LV-RB5 animals. *LV-GFP and LV-RB5 animals did not differ significantly in their locomotor activity. The average number of beam breaks made by LV-GFP and LV-RB5 mice during one hour time bins over the entire 24 hour testing period, with light and dark phases indicated (A), 24 hour locomotor activity data was split into 12 hours non-contiguous light phase and 12 hours contiguous dark phase as well as being assessed as a total (B), the first 30 minutes of beam breaks during the testing period was taken and assessed in 5 minute time bins (C) as well as being assessed as the total number of beam breaks over the entire 30 minute period (D). Significant differences in the number of beam breaks are signified by dashed lines, with significance levels represented by $p \leq 0.05$*, $p \leq 0.01$**, and $p \leq 0.001$***. Values are expressed as means ± SEM. All LV-GFP n = 12, LV-RB5 n = 10.*

Animals were tested for differences in locomotor activity over a 24-hour period (Figure 4.13A - B). LV-GFP and LV-RB5 did not differ in activity at equivalent time-points over the 24-hour testing period ($F(1, 20) = 2.571$, p = n.s.) (Figure 4.13A) with no significant interaction between group and time-point ($F(23, 460) = 0.795$, p = n.s.). Both groups displayed the elevation in

activity typical of mice during the dark phase compared to the light phase ($F(1, 20) = 100.412$, $p < 0.001$) (Figure 4.13B) with no difference in activity between groups in each respective phase ($F(1, 20) = 1.694$, p = n.s.) or the whole 24-hour period ($t(20) = 1.492$, p = n.s.).

LV-GFP and LV-RB5 mice displayed comparable levels of exploratory activity at equivalent time-points across the first 30 minutes of testing ($F(1, 20) = 2.525$, p = n.s.) (Figure 4.13C) with both groups demonstrating an equivalent typical reduction in activity as animals habituate to the novel environment ($F(5, 100) = 10.778$, $p < 0.001$). Furthermore, the total number of beam breaks did not differ between LV groups ($t(20) = -1.588$, p = n.s.), suggesting that animals were equally active across the entire 30-minute testing period.

4.4.2.4. Open Field

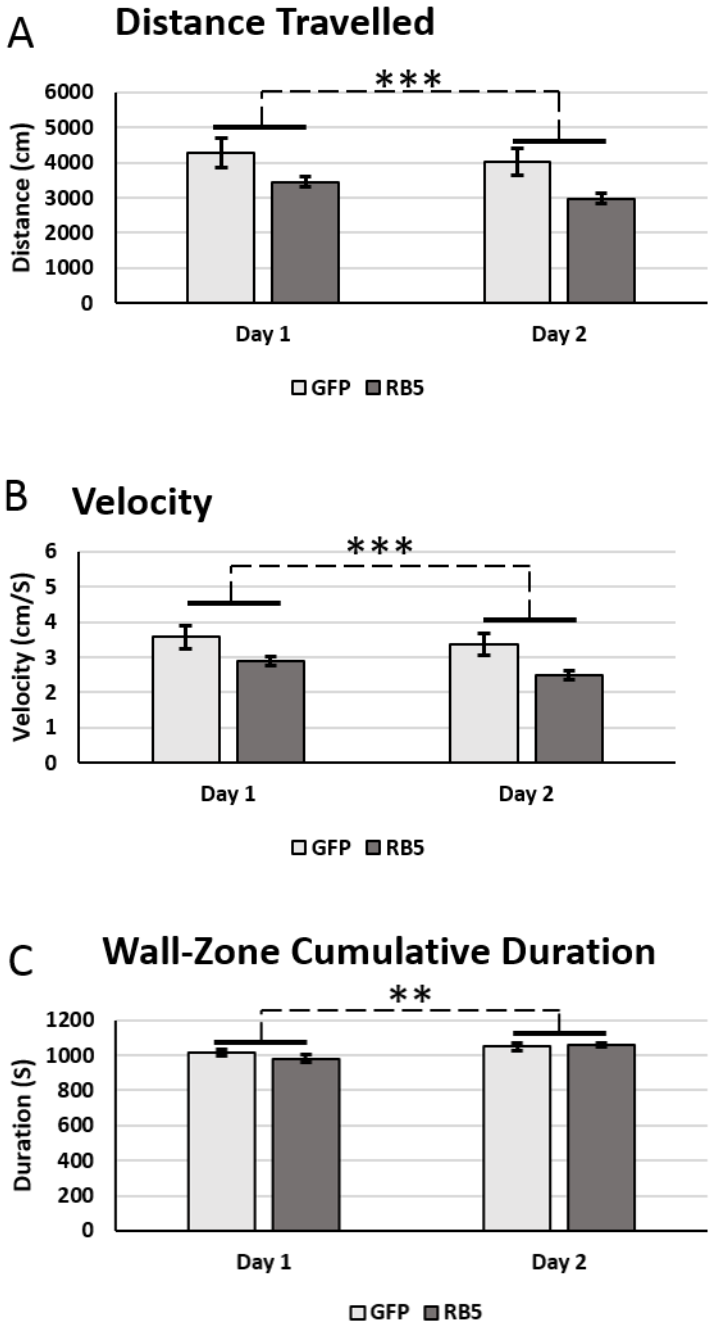

Figure 4.14. Performance of LV-GFP and LV-RB5 in the open field. *LV-GFP and LV-RB5 animals did not significantly differ in any measures recorded in the open field test and showed normal habituation with time. The distance animals travelled (A), the velocity at which animals travelled at (B), and the cumulative duration animals spent in the wall-zone (C). Significant differences between days are signified by significant bars connected by dashed lines, with significance levels represented by p ≤ 0.05*, p ≤ 0.01**, and p ≤ 0.001***. Values are expressed as means ± SEM. All LV-GFP n = 12, LV-RB5 n = 10.*

Animals were tested in the open field on two consecutive days to explore activity and habituation to a novel environment in more detail, as well as to investigate potential differences in thigmotaxis (Figure 4.14). Both groups demonstrated reductions in distance travelled ($F(1, 20) = 10.066$, $p = 0.005$) (Figure 4.14A) and velocity ($F(1, 20) = 10.057$, $p = 0.005$) (Figure 4.14B) between days 1 and 2 indicating habituation to the novel environment and a corresponding decrease in activity on the second day. LV group did not impact on either distance travelled ($F(1, 20) = 4.435$, p = n.s.) or velocity ($F(1, 20) = 4.428$, p = n.s.), reflecting comparable activity and habituation.

Next, to give a measure of thigmotaxis, the cumulative durations animals spent in the wall-zone around the perimeter of the arena and the centre-zone of the arena were recorded and compared (Figure 4.14C). Mice spent a longer duration in the wall-zone on the second day of testing compared to the first ($F(1, 20) = 9.453$, $p = 0.006$) implying that mice were habituated to the arena and explored less on the second day than the first. LV-GFP and LV-RB5 animals spent equivalent durations in the wall-zone ($F(1, 20) = 0.441$, p = n.s.) indicating that they did not differ in thigmotaxic behaviour.

4.4.2.5. Fixed Ratio Operant Conditioning

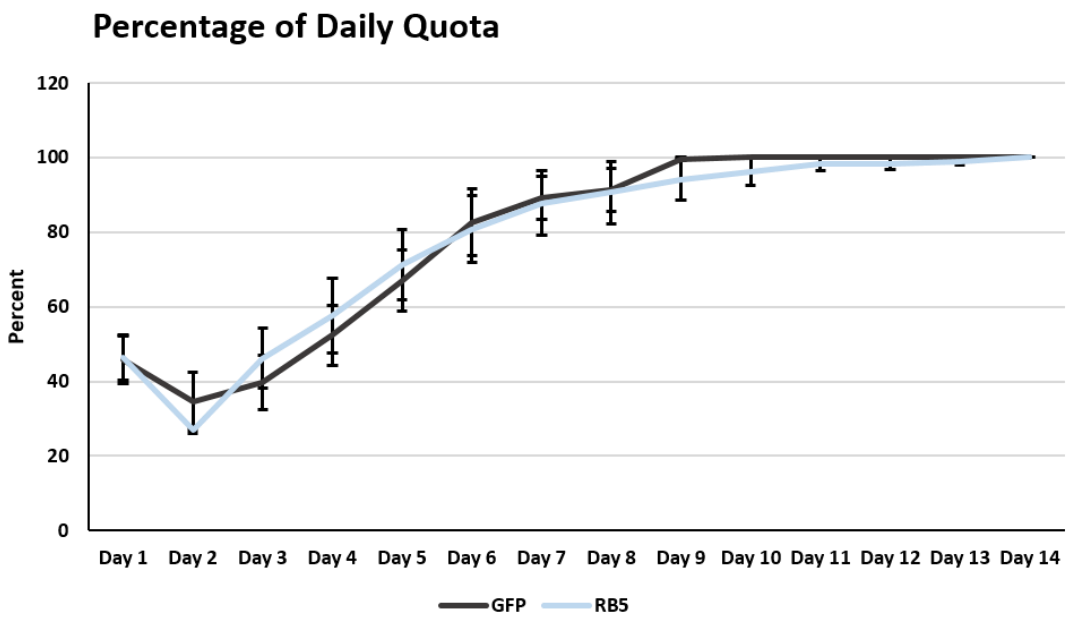

Figure 4.15. Performance of LV-GFP and LV-RB5 on the FR1 task. *LV-GFP and LV-RB5 animals did not significantly differ in the FR1 measure of associative learning and performance. The percentages of the daily quota of nose-pokes (100%) reached are plotted for each group over the course of 14 days. Values are expressed as means ± SEM. All LV-GFP n = 12, LV-RB5 n = 10.*

Animals were tested on the striatal-dependent fixed-ratio schedule 1 (FR1) to probe associative learning and performance (Figure 4.15). Both LV-GFP and LV-RB5 mice learned the association over time Animals were tested on the striatal-dependent fixed-ratio schedule 1 (FR1) to probe associative learning and performance (Figure 4.15) but LV had no effect on performance (1, 20) = 0.014, p = n.s.).

4.4.3. Histological Characterisation

4.4.3.1. Stereology

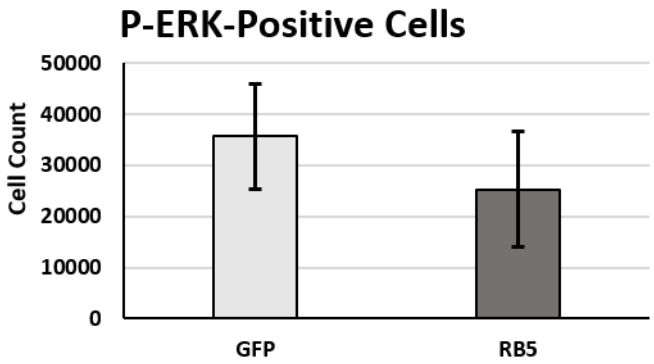

Figure 4.16. Stereological count of P-ERK-positive cells within the dorsal striatum. *LV-RB5 did not significantly increase the number of P-ERK-positive cells in the dorsal striatum, relative to LV-GFP. Brain sections were immunohistochemically stained against P-ERK and the number of P-ERK-positive striatal cells assessed with stereology. Values are expressed as means ± SEM. LV-GFP n = 5, LV-RB5 n = 5.*

Given that LV-RB5 did not significantly affect the behaviour of WT mice on any of the parameters measured when compared to LV-GFP, the ability of LV-RB5 to result in an increase in striatal ERK activation was assessed. A sample of brains displaying large areas of fluorescence from 5 LV-GFP and 5 LV-RB5 animals were stained them against P-ERK (Figure 4.17) and stereological counting of P-ERK-positive cells was conducted within the dorsal striatum. LV-RB5 administration did not increase the number of P-ERK-positive cells in the dorsal striatum relative to LV-GFP controls ($t(8) = 0.682$, p = n.s.) (Figure 4.16) suggesting that RB5 was unable to increase striatal ERK activation despite widespread transduction and high GFP transgene expression.

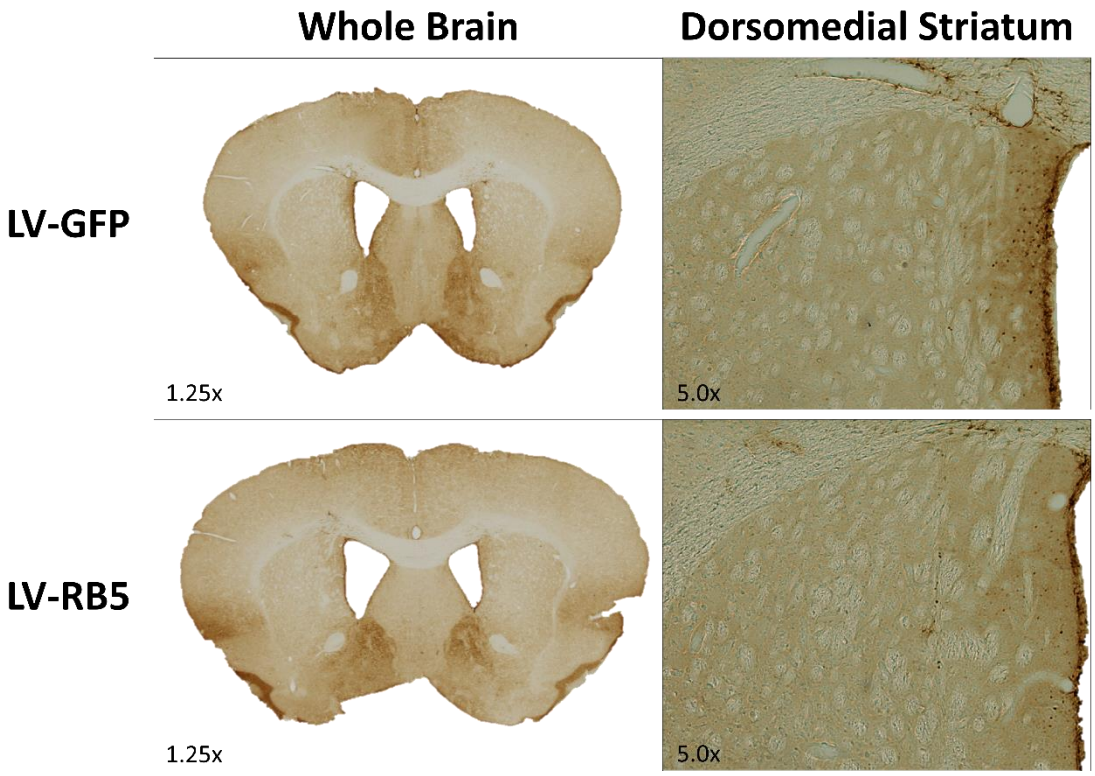

Figure 4.17. Representative samples of LV-GFP and LV-RB5-treated brains stained for P-ERK. *Whole brains (1.25x magnification) and samples of the dorsomedial striatum (5.0x magnification) are displayed with more P-ERK-positive neurons evident in the medial aspect of the striatum.*

4.4.3.2. Neurodegeneration

Upon section and mounting brains, it became readily apparent that a significant number of them displayed extensive neurodegeneration (Figure 4.18). LV-GFP- and LV-RB5-administered animals were affected to a comparable extent. In cases of particularly extensive neurodegeneration, animals were removed from behavioural analyses to limit confounding factors to behavioural analyses as far as possible (LV-GFP – 8 removed, LV-RB5 – 9 removed). Neurodegeneration was associated with enlarged brains, enlarged ventricles, striatal peeling from overlying cortex (particularly at the lateral aspect), general fragility, and lack of cresyl violet stained cells around needle tracts (Figures 4.18A & B). Sections were extremely difficult to handle and mount and the extent of damage was made worse with each manipulation.

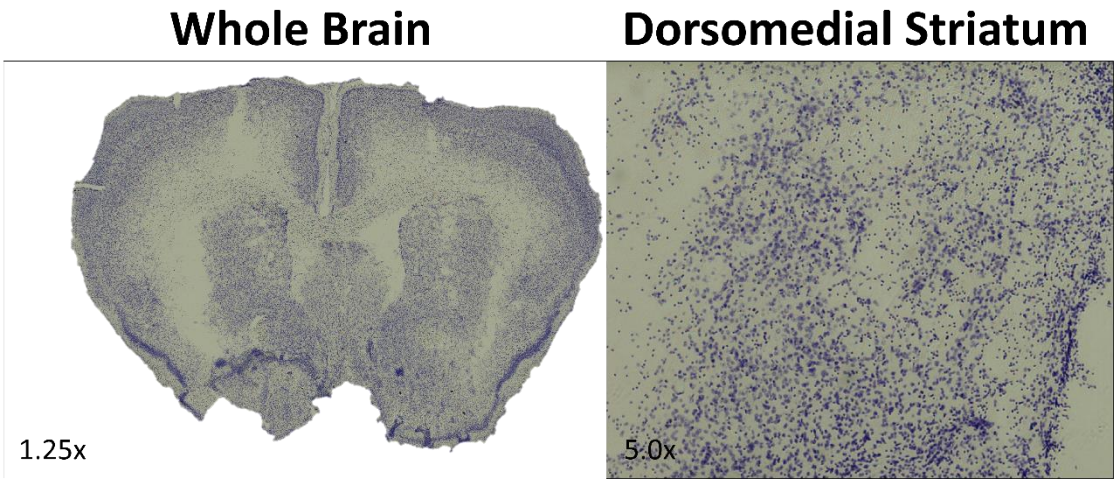

Figure 4.18. Representative samples of an LV-RB5-treated brain displaying gross neurodegeneration stained with cresyl violet. *An image of the whole brain (at 1.25x magnification) and a sample of dorsomedial striatum (at 5.0x magnification) are displayed.*

4.4.4. RB5 Pharmacokinetics

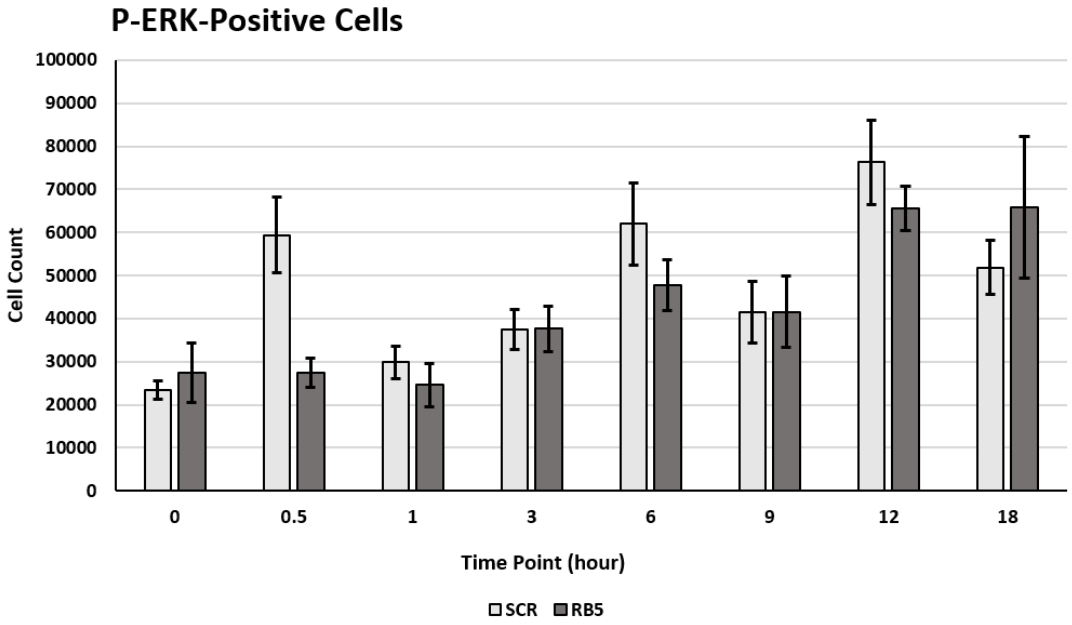

Figure 4.19. Stereological counts of striatal P-ERK-positive cells following SCR or RB5 systemic injection*. There was no significant increase in the number of P-ERK-positive striatal cells in RB5-treated animals comparted to SCR-treated controls. However, the number of P-ERK-positive cells significantly differed between time-points. The number of P-ERK positive cells within the dorsal striatum was stereologically counted after mice were intraperitoneally injected with either SCR or RB5 peptide and perfused at one of eight time-points post-injection.*

Given that LV-RB5 did not increase striatal ERK activation or affect behaviour relative to LV-GFP controls, the pharmacokinetics of the RB5 peptide was evaluated (Figure 4.19). Wild-type animals received i.p. injections of either RB5 or scrambled (SCR) control peptide at a dose of 10mg/kg, before being perfused at the appropriate time-point post-injection. Administration with RB5 peptide did not result in a significantly higher number of P-ERK-positive striatal cells when compared to SCR control ($F(1, 64) = 2.139$, p = n.s.), suggesting that RB5 does not result in increased ERK activation when administered systemically. Interestingly, the number of P-ERK-positive cells differed between time-points ($F(7, 64) = 8.744$, $p < 0.001$), possibly reflecting different basal ERK activation levels. No significant interactions between time-point and peptide were reported ($F(7, 64) = 1.685$, p = n.s.). A sample of P-ERK-positive stained brains are displayed in Figure 4.20). The histological results from this systemic study mirror those obtained from the LV study, with both experiments strongly suggesting that RB5 does not significantly increase ERK activation in the striatum of wild-type animals.

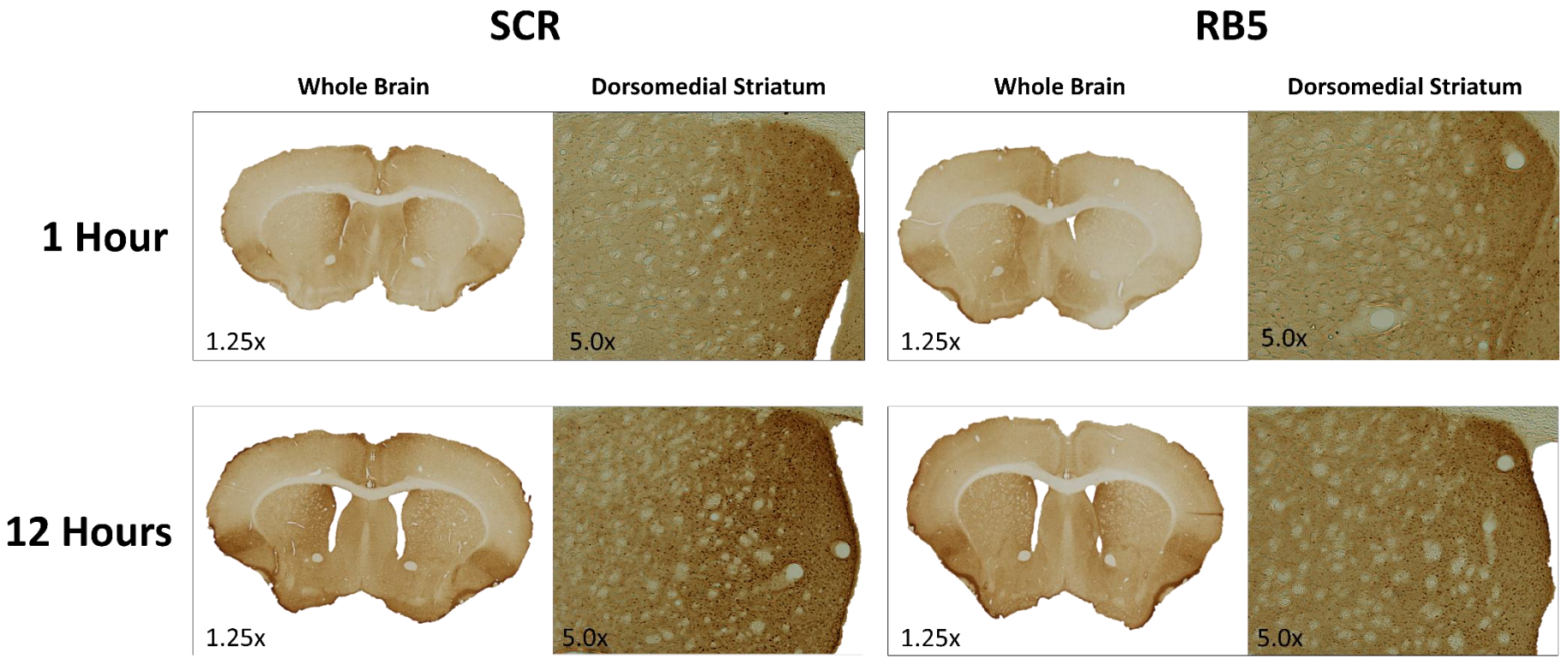

Figure 4.20. Representation of P-ERK-stained brains of SCR and RB5-administered animals at 1 hour and 12 hour time-points. *The whole brain (at 1.25x magnification) and a sample of the dorsomedial striatum (at 5.0x magnification) are displayed.*

4.4. Discussion

4.4.1. Summary

Over the course of this study, the long-term ERK signalling and behavioural effects of intrastriatal, high titre LV-GFP and LV-RB5 were investigated in WT animals. Although constructed for use in HD, it was important to first evaluate LV-SCR and LV-RB5 for any effect on commonly-used motor and cognitive tasks in WT animals to determine whether treatment with both LVs is safe, well-tolerated and without side-effects. Testing was not conducted before viral infusion in order to identify any effects of LV on learning. Observing no differences in performance between LV groups on any of the tasks, animals were perfused and selected brains from each group were stained for P-ERK. Next, stereological counts of P-ERK-positive cells in the striata were taken, revealing no difference in ERK activation between viral groups. A significant number of animals in both groups displayed extensive and unexpected neurodegeneration likely caused by high expression of GFP within LV-GFP and LV-RB5 transduced cells. Given that no effect on ERK signalling and no behavioural change was elicited by LV-RB5, in contrast to previous data collected by other members of the research group, a pharmacokinetic time-course study was conducted to characterise the acute effects of RB5 peptide on striatal P-ERK in WT animals. Mice received an i.p. injection of either control SCR peptide or RB5 peptide at 10 mg/kg, before being returned to their home cage for a defined period of time and then perfused. Brains taken at each time-point were then stained for P-ERK and cell counts conducted using stereology within the striatum. As in the previous arm of the experiment, no difference in the number of striatal P-ERK-positive cells was observed between groups, suggesting that RB5 is unable to increase ERK signalling acutely, as well as in the long term.

4.4.2. LV-RB5

4.4.2.1. Behavioural Evaluation

No difference in performance between LV-GFP and LV-RB5 animals was observed on any of the tasks used (Section 4.4.2.), suggesting that LV-RB5 did not affect the motor of cognitive abilities of mice relative to controls. Figure 4.10 demonstrates that both LV groups exhibited comparable motor coordination on the rotarod and that LV-RB5 had no effect on learning of this task relative to controls. ERK signalling being shown to be responsible for consolidation of motor learning on the rotarod (Bureau *et al*., 2010) and increased ERK signalling has been shown to improve motor learning in a mouse model of autism (Ash *et al.*, 2017) an effect which was not observed here. Supporting the rotarod data, LV groups showed no discernible difference in motor coordination or balance on any of the three balance beam parameters

(Figure 4.11). In addition, neither group differed in their latency to fall from the inverted grid (Figure 4.12), showing that limb muscle strength does not differ between animals – unsurprising in WT animals given a 60 second ceiling. Striatal ERK activity has been shown to regulate locomotor activity (Bessuso *et al*., 2013) in a pathway-specific manner (Hutton *et al*., 2017). However, LV-RB5 did not affect the locomotor activity of WT mice relative to LV-GFP during the light or dark phase (Figure 4.13B) or during the first 30 minutes of testing (Figure 4.13C – D), suggesting no effect on locomotor activity or habituation. Furthermore, in a shorter-term measure of activity, LV-GFP and LV-RB5 displayed comparable distance travelled and velocity in the open field (Figure 4.14A – B), with no difference in the cumulative duration spent exploring the wall-zone (Figure 4.14C), suggesting that neither LV acted to disinhibit mice. In addition, both groups of animals showed normal longer-term habituation to the open field between days 1 and 2 (Figure 4.14), again mirroring the general activity and habituation results produced in the spontaneous locomotor activity task. Striatal ERK signalling has also been shown to be essential for striatal-dependent associative learning (Shiflett and Balleine, 2011). Through simple FR1 training (Figure 4.15), it was readily apparent that associative learning did not differ between groups.

4.4.2.2. Evaluation of Cellular Effects

4.4.2.2.1 Effect on ERK Activation

Following the lack of behavioural differences between LV-GFP and LV-RB5 animals, the ability of LV-RB5 to increase striatal ERK signalling was evaluated by staining brains for P-ERK. When evaluated with stereology, no difference in the number of P-ERK-positive cells was observed in the striata of LV-RB5 and control group animals (Figure 4.16). Thus, it appears that constitutively-expressed RB5 peptide is not capable of elevating striatal ERK signalling above LV-GFP in WT mice in the long-term. The intensity and localisation of GFP demonstrates that LVs were injected correctly and that the LVs were capable of transducing cells and integrating transgenes into the host genome. Although indirect evidence, the presence of GFP expression makes it likely that the RB5 sequence was also incorporated into the host genome, but it is possible that is was not highly expressed. However, the transgene downstream of the IRES is usually less expressed than the upstream transgene (Section 1.6.5.3.6). Given the high expression of GFP, it seems unlikely that RB5 would not be expressed; unless the IRES interacts and prevents its function. Another possibility is that the peptide was initially efficacious in increasing P-ERK but that cellular regulatory mechanisms acted to dampen ERK activity following sustained elevation. Another possibility is that the peptide was unable to increase striatal ERK signalling in the striatum of WT mice.

4.4.2.2.3. Lentiviral Vector Efficacy

The spread of each LV within the striatum was evaluated through fluorescence microscopy. The intensity, spread, and localisation of striatal GFP (Figure 4.9) demonstrates that both LVs were injected correctly and that the LVs were capable of transducing cells - integrating transgenes into the host genome which are then expressed. GFP has been shown to be a quantitative reporter of gene expression *in vitro* (Soboleski, Oaks and Halford, 2005). Under the microscope, both LV-GFP and LV-RB5 fluoresced very intensely and fluorescence was readily apparent at a magnification of 1.6 X. As fluorescence of GFP is directly proportional to GFP gene copy number, and intensity is directly proportional to GFP mRNA abundance in single cells (Soboleski *et al*, 2005), the GFP transgene incorporated into the striatum of LV-GFP- and LV-RB5-treated mice appears to have been expressed at a very high level. One possibility is that an overly high expression of GFP masked any effect of RB5 on ERK signalling.

4.4.2.2.4. Neurodegeneration

Unexpectedly, a proportion of animals in each group exhibited significant neurodegeneration in the absence of any overt signs of illness or abnormal behaviour, probably representing a slow process. Introduction of infection through surgery is also unlikely as it is done in a sterile setting. An alternative explanation for the observed damage could be that the viral vector itself, rather than the transgene products, was responsible. However, this also seems unlikely given that the same LV construct has previously been used in the lab *in vitro* and *in vivo* with no ill effects noted (Indrigo *et al.*, 2010). However, previous *in vivo* experiments were conducted over a shorter time-frame of around 4 weeks from LV infusion to termination compared to 4 months in the present study. The length of these experiments lends credence to the notion that degeneration was not caused by the LV itself, given that the vectors themselves are degraded relatively quickly post-injection. Therefore, the transgene products appear to be the culprit for neurodegeneration in the current experiment. Given that GFP was included in both LV-GFP and LV-RB5 constructs, has a downstream WPRE element, that both groups showed very high fluorescence levels, and that both groups were affected by degeneration to a comparable degree it seems likely that overexpression of GFP was causative in cell death.

4.4.2.2.4.1. GFP-mediated toxicity

Although widely-used as a fluorescent reporter, GFP has been shown to cause toxicity under certain circumstances. GFP expression has been shown to trigger apoptosis (Liu *et al.*, 1999), cause *in vivo* damage (Huang *et al.*, 2000) and produce oxidative stress upon maturation (Goto *et al.*, 2003; Ganini *et al.*, 2017). GFP has also been shown to result in titre-dependent cell death in the rat substantia nigra when administered via an AAV8 (Klein *et al.*, 2006). The study by Klein and colleagues has particular importance to the current project as degeneration was site-

specific and, similar to the striatum, the substantia nigra is known to be susceptible to oxidative stress. GFP-induced degeneration of neurons has key implications for preclinical work, and the use of such reporters in viral vectors should be reconsidered. Sufficiently high expression of GFP could have a very detrimental impact on experimental integrity if treated as a non-functional control.

4.4.3. Re-evaluation of RB5 Pharmacokinetics

LV-RB5 was constructed and tested as a gene therapy on the basis that previous work by the Brambilla lab found an increase in P-ERK in response to acute, systemic administration of RB5 peptide in WT animals. Given the absence of increased striatal P-ERK in LV-RB5-treated animals, the ability of the RB5 cell-penetrating peptide to increase striatal P-ERK levels relative to SCR control was investigated in WT mice. No increase in P-ERK was seen in WT animals receiving RB5, mirroring the results obtained with LV-RB5 (Figure 4.19). There were significant differences in the amount of P-ERK between time-points, but this could reflect natural oscillations in ERK activation or be due to the small group sizes used. The lack of increased ERK activity at even the earliest time-point, coupled with the use of stereoisomeric amino acids at essential residues within the peptide, suggests an intrinsic lack of efficacy of the peptide. However, there are key differences between previous experiments and the one detailed here. Firstly, as mentioned, natural variation in ERK activation was observed between different time-points in this study. The presence of only one SCR control group at one time-point in the previous study conducted by the Brambilla lab (Figure 4.3) could mean that significant differences obtained in the previous study were false positives. Secondly, unbiased stereological analysis was used in the current study, in contrast to the previous experiment which used manual counting. As such, the differences in results between both studies could be due to key differences in techniques, but it should be noted that the methods used here are more conservative.

A naïve control group was not included in the present study, making comparisons between LV-GFP and LV-RB5 animals difficult. However, LV-GFP and LV-RB5 animals performed to a comparable level to WT mice of a similar age on the same genetic background and behavioural equipment (Yhnell, Dunnett and Brooks, 2016).

4.4.4. Conclusions

No increase in levels of striatal P-ERK were seen using LV-RB5 in WT animals, or when RB5 was administered systemically as a cell-penetrating peptide. RB5 was designed based on the 20 amino acids situated at the N-terminal of ERK1. Previous reports indicated that this region was responsible for reduced nuclear shuttling speed of ERK1 compared to ERK2 (Marchi *et al*., 2008), providing an entry point for potential modulation of ERK signalling. However, the argument over isoform functional redundancy vs functional specificity continues. Furthermore, studies by additional groups disagree with the interpretation of the paper and instead propose a functional redundancy model of ERK signalling whereby apparent functional differences between isoforms is due to relative expression levels. Conducting similar studies as those detailed by Marchi and colleagues, Voison *et al*. (2010) report a failure to replicate findings and propose that the slower nuclear shuttling of ERK1 is due to slower phosphorylation by upstream MEK as a consequence of higher ERK2 competition. Furthermore, there is no clear mechanism for slower shuttling of ERK1. Reports functional redundancy and evidence for lack of RB5 efficacy in this thesis call into question the validity of RB5 as treatment strategy.

In principle ERK modulation remains an attractive target for HD therapy if ERK signalling is decreased in HD. ERK has demonstrated neuroprotective roles and has been shown to be key for BDNF-TrkB gene expression changes. Since BDNF signalling is dysfunctional in HD and ERK has been shown to be lower in HD knock-in animals, boosting ERK signalling could protect MSNs from HD-related damage and degeneration and help to maintain synaptic plasticity while bypassing problems associated with BDNF receptor deficits and imbalances. Before such therapies are possible, more work must be done to characterise the Ras-ERK signalling pathway as dysregulated ERK signalling leads to some forms of cancer in addition to RASopathies such as NF1. Therefore care must be taken and the benefits of modulating this pathway weighed carefully against the potential risks. Future research should aim to investigate whether regulatory networks are in place to prevent long-term elevation of ERK signalling, characterise the efficacy of RB5 and determine the optimal titre for use.

Chapter 5: General Discussion

5.1. The Pros and Cons of Animal Models

Animal models have an indisputable place in biological research. Although ethical concerns clearly exist, the use of animals is a standard feature at every stage of basic preclinical research and drug development. However, modelling a complex disease such as PD in a rodent model is evidently challenging. Even widely-used "successful" animal models of disease like HD mice do not fully recapitulate the human condition and lack some of the essential characteristics of the disease they are modelling, such as pronounced striatal degeneration. They do however display clear cognitive and motor deficits, and the knock-in models feature an age-dependent progressive phenotype (Yhnell, Dunnett and Brooks, 2016). However, the germline Parkin null mouse models previously reported displayed subtle, variable motor and non-motor phenotypes in the absence of nigral degeneration (Section 2.1.3.) and the Parkin$^{S65A/S65A}$ mouse characterised in Chapter 2 cannot be thought of as a robust model of PD. The presence or absence of a parkinsonian phenotype in Parkin mutants appears to rely more heavily on the genetic characteristics outside the *Parkin* locus than it does on the *Parkin* mutation itself, in the sense that various germline mutations in the *Parkin* gene analogous to those in the human disease are not causative of a phenotype in animals in isolation. Instead, as shown by Perez and Palmiter (2005) and the study detailed in Chapter 2 using more similar background strains, detection of a parkinsonian phenotype could be attributable to genetic background in non-congenic animals of mixed strains. In addition, crossing inducible and stressor models with Parkin null mice result in a clear phenotype (Section 2.1.3.2.) suggesting mechanisms of compensation in mice which may make modelling PD through germline mutations difficult given the short lifespan of rodents. In consideration of age being the greatest risk factor for PD, introducing germline mutations into large animal models may represent a step forward due to an extended lifespan of these animals.

Use of mice of mixed genetic background in addition to different tests and operators makes a retrospective analysis of these early *Parkin* models difficult. In light of this, a more unified strategy towards phenotypic characterisation of genetically engineered animals should be pursued. Firstly, ARRIVE (Animal research: reporting *in vivo* experiments) guidelines should be followed for reporting animal and experimental information (Kilkenny *et al.*, 2013), with particular emphasis on mouse background strain. In the case of a mouse line being generated on a mixed genetic background strain, a statement on whether the animals used for testing are congenic or not should be made. In the case of non-congenic animals, the filial generation of

animals used for testing should be stated and a coisogenic mouse line should ideally be included for side-by-side comparison. In the case of phenotypic differences, genomic differences between congenic and mixed mice could be identified through sequencing. At the behavioural level, the variation in which tests were used to screen germline *Parkin* null mice and how they were conducted makes comparison between models difficult. Although variation between laboratories conducting the same tests has been reported, these differences are typically more influenced by genetic background rather than operator conduct (Wahlsten *et al.*, 2003). Therefore standardising tests across different laboratories would permit better evaluation of phenotype in different - and the same - animal models between research groups and permit meta-analysis of results. In addition to standardisation, establishing preclinical trial centres and publishing predefined outcomes specific to the disease under investigation would encourage a uniform approach and reporting methodology to individual groups, again aiding comparisons and reproducibility (Jucker, 2010; van der Worp *et al.*, 2010). A grading system could also be established to score the deficits in animals on tasks probing different behavioural domains (e.g. cognitive or motor) and sub-domains (e.g. spatial memory vs associative learning) to easily enable researchers to choose the most appropriate model for their particular experiment.

Although genetic models of disease are invaluable for understanding the underlying pathophysiology of disease, the experiments described in this thesis demonstrate the importance of neurotoxin models of disease and healthy WT mice for mechanistic insight and primary analysis of therapies, respectively. In the case of Chapter 3, trialling a symptomatic-targeted striatal dopamine replacement therapy in 6-OHDA rats is perfectly sensible, given that dopaminergic cell death and subsequent reductions in striatal dopamine levels can be readily and reproducibly induced in these animal models. In the case of Chapter 4, the use of WT mice as the first *in vivo* model for characterisation of RB5 transgene expression proved extremely valuable. As a potential disease-modifying therapy, initial characterisation in a knock-in HD model, while attractive, would have led to a long, expensive experiment which, at termination, would have been inconclusive owing to confounding pathology attributed to both LV-GFP and LV-RB5. In addition, characterisation of RB5's capacity to increase ERK activation demonstrated a lack of efficacy by both routes of administration in the presence of adequate control groups and unbiased stereology. Chapter 4 demonstrates the ethical and experimental advantages of therapy characterisation in WT animals, prior to advancing the study prematurely. This chapter also demonstrates that strong controls are needed, with the inclusion of a naïve group key to future experiments.

As described in Chapter 2, the dogma of PINK1-Parkin-mediated mitophagy in SNc neurons was based on *in vitro* experiments conducted using mitochondrial toxins largely in proliferative cell-types. Production of Parkin null Drosophila produced a degenerative phenotype and a flurry of activity to create Parkin null mouse lines generated several models which displayed a very mild phenotype or absence of phenotype (Section 1.5.4.2.4.). Later work demonstrated that basal mitophagy occurred independently of PINK1 in mouse SNc and that mitophagy was unaffected in the SNc of *Parkin*$^{S65A/S65A}$ mice (Mcwilliams *et al.*, 2018). These discrepancies represent a failure in translation between cell and animal models of disease. The advent of iPSC technology could allow a more in-depth study of the disease pathways and dysfunction in neurons derived from PD patient tissue before introducing the mutations into animal models (Falkenburger, Saridaki and Dinter, 2016; Mishima *et al.*, 2018; Amin *et al.*, 2019). However, study of diseases such as PD, in which age is the greatest risk factor, may not reproduce the disease sufficiently given the immaturity of the system (Doss and Sachinidis, 2019). Another clear drawback is the inability to investigate non-cell autonomous pathophysiological process or changes at the behavioural level.

5.2. Optimisation of Therapies

Optimisation is an essential step for any therapy. The ProSavin clinical trial (Palfi *et al*., 2014) utilised an LV approach to gene therapy. Although safe and well-tolerated, subsequent approaches have taken advantage of the better safety profile of AAVs: they are not pathogenic to human in their native form, they are less immunogenic, they cut the risk of insertional mutagenesis, they require a helper virus for replication, and their serotype can be manipulated to confer preference for certain cell-types, thus conferring specificity (Choudhury *et al.*, 2017). The transition from multiple monocistronic AAVs to bicistronic AAVs (Cederfjäll *et al*., 2012) represents a significant refinement in approach, also. The inclusion of linkers detailed in Chapter 3 (although unsuccessful at this time) also represents an attractive target for optimisation given the issues associated with scaling up from small animal models to NHPs to humans even when using high titrations (Cederfjäll *et al*., 2013; Palfi *et al*., 2014). The ability to ensure robust co-expression of transgenes such as *TH* and *GCH1* from a single AAV at a low titre would ensure therapy was optimal, and efficient co-expression may mitigate the issues of transducing a much larger volume in larger models. In addition, gene therapy, as with any therapy, lies within a defined therapeutic window. Once administered, the promoter under which transgene expression is driven cannot be modulated. Too low a titre, such as that administered in the MPTP model NHP detailed by Cederfjäll *et al*., (2013) and in Chapter 3 of this thesis, will result in little-to-no therapeutic benefit and the prevention from efficiently administering a further dose due to an increased immune response upon re-exposure

(Choudhury *et al.,* 2017). On the other hand, too high a titre can lead to transgene over-expression and neurodegeneration, such as that described by Cederfjäll *et al*., 2012, 2013; Klein *et al*., 2006 and Chapter 4 of this thesis. Therefore, to prevent the ethical issues associated with administrating a low dose and the health issues associated with administering a high dose, optimisation and characterisation of doses in various models must first be undertaken, and transgene expression must be sufficiently maximised. As in Section 5.1.1., consistency in generation of therapeutic AAVs should also be an essential step in translation. As detailed in Section 3.5., the sequence targeted for PCR can greatly influence the titre of the AAV reported, potentially preventing replication between studies as was the case in Chapter 3.

5.3. Scientific Reporting and the Differences Between Models

Lack of sufficient reporting and the technical difficulties associated with characterisation and drug testing in different models can also lead to difficulties in producing accurate animal models of disease or developing therapies. In the case of Chapter 2, a huge amount of research characterised Parkin, and more specifically phosphorylation of Parkin at Ser65, as being essential for mitophagy, linking this cellular pathway to PD. However, the majority of this work took place in cellular models where Parkin was overexpressed or where mitochondrial potential was manipulated through mitochondrial uncouplers. It is only recently, through production of complex *in vivo* models capable of characterising mitophagy, that it is possible to see that basal mitophagy occurs independently of the PINK1-Parkin pathway in mouse SNc neurons (McWilliams *et al*., 2018) and that germline PD causative mutations in *Parkin* do not affect basal mitophagy in this region (McWilliams *et al*., 2018). The expectation of a parkinsonian phenotype in Parkin null mice also lead to reporting of parkinsonian phenotypes in the absence of supporting pathology without the consideration of genetic background, despite the importance of background being known at the time. Only Perez and Palmiter (2005) controlled for this, and subsequently titled their paper “Parkin-deficient mice are not a robust model of parkinsonism”. Accordingly, the separate work demonstrating the importance of the PINK1-Parkin pathway for mitophagy *in vitro* and the effect of mutations in *Parkin* in human PD have not converged, with the Parkin$^{S65A/S65A}$ mouse failing to show any deficits in mitophagy, any nigral degeneration or alteration in dopamine transmission, of any overt parkinsonian phenotype.

GFP is commonly used as a reporter *in vitro* and *in vivo*, often as a control, as in Chapter 4. However, expression of this protein has a physiological effect, promoting oxidative stress and causing cell death if expressed at high enough levels (Ganini *et al*., 2017; Klein et al., 2006), Chapter 4. Of particular note is the vulnerability of neurons of the substantia nigra and striatum

to oxidative stress, coupled with the demonstration by Klein and colleagues and Chapter 4 that GFP expression is sufficient to induce cell death in these areas. Considering that both of these regions represent prime targets for gene therapy in PD and HD/PD respectively, the use of GFP as a control or as a reporter in the experimental vector during preclinical evaluation raises important questions. GFP-mediated oxidative stress in cells already undergoing disease-mediated oxidative stress could worsen the phenotype of animals to diminish or mask the effects of a potential treatment. In addition, the use of GFP in WT animals (as in Chapter 4) is sufficient to cause cell death within the striatum, carrying the potential to cause dysfunction in WT animals, compromising their purpose as healthy controls. From these reports, it is apparent that the harmful role of GFP is clearly known, but also that it is under-reported and underappreciated.

Although the ERK signalling pathway has been extensively characterised, debate is still ongoing as to whether the ERK1 and ERK2 isoforms are functionally redundant. Both *in vitro* and *in vivo* data have led to multiple reports of functional specificity and an associated alteration in ERK signalling upon isoform-specific manipulation which can cause behavioural changes (See Chapter 4). The production and therapeutic investigation of RB5 was based on evidence of differential nuclear shuttling of ERK isoforms and associated alterations in signalling through relief of isoform partial agonism (Marchi *et al*., 2008). However, more recent work has pointed to a more simple explanation for ERK isoform "functional specificity" – different levels of expression of the *MAPK3* and *MAPK1* genes. As demonstrated by Busca, Pouyyssegur, and Lenormand (2016), a surprising number of studies reporting on ERK isoform functional specificity fail to take into account or report the relative expression of isoforms within their model of interest. Considering that relative amounts of each isoform would certainly influence their relative signalling contributions due to a shared activator, this lack of investigation is a concerning prospect. If relative expression is to blame for the apparent functional specificity of ERK1 and ERK2, it is not readily apparently how RB5 would be able to affect ERK signalling.

5.4. Conclusions

This thesis aimed to follow three key objectives: to characterise a potential animal model of PD, to optimise an existing therapy, and to validate the cellular and behavioural effects of a potential disease-modifying treatment for HD in WT animals. Although largely "negative", the data in this thesis highlight the key challenges for preclinical study of neurodegeneration and progress towards translation. However, it also provides some key steps that should be taken to promote reliable, replicable, and accurate models of disease and treatments. They key conclusions will be listed here:

- *Parkin* $^{S65A/S65A}$ mice are not a robust model of Parkinson's disease – they do not exhibit a clear motor phenotype and the nigrostriatal system is intact with no alterations in basal mitophagy. Roles of the PINK1-Parkin pathway outside of mitophagy should be explored.
- AAV-mediated dopamine replacement therapy has the potential to optimise current oral L-DOPA therapy. Evaluation of linkers was not possible due to an insufficient titre of virus being delivered, but this highlights the fact that increasing attention needs to be focussed on the methodology of titrating viral vectors and evaluating the best dose for therapeutic benefit before progressing into clinical trials.
- RB5 does not increase striatal P-ERK signalling in wild-type mice when administered systemically or via an LV. The efficacy of this peptide must be reconsidered and, as above, the titre of LV carefully reconsidered in light of the extensive neurodegeneration observed in some animals. Furthermore, the debate of functional redundancy/specificity between ERK isoforms should be investigated with consideration of relative expression levels.

Bibliography

Aarsland, D. *et al.* (1999) 'Mental symptoms in Parkinson's disease are important contributors to caregiver distress.', *International journal of geriatric psychiatry*. England, 14(10), pp. 866–874.

Adam, O. R. and Jankovic, J. (2008) 'Symptomatic treatment of Huntington disease.', *Neurotherapeutics : the journal of the American Society for Experimental NeuroTherapeutics*, 5(2), pp. 181–197. doi: 10.1016/j.nurt.2008.01.008.

Adams, J. P. and Sweatt, J. D. (2002) 'Molecular psychology: roles for the ERK MAP kinase cascade in memory.', *Annual review of pharmacology and toxicology*, 42(1), pp. 135–163. doi: 10.1146/annurev.pharmtox.42.082701.145401.

Akinleye, A. *et al.* (2013) 'MEK and the inhibitors: From bench to bedside', *Journal of Hematology and Oncology*, 6(1), pp. 1–11. doi: 10.1186/1756-8722-6-27.

Akkina, R. K. *et al.* (1996) 'High-efficiency gene transfer into CD34+ cells with a human immunodeficiency virus type 1-based retroviral vector pseudotyped with vesicular stomatitis virus envelope glycoprotein G.', *Journal of virology*. United States, 70(4), pp. 2581–2585.

Alberico, S. L., Cassell, M. D. and Narayanan, N. S. (2015) 'The Vulnerable Ventral Tegmental Area in Parkinson's Disease.', *Basal ganglia*. Netherlands, 5(2–3), pp. 51–55. doi: 10.1016/j.baga.2015.06.001.

Albin, R. L., Young, A. B. and Penney, J. B. (1989) 'The functional anatomy of basal ganglia disorders', *Trends in Neurosciences*, 12(10), pp. 366–375. doi: https://doi.org/10.1016/0166-2236(89)90074-X.

Alexander, G. (1986) 'Parallel Organization of Functionally Segregated Circuits Linking Basal Ganglia and Cortex', *Annual Review of Neuroscience*, 9(1), pp. 357–381. doi: 10.1146/annurev.neuro.9.1.357.

Allen, G. I. and Tsukahara, N. (1974) 'Cerebrocerebellar Communication Systems', *Physiological Reviews*, 54(4), pp. 957–1006.

Allera-Moreau, C. *et al.* (2006) 'The use of IRES-based bicistronic vectors allows the stable expression of recombinant G-protein coupled receptors such as NPY5 and histamine 4', *Biochimie*, 88(6), pp. 737–746. doi: 10.1016/j.biochi.2006.05.019.

Allera-Moreau, C. *et al.* (2007) 'Long term expression of bicistronic vector driven by the FGF-1

IRES in mouse muscle', *BMC Biotechnology*, 7, pp. 1–12. doi: 10.1186/1472-6750-7-74.

Alonso Canovas, A. *et al.* (2014) 'Dopaminergic agonists in Parkinson's disease.', *Neurologia (Barcelona, Spain)*. Spain, 29(4), pp. 230–241. doi: 10.1016/j.nrl.2011.04.012.

Altar, C. A. *et al.* (1997) 'Anterograde transport of brain-derived neurotrophic factor and its role in the brain.', *Nature*. England, 389(6653), pp. 856–860. doi: 10.1038/39885.

Amin, N. *et al.* (2019) 'Recent advances of induced pluripotent stem cells application in neurodegenerative diseases', *Progress in Neuro-Psychopharmacology and Biological Psychiatry*. Elsevier, 95(March), p. 109674. doi: 10.1016/j.pnpbp.2019.109674.

Andrew, S. E. *et al.* (1993) 'The relationship between trinucleotide (CAG) repeat length and clinical features of Huntington's disease.', *Nature genetics*. United States, 4(4), pp. 398–403. doi: 10.1038/ng0893-398.

Andrews, R. M. *et al.* (1999) 'Reanalysis and revision of the Cambridge reference sequence for human mitochondrial DNA', *Nature Genetics*, 23(2), p. 147. doi: 10.1038/13779.

Annoni, A. *et al.* (2018) 'Modulation of immune responses in lentiviral vector-mediated gene transfer', *Cellular Immunology*. Elsevier, 342(April 2018), p. 103802. doi: 10.1016/j.cellimm.2018.04.012.

Apostol, B. L. *et al.* (2006) 'Mutant huntingtin alters MAPK signaling pathways in PC12 and striatal cells: ERK1/2 protects against mutant huntingtin-associated toxicity.', *Human molecular genetics*, 15(2), pp. 273–85. doi: 10.1093/hmg/ddi443.

Apostol, B. L. *et al.* (2008) 'CEP-1347 reduces mutant huntingtin-associated neurotoxicity and restores BDNF levels in R6/2 mice', *Molecular and Cellular Neuroscience*, 39(1), pp. 8–20. doi: 10.1016/j.mcn.2008.04.007.

Arai, R. *et al.* (1994) 'Immunohistochemical evidence that central serotonin neurons produce dopamine from exogenousl-DOPA in the rat, with reference to the involvement of aromaticl-amino acid decar□ylase', *Brain Research*, 667(2), pp. 295–299. doi: https://doi.org/10.1016/0006-8993(94)91511-3.

Arregui, L. *et al.* (2011) 'Adenoviral astrocyte-specific expression of BDNF in the striata of mice transgenic for Huntington's disease delays the onset of the motor phenotype', *Cellular and Molecular Neurobiology*, 31(8), pp. 1229–1243. doi: 10.1007/s10571-011-9725-y.

Arumugam, V. *et al.* (2017) 'The impact of antidepressant treatment on brain-derived neurotrophic factor level: An evidence-based approach through systematic review and meta-

analysis.', *Indian journal of pharmacology*, 49(3), pp. 236–242. doi: 10.4103/ijp.IJP_700_16.

Ash, R. T. *et al.* (2017) 'Excessive ERK-dependent synaptic clustering drives enhanced motor learning in the MECP2 duplication syndrome mouse model of autism', *Doi.Org*, pp. 1–51. doi: 10.1101/100875.

Atchison, R. W., Casto, B. C. and Hammon, W. M. (1965) 'Adenovirus-Associated Defective Virus Particles', *Science*. United States, 149(3685), pp. 754–755. doi: 10.1126/science.149.3685.754.

Atkins, C. M. *et al.* (1998) 'The MAPK cascade is required for mammalian associative learning.', *Nature neuroscience*, 1(7), pp. 602–609. doi: 10.1038/2836.

Bachoud-Lévi, A. C. *et al.* (2000) 'Motor and cognitive improvements in patients with Huntington's disease after neural transplantation', *Lancet*. England, 356(9246), pp. 1975–1979. doi: 10.1016/S0140-6736(00)03310-9.

Bachoud-Lévi, A. C. (2017) 'From open to large-scale randomized cell transplantation trials in Huntington's disease: Lessons from the multicentric intracerebral grafting in Huntington's disease trial (MIG-HD) and previous pilot studies', *Progress in Brain Research*, 230, pp. 227–261. doi: 10.1016/bs.pbr.2016.12.011.

Badin, R. A. *et al.* (2019) 'Gene Therapy for Parkinson's Disease: Preclinical Evaluation of Optimally Configured TH:CH1 Fusion for Maximal Dopamine Synthesis', *Molecular Therapy - Methods & Clinical Development*, 14(September), pp. 206–216. doi: 10.1016/j.omtm.2019.07.002.

Bae, E.-J. *et al.* (2018) 'LRRK2 kinase regulates α-synuclein propagation via RAB35 phosphorylation', *Nature Communications*, 9(1), p. 3465. doi: 10.1038/s41467-018-05958-z.

Baig, F. *et al.* (2015) 'Delineating nonmotor symptoms in early Parkinson's disease and first-degree relatives.', *Movement disorders : official journal of the Movement Disorder Society*. United States, 30(13), pp. 1759–1766. doi: 10.1002/mds.26281.

Barde, Y. A., Edgar, D. and Thoenen, H. (1982) 'Purification of a new neurotrophic factor from mammalian brain.', *The EMBO journal*. England, 1(5), pp. 549–553.

Barker, R. A. *et al.* (2013) 'Fetal dopaminergic transplantation trials and the future of neural grafting in Parkinson's disease.', *The Lancet. Neurology*. England, 12(1), pp. 84–91. doi: 10.1016/S1474-4422(12)70295-8.

Barker, R. A. *et al.* (2019) 'Designing stem-cell-based dopamine cell replacement trials for

Parkinson's disease', *Nature Medicine*, 25(July). doi: 10.1038/s41591-019-0507-2.

Bartels, A. L. *et al.* (2003) 'Relationship between freezing of gait (FOG) and other features of Parkinson's: FOG is not correlated with bradykinesia', *Journal of Clinical Neuroscience*, 10(5), pp. 584–588. doi: 10.1016/S0967-5868(03)00192-9.

Bates, G. P. *et al.* (2015) 'Huntington disease', *Nature Reviews Disease Primers*, (April), p. 15005. doi: 10.1038/nrdp.2015.5.

Beal, M. F. *et al.* (1986) 'Replication of the neurochemical characteristics of Huntington's disease by quinolinic acid.', *Nature*. England, 321(6066), pp. 168–171. doi: 10.1038/321168a0.

Beal, M. F. *et al.* (1993) 'Age-dependent striatal excitotoxic lesions produced by the endogenous mitochondrial inhibitor malonate.', *Journal of neurochemistry*. England, 61(3), pp. 1147–1150. doi: 10.1111/j.1471-4159.1993.tb03633.x.

Beal, M. F. (2010) 'Parkinson's disease: a model dilemma', *Nature*, 466(7310), pp. S8–S10. doi: 10.1038/466S8a.

Beglinger, L. J. *et al.* (2014) 'Results of the citalopram to enhance cognition in Huntington disease trial.', *Movement disorders : official journal of the Movement Disorder Society*. United States, 29(3), pp. 401–405. doi: 10.1002/mds.25750.

Bemelmans, A. P. *et al.* (1999) 'Brain-derived neurotrophic factor-mediated protection of striatal neurons in an excitotoxic rat model of Huntington's disease, as demonstrated by adenoviral gene transfer.', *Human gene therapy*. United States, 10(18), pp. 2987–2997. doi: 10.1089/10430349950016393.

Benazzouz, A. *et al.* (2002) 'Intraoperative microrecordings of the subthalamic nucleus in Parkinson's disease.', *Movement disorders : official journal of the Movement Disorder Society*. United States, 17 Suppl 3, pp. S145-9.

Bencsics, C. *et al.* (1996) 'Double transduction with GTP cyclohydrolase I and tyrosine hydroxylase is necessary for spontaneous synthesis of L-DOPA by primary fibroblasts.', *The Journal of neuroscience : the official journal of the Society for Neuroscience*, 16(14), pp. 4449–56. doi: 10.1071/SR9950321.

Bender, A. *et al.* (2006) 'High levels of mitochondrial DNA deletions in substantia nigra neurons in aging and Parkinson disease.', *Nature genetics*. United States, 38(5), pp. 515–517. doi: 10.1038/ng1769.

Bendor, J. T., Logan, T. P. and Edwards, R. H. (2013) 'The function of alpha-synuclein.', *Neuron*. United States, 79(6), pp. 1044–1066. doi: 10.1016/j.neuron.2013.09.004.

Bereiter-Hahn, J. and Vöth, M. (1994) 'Dynamics of mitochondria in living cells: Shape changes, dislocations, fusion, and fission of mitochondria', *Microscopy Research and Technique*, 27(3), pp. 198–219. doi: 10.1002/jemt.1070270303.

Bergman, H. *et al.* (1994) 'The primate subthalamic nucleus. II. Neuronal activity in the MPTP model of parkinsonism.', *Journal of neurophysiology*. United States, 72(2), pp. 507–520. doi: 10.1152/jn.1994.72.2.507.

Besusso, D. *et al.* (2013) 'BDNF-TrkB signaling in striatopallidal neurons controls inhibition of locomotor behavior.', *Nature communications*. Nature Publishing Group, 4(May), p. 2031. doi: 10.1038/ncomms3031.

Betarbet, R. *et al.* (2000) 'Chronic systemic pesticide exposure reproduces features of Parkinson's disease.', *Nature neuroscience*. United States, 3(12), pp. 1301–1306. doi: 10.1038/81834.

Bhakar, A. L. *et al.* (2003) 'Apoptosis induced by p75NTR overexpression requires Jun kinase-dependent phosphorylation of Bad.', *The Journal of neuroscience : the official journal of the Society for Neuroscience*, 23(36), pp. 11373–11381. doi: 23/36/11373 [pii].

Billingsley, K. J. *et al.* (2018) 'Genetic risk factors in Parkinson's disease.', *Cell and tissue research*. Germany, 373(1), pp. 9–20. doi: 10.1007/s00441-018-2817-y.

Björklund, A. and Dunnett, S. B. (2019) 'The Amphetamine Induced Rotation Test: A Re-Assessment of Its Use as a Tool to Monitor Motor Impairment and Functional Recovery in Rodent Models of Parkinson's Disease.', *Journal of Parkinson's disease*, 9(1), pp. 17–29. doi: 10.3233/JPD-181525.

Björklund, A., Schmidt, R. H. and Stenevi, U. (1980) 'Functional reinnervation of the neostriatum in the adult rat by use of intraparenchymal grafting of dissociated cell suspensions from the substantia nigra', *Cell and Tissue Research*. Germany, 212(1), pp. 39–45. doi: 10.1007/BF00234031.

Björklund, T. *et al.* (2009) 'Optimization of continuous in vivo DOPA production and studies on ectopic da synthesis using rAAV5 vectors in Parkinsonian rats', *Journal of Neurochemistry*, 111(2), pp. 355–367. doi: 10.1111/j.1471-4159.2009.06340.x.

Björklund, T. *et al.* (2010) 'Optimized adeno-associated viral vector-mediated striatal DOPA delivery restores sensorimotor function and prevents dyskinesias in a model of advanced

Parkinson's disease', *Brain*, 133(2), pp. 496–511. doi: 10.1093/brain/awp314.

Björklund, T., Cederfjäll, E. A. and Kirik, D. (2010) 'Gene therapy for dopamine replacement', *Progress in Brain Research*, 184(C), pp. 220–235. doi: 10.1016/S0079-6123(10)84012-9.

Blanchet, P. J. and Brefel-Courbon, C. (2018) 'Chronic pain and pain processing in Parkinson's disease', *Progress in Neuro-Psychopharmacology and Biological Psychiatry*. Elsevier, 87(September 2017), pp. 200–206. doi: 10.1016/j.pnpbp.2017.10.010.

Blank, J. L. *et al.* (1996) 'Molecular Cloning of Mitogen-activated Protein/ERK Kinase Kinases (MEKK) 2 and 3', *The Journal of Biological Chemistry*, 271(10), pp. 5361–5368. doi: 10.1074/jbc.271.10.5361.

Blaschko, H. (1942) 'The activity of l(-)-dopa decarboxylase.', *The Journal of physiology*, 101(3), pp. 337–349. doi: 10.1113/jphysiol.1942.sp003988.

Blauwendraat, C. *et al.* (2019) 'Parkinson's disease age at onset genome-wide association study: Defining heritability, genetic loci, and α-synuclein mechanisms', *Movement Disorders*, 34(6), pp. 866–875. doi: 10.1002/mds.27659.

Blum, S. *et al.* (1999) 'A mitogen-activated protein kinase cascade in the CA1/CA2 subfield of the dorsal hippocampus is essential for long-term spatial memory.', *The Journal of neuroscience : the official journal of the Society for Neuroscience*. United States, 19(9), pp. 3535–3544.

Bodai, Laszlo; Marsh, J. L. (2013) 'A novel target for Huntington's disease: ERK at the crossroads of signaling', *Bioessays*, 34(2), pp. 142–148.

Bokhoven, M. *et al.* (2009) 'Insertional Gene Activation by Lentiviral and Gammaretroviral Vectors', *Journal of Virology*. American Society for Microbiology Journals, 83(1), pp. 283–294. doi: 10.1128/JVI.01865-08.

Bonfini, L. *et al.* (1992) 'The Son of sevenless gene product: A putative activator of Ras', *Science*, 255(5044), pp. 603–606. doi: 10.1126/science.1736363.

Bonifati, V. *et al.* (2003) 'Mutations in the DJ-1 gene associated with autosomal recessive early-onset parkinsonism.', *Science (New York, N.Y.)*. United States, 299(5604), pp. 256–259. doi: 10.1126/science.1077209.

Borrell-Pagès, M. *et al.* (2006) 'Cystamine and cysteamine increase brain levels of BDNF in Huntington disease via HSJ1b and transglutaminase', *The Journal of clinical investigation*. 2006/04/06. American Society for Clinical Investigation, 116(5), pp. 1410–1424. doi:

10.1172/JCI27607.

Bothe, G. W. M. *et al.* (2004) 'Genetic and behavioral differences among five inbred mouse strains commonly used in the production of transgenic and knockout mice.', *Genes, brain, and behavior*. England, 3(3), pp. 149–157. doi: 10.1111/j.1601-183x.2004.00064.x.

Boutin, S. *et al.* (2010) 'Prevalence of serum IgG and neutralizing factors against adeno-associated virus (AAV) types 1, 2, 5, 6, 8, and 9 in the healthy population: implications for gene therapy using AAV vectors.', *Human gene therapy*. United States, 21(6), pp. 704–712. doi: 10.1089/hum.2009.182.

Bowles, K. R. and Jones, L. (2014) 'Kinase Signalling in Huntington ' s Disease', 3, pp. 89–123. doi: 10.3233/JHD-140106.

Braak, H. *et al.* (2003) 'Staging of brain pathology related to sporadic Parkinson's disease', *Neurobiology of Aging*, 24(2), pp. 197–211. doi: 10.1016/S0197-4580(02)00065-9.

Brambilla, R. *et al.* (1997) 'A role for the Ras signalling pathway in synaptic transmission and long-term memory.', *Nature*, 390(6657), pp. 281–286. doi: 10.1038/36849.

Branch, S. Y. *et al.* (2016) 'Dopaminergic Neurons Exhibit an Age-Dependent Decline in Electrophysiological Parameters in the MitoPark Mouse Model of Parkinson's Disease.', *The Journal of neuroscience : the official journal of the Society for Neuroscience*. United States, 36(14), pp. 4026–4037. doi: 10.1523/JNEUROSCI.1395-15.2016.

Breese, G. R. and Traylor, T. D. (1971) 'Depletion of brain noradrenaline and dopamine by 6-hydroxydopamine.', *British journal of pharmacology*. England, 42(1), pp. 88–99. doi: 10.1111/j.1476-5381.1971.tb07089.x.

Breger, L. S. and Fuzzati Armentero, M. T. (2019) 'Genetically engineered animal models of Parkinson's disease: From worm to rodent', *European Journal of Neuroscience*, 49(4), pp. 533–560. doi: 10.1111/ejn.14300.

Brito, V. *et al.* (2013) 'Imbalance of p75(NTR)/TrkB protein expression in Huntington's disease: implication for neuroprotective therapies.', *Cell death & disease*, 4, p. e595. doi: 10.1038/cddis.2013.116.

den Brok, M. G. H. E. *et al.* (2015) 'Apathy in Parkinson's disease: A systematic review and meta-analysis.', *Movement disorders : official journal of the Movement Disorder Society*. United States, 30(6), pp. 759–769. doi: 10.1002/mds.26208.

Brooks, S. P., Jones, L. and Dunnett, S. B. (2012) 'Comparative analysis of pathology and

behavioural phenotypes in mouse models of Huntington's disease.', *Brain research bulletin*. Elsevier Inc., 88(2–3), pp. 81–93. doi: 10.1016/j.brainresbull.2011.10.002.

Brouillet, E. *et al.* (1993) 'Age-dependent vulnerability of the striatum to the mitochondrial toxin 3-nitropropionic acid.', *Journal of neurochemistry*. England, 60(1), pp. 356–359. doi: 10.1111/j.1471-4159.1993.tb05859.x.

Brunet, F. G. *et al.* (2006) 'Gene loss and evolutionary rates following whole-genome duplication in teleost fishes.', *Molecular biology and evolution*. United States, 23(9), pp. 1808–1816. doi: 10.1093/molbev/msl049.

Bryant, C. D. *et al.* (2008) 'Behavioral differences among C57BL/6 substrains: implications for transgenic and knockout studies.', *Journal of neurogenetics*. England, 22(4), pp. 315–331. doi: 10.1080/01677060802357388.

Bryant, C. D. (2011) 'The blessings and curses of C57BL/6 substrains in mouse genetic studies.', *Annals of the New York Academy of Sciences*, 1245, pp. 31–33. doi: 10.1111/j.1749-6632.2011.06325.x.

Bukrinsky, M. I. *et al.* (1993) 'Association of integrase, matrix, and reverse transcriptase antigens of human immunodeficiency virus type 1 with viral nucleic acids following acute infection.', *Proceedings of the National Academy of Sciences of the United States of America*. United States, 90(13), pp. 6125–6129. doi: 10.1073/pnas.90.13.6125.

Büning, H. *et al.* (2015) 'Engineering the AAV capsid to optimize vector–host-interactions', *Current Opinion in Pharmacology*, 24, pp. 94–104. doi: https://doi.org/10.1016/j.coph.2015.08.002.

Bureau, G. *et al.* (2010) 'Intrastriatal inhibition of extracellular signal-regulated kinases impaired the consolidation phase of motor skill learning', *Neurobiology of Learning and Memory*. Elsevier Inc., 94(1), pp. 107–115. doi: 10.1016/j.nlm.2010.04.008.

Buscà, R. *et al.* (2015) 'ERK1 and ERK2 present functional redundancy in tetrapods despite higher evolution rate of ERK1.', *BMC evolutionary biology*. BMC Evolutionary Biology, 15(1), p. 179. doi: 10.1186/s12862-015-0450-x.

Buscà, R., Pouysségur, J. and Lenormand, P. (2016) 'ERK1 and ERK2 Map Kinases: Specific Roles or Functional Redundancy?', *Frontiers in Cell and Developmental Biology*, 4(June), pp. 1–23. doi: 10.3389/fcell.2016.00053.

Cackovic, J. *et al.* (2018) 'Vulnerable Parkin Loss-of-Function Drosophila Dopaminergic Neurons Have Advanced Mitochondrial Aging, Mitochondrial Network Loss and Transiently

Reduced Autophagosome Recruitment', *Frontiers in Cellular Neuroscience*, 12(February), pp. 1–14. doi: 10.3389/fncel.2018.00039.

Calabresi, P. *et al.* (2000) 'Dopamine and cAMP-regulated phosphoprotein 32 kDa controls both striatal long-term depression and long-term potentiation, opposing forms of synaptic plasticity.', *The Journal of neuroscience : the official journal of the Society for Neuroscience*. United States, 20(22), pp. 8443–8451.

Calabresi, P. A. *et al.* (2014) 'Safety and efficacy of fingolimod in patients with relapsing-remitting multiple sclerosis (FREEDOMS II): a double-blind, randomised, placebo-controlled, phase 3 trial.', *The Lancet. Neurology*. England, 13(6), pp. 545–556. doi: 10.1016/S1474-4422(14)70049-3.

Canals, J. M. *et al.* (2004) 'Brain-derived neurotrophic factor regulates the onset and severity of motor dysfunction associated with enkephalinergic neuronal degeneration in Huntington's disease', *Journal of Neuroscience*, 24(35), pp. 7727–7739. doi: 10.1523/JNEUROSCI.1197-04.2004.

Cargnello, M. and Roux, P. P. (2011) 'Activation and Function of the MAPKs and Their Substrates, the MAPK-Activated Protein Kinases', *Microbiology and molecular biology reviews : MMBR*, 75(1), pp. 50–83. doi: 10.1128/MMBR.00031-10.

Carlson, G. A. *et al.* (1997) 'Genetic modification of the phenotypes produced by amyloid precursor protein overexpression in transgenic mice.', *Human molecular genetics*. England, 6(11), pp. 1951–1959. doi: 10.1093/hmg/6.11.1951.

Caron, N. S., Dorsey, E. R. and Hayden, M. R. (2018) 'Therapeutic approaches to huntington disease: From the bench to the clinic', *Nature Reviews Drug Discovery*. Nature Publishing Group, 17(10), pp. 729–750. doi: 10.1038/nrd.2018.133.

Carriere, A. *et al.* (2008) 'The RSK factors of activating the Ras/MAPK signaling cascade.', *Frontiers in bioscience : a journal and virtual library*. United States, 13, pp. 4258–4275. doi: 10.2741/3003.

Casar, B. and Crespo, P. (2016) 'ERK Signals: Scaffolding Scaffolds?', *Frontiers in Cell and Developmental Biology*, 4(May), pp. 1–11. doi: 10.3389/fcell.2016.00049.

Castrén, E. and Antila, H. (2017) 'Neuronal plasticity and neurotrophic factors in drug responses Europe PMC Funders Author Manuscripts Neurotrophins in Plasticity', 22(8), pp. 1085–1095. doi: 10.1038/mp.2017.61.Neuronal.

Cebrian, C. *et al.* (2014) 'MHC-I expression renders catecholaminergic neurons susceptible to

T-cell-mediated degeneration.', *Nature communications*. England, 5, p. 3633. doi: 10.1038/ncomms4633.

Cederfjäll, E. *et al.* (2012) 'Design of a single AAV vector for coexpression of TH and GCH1 to establish continuous DOPA synthesis in a rat model of parkinson's disease', *Molecular Therapy*. Nature Publishing Group, 20(7), pp. 1315–1326. doi: 10.1038/mt.2012.1.

Cederfjäll, E. *et al.* (2013) 'Continuous DOPA synthesis from a single AAV: dosing and efficacy in models of Parkinson's disease.', *Scientific reports*, 3, p. 2157. doi: 10.1038/srep02157.

Cha, G.-H. *et al.* (2005) 'Parkin negatively regulates JNK pathway in the dopaminergic neurons of Drosophila', *Pnas*, 102(29), pp. 10345–10350. doi: 10.1073/pnas.0500346102.

Chaban, Y., Boekema, E. J. and Dudkina, N. V (2014) 'Structures of mitochondrial oxidative phosphorylation supercomplexes and mechanisms for their stabilisation', *Biochimica et Biophysica Acta (BBA) - Bioenergetics*, 1837(4), pp. 418–426. doi: https://doi.org/10.1016/j.bbabio.2013.10.004.

Chan-Palay, V. and Asan, E. (1989) 'Alterations in catecholamine neurons of the locus coeruleus in senile dementia of the Alzheimer type and in Parkinson's disease with and without dementia and depression.', *The Journal of comparative neurology*. United States, 287(3), pp. 373–392. doi: 10.1002/cne.902870308.

Chandler, R. J., Sands, M. S. and Venditti, C. P. (2017) 'Recombinant Adeno-Associated Viral Integration and Genotoxicity: Insights from Animal Models', *Human Gene Therapy*, 28(4), pp. 314–322. doi: 10.1089/hum.2017.009.

Chang, D. *et al.* (2017) 'A meta-analysis of genome-wide association studies identifies 17 new Parkinson's disease risk loci.', *Nature genetics*. United States, 49(10), pp. 1511–1516. doi: 10.1038/ng.3955.

Chao, M. V (2003) 'Neurotrophins and their receptors: a convergence point for many signalling pathways.', *Nature reviews. Neuroscience*, 4(4), pp. 299–309. doi: 10.1038/nrn1078.

Charreau, B. *et al.* (1996) 'Transgenesis in rats: technical aspects and models.', *Transgenic research*. Netherlands, 5(4), pp. 223–234.

Chen, B. *et al.* (2001) 'Increased hippocampal BDNF immunoreactivity in subjects treated with antidepressant medication', *Biological Psychiatry*, 50(4), pp. 260–265. doi: 10.1016/S0006-3223(01)01083-6.

Chiu, C. T. *et al.* (2011) 'Combined treatment with the mood stabilizers lithium and valproate produces multiple beneficial effects in transgenic mouse models of huntington's disease', *Neuropsychopharmacology*. Nature Publishing Group, 36(12), pp. 2406–2421. doi: 10.1038/npp.2011.128.

Choi-Lundberg, D. L. *et al.* (1998) 'Behavioral and cellular protection of rat dopaminergic neurons by an adenoviral vector encoding glial cell line-derived neurotrophic factor.', *Experimental neurology*. United States, 154(2), pp. 261–275. doi: 10.1006/exnr.1998.6887.

Choi, K. A., Choi, Y. and Hong, S. (2018) 'Stem cell transplantation for Huntington's diseases', *Methods*, 133, pp. 104–112. doi: 10.1016/j.ymeth.2017.08.017.

Choudhury, S. R. *et al.* (2017) 'Viral vectors for therapy of neurologic diseases', *Neuropharmacology*, 120, pp. 63–80. doi: 10.1016/j.neuropharm.2016.02.013.

Christine, C. W. *et al.* (2009) 'Safety and tolerability of putaminal AADC gene therapy for Parkinson disease', *Neurology*, 73(20), pp. 1662–1669. doi: 10.1212/WNL.0b013e3181c29356.

Christine, C. W. *et al.* (2019) 'Magnetic resonance imaging–guided phase 1 trial of putaminal AADC gene therapy for Parkinson's disease', *Annals of Neurology*, 85(5), pp. 704–714. doi: 10.1002/ana.25450.

Cichowski, K. *et al.* (2003) 'Dynamic regulation of the Ras pathway via proteolysis of the NF1 tumor suppressor.', *Genes & development*, 17(4), pp. 449–454. doi: 10.1101/gad.1054703.

Ciechanover, A. *et al.* (1980) 'Characterization of the heat-stable polypeptide of the ATP-dependent proteolytic system from reticulocytes.', *The Journal of biological chemistry*. United States, 255(16), pp. 7525–7528.

Ciechanover, A. (1994) 'The ubiquitin-proteasome proteolytic pathway', *Cell*, 79(1), pp. 13–21. doi: https://doi.org/10.1016/0092-8674(94)90396-4.

Ciesielska, A. *et al.* (2017) 'Depletion of AADC activity in caudate nucleus and putamen of Parkinson's disease patients; Implications for ongoing AAV2-AADC gene therapy trial', *PLoS ONE*, 12(2), pp. 1–13. doi: 10.1371/journal.pone.0169965.

Clark, I. E. *et al.* (2006) 'Drosophila pink1 is required for mitochondrial function and interacts genetically with parkin', *Nature*, 441(7097), pp. 1162–1166. doi: 10.1038/nature04779.

Von Coelln, R. *et al.* (2004) 'Loss of locus coeruleus neurons and reduced startle in parkin null mice.', *Proceedings of the National Academy of Sciences of the United States of America*.

United States, 101(29), pp. 10744–10749. doi: 10.1073/pnas.0401297101.

Colella, P., Ronzitti, G. and Mingozzi, F. (2018) 'Emerging Issues in AAV-Mediated In Vivo Gene Therapy', *Molecular Therapy - Methods and Clinical Development*. Elsevier Ltd., 8(March), pp. 87–104. doi: 10.1016/j.omtm.2017.11.007.

Como, P. G. *et al.* (1997) 'A controlled trial of fluoxetine in nondepressed patients with Huntington's disease', *Movement Disorders*, 12(3), pp. 397–401. doi: 10.1002/mds.870120319.

Cong, W. N. *et al.* (2015) 'Amitriptyline improves motor function via enhanced neurotrophin signaling and mitochondrial functions in the murine N171-82Q Huntington disease model', *Journal of Biological Chemistry*, 290(5), pp. 2728–2743. doi: 10.1074/jbc.M114.588608.

Connor, B. (2018) 'Concise Review: The Use of Stem Cells for Understanding and Treating Huntington's Disease', *Stem Cells*, 36(2), pp. 146–160. doi: 10.1002/stem.2747.

Correia Guedes, L. *et al.* (2010) 'Worldwide frequency of G2019S LRRK2 mutation in Parkinson's disease: a systematic review.', *Parkinsonism & related disorders*. England, 16(4), pp. 237–242. doi: 10.1016/j.parkreldis.2009.11.004.

Costa, R. M. *et al.* (2002) 'Mechanism for the learning deficits in a mouse model of neurofibromatosis type 1.', *Nature*, 415(6871), pp. 526–530. Available at: http://eutils.ncbi.nlm.nih.gov/entrez/eutils/elink.fcgi?dbfrom=pubmed&id=11793011&retmode=ref&cmd=prlinks.

Crawley, J. N. *et al.* (1997) 'Behavioral phenotypes of inbred mouse strains: Implications and recommendations for molecular studies', *Psychopharmacology*, 132(2), pp. 107–124. doi: 10.1007/s002130050327.

Crusio, W. E. (2004) 'Flanking gene and genetic background problems in genetically manipulated mice.', *Biological psychiatry*. United States, 56(6), pp. 381–385. doi: 10.1016/j.biopsych.2003.12.026.

Cuenda, A. and Rousseau, S. (2007) 'p38 MAP-Kinases pathway regulation, function and role in human diseases', *Biochimica et Biophysica Acta (BBA) - Molecular Cell Research*, 1773(8), pp. 1358–1375. doi: https://doi.org/10.1016/j.bbamcr.2007.03.010.

Curtin, J. A. *et al.* (2008) 'Bidirectional promoter interference between two widely used internal heterologous promoters in a late-generation lentiviral construct', *Gene Therapy*, 15(5), pp. 384–390. doi: 10.1038/sj.gt.3303105.

Cyron, D. (2016) 'Mental Side Effects of Deep Brain Stimulation (DBS) for Movement Disorders: The Futility of Denial.', *Frontiers in integrative neuroscience*, 10, p. 17. doi: 10.3389/fnint.2016.00017.

D'Costa, S. *et al.* (2016) 'Practical utilization of recombinant AAV vector reference standards: focus on vector genomes titration by free ITR qPCR', *Molecular Therapy - Methods and Clinical Development*, 3(July 2015), p. 16019. doi: 10.1038/mtm.2016.19.

Dauer, W. *et al.* (2002) 'Resistance of alpha -synuclein null mice to the parkinsonian neurotoxin MPTP.', *Proceedings of the National Academy of Sciences of the United States of America*. United States, 99(22), pp. 14524–14529. doi: 10.1073/pnas.172514599.

Davis, G. C. *et al.* (1979) 'Chronic Parkinsonism secondary to intravenous injection of meperidine analogues.', *Psychiatry research*. Ireland, 1(3), pp. 249–254. doi: 10.1016/0165-1781(79)90006-4.

Deas, E. *et al.* (2011) 'PINK1 cleavage at position A103 by the mitochondrial protease PARL.', *Human molecular genetics*. England, 20(5), pp. 867–879. doi: 10.1093/hmg/ddq526.

Deeks, S. G. *et al.* (2015) 'HIV infection', *Nature Reviews Disease Primers*, 1(1), p. 15035. doi: 10.1038/nrdp.2015.35.

Dehay, B. *et al.* (2012) 'Lysosomal dysfunction in Parkinson disease: ATP13A2 gets into the groove.', *Autophagy*. United States, 8(9), pp. 1389–1391. doi: 10.4161/auto.21011.

DeLong, M. R. (1990) 'Primate models of movement disorders of basal ganglia origin', *Trends in Neurosciences*, 13(7), pp. 281–285. doi: https://doi.org/10.1016/0166-2236(90)90110-V.

DeMarch, Z. *et al.* (2008) 'Beneficial effects of rolipram in the R6/2 mouse model of Huntington's disease', *Neurobiology of Disease*. Elsevier Inc., 30(3), pp. 375–387. doi: 10.1016/j.nbd.2008.02.010.

Denayer, T., Stöhrn, T. and Van Roy, M. (2014) 'Animal models in translational medicine: Validation and prediction', *New Horizons in Translational Medicine*. Elsevier, 2(1), pp. 5–11. doi: 10.1016/j.nhtm.2014.08.001.

Deng, H., Wang, P. and Jankovic, J. (2018) 'The genetics of Parkinson disease', *Ageing Research Reviews*. Elsevier, 42(September 2017), pp. 72–85. doi: 10.1016/j.arr.2017.12.007.

Deng, H. and Yuan, L. (2014) 'Genetic variants and animal models in SNCA and Parkinson disease', *Ageing Research Reviews*, 15, pp. 161–176. doi: https://doi.org/10.1016/j.arr.2014.04.002.

Deng, P. *et al.* (2016) 'Engineered BDNF producing cells as a potential treatment for neurologic disease.', *Expert opinion on biological therapy*, 16(8), pp. 1025–1033. doi: 10.1080/14712598.2016.1183641.

Deogracias, R. *et al.* (2012) 'Fingolimod, a sphingosine-1 phosphate receptor modulator, increases BDNF levels and improves symptoms of a mouse model of Rett syndrome.', *Proceedings of the National Academy of Sciences of the United States of America*, 109(35), pp. 14230–5. doi: 10.1073/pnas.1206093109.

Desai, V. G. *et al.* (1996) 'MPP(+)-induced neurotoxicity in mouse is age-dependent: evidenced by the selective inhibition of complexes of electron transport.', *Brain research*. Netherlands, 715(1–2), pp. 1–8. doi: 10.1016/0006-8993(95)01255-9.

DiFiglia, M. *et al.* (1997) 'Aggregation of huntingtin in neuronal intranuclear inclusions and dystrophic neurites in brain.', *Science (New York, N.Y.)*. United States, 277(5334), pp. 1990–1993. doi: 10.1126/science.277.5334.1990.

Dodiya, H. B. *et al.* (2010) 'Differential transduction following basal ganglia administration of distinct pseudotyped AAV capsid serotypes in nonhuman primates', *Molecular Therapy*. Nature Publishing Group, 18(3), pp. 579–587. doi: 10.1038/mt.2009.216.

Dorsey, E. R. *et al.* (2007) 'Projected number of people with Parkinson disease in the most populous nations, 2005 through 2030.', *Neurology*. United States, 68(5), pp. 384–386. doi: 10.1212/01.wnl.0000247740.47667.03.

Dorsey, E. R. *et al.* (2018) 'Global, regional, and national burden of Parkinson's disease, 1990–2016: a systematic analysis for the Global Burden of Disease Study 2016', *The Lancet Neurology*, 17(11), pp. 939–953. doi: 10.1016/S1474-4422(18)30295-3.

Doss, M. X. and Sachinidis, A. (2019) 'Current Challenges of iPSC-Based Disease Modeling and Therapeutic Implications.', *Cells*, 8(5). doi: 10.3390/cells8050403.

Doty, R. L., Deems, D. A. and Stellar, S. (1988) 'Olfactory dysfunction in parkinsonism: a general deficit unrelated to neurologic signs, disease stage, or disease duration.', *Neurology*. United States, 38(8), pp. 1237–1244. doi: 10.1212/wnl.38.8.1237.

Dreas, A. *et al.* (2017) 'Mitogen-activated Protein Kinase (MAPK) Interacting Kinases 1 and 2 (MNK1 and MNK2) as Targets for Cancer Therapy: Recent Progress in the Development of MNK Inhibitors.', *Current medicinal chemistry*. United Arab Emirates, 24(28), pp. 3025–3053. doi: 10.2174/0929867324666170203123427.

Drouin, L. M. and Agbandje-McKenna, M. (2013) 'Adeno-associated virus structural biology as

a tool in vector development.', *Future virology*. England, 8(12), pp. 1183–1199. doi: 10.2217/fvl.13.112.

Drucker-Colín, R. and García-Hernández, F. (1991) 'A new motor test sensitive to aging and dopaminergic function', *Journal of Neuroscience Methods*, 39(2), pp. 153–161. doi: 10.1016/0165-0270(91)90081-A.

Duan, W. *et al.* (2004) 'Paroxetine Retards Disease Onset and Progression in Huntingtin Mutant Mice', *Annals of Neurology*, 55(4), pp. 590–594. doi: 10.1002/ana.20075.

Dull, T. *et al.* (1998) 'A third-generation lentivirus vector with a conditional packaging system.', *Journal of virology*, 72(11), pp. 8463–8471. doi: 98440501.

Durães, F., Pinto, M. and Sousa, E. (2018) 'Old drugs as new treatments for neurodegenerative diseases', *Pharmaceuticals*, 11(2), pp. 1–21. doi: 10.3390/ph11020044.

Duyao, M. *et al.* (1993) 'Trinucleotide repeat length instability and age of onset in Huntington's disease.', *Nature genetics*. United States, 4(4), pp. 387–392. doi: 10.1038/ng0893-387.

Eaton, S. L. and Wishart, T. M. (2017) 'Bridging the gap: large animal models in neurodegenerative research', *Mammalian Genome*. Springer US, 28(7–8), pp. 324–337. doi: 10.1007/s00335-017-9687-6.

Edvardson, S. *et al.* (2012) 'A deleterious mutation in DNAJC6 encoding the neuronal-specific clathrin-uncoating co-chaperone auxilin, is associated with juvenile parkinsonism.', *PloS one*. United States, 7(5), p. e36458. doi: 10.1371/journal.pone.0036458.

Eisener-Dorman, A. F., Lawrence, D. A. and Bolivar, V. J. (2009) 'Cautionary insights on knockout mouse studies: the gene or not the gene?', *Brain, behavior, and immunity*, 23(3), pp. 318–324. doi: 10.1016/j.bbi.2008.09.001.

Eisinger, R. S. *et al.* (2019) 'A review of basal ganglia circuits and physiology: Application to deep brain stimulation', *Parkinsonism and Related Disorders*. Elsevier, 59(January), pp. 9–20. doi: 10.1016/j.parkreldis.2019.01.009.

Ekstrand, M. I. *et al.* (2007) 'Progressive parkinsonism in mice with respiratory-chain-deficient dopamine neurons', *Proceedings of the National Academy of Sciences of the United States of America*, 104(4), pp. 1325–1330. doi: 10.1073/pnas.0605208103.

Ellrichmann, G. *et al.* (2017) 'Laquinimod treatment in the R6/2 mouse model', *Scientific Reports*, 7(1), pp. 1–13. doi: 10.1038/s41598-017-04990-1.

English, J. D. and Sweatt, J. D. (1997) 'A requirement for the mitogen-activated protein kinase cascade in hippocampal long term potentiation.', *The Journal of biological chemistry*. United States, 272(31), pp. 19103–19106. doi: 10.1074/jbc.272.31.19103.

Eriksen, J. L., Przedborski, S. and Petrucelli, L. (2005) 'Gene dosage and pathogenesis of Parkinson's disease', *Trends in Molecular Medicine*, 11(3), pp. 91–96. doi: https://doi.org/10.1016/j.molmed.2005.01.001.

Ertekin-Taner, N. (2007) 'Genetics of Alzheimer's disease: a centennial review.', *Neurologic clinics*, 25(3), pp. 611–67, v. doi: 10.1016/j.ncl.2007.03.009.

Faber, P. W. *et al.* (1999) 'Polyglutamine-mediated dysfunction and apoptotic death of a Caenorhabditis elegans sensory neuron.', *Proceedings of the National Academy of Sciences of the United States of America*. United States, 96(1), pp. 179–184. doi: 10.1073/pnas.96.1.179.

Falkenburger, B. H., Saridaki, T. and Dinter, E. (2016) 'Cellular models for Parkinson's disease', *Journal of Neurochemistry*, 139, pp. 121–130. doi: 10.1111/jnc.13618.

Falkenburger, B. H. and Schulz, J. B. (2006) 'Limitations of cellular models in Parkinson's disease research.', *Journal of neural transmission. Supplementum*. Austria, (70), pp. 261–268.

Fearnley, J. M. and Lees, A. J. (1991) 'Ageing and Parkinson's Disease: Sunstantia Nigra Regional Selectivity', *Brain*, 114(5), pp. 2283–2301. doi: 10.1093/brain/114.5.2283.

Feigin, V. L. *et al.* (2017) 'Global, regional, and national burden of neurological disorders during 1990–2015: a systematic analysis for the Global Burden of Disease Study 2015', *The Lancet Neurology*. England, 16(11), pp. 877–897. doi: 10.1016/S1474-4422(17)30299-5.

Fenelon, G. *et al.* (2010) 'The changing face of Parkinson's disease-associated psychosis: a cross-sectional study based on the new NINDS-NIMH criteria.', *Movement disorders : official journal of the Movement Disorder Society*. United States, 25(6), pp. 763–766. doi: 10.1002/mds.22839.

Ferese, R. *et al.* (2015) 'Four Copies of SNCA Responsible for Autosomal Dominant Parkinson's Disease in Two Italian Siblings.', *Parkinson's disease*. United States, 2015, p. 546462. doi: 10.1155/2015/546462.

Fernagut, P.-O. and Chesselet, M.-F. (2004) 'Alpha-synuclein and transgenic mouse models.', *Neurobiology of disease*. United States, 17(2), pp. 123–130. doi: 10.1016/j.nbd.2004.07.001.

Fernández-Ruiz, J. (2019) 'The biomedical challenge of neurodegenerative disorders: an opportunity for cannabinoid-based therapies to improve on the poor current therapeutic

outcomes', *British Journal of Pharmacology*, 176(10), pp. 1370–1383. doi: 10.1111/bph.14382.

Ferrante, R. J. (2009) 'Mouse models of Huntington's disease and methodological considerations for therapeutic trials.', *Biochimica et biophysica acta*. Elsevier B.V., 1792(6), pp. 506–520. doi: 10.1016/j.bbadis.2009.04.001.

Ferrer, I. *et al.* (2000) 'Brain-derived neurotrophic factor in Huntington disease', *Brain Research*, 866, pp. 257–261. doi: 10.1016/S0006-8993(00)02237-X.

Filion, M. and Tremblay, L. (1991) 'Abnormal spontaneous activity of globus pallidus neurons in monkeys with MPTP-induced parkinsonism.', *Brain research*. Netherlands, 547(1), pp. 142–151.

Fineberg, N. A. *et al.* (2013) 'The size, burden and cost of disorders of the brain in the UK', *Journal of Psychopharmacology*, 27(9), pp. 761–770. doi: 10.1177/0269881113495118.

Finkel, R. S. *et al.* (2017) 'Nusinersen versus sham control in infantile-onset spinal muscular atrophy', *New England Journal of Medicine*, 377(18), pp. 1723–1732. doi: 10.1056/NEJMoa1702752.

Fleming, S. M. *et al.* (2004) 'Behavioral and immunohistochemical effects of chronic intravenous and subcutaneous infusions of varying doses of rotenone.', *Experimental neurology*. United States, 187(2), pp. 418–429. doi: 10.1016/j.expneurol.2004.01.023.

Fontaine, D. A. and Davis, D. B. (2016) 'Attention to background strain is essential for metabolic research: C57BL/6 and the international knockout mouse consortium', *Diabetes*, 65(1), pp. 25–33. doi: 10.2337/db15-0982.

Forsaa, E. B. *et al.* (2010) 'A 12-year population-based study of psychosis in Parkinson disease.', *Archives of neurology*. United States, 67(8), pp. 996–1001. doi: 10.1001/archneurol.2010.166.

Frank, S. *et al.* (2016) 'Effect of Deutetrabenazine on Chorea Among Patients With Huntington Disease: A Randomized Clinical Trial.', *JAMA*. United States, 316(1), pp. 40–50. doi: 10.1001/jama.2016.8655.

Freed, C. R. *et al.* (2001) 'Transplantation of embryonic dopamine neurons for severe Parkinson's disease', *New England Journal of Medicine*. United States, 344(10), pp. 710–719. doi: 10.1056/NEJM200103083441002.

Frémin, C. *et al.* (2015) 'Functional Redundancy of ERK1 and ERK2 MAP Kinases during

Development', *Cell Reports*, 12(6), pp. 913–921. doi: 10.1016/j.celrep.2015.07.011.

Fukumoto, T. *et al.* (2001) 'Chronic lithium treatment increases the expression of brain-derived neurotrophic factor in the rat brain', *Psychopharmacology*, 158(1), pp. 100–106. doi: 10.1007/s002130100871.

Furler, S. *et al.* (2001) 'Recombinant AAV vectors containing the foot and mouth disease virus 2A sequence confer efficient bicistronic gene expression in cultured cells and rat substantia nigra neurons', *Gene Therapy*, 8(11), pp. 864–873. doi: 10.1038/sj.gt.3301469.

Ganini, D. *et al.* (2017) 'Fluorescent proteins such as eGFP lead to catalytic oxidative stress in cells', *Redox Biology*. Elsevier B.V., 12(February), pp. 462–468. doi: 10.1016/j.redox.2017.03.002.

Garrido, C. *et al.* (2006) 'Mechanisms of cytochrome c release from mitochondria', *Cell Death & Differentiation*, 13(9), pp. 1423–1433. doi: 10.1038/sj.cdd.4401950.

Gauthier, L. R. *et al.* (2004) 'Huntingtin controls neurotrophic support and survival of neurons by enhancing BDNF vesicular transport along microtubules', *Cell*, 118(1), pp. 127–138. doi: 10.1016/j.cell.2004.06.018.

Gelderblom, H. *et al.* (2017) 'Bupropion for the treatment of apathy in Huntington's disease: A multicenter, randomised, double-blind, placebocontrolled, prospective crossover trial', *PLoS ONE*, 12(3), pp. 1–17. doi: 10.1371/journal.pone.0173872.

GeM-HD Consortium (2015) 'Identification of Genetic Factors that Modify Clinical Onset of Huntington's Disease.', *Cell*, 162(3), pp. 516–526. doi: 10.1016/j.cell.2015.07.003.

Gerfen, C. R. *et al.* (1990) 'D1 and D2 dopamine receptor-regulated gene expression of striatonigral and striatopallidal neurons.', *Science (New York, N.Y.)*. United States, 250(4986), pp. 1429–1432. doi: 10.1126/science.2147780.

Gerlai, R. (1996) 'Gene-targeting studies of mammalian behavior: is it the mutation or the background genotype?', *Trends in neurosciences*. England, 19(5), pp. 177–181. doi: 10.1016/s0166-2236(96)20020-7.

Gharami, K. *et al.* (2008) 'Brain-derived neurotrophic factor over-expression in the forebrain ameliorates Huntington's disease phenotypes in mice', *Journal of Neurochemistry*, 105(2), pp. 369–379. doi: 10.1111/j.1471-4159.2007.05137.x.

Giampà, C. *et al.* (2010) 'Inhibition of the Striatal Specific Phosphodiesterase PDE10A Ameliorates Striatal and Cortical Pathology in R6/2 Mouse Model of Huntington's Disease',

PLOS ONE. Public Library of Science, 5(10), p. e13417. Available at: https://doi.org/10.1371/journal.pone.0013417.

Ginés, S., Paoletti, P. and Alberch, J. (2010) 'Impaired TrkB-mediated ERK1/2 activation in huntington disease knock-in striatal cells involves reduced p52/p46 Shc expression', *Journal of Biological Chemistry*, 285(28), pp. 21537–21548. doi: 10.1074/jbc.M109.084202.

Giralt, A. *et al.* (2009) 'Brain-derived neurotrophic factor modulates the severity of cognitive alterations induced by mutant huntingtin: Involvement of phospholipaseCγ activity and glutamate receptor expression', *Neuroscience*. IBRO, 158(4), pp. 1234–1250. doi: 10.1016/j.neuroscience.2008.11.024.

Giralt, A. *et al.* (2011) 'Conditional BDNF release under pathological conditions improves Huntington's disease pathology by delaying neuronal dysfunction', *Molecular Neurodegeneration*. BioMed Central Ltd, 6(1), p. 71. doi: 10.1186/1750-1326-6-71.

Girault, J. A. *et al.* (2007) 'ERK2: a logical AND gate critical for drug-induced plasticity?', *Current Opinion in Pharmacology*, 7(1), pp. 77–85. doi: 10.1016/j.coph.2006.08.012.

Glass, D. J. *et al.* (1991) 'TrkB mediates BDNF/NT-3-dependent survival and proliferation in fibroblasts lacking the low affinity NGF receptor.', *Cell*. United States, 66(2), pp. 405–413. doi: 10.1016/0092-8674(91)90629-d.

Glauser, L. *et al.* (2011) 'Parkin promotes the ubiquitination and degradation of the mitochondrial fusion factor mitofusin 1.', *Journal of neurochemistry*. England, 118(4), pp. 636–645. doi: 10.1111/j.1471-4159.2011.07318.x.

Goedert, M. *et al.* (2013) '100 years of Lewy pathology', *Nature Reviews Neurology*. Nature Publishing Group, 9(1), pp. 13–24. doi: 10.1038/nrneurol.2012.242.

Goldberg, M. S. *et al.* (2003) 'Parkin-deficient Mice Exhibit Nigrostriatal Deficits but not Loss of Dopaminergic Neurons', *Journal of Biological Chemistry*, 278(44), pp. 43628–43635. doi: 10.1074/jbc.M308947200.

Goold, R. *et al.* (2019) 'FAN1 modifies Huntington's disease progression by stabilizing the expanded HTT CAG repeat.', *Human molecular genetics*. England, 28(4), pp. 650–661. doi: 10.1093/hmg/ddy375.

Goto, H. *et al.* (2003) 'Transduction of green fluorescent protein increased oxidative stress and enhanced sensitivity to cytotoxic drugs in neuroblastoma cell lines.', *Molecular cancer therapeutics*. United States, 2(9), pp. 911–917.

Graham, R. K. *et al.* (2006) 'Cleavage at the Caspase-6 Site Is Required for Neuronal Dysfunction and Degeneration Due to Mutant Huntingtin', *Cell*, 125(6), pp. 1179–1191. doi: 10.1016/j.cell.2006.04.026.

Gray, M. *et al.* (2008) 'Full-length human mutant huntingtin with a stable polyglutamine repeat can elicit progressive and selective neuropathogenesis in BACHD mice.', *The Journal of neuroscience : the official journal of the Society for Neuroscience*, 28(24), pp. 6182–6195. doi: 10.1523/JNEUROSCI.0857-08.2008.

Gray, S. J. *et al.* (2011) 'Optimizing promoters for recombinant adeno-associated virus-mediated gene expression in the peripheral and central nervous system using self-complementary vectors', *Human Gene Therapy*, 22(9), pp. 1143–1153. doi: 10.1089/hum.2010.245.

Greene, A. W. *et al.* (2012) 'Mitochondrial processing peptidase regulates PINK1 processing, import and Parkin recruitment.', *EMBO reports*. England, 13(4), pp. 378–385. doi: 10.1038/embor.2012.14.

Greene, J. C. *et al.* (2003) 'Mitochondrial pathology and apoptotic muscle degeneration in Drosophila parkin mutants', *Proceedings of the National Academy of Sciences*, 100(7), pp. 4078–4083. doi: 10.1073/pnas.0737556100.

Grillner, S. and Robertson, B. (2016) 'The Basal Ganglia Over 500 Million Years', *Current Biology*. Elsevier Ltd, 26(20), pp. R1088–R1100. doi: 10.1016/j.cub.2016.06.041.

Grotewiel, M. and Bettinger, J. C. (2015) 'Drosophila and Caenorhabditis elegans as Discovery Platforms for Genes Involved in Human Alcohol Use Disorder.', *Alcoholism, clinical and experimental research*. England, 39(8), pp. 1292–1311. doi: 10.1111/acer.12785.

Group, H. S. (2006) 'Tetrabenazine as antichorea therapy in Huntington disease: a randomized controlled trial.', *Neurology*. United States, 66(3), pp. 366–372. doi: 10.1212/01.wnl.0000198586.85250.13.

Grünewald, A., Kumar, K. R. and Sue, C. M. (2019) 'New insights into the complex role of mitochondria in Parkinson's disease', *Progress in Neurobiology*. Elsevier, 177(September), pp. 73–93. doi: 10.1016/j.pneurobio.2018.09.003.

Gupta, H. V., Lyons, K. E. and Pahwa, R. (2019) 'Old Drugs, New Delivery Systems in Parkinson's Disease', *Drugs and Aging*. Springer International Publishing. doi: 10.1007/s40266-019-00682-9.

Halliday, G. M. *et al.* (1990) 'Loss of brainstem serotonin- and substance P-containing neurons

in Parkinson's disease.', *Brain research*. Netherlands, 510(1), pp. 104–107. doi: 10.1016/0006-8993(90)90733-r.

Halliday, G. M. *et al.* (2011) 'Neuropathology underlying clinical variability in patients with synucleinopathies', *Acta Neuropathologica*, 122(2), pp. 187–204. doi: 10.1007/s00401-011-0852-9.

Han, C. *et al.* (2018) 'Open science meets stem cells: A new drug discovery approach for neurodegenerative disorders', *Frontiers in Neuroscience*, 12(FEB), pp. 1–8. doi: 10.3389/fnins.2018.00047.

Hauge, C. and Frödin, M. (2006) 'RSK and MSK in MAP kinase signalling', *Journal of Cell Science*. The Company of Biologists Ltd, 119(15), pp. 3021–3023. doi: 10.1242/jcs.02950.

Hauser, D. N., Primiani, C. T. and Cookson, M. R. (2016) 'The Effects of Variants in the Parkin, PINK1, and DJ-1 Genes along with Evidence for their Pathogenicity', *Current Protein & Peptide Science*, 18(7), pp. 702–714. doi: 10.2174/1389203717666160311121954.

Hawkes, C. H., Del Tredici, K. and Braak, H. (2007) 'Parkinson's disease: a dual-hit hypothesis.', *Neuropathology and applied neurobiology*. England, 33(6), pp. 599–614. doi: 10.1111/j.1365-2990.2007.00874.x.

Hawkes, C. H., Del Tredici, K. and Braak, H. (2009) 'Parkinson's disease: The dual hit theory revisited', *Annals of the New York Academy of Sciences*, 1170, pp. 615–622. doi: 10.1111/j.1749-6632.2009.04365.x.

Hayes, M. T. (2019) 'Parkinson's Disease and Parkinsonism', *The American Journal of Medicine*, 132(7), pp. 802–807. doi: https://doi.org/10.1016/j.amjmed.2019.03.001.

Healy, D. G. *et al.* (2008) 'Phenotype, genotype, and worldwide genetic penetrance of LRRK2-associated Parkinson's disease: a case-control study.', *The Lancet. Neurology*, 7(7), pp. 583–590. doi: 10.1016/S1474-4422(08)70117-0.

Hedrich, K. *et al.* (2004) 'Distribution, type and origin of Parkin mutations: Review and case studies', *Movement Disorders*, 19(10), pp. 1146–1157. doi: 10.1002/mds.20234.

Heiman-Patterson, T. D. *et al.* (2015) 'Genetic background effects on disease onset and lifespan of the mutant dynactin p150Glued mouse model of motor neuron disease.', *PloS one*, 10(3), p. e0117848. doi: 10.1371/journal.pone.0117848.

Heinsen, H. *et al.* (1994) 'Cortical and striatal neurone number in Huntington's disease.', *Acta neuropathologica*. Germany, 88(4), pp. 320–333. doi: 10.1007/bf00310376.

Helmich, R. C. *et al.* (2012) 'Cerebral causes and consequences of parkinsonian resting tremor: A tale of two circuits?', *Brain*, 135(11), pp. 3206–3226. doi: 10.1093/brain/aws023.

Hely, M. A. *et al.* (2008) 'The Sydney multicenter study of Parkinson's disease: The inevitability of dementia at 20 years', *Movement Disorders*, 23(6), pp. 837–844. doi: 10.1002/mds.21956.

Hernandez-Baltazar, D., Zavala-Flores, L. M. and Villanueva-Olivo, A. (2017) 'The 6-hydroxydopamine model and parkinsonian pathophysiology: Novel findings in an older model', *Neurología (English Edition)*. Sociedad Española de Neurología, 32(8), pp. 533–539. doi: 10.1016/j.nrleng.2015.06.019.

Hernandez, D. G., Reed, X. and Singleton, A. B. (2016) 'Genetics in Parkinson disease: Mendelian versus non-Mendelian inheritance', *Journal of Neurochemistry*, 139(Suppl 1), pp. 59–74. doi: 10.1111/jnc.13593.

Hersch, S. *et al.* (2017) 'Multicenter, Randomized, Double-blind, Placebo-controlled Phase 1b/2a Studies of WVE-120101 and WVE-120102 in Patients with Huntington{\textquoteright}s Disease (P2.006)', *Neurology*. Wolters Kluwer Health, Inc. on behalf of the American Academy of Neurology, 88(16 Supplement). Available at: https://n.neurology.org/content/88/16_Supplement/P2.006.

Hershko, A. *et al.* (1983) 'Components of ubiquitin-protein ligase system. Resolution, affinity purification, and role in protein breakdown.', *The Journal of biological chemistry*. United States, 258(13), pp. 8206–8214.

Hervé, D., Rogard, M. and Lévi-Strauss, M. (1995) 'Molecular analysis of the multiple Golf α subunit mRNAs in the rat brain', *Molecular Brain Research*, 32(1), pp. 125–134. doi: 10.1016/0169-328X(95)00070-9.

Ho, D. H. *et al.* (2016) 'G2385R and I2020T Mutations Increase LRRK2 GTPase Activity.', *BioMed research international*. United States, 2016, p. 7917128. doi: 10.1155/2016/7917128.

Hobbs, G. A., Der, C. J. and Rossman, K. L. (2016) 'RAS isoforms and mutations in cancer at a glance', *Journal of Cell Science*, 129(7), pp. 1287–1292. doi: 10.1242/jcs.182873.

Hoehn, M. M. and Yahr, M. D. (1967) 'Parkinsonism: onset, progression and mortality.', *Neurology*. United States, 17(5), pp. 427–442. doi: 10.1212/wnl.17.5.427.

Hornykiewicz, O. (1966) 'Dopamine (3-hydroxytyramine) and brain function.', *Pharmacological reviews*. United States, 18(2), pp. 925–964.

Huang, E. J. and Reichardt, L. F. (2001) 'Neurotrophins: roles in neuronal development and function.', *Annual review of neuroscience*, 24, pp. 677–736. doi: 10.1146/annurev.neuro.24.1.677.

Huang, M. *et al.* (2019) 'α-Synuclein: A Multifunctional Player in Exocytosis, Endocytosis, and Vesicle Recycling', *Frontiers in Neuroscience*, 13, p. 28. doi: 10.3389/fnins.2019.00028.

Huang, W. Y. *et al.* (2000) 'Transgenic expression of green fluorescence protein can cause dilated cardiomyopathy.', *Nature medicine*. United States, pp. 482–483. doi: 10.1038/74914.

Hulme, A. E., Perez, O. and Hope, T. J. (2011) 'Complementary assays reveal a relationship between HIV-1 uncoating and reverse transcription.', *Proceedings of the National Academy of Sciences of the United States of America*. United States, 108(24), pp. 9975–9980. doi: 10.1073/pnas.1014522108.

Huot, P. *et al.* (2013) 'The pharmacology of L-DOPA-induced dyskinesia in Parkinson's disease.', *Pharmacological reviews*. United States, 65(1), pp. 171–222. doi: 10.1124/pr.111.005678.

Hutton, S. R. *et al.* (2017) 'ERK/MAPK Signaling Is Required for Pathway-Specific Striatal Motor Functions', *Journal of Neuroscience*. Society for Neuroscience, 37(34), pp. 8102–8115. doi: 10.1523/JNEUROSCI.0473-17.2017.

Indrigo, M. *et al.* (2010) 'Lentiviral Vectors to Study the Differential Function of ERK1 and ERK2 MAP Kinases'. Edited by R. Seger. Totowa, NJ: Humana Press (Methods in Molecular Biology), 661, pp. 205–220. doi: 10.1007/978-1-60761-795-2.

Itier, J. M. *et al.* (2003) 'Parkin gene inactivation alters behaviour and dopamine neurotransmission in the mouse', *Human Molecular Genetics*, 12(18), pp. 2277–2291. doi: 10.1093/hmg/ddg239.

Jackson-Lewis, V., Blesa, J. and Przedborski, S. (2012) 'Animal models of Parkinson's disease', *Parkinsonism & Related Disorders*, 18, pp. S183–S185. doi: https://doi.org/10.1016/S1353-8020(11)70057-8.

Jackson-Lewis, V. and Przedborski, S. (2007) 'Protocol for the MPTP mouse model of Parkinson's disease.', *Nature protocols*. England, 2(1), pp. 141–151. doi: 10.1038/nprot.2006.342.

Jackson, G. R. *et al.* (1998) 'Polyglutamine-expanded human huntingtin transgenes induce degeneration of Drosophila photoreceptor neurons', *Neuron*, 21(3), pp. 633–642. doi: 10.1016/S0896-6273(00)80573-5.

Jacobsen, J. C. *et al.* (2010) 'An ovine transgenic Huntington's disease model.', *Human molecular genetics*. England, 19(10), pp. 1873–1882. doi: 10.1093/hmg/ddq063.

Jagmag, S. A. *et al.* (2016) 'Evaluation of models of Parkinson's disease', *Frontiers in Neuroscience*, 9(JAN). doi: 10.3389/fnins.2015.00503.

Jarraya, B. *et al.* (2009) 'Dopamine gene therapy for Parkinson's disease in a nonhuman primate without associated dyskinesia', *Science Translational Medicine*, 1(2), p. 2ra4. doi: 10.1126/scitranslmed.3000130.

Jeibmann, A. and Paulus, W. (2009) 'Drosophila melanogaster as a model organism of brain diseases.', *International journal of molecular sciences*, 10(2), pp. 407–440. doi: 10.3390/ijms10020407.

Jeromin, A. and Bowser, R. (2017) 'Biomarkers in Neurodegenerative Diseases.', *Advances in neurobiology*. United States, 15, pp. 491–528. doi: 10.1007/978-3-319-57193-5_20.

Jin, S. M. *et al.* (2010) 'Mitochondrial membrane potential regulates PINK1 import and proteolytic destabilization by PARL.', *The Journal of cell biology*, 191(5), pp. 933–942. doi: 10.1083/jcb.201008084.

Jin, S. M. and Youle, R. J. (2012) 'PINK1- and Parkin-mediated mitophagy at a glance', *Journal of Cell Science*. The Company of Biologists Ltd, 125(4), pp. 795–799. doi: 10.1242/jcs.093849.

Johansen, T. and Lamark, T. (2011) 'Selective autophagy mediated by autophagic adapter proteins.', *Autophagy*, 7(3), pp. 279–296. doi: 10.4161/auto.7.3.14487.

Jucker, M. (2010) 'The benefits and limitations of animal models for translational research in neurodegenerative diseases.', *Nature medicine*. United States, 16(11), pp. 1210–1214. doi: 10.1038/nm.2224.

Julienne, H. *et al.* (2017) 'Drosophila PINK1 and parkin loss-of-function mutants display a range of non-motor Parkinson's disease phenotypes', *Neurobiology of Disease*. Elsevier Inc., 104, pp. 15–23. doi: 10.1016/j.nbd.2017.04.014.

Juorio, A. V *et al.* (1993) 'Decarboxylation of L-dopa by cultured mouse astrocytes.', *Brain research*. Netherlands, 626(1–2), pp. 306–309. doi: 10.1016/0006-8993(93)90592-b.

Kalinderi, K., Bostantjopoulou, S. and Fidani, L. (2016) 'The genetic background of Parkinson's disease: current progress and future prospects', *Acta Neurologica Scandinavica*, 134(5), pp. 314–326. doi: 10.1111/ane.12563.

Kane, L. A. *et al.* (2014) 'PINK1 phosphorylates ubiquitin to activate parkin E3 ubiquitin ligase

activity', *Journal of Cell Biology*, 205(2), pp. 143–153. doi: 10.1083/jcb.201402104.

Kang, S. K., Hawkins, N. A. and Kearney, J. A. (2019) 'C57BL/6J and C57BL/6N substrains differentially influence phenotype severity in the Scn1a (+/-) mouse model of Dravet syndrome.', *Epilepsia open*. United States, 4(1), pp. 164–169. doi: 10.1002/epi4.12287.

Kang, U.-B. and Marto, J. A. (2017) 'Leucine-rich repeat kinase 2 and Parkinson's disease', *PROTEOMICS*, 17(1–2), p. 1600092. doi: 10.1002/pmic.201600092.

Kaplitt, M. G. *et al.* (1994) 'Long-term gene expression and phenotypic correction using adeno-associated virus vectors in the mammalian brain.', *Nature genetics*. United States, 8(2), pp. 148–154. doi: 10.1038/ng1094-148.

Karimi-Moghadam, A. *et al.* (2018) 'Parkinson Disease from Mendelian Forms to Genetic Susceptibility: New Molecular Insights into the Neurodegeneration Process', *Cellular and Molecular Neurobiology*. Springer US, 38(6), pp. 1153–1178. doi: 10.1007/s10571-018-0587-4.

Kawasaki, H. *et al.* (1999) 'Requirement for mitogen-activated protein kinase in cerebellar long term depression.', *The Journal of biological chemistry*. United States, 274(19), pp. 13498–13502. doi: 10.1074/jbc.274.19.13498.

Kazlauskaite, A. *et al.* (2014) 'Parkin is activated by PINK1-dependent phosphorylation of ubiquitin at Ser ^{65}', *Biochemical Journal*, 460(1), pp. 127–141. doi: 10.1042/BJ20140334.

Kells, A. P., Henry, R. A. and Connor, B. (2008) 'AAV-BDNF mediated attenuation of quinolinic acid-induced neuropathology and motor function impairment', *Gene Therapy*, 15(13), pp. 966–977. doi: 10.1038/gt.2008.23.

Kennedy, L. *et al.* (2003) 'Dramatic tissue-specific mutation length increases are an early molecular event in Huntington disease pathogenesis.', *Human molecular genetics*. England, 12(24), pp. 3359–3367. doi: 10.1093/hmg/ddg352.

Kessler, P. D. *et al.* (1996) 'Gene delivery to skeletal muscle results in sustained expression and systemic delivery of a therapeutic protein', *Proceedings of the National Academy of Sciences*. National Academy of Sciences, 93(24), pp. 14082–14087. doi: 10.1073/pnas.93.24.14082.

Khoo, T. K. *et al.* (2013) 'The spectrum of nonmotor symptoms in early Parkinson disease', *Neurology*, 80, pp. 276–281.

Kilkenny, C. *et al.* (2013) 'Improving bioscience research reporting: The arrive guidelines for

reporting animal research', *Animals*. Kilkenny et al. This is an open-access article distributed under the terms of the Creative Commons Attribution License, which permits unrestricted use, distribution, and reproduction in any medium, provided the original author and source are credited, 4(1), pp. 35–44. doi: 10.3390/ani4010035.

Kim, C. and Lee, S.-J. (2008) 'Controlling the mass action of α-synuclein in Parkinson's disease', *Journal of Neurochemistry*, 107(2), pp. 303–316. doi: 10.1111/j.1471-4159.2008.05612.x.

Kim, E. *et al.* (2014) 'Transient inhibition of the ERK pathway prevents cerebellar developmental defects and improves long-term motor functions in murine models of neurofibromatosis type 1', *eLife*, 3, pp. 1–27. doi: 10.7554/eLife.05151.

Kim, S. *et al.* (2019) 'Transneuronal Propagation of Pathologic α-Synuclein from the Gut to the Brain Models Parkinson's Disease', *Neuron*. Elsevier Inc., 103(4), pp. 627-641.e7. doi: 10.1016/j.neuron.2019.05.035.

Kirik, D., Rosenblad, C., *et al.* (2002) 'Parkinson-like neurodegeneration induced by targeted overexpression of alpha-synuclein in the nigrostriatal system.', *The Journal of neuroscience : the official journal of the Society for Neuroscience*, 22(7), pp. 2780–91. doi: 20026246.

Kirik, D., Georgievska, B., *et al.* (2002) 'Reversal of motor impairments in parkinsonian rats by continuous intrastriatal delivery of L-dopa using rAAV-mediated gene transfer', *Proceedings of the National Academy of Sciences of the United States of America*, 99(7), pp. 4708–4713. doi: 10.1073/pnas.062047599.

Kirik, D. *et al.* (2003) 'Nigrostriatal alpha-synucleinopathy induced by viral vector-mediated overexpression of human alpha-synuclein: a new primate model of Parkinson's disease.', *Proceedings of the National Academy of Sciences of the United States of America*. United States, 100(5), pp. 2884–2889. doi: 10.1073/pnas.0536383100.

Kitada, T. *et al.* (1998a) 'Mutations in the parkin gene cause autosomal recessive juvenile parkinsonism', *Nature*, 392(6676), pp. 605–608. doi: 10.1038/33416.

Kitada, T. *et al.* (1998b) 'Mutations in the parkin gene cause autosomal recessive juvenile parkinsonism', *Nature*, 392(6676), pp. 605–608. doi: 10.1038/33416.

Klein, C. and Westenberger, A. (2012) 'Genetics of Parkinson's disease.', *Cold Spring Harbor perspectives in medicine*, 2(1), p. a008888. doi: 10.1101/cshperspect.a008888.

Klein, R. *et al.* (1991) 'The trkB tyrosine protein kinase is a receptor for brain-derived neurotrophic factor and neurotrophin-3.', *Cell*, 66(2), pp. 395–403. doi: 10.1016/0092-

8674(91)90628-c.

Klein, R. L. *et al.* (2006) 'Efficient Neuronal Gene Transfer with AAV8 Leads to Neurotoxic Levels of Tau or Green Fluorescent Proteins', *In Vivo*, 13(3), pp. 517–527. doi: 10.1016/j.ymthe.

Kola, I. and Landis, J. (2004) 'Can the pharmaceutical industry reduce attrition rates?', *Nature Reviews Drug Discovery*, 3(8), pp. 711–716. doi: 10.1038/nrd1470.

Kondapalli, C. *et al.* (2012) 'PINK1 is activated by mitochondrial membrane potential depolarization and stimulates Parkin E3 ligase activity by phosphorylating Serine 65', *Open Biology*, 2(5), pp. 120080–120080. doi: 10.1098/rsob.120080.

Kondoh, K. and Nishida, E. (2007) 'Regulation of MAP kinases by MAP kinase phosphatases', *Biochimica et Biophysica Acta (BBA) - Molecular Cell Research*, 1773(8), pp. 1227–1237. doi: https://doi.org/10.1016/j.bbamcr.2006.12.002.

Kopyov, O. V *et al.* (1998) 'Safety of intrastriatal neurotransplantation for Huntington's disease patients.', *Experimental neurology*. United States, 149(1), pp. 97–108. doi: 10.1006/exnr.1997.6685.

Kostrzewa, R. M. and Jacobowitz, D. M. (1974) 'Pharmacological actions of 6-hydroxydopamine.', *Pharmacological reviews*. United States, 26(3), pp. 199–288.

Koyano, F. *et al.* (2014) 'Ubiquitin is phosphorylated by PINK1 to activate parkin', *Nature*. Nature Publishing Group, 510(7503), pp. 162–166. doi: 10.1038/nature13392.

Krapivinsky, G. *et al.* (2003) 'The NMDA Receptor Is Coupled to the ERK Pathway by a Direct Interaction between NR2B and RasGRF1', *Neuron*, 40(4), pp. 775–784. doi: https://doi.org/10.1016/S0896-6273(03)00645-7.

Kreiner, G. (2018) 'What have we learned recently from transgenic mouse models about neurodegeneration? The most promising discoveries of this millennium', *Pharmacological Reports*. Institute of Pharmacology, Polish Academy of Sciences, 70(6), pp. 1105–1115. doi: 10.1016/j.pharep.2018.09.006.

Von Kriegsheim, A. *et al.* (2009) 'Cell fate decisions are specified by the dynamic ERK interactome', *Nature Cell Biology*. England, 11(12), pp. 1458–1464. doi: 10.1038/ncb1994.

Krishna, M. and Narang, H. (2008) 'The complexity of mitogen-activated protein kinases (MAPKs) made simple', *Cellular and Molecular Life Sciences*, 65(22), pp. 3525–3544. doi: 10.1007/s00018-008-8170-7.

Kruger, R. *et al.* (1998) 'Ala30Pro mutation in the gene encoding alpha-synuclein in Parkinson's disease.', *Nature genetics*. United States, pp. 106–108. doi: 10.1038/ng0298-106.

Kumar, S. R. *et al.* (2016) 'Clinical development of gene therapy: results and lessons from recent successes.', *Molecular therapy. Methods & clinical development*, 3, p. 16034. doi: 10.1038/mtm.2016.34.

Kupsch, A. *et al.* (2001) 'Monoamine oxidase-inhibition and MPTP-induced neurotoxicity in the non-human primate: comparison of rasagiline (TVP 1012) with selegiline.', *Journal of neural transmission (Vienna, Austria : 1996)*. Austria, 108(8–9), pp. 985–1009. doi: 10.1007/s007020170018.

Kurtis, M. M., Rodriguez-Blazquez, C. and Martinez-Martin, P. (2013) 'Relationship between sleep disorders and other non-motor symptoms in Parkinson's disease', *Parkinsonism and Related Disorders*, 19(12), pp. 1152–1155. doi: 10.1016/j.parkreldis.2013.07.026.

Kuzuhara, S. *et al.* (1988) 'Lewy bodies are ubiquitinated. A light and electron microscopic immunocytochemical study.', *Acta neuropathologica*. Germany, 75(4), pp. 345–353. doi: 10.1007/bf00687787.

Lagouge, M. and Larsson, N.-G. (2013) 'The role of mitochondrial DNA mutations and free radicals in disease and ageing.', *Journal of internal medicine*, 273(6), pp. 529–543. doi: 10.1111/joim.12055.

Lang, A. E. *et al.* (2006) 'Randomized controlled trial of intraputamenal glial cell line-derived neurotrophic factor infusion in Parkinson disease.', *Annals of neurology*. United States, 59(3), pp. 459–466. doi: 10.1002/ana.20737.

Lang, A. E. (2010) 'Clinical trials of disease-modifying therapies for neurodegenerative diseases: The challenges and the future', *Nature Medicine*. Nature Publishing Group, 16(11), pp. 1223–1226. doi: 10.1038/nm.2220.

Langston, J. *et al.* (1983) 'Chronic Parkinsonism in humans due to a product of meperidine-analog synthesis', *Science*, 219(4587), pp. 979–980. doi: 10.1126/science.6823561.

Lawrence, B. J., Gasson, N. and Loftus, A. M. (2016) 'Prevalence and Subtypes of Mild Cognitive Impairment in Parkinson's Disease.', *Scientific reports*. England, 6, p. 33929. doi: 10.1038/srep33929.

Lazarou, M. *et al.* (2012) 'Role of PINK1 binding to the TOM complex and alternate intracellular membranes in recruitment and activation of the E3 ligase Parkin.', *Developmental cell*. United States, 22(2), pp. 320–333. doi: 10.1016/j.devcel.2011.12.014.

Lazarou, M. *et al.* (2015) 'The ubiquitin kinase PINK1 recruits autophagy receptors to induce mitophagy', *Nature*, 524(7565), pp. 309–314. doi: 10.1038/nature14893.

Lee, A. L. *et al.* (2017) 'A new Caenorhabditis elegans model of human huntingtin 513 aggregation and toxicity in body wall muscles.', *PloS one*, 12(3), p. e0173644. doi: 10.1371/journal.pone.0173644.

Lee, J.-M. *et al.* (2012) 'CAG repeat expansion in Huntington disease determines age at onset in a fully dominant fashion.', *Neurology*. United States, 78(10), pp. 690–695. doi: 10.1212/WNL.0b013e318249f683.

Lee, J.-M. *et al.* (2017) 'A modifier of Huntington's disease onset at the MLH1 locus', *Human Molecular Genetics*, 26(19), pp. 3859–3867. doi: 10.1093/hmg/ddx286.

Lee, J.-M. *et al.* (2019) 'CAG Repeat Not Polyglutamine Length Determines Timing of Huntington's Disease Onset', *Cell*, 178(4), pp. 887-900.e14. doi: https://doi.org/10.1016/j.cell.2019.06.036.

Lee, J. J. *et al.* (2018) 'Basal mitophagy is widespread in Drosophila but minimally affected by loss of Pink1 or parkin', *Journal of Cell Biology*, 217(5), pp. 1613–1622. doi: 10.1083/jcb.201801044.

Lee, S.-J. *et al.* (2010) 'Cell-to-cell transmission of non-prion protein aggregates.', *Nature reviews. Neurology*. England, pp. 702–706. doi: 10.1038/nrneurol.2010.145.

Lee, S.-T. *et al.* (2009) 'Slowed progression in models of Huntington disease by adipose stem cell transplantation.', *Annals of neurology*. United States, 66(5), pp. 671–681. doi: 10.1002/ana.21788.

Lee, T. *et al.* (2004) 'Docking motif interactions in MAP kinases revealed by hydrogen exchange mass spectrometry.', *Molecular cell*. United States, 14(1), pp. 43–55. doi: 10.1016/s1097-2765(04)00161-3.

Lefloch, R., Pouyssegur, J. and Lenormand, P. (2008) 'Single and combined silencing of ERK1 and ERK2 reveals their positive contribution to growth signaling depending on their expression levels.', *Molecular and cellular biology*. United States, 28(1), pp. 511–527. doi: 10.1128/MCB.00800-07.

Lehtonen, Š. *et al.* (2019) 'Dysfunction of Cellular Proteostasis in Parkinson's Disease', *Frontiers in Neuroscience*, 13, p. 457. doi: 10.3389/fnins.2019.00457.

Lei, Z., Cao, G. and Wei, G. (2019) 'A30P mutant α-synuclein impairs autophagic flux by

inactivating JNK signaling to enhance ZKSCAN3 activity in midbrain dopaminergic neurons', *Cell Death and Disease*. Springer US, 10(2). doi: 10.1038/s41419-019-1364-0.

Leibrock, J. *et al.* (1989) 'Molecular cloning and expression of brain-derived neurotrophic factor.', *Nature*. England, 341(6238), pp. 149–152. doi: 10.1038/341149a0.

Leonard, D. P. *et al.* (1975) 'A Double Blind Trial of Lithium Carbonate and Haloperidol in Huntington's Chorea', *Australian & New Zealand Journal of Psychiatry*, 9(2), pp. 115–118. doi: 10.3109/00048677509159834.

Lesage, S. *et al.* (2016) 'Loss of VPS13C Function in Autosomal-Recessive Parkinsonism Causes Mitochondrial Dysfunction and Increases PINK1/Parkin-Dependent Mitophagy.', *American journal of human genetics*, 98(3), pp. 500–513. doi: 10.1016/j.ajhg.2016.01.014.

Lewis, E. A. and Smith, G. A. (2016) 'Using Drosophila models of Huntington's disease as a translatable tool', *Journal of Neuroscience Methods*, 265, pp. 89–98. doi: https://doi.org/10.1016/j.jneumeth.2015.07.026.

Li, M. and Rosser, A. E. (2017) 'Pluripotent stem cell-derived neurons for transplantation in Huntington's disease.', *Progress in brain research*. Netherlands, 230, pp. 263–281. doi: 10.1016/bs.pbr.2017.02.009.

Li, W. *et al.* (2005) 'The HMG-CoA reductase inhibitor lovastatin reverses the learning and attention deficits in a mouse model of Neurofibromatosis Type 1', *Current Biology*, 15(21), pp. 1961–1967. doi: 10.1016/j.cub.2005.09.043.

Li, Z. *et al.* (2011) 'Essential roles of enteric neuronal serotonin in gastrointestinal motility and the development/survival of enteric dopaminergic neurons.', *The Journal of neuroscience : the official journal of the Society for Neuroscience*. United States, 31(24), pp. 8998–9009. doi: 10.1523/JNEUROSCI.6684-10.2011.

Limaye, A., Hall, B. and Kulkarni, A. B. (2009) 'Manipulation of mouse embryonic stem cells for knockout mouse production.', *Current protocols in cell biology*, Chapter 19, p. Unit 19.13 19.13.1-24. doi: 10.1002/0471143030.cb1913s44.

Linder, C. C. (2006) 'Genetic variables that influence phenotype', *ILAR Journal*, 47(2), pp. 132–140. doi: 10.1093/ilar.47.2.132.

Lindvall, O. *et al.* (1989) 'Human fetal dopamine neurons grafted into the striatum in two patients with severe Parkinson's disease. A detailed account of methodology and a 6-month follow-up.', *Archives of neurology*. United States, 46(6), pp. 615–631. doi: 10.1001/archneur.1989.00520420033021.

Litvan, I. *et al.* (2012) 'Diagnostic criteria for mild cognitive impairment in Parkinson's disease: Movement Disorder Society Task Force guidelines.', *Movement disorders : official journal of the Movement Disorder Society*, 27(3), pp. 349–356. doi: 10.1002/mds.24893.

Liu, G. *et al.* (2017) 'Prediction of cognition in Parkinson's disease with a clinical–genetic score: a longitudinal analysis of nine cohorts', *The Lancet Neurology*, 16(8), pp. 620–629. doi: https://doi.org/10.1016/S1474-4422(17)30122-9.

Liu, H. *et al.* (1999) 'Is Green Fluorescent Protein Toxic to the Living Cells? - 20081211_94c62335071dba3032eaoeSWWCB0wBfE.attach.pdf', 717, pp. 712–717. Available at: http://download.bioon.com/view/upload/month_0812/20081211_94c62335071dba3032eaoeSWWCB0wBfE.attach.pdf.

Liu, L. *et al.* (2016) 'Induced Pluripotent Stem Cells in Huntington's Disease: Disease Modeling and the Potential for Cell-Based Therapy.', *Molecular neurobiology*, 53(10), pp. 6698–6708. doi: 10.1007/s12035-015-9601-8.

Liu, Z. *et al.* (2017) 'Systematic comparison of 2A peptides for cloning multi-genes in a polycistronic vector', *Scientific Reports*. Springer US, 7(1), pp. 1–9. doi: 10.1038/s41598-017-02460-2.

Lu, B., Nagappan, G. and Lu, Y. (2014) 'BDNF and synaptic plasticity, cognitive function, and dysfunction.', *Handbook of experimental pharmacology*. Germany, 220, pp. 223–250. doi: 10.1007/978-3-642-45106-5_9.

Lücking, C. B. *et al.* (2000) 'Association between Early-Onset Parkinson's Disease and Mutations in the Parkin Gene', *New England Journal of Medicine*, 342(21), pp. 1560–1567. doi: 10.1056/NEJM200005253422103.

Luk, K. C. *et al.* (2009) 'Exogenous alpha-synuclein fibrils seed the formation of Lewy body-like intracellular inclusions in cultured cells.', *Proceedings of the National Academy of Sciences of the United States of America*. United States, 106(47), pp. 20051–20056. doi: 10.1073/pnas.0908005106.

MacDonald, M. E. *et al.* (1993) 'A novel gene containing a trinucleotide repeat that is expanded and unstable on Huntington's disease chromosomes. The Huntington's Disease Collaborative Research Group.', *Cell*. Elsevier, 72(6), pp. 971–83. doi: 10.1016/0092-8674(93)90585-E.

Maher, P. *et al.* (2011) 'Erk activation by the polyphenols fisetin and resveratrol provides

neuroprotection in multiple models of Huntington's disease', *Human Molecular Genetics*, 20(2), pp. 261–270. doi: 10.1093/hmg/ddq460.

Manfré, G. *et al.* (2017) 'The BACHD Rat Model of Huntington Disease Shows Specific Deficits in a Test Battery of Motor Function.', *Frontiers in behavioral neuroscience*, 11, p. 218. doi: 10.3389/fnbeh.2017.00218.

Mangiarini, L. *et al.* (1996) 'Exon I of the HD gene with an expanded CAG repeat is sufficient to cause a progressive neurological phenotype in transgenic mice', *Cell*, 87(3), pp. 493–506. doi: 10.1016/S0092-8674(00)81369-0.

Mann, D. M., Oliver, R. and Snowden, J. S. (1993) 'The topographic distribution of brain atrophy in Huntington's disease and progressive supranuclear palsy.', *Acta neuropathologica*. Germany, 85(5), pp. 553–559. doi: 10.1007/bf00230496.

Manning-Bog, A. B. *et al.* (2002) 'The herbicide paraquat causes up-regulation and aggregation of alpha-synuclein in mice: paraquat and alpha-synuclein.', *The Journal of biological chemistry*. United States, 277(3), pp. 1641–1644. doi: 10.1074/jbc.C100560200.

Manning-Boğ, A. B. and Langston, J. W. (2007) 'Model fusion: The next phase in developing animal models for Parkinson's disease', *Neurotoxicity Research*, 11(3–4), pp. 219–240. doi: 10.1007/BF03033569.

Maraganore, D. M. *et al.* (2006) 'Collaborative analysis of alpha-synuclein gene promoter variability and Parkinson disease.', *JAMA*. United States, 296(6), pp. 661–670. doi: 10.1001/jama.296.6.661.

Marchi, M. *et al.* (2008) 'The N-terminal domain of ERK1 accounts for the functional differences with ERK2', *PLoS ONE*, 3(12). doi: 10.1371/journal.pone.0003873.

Markesbery, W. R. *et al.* (2009) 'Lewy body pathology in normal elderly subjects.', *Journal of neuropathology and experimental neurology*, 68(7), pp. 816–822. doi: 10.1097/NEN.0b013e3181ac10a7.

Maroteaux, L., Campanelli, J. T. and Scheller, R. H. (1988) 'Synuclein: a neuron-specific protein localized to the nucleus and presynaptic nerve terminal.', *The Journal of neuroscience : the official journal of the Society for Neuroscience*. United States, 8(8), pp. 2804–2815.

Martin, I. *et al.* (2014) 'LRRK2 pathobiology in Parkinson's disease.', *Journal of neurochemistry*, 131(5), pp. 554–565. doi: 10.1111/jnc.12949.

Masters, C. L. *et al.* (2015) 'Alzheimer's disease', *Nature Reviews Disease Primers*, 1(1), p.

15056. doi: 10.1038/nrdp.2015.56.

Mata, I. F. *et al.* (2006) 'LRRK2 in Parkinson's disease: protein domains and functional insights', *Trends in Neurosciences*, 29(5), pp. 286–293. doi: https://doi.org/10.1016/j.tins.2006.03.006.

Matsuda, W. *et al.* (2009) 'Single nigrostriatal dopaminergic neurons form widely spread and highly dense axonal arborizations in the neostriatum.', *The Journal of neuroscience : the official journal of the Society for Neuroscience*, 29(2), pp. 444–453. doi: 10.1523/JNEUROSCI.4029-08.2009.

Matsuo, N. *et al.* (2010) 'Behavioral profiles of three C57BL/6 substrains.', *Frontiers in behavioral neuroscience*, 4, p. 29. doi: 10.3389/fnbeh.2010.00029.

Mazzucchelli, C. *et al.* (2002) 'Knockout of ERK1 MAP Kinase Enhances Synaptic Plasticity in the Striatum and Facilitates Striatal-Mediated Learning and Memory', 34, pp. 807–820.

McBride, J. L. *et al.* (2004) 'Human neural stem cell transplants improve motor function in a rat model of Huntington's disease', *Journal of Comparative Neurology*, 475(2), pp. 211–219. doi: 10.1002/cne.20176.

McCord, J. M. and Fridovich, I. (1969) 'Superoxide dismutase. An enzymic function for erythrocuprein (hemocuprein).', *The Journal of biological chemistry*. United States, 244(22), pp. 6049–6055.

McCormack, A. L. *et al.* (2002) 'Environmental risk factors and Parkinson's disease: selective degeneration of nigral dopaminergic neurons caused by the herbicide paraquat.', *Neurobiology of disease*. United States, 10(2), pp. 119–127.

McGregor, M. M. and Nelson, A. B. (2019) 'Circuit Mechanisms of Parkinson's Disease', *Neuron*. Elsevier Inc., 101(6), pp. 1042–1056. doi: 10.1016/j.neuron.2019.03.004.

McLelland, G.-L. *et al.* (2018) 'Mfn2 ubiquitination by PINK1/parkin gates the p97-dependent release of ER from mitochondria to drive mitophagy.', *eLife*. England, 7. doi: 10.7554/eLife.32866.

Mcwilliams, T. G. *et al.* (2018) 'Phosphorylation of Parkin at serine 65 is essential for its activation in vivo', *Open biology*, 8(11). doi: 10.1098/rsob.180108.

McWilliams, T. G. *et al.* (2018) 'Basal Mitophagy Occurs Independently of PINK1 in Mouse Tissues of High Metabolic Demand', *Cell Metabolism*, pp. 1–11. doi: 10.1016/j.cmet.2017.12.008.

McWilliams, T. G. and Muqit, M. M. (2017) 'PINK1 and Parkin: emerging themes in mitochondrial homeostasis', *Current Opinion in Cell Biology*. Elsevier Ltd, 45, pp. 83–91. doi: 10.1016/j.ceb.2017.03.013.

Meade, R. M., Fairlie, D. P. and Mason, J. M. (2019) 'Alpha-synuclein structure and Parkinson's disease – lessons and emerging principles', *Molecular Neurodegeneration*, 14(1), p. 29. doi: 10.1186/s13024-019-0329-1.

Mealer, R. G. *et al.* (2014) 'Rhes, a Striatal-selective Protein Implicated in Huntington Disease, Binds Beclin-1 and activates autophagy', *Journal of Biological Chemistry*, 289(6), pp. 3547–3554. doi: 10.1074/jbc.M113.536912.

Meiser, J., Weindl, D. and Hiller, K. (2013) 'Complexity of dopamine metabolism.', *Cell communication and signaling : CCS*, 11(1), p. 34. doi: 10.1186/1478-811X-11-34.

Menalled, L. B. *et al.* (2012) 'Comprehensive Behavioral and Molecular Characterization of a New Knock-In Mouse Model of Huntington's Disease: ZQ175', *PLoS ONE*, 7(12). doi: 10.1371/journal.pone.0049838.

Merten, O. W., Hebben, M. and Bovolenta, C. (2016) 'Production of lentiviral vectors', *Molecular Therapy - Methods and Clinical Development*, 3(December 2015), p. 16017. doi: 10.1038/mtm.2016.17.

Mestre, T. A. (2019) 'Recent advances in the therapeutic development for Huntington disease', *Parkinsonism and Related Disorders*. Elsevier, 59(November 2018), pp. 125–130. doi: 10.1016/j.parkreldis.2018.12.003.

Miguez, a. *et al.* (2015) 'Fingolimod (FTY720) enhances hippocampal synaptic plasticity and memory in Huntington's disease by preventing p75NTR up-regulation and astrocyte-mediated inflammation', *Human Molecular Genetics*, 24(17), pp. 4958–4970. doi: 10.1093/hmg/ddv218.

Miller, G. W. (2007) 'Paraquat: the red herring of Parkinson's disease research.', *Toxicological sciences : an official journal of the Society of Toxicology*. United States, pp. 1–2. doi: 10.1093/toxsci/kfm223.

Milone, M. C. and O'Doherty, U. (2018) 'Clinical use of lentiviral vectors.', *Leukemia*. England, 32(7), pp. 1529–1541. doi: 10.1038/s41375-018-0106-0.

Mingozzi, F. and Buning, H. (2015) 'Adeno-Associated Viral Vectors at the Frontier between Tolerance and Immunity.', *Frontiers in immunology*. Switzerland, 6, p. 120. doi: 10.3389/fimmu.2015.00120.

Mingozzi, F. and High, K. A. (2017) 'Overcoming the Host Immune Response to Adeno-Associated Virus Gene Delivery Vectors: The Race Between Clearance, Tolerance, Neutralization, and Escape', *Annual Review of Virology*, 4(1), pp. 511–534. doi: 10.1146/annurev-virology-101416-041936.

Mink, J. W. (1996) 'The Basal Ganglia: Focused Selection and Inhibition of Competing Motor Programs', *Progress in Neurobiology*, 50, pp. 381–425. doi: 10.1016/S0301-0082(96)00042-1.

Minskaia, E. and Ryan, M. D. (2013) 'Protein coexpression using FMDV 2A: Effect of "linker" residues', *BioMed Research International*, 2013. doi: 10.1155/2013/291730.

Mishima, T. *et al.* (2018) 'Modeling Parkinson's disease and atypical parkinsonian syndromes using induced pluripotent stem cells', *International Journal of Molecular Sciences*, 19(12). doi: 10.3390/ijms19123870.

Mizuguchi, H. *et al.* (2000) 'IRES-Dependent Second Gene Expression Is Significantly Lower Than Cap-Dependent First Gene Expression in a Bicistronic Vector', *Molecular Therapy*. American Society for Gene Therapy, 1(4), pp. 376–382. doi: 10.1006/mthe.2000.0050.

Mohs, R. C. and Greig, N. H. (2017) 'Drug discovery and development: Role of basic biological research', *Alzheimer's and Dementia: Translational Research and Clinical Interventions*. Elsevier Inc., 3(4), pp. 651–657. doi: 10.1016/j.trci.2017.10.005.

Montserrat, A. *et al.* (2004) 'Inclusion body formation reduces levels of mutant huntingtin and the risk of neuronal death', 431(October).

Moore, R. Y. and Bloom, F. E. (1978) 'Central Catecholamine Neuron Systems : Anatomy and Physiology of the Dopamine Systems', *Annual Reviews Neuroscience*, 1, pp. 129–69.

Morozov, A. *et al.* (2003) 'Rap1 couples cAMP signaling to a distinct pool of p42/44MAPK regulating excitability, synaptic plasticity, learning, and memory.', *Neuron*. United States, 39(2), pp. 309–325. doi: 10.1016/s0896-6273(03)00404-5.

Moustafa, A. A. *et al.* (2016) 'Motor symptoms in Parkinson's disease: A unified framework', *Neuroscience and Biobehavioral Reviews*. Elsevier Ltd, 68, pp. 727–740. doi: 10.1016/j.neubiorev.2016.07.010.

Muller, F. L., Liu, Y. and Van Remmen, H. (2004) 'Complex III releases superoxide to both sides of the inner mitochondrial membrane.', *The Journal of biological chemistry*. United States, 279(47), pp. 49064–49073. doi: 10.1074/jbc.M407715200.

Muqit, M. M. K. *et al.* (2006) 'Altered cleavage and localization of PINK1 to aggresomes in the

presence of proteasomal stress', *Journal of Neurochemistry*, 98(1), pp. 156–169. doi: 10.1111/j.1471-4159.2006.03845.x.

Mura, A. *et al.* (1995) 'Aromatic L-amino acid decarboxylase immunoreactive cells in the rat striatum: a possible site for the conversion of exogenous L-DOPA to dopamine.', *Brain research*. Netherlands, 704(1), pp. 51–60. doi: 10.1016/0006-8993(95)01104-8.

Muramatsu, S.-I. *et al.* (2002) 'Behavioral recovery in a primate model of Parkinson's disease by triple transduction of striatal cells with adeno-associated viral vectors expressing dopamine-synthesizing enzymes.', *Human gene therapy*. United States, 13(3), pp. 345–354. doi: 10.1089/10430340252792486.

Muramatsu, S. I. *et al.* (2010) 'A phase i study of aromatic l-amino acid decarboxylase gene therapy for parkinson's disease', *Molecular Therapy*. Nature Publishing Group, 18(9), pp. 1731–1735. doi: 10.1038/mt.2010.135.

Murphy, M. P. (2009) 'How mitochondria produce reactive oxygen species.', *The Biochemical journal*. England, 417(1), pp. 1–13. doi: 10.1042/BJ20081386.

Nadeau, J. H. (2001) 'Modifier genes in mice and humans', *Nature Reviews Genetics*, 2(3), pp. 165–174. doi: 10.1038/35056009.

Nagatsu, T. and Sawada, M. (2007) 'Biochemistry of postmortem brains in Parkinson's disease: historical overview and future prospects.', *Journal of neural transmission. Supplementum*. Austria, (72), pp. 113–120.

Naldini, L. *et al.* (1996) 'Efficient transfer, integration, and sustained long-term expression of the transgene in adult rat brains injected with a lentiviral vector.', *Proceedings of the National Academy of Sciences of the United States of America*. United States, 93(21), pp. 11382–11388. doi: 10.1073/pnas.93.21.11382.

Nalls, M. A. *et al.* (2018) 'Parkinson's disease genetics: identifying novel risk loci, providing causal insights and improving estimates of heritable risk', *bioRxiv*. Cold Spring Harbor Laboratory. doi: 10.1101/388165.

Nambu, A. (2005) 'A new approach to understand the pathophysiology of Parkinson's disease', *Journal of Neurology*, 252(SUPPL. 4), pp. 1–4. doi: 10.1007/s00415-005-4002-y.

Narendra, D. *et al.* (2008) 'Parkin is recruited selectively to impaired mitochondria and promotes their autophagy', *Journal of Cell Biology*, 183(5), pp. 795–803. doi: 10.1083/jcb.200809125.

Nash, K., Chen, W. and Muzyczka, N. (2008) 'Complete in vitro reconstitution of adeno-associated virus DNA replication requires the minichromosome maintenance complex proteins.', *Journal of virology*. United States, 82(3), pp. 1458–1464. doi: 10.1128/JVI.01968-07.

Naso, M. F. *et al.* (2017) 'Adeno-Associated Virus (AAV) as a Vector for Gene Therapy', *BioDrugs*. Springer International Publishing, 31(4), pp. 317–334. doi: 10.1007/s40259-017-0234-5.

Nelson, A. B. and Kreitzer, A. C. (2014) 'Reassessing Models of Basal Ganglia Function and Dysfunction', *Annual Review of Neuroscience*, 37(1), pp. 117–135. doi: 10.1146/annurev-neuro-071013-013916.

Nelson, M. R. *et al.* (2015) 'The support of human genetic evidence for approved drug indications', *Nature Genetics*. Nature Publishing Group, 47(8), pp. 856–860. doi: 10.1038/ng.3314.

Neupert, W. and Herrmann, J. M. (2007) 'Translocation of proteins into mitochondria.', *Annual review of biochemistry*. United States, 76, pp. 723–749. doi: 10.1146/annurev.biochem.76.052705.163409.

Nguyen, K. Q., Rymar, V. V. and Sadikot, A. F. (2016) 'Impaired TrkB Signaling Underlies Reduced BDNF-Mediated Trophic Support of Striatal Neurons in the R6/2 Mouse Model of Huntington's Disease', *Frontiers in Cellular Neuroscience*, 10(February), pp. 1–12. doi: 10.3389/fncel.2016.00037.

Ni, H.-M., Williams, J. A. and Ding, W.-X. (2015) 'Mitochondrial dynamics and mitochondrial quality control.', *Redox biology*. Netherlands, 4, pp. 6–13. doi: 10.1016/j.redox.2014.11.006.

Nibuya, M., Morinobu, S. and Duman, R. S. (1995) 'Regulation of BDNF and trkB mRNA in rat brain by chronic electroconvulsive seizure and antidepressant drug treatments.', *The Journal of neuroscience : the official journal of the Society for Neuroscience*. United States, 15(11), pp. 7539–7547.

Nunnari, J. and Suomalainen, A. (2012) 'Mitochondria: in sickness and in health.', *Cell*. United States, 148(6), pp. 1145–1159. doi: 10.1016/j.cell.2012.02.035.

Obeso, J. A. *et al.* (2017) 'Past, present, and future of Parkinson's disease: A special essay on the 200th Anniversary of the Shaking Palsy', *Movement Disorders*, 32(9), pp. 1264–1310. doi: 10.1002/mds.27115.

Ochs, G. *et al.* (2000) 'A phase I/II trial of recombinant methionyl human brain derived

neurotrophic factor administered by intrathecal infusion to patients with amyotrophic lateral sclerosis', *Amyotrophic Lateral Sclerosis*, 1(3), pp. 201–206. doi: 10.1080/14660820050515197.

Olanow, C. W. *et al.* (2003) 'A double-blind controlled trial of bilateral fetal nigral transplantation in Parkinson's disease.', *Annals of neurology*. United States, 54(3), pp. 403–414. doi: 10.1002/ana.10720.

Ordureau, A. *et al.* (2015) 'Quantitative proteomics reveal a feed-forward model for mitochondrial PARKIN translocation and UB chain synthesis', *Molecular Cell*, 56(3), pp. 360–375. doi: 10.1016/j.molcel.2014.09.007.Quantitative.

Osborne, A. *et al.* (2018) 'Design of a Novel Gene Therapy Construct to Achieve Sustained Brain-Derived Neurotrophic Factor Signaling in Neurons', *Human Gene Therapy*, 29(7), pp. 828–841. doi: 10.1089/hum.2017.069.

Pagès, G. *et al.* (1999) 'Defective thymocyte maturation in p44 MAP kinase (Erk 1) knockout mice.', *Science*, 286(5443), pp. 1374–1377. doi: 10.1126/science.286.5443.1374.

Paisan-Ruiz, C. *et al.* (2004) 'Cloning of the gene containing mutations that cause PARK8-linked Parkinson's disease.', *Neuron*. United States, 44(4), pp. 595–600. doi: 10.1016/j.neuron.2004.10.023.

Palfi, S. *et al.* (2014) 'Long-term safety and tolerability of ProSavin, a lentiviral vector-based gene therapy for Parkinson's disease: a dose escalation, open-label, phase 1/2 trial', *The Lancet*. Elsevier, 383(9923), pp. 1138–1146. doi: 10.1016/S0140-6736(13)61939-X.

Palfi, S. *et al.* (2018) 'Long-Term Follow-Up of a Phase I/II Study of ProSavin, a Lentiviral Vector Gene Therapy for Parkinson's Disease', *Human Gene Therapy Clinical Development*, 29(3), pp. 148–155. doi: 10.1089/humc.2018.081.

Palikaras, K., Lionaki, E. and Tavernarakis, N. (2018) 'Mechanisms of mitophagy in cellular homeostasis, physiology and pathology', *Nature Cell Biology*. Springer US, 20(9), pp. 1013–1022. doi: 10.1038/s41556-018-0176-2.

Pandey, U. B. and Nichols, C. D. (2011) 'Human disease models in Drosophila melanogaster and the role of the fly in therapeutic drug discovery.', *Pharmacological reviews*, 63(2), pp. 411–436. doi: 10.1124/pr.110.003293.

Pangalos, M. N., Schechter, L. E. and Hurko, O. (2007) 'Drug development for CNS disorders: strategies for balancing risk and reducing attrition.', *Nature reviews. Drug discovery*. England, 6(7), pp. 521–532. doi: 10.1038/nrd2094.

Papagno, C. and Trojano, L. (2018) 'Cognitive and behavioral disorders in Parkinson's disease: an update. II: behavioral disorders', *Neurological Sciences*. Neurological Sciences, 39(1), pp. 53–61. doi: 10.1007/s10072-017-3155-7.

Papapetropoulos, S. *et al.* (2001) 'Clinical phenotype in patients with alpha-synuclein Parkinson's disease living in Greece in comparison with patients with sporadic Parkinson's disease.', *Journal of neurology, neurosurgery, and psychiatry*. England, 70(5), pp. 662–665. doi: 10.1136/jnnp.70.5.662.

Papavasiliou, P. S. *et al.* (1972) 'Levodopa in Parkinsonism: potentiation of central effects with a peripheral inhibitor.', *The New England journal of medicine*. United States, 286(1), pp. 8–14. doi: 10.1056/NEJM197201062860102.

Di Pardo, A. *et al.* (2014) 'FTY720 (fingolimod) is a neuroprotective and disease-modifying agent in cellular and mouse models of huntington disease', *Human Molecular Genetics*, 23(9), pp. 2251–2265. doi: 10.1093/hmg/ddt615.

Di Pardo, A. *et al.* (2017) 'Defective Sphingosine-1-phosphate metabolism is a druggable target in Huntington's disease', *Scientific Reports*, 7(1), pp. 1–14. doi: 10.1038/s41598-017-05709-y.

Parent, A., Smith, Y. and Bellefeuille, L. (1984) 'The Output Organization of the Pallidum and Substantia Nigra in Primate as Revealed by a Retrograde Double-Labeling Method', in McKenzie, J. S., Kemm, R. E., and Wilcock, L. N. (eds) *The Basal Ganglia: Structure and Function*. Boston, MA: Springer US, pp. 147–160. doi: 10.1007/978-1-4684-1212-3_7.

Park, J. *et al.* (2006) 'Mitochondrial dysfunction in Drosophila PINK1 mutants is complemented by parkin', *Nature*, 441(7097), pp. 1157–1161. doi: 10.1038/nature04788.

Parkinson, J. (2002) 'An Essay on the Shaking Palsy (Originally published in 1817)', *Journal of Neuropsychiatry*, 14(2), pp. 223–236. doi: 10.1176/appi.neuropsych.14.2.223.

Parmar, M., Torper, O. and Drouin-Ouellet, J. (2019) 'Cell-based therapy for Parkinson's disease: A journey through decades toward the light side of the Force', *European Journal of Neuroscience*, 49(4), pp. 463–471. doi: 10.1111/ejn.14109.

Patapoutian, A. and Reichardt, L. F. (2001) 'Trk receptors: mediators of neurotrophin action', *Current Opinion in Neurobiology*, 11(3), pp. 272–280. doi: https://doi.org/10.1016/S0959-4388(00)00208-7.

Pedersen, K. F. *et al.* (2013) 'Prognosis of mild cognitive impairment in early Parkinson disease: the Norwegian ParkWest study.', *JAMA neurology*. United States, 70(5), pp. 580–

586. doi: 10.1001/jamaneurol.2013.2110.

Peng, Q. *et al.* (2008) 'The antidepressant sertraline improves the phenotype, promotes neurogenesis and increases BDNF levels in the R6/2 Huntington's disease mouse model', *Experimental neurology*. 2007/11/09, 210(1), pp. 154–163. doi: 10.1016/j.expneurol.2007.10.015.

Penney, J. B. and Young, A. B. (1983) 'Speculations on the Functional Anatomy of Basal Ganglia Disorders', *Annual Review of Neuroscience*, 6(1), pp. 73–94. doi: 10.1146/annurev.ne.06.030183.000445.

Perese, D. A. *et al.* (1989) 'A 6-hydroxydopamine-induced selective parkinsonian rat model (perese 1989).pdf', 494, pp. 285–293.

Perez, F. A. and Palmiter, R. D. (2005) 'Parkin-deficient mice are not a robust model of parkinsonism', *Proceedings of the National Academy of Sciences*, 102(6), pp. 2174–2179. doi: 10.1073/pnas.0409598102.

Pesah, Y. *et al.* (2004) 'Drosophila parkin mutants have decreased mass and cell size and increased sensitivity to oxygen radical stress', *Development*, 131(9), pp. 2183–2194. doi: 10.1242/dev.01095.

Pfeiffer, R. F. (2016) 'Non-motor symptoms in Parkinson's disease', *Parkinsonism and Related Disorders*. Elsevier Ltd, 22, pp. S119–S122. doi: 10.1016/j.parkreldis.2015.09.004.

Pickart, C. M. and Eddins, M. J. (2004) 'Ubiquitin: structures, functions, mechanisms', *Biochimica et Biophysica Acta (BBA) - Molecular Cell Research*, 1695(1), pp. 55–72. doi: https://doi.org/10.1016/j.bbamcr.2004.09.019.

Pickrell, A. M. *et al.* (2015) 'Endogenous Parkin Preserves Dopaminergic Substantia Nigral Neurons following Mitochondrial DNA Mutagenic Stress', *Neuron*, 87(2), pp. 371–381. doi: 10.1002/nbm.3369.Three.

Pierre, S., Bats, A. S. and Coumoul, X. (2011) 'Understanding SOS (Son of Sevenless)', *Biochemical Pharmacology*, 82(9), pp. 1049–1056. doi: 10.1016/j.bcp.2011.07.072.

Pigott, K. *et al.* (2015) 'Longitudinal study of normal cognition in Parkinson disease.', *Neurology*, 85(15), pp. 1276–1282. doi: 10.1016/j.pnpbp.2005.06.015.

Pinto, M., Nissanka, N. and Moraes, C. T. (2017) 'Lack of Parkin anticipates the phenotype and affects mitochondrial morphology and mtDNA levels in a mouse model of Parkinson's Disease', *The Journal of Neuroscience*, 38(4), pp. 1384–17. doi: 10.1523/JNEUROSCI.1384-

17.2017.

Pinto, M., Nissanka, N. and Moraes, C. T. (2018) 'Lack of Parkin Anticipates the Phenotype and Affects Mitochondrial Morphology and mtDNA Levels in a Mouse Model of Parkinson's Disease.', *The Journal of neuroscience : the official journal of the Society for Neuroscience*. United States, 38(4), pp. 1042–1053. doi: 10.1523/JNEUROSCI.1384-17.2017.

Pinto, S. *et al.* (2016) 'Dysarthria in individuals with Parkinson's disease: A protocol for a binational, cross-sectional, case-controlled study in French and European Portuguese (FraLusoPark)', *BMJ Open*, 6(11), pp. 1–10. doi: 10.1136/bmjopen-2016-012885.

Pistacchi, M. *et al.* (2017) 'Gait analysis and clinical correlations in early Parkinson's disease.', *Functional neurology*, 32(1), pp. 28–34. doi: 10.11138/FNeur/2017.32.1.028.

Plotkin, J. L. *et al.* (2014) 'Impaired TrkB receptor signaling underlies corticostriatal dysfunction in Huntington's disease', *Neuron*. Elsevier Inc., 83(1), pp. 178–188. doi: 10.1016/j.neuron.2014.05.032.

Poewe, W. *et al.* (2017) 'Parkinson disease', *Nature Reviews Disease Primers*, 3(1), p. 17013. doi: 10.1038/nrdp.2017.13.

Pollak, P. *et al.* (1993) 'Effects of the stimulation of the subthalamic nucleus in Parkinson disease', *Revue neurologique*. France, 149(3), pp. 175–6. Available at: http://www.ncbi.nlm.nih.gov/pubmed/8235208.

Pollock, K. *et al.* (2016) 'Human Mesenchymal Stem Cells Genetically Engineered to Overexpress Brain-derived Neurotrophic Factor Improve Outcomes in Huntington's Disease Mouse Models.', *Molecular therapy : the journal of the American Society of Gene Therapy*. United States, 24(5), pp. 965–977. doi: 10.1038/mt.2016.12.

Polymeropoulos, M. H. *et al.* (1997) 'Mutation in the alpha-synuclein gene identified in families with Parkinson's disease.', *Science (New York, N.Y.)*. United States, 276(5321), pp. 2045–2047. doi: 10.1126/science.276.5321.2045.

Porras, G., Li, Q. and Bezard, E. (2012) 'Modeling Parkinson's disease in primates: The MPTP model', *Cold Spring Harbor Perspectives in Medicine*, 2(3), pp. 1–10. doi: 10.1101/cshperspect.a009308.

Potkin, K. T. and Potkin, S. G. (2018) 'New directions in therapeutics for Huntington disease.', *Future neurology*. England, 13(2), pp. 101–121. doi: 10.2217/fnl-2017-0035.

Pouladi, M. a, Morton, a J. and Hayden, M. R. (2013) 'Choosing an animal model for the study

of Huntington's disease.', *Nature reviews. Neuroscience*. Nature Publishing Group, 14(10), pp. 708–21. doi: 10.1038/nrn3570.

Poulopoulos, M. *et al.* (2012) 'Clinical and pathological characteristics of LRRK2 G2019S patients with PD.', *Journal of molecular neuroscience : MN*, 47(1), pp. 139–143. doi: 10.1007/s12031-011-9696-y.

Pradhan, B. S. and Majumdar, S. S. (2016) 'An Efficient Method for Generation of Transgenic Rats Avoiding Embryo Manipulation.', *Molecular therapy. Nucleic acids*, 5(3), p. e293. doi: 10.1038/mtna.2016.9.

Pringsheim, T. *et al.* (2014) 'The prevalence of Parkinson's disease: A systematic review and meta-analysis', *Movement Disorders*, 29(13), pp. 1583–1590. doi: 10.1002/mds.25945.

Pryde, K. R. *et al.* (2016) 'PINK1 disables the anti-fission machinery to segregate damaged mitochondria for mitophagy.', *The Journal of cell biology*, 213(2), pp. 163–171. doi: 10.1083/jcb.201509003.

Purisai, M. G. *et al.* (2005) 'Alpha-synuclein expression in the substantia nigra of MPTP-lesioned non-human primates.', *Neurobiology of disease*. United States, 20(3), pp. 898–906. doi: 10.1016/j.nbd.2005.05.028.

Ramezani, A. and Hawley, R. G. (2002) 'Overview of the HIV-1 Lentiviral Vector System', *Current Protocols in Molecular Biology*, 60(1), pp. 16.21.1-16.21.15. doi: 10.1002/0471142727.mb1621s60.

Ramirez, A. *et al.* (2006) 'Hereditary parkinsonism with dementia is caused by mutations in ATP13A2, encoding a lysosomal type 5 P-type ATPase.', *Nature genetics*. United States, 38(10), pp. 1184–1191. doi: 10.1038/ng1884.

Ranzani, M. *et al.* (2013) 'Lentiviral vector-based insertional mutagenesis identifies genes associated with liver cancer.', *Nature methods*, 10(2), pp. 155–161. doi: 10.1038/nmeth.2331.

Rauen, K. a (2013) 'The RASopathies', *Annu Rev Genomics Hum Genet.*, 14, pp. 355–369. doi: 10.1146/annurev-genom-091212-153523.The.

Reed, X. *et al.* (2019) 'The role of monogenic genes in idiopathic Parkinson's disease', *Neurobiology of Disease*. Elsevier, 124(November 2018), pp. 230–239. doi: 10.1016/j.nbd.2018.11.012.

Reijnders, J. S. A. M. *et al.* (2008) 'A systematic review of prevalence studies of depression in

Parkinson's disease.', *Movement disorders : official journal of the Movement Disorder Society*. United States, 23(2), pp. 183–9; quiz 313. doi: 10.1002/mds.21803.

Reilmann, R. *et al.* (2018) 'J05 Legato-hd study: a phase 2 study assessing the efficacy and safety of laquinimod as a treatment for huntington disease', *Journal of Neurology, Neurosurgery & Psychiatry*, 89(Suppl 1), pp. A99–A99. doi: 10.1136/jnnp-2018-ehdn.265.

Reilmann, R. *et al.* (2019) 'Safety and efficacy of pridopidine in patients with Huntington's disease (PRIDE-HD): a phase 2, randomised, placebo-controlled, multicentre, dose-ranging study', *The Lancet Neurology*, 18(2), pp. 165–176. doi: 10.1016/S1474-4422(18)30391-0.

Reiner, A. *et al.* (1988) 'Differential loss of striatal projection neurons in Huntington disease.', *Proceedings of the National Academy of Sciences of the United States of America*, 85(15), pp. 5733–7. Available at: http://www.pubmedcentral.nih.gov/articlerender.fcgi?artid=281835&tool=pmcentrez&rendertype=abstract.

Reiner, A., Dragatsis, I. and Dietrich, P. (2011) *GENETICS AND NEUROPATHOLOGY OF HUNTINGTON'S DISEASE*. doi: 10.1002/oby.21042.Prevalence.

Renaud-Gabardos, E. (2015) 'Internal ribosome entry site-based vectors for combined gene therapy', *World Journal of Experimental Medicine*, 5(1), p. 11. doi: 10.5493/wjem.v5.i1.11.

Rial, D. *et al.* (2014) 'Behavioral phenotyping of Parkin-deficient mice: Looking for early preclinical features of Parkinson's disease', *PLoS ONE*, 9(12), pp. 1–21. doi: 10.1371/journal.pone.0114216.

Rietdijk, C. D. *et al.* (2017) 'Exploring Braak's hypothesis of parkinson's disease', *Frontiers in Neurology*, 8(FEB). doi: 10.3389/fneur.2017.00037.

De Rijck, J. *et al.* (2007) 'Lentiviral nuclear import: A complex interplay between virus and host', *BioEssays*, 29(5), pp. 441–451. doi: 10.1002/bies.20561.

Rodriguez-Tebar, A., Dechant, G. and Barde, Y.-A. (1990) 'Binding of brain-derived neurotrophic factor to the nerve growth factor receptor', *Neuron*, 4(4), pp. 487–492. doi: https://doi.org/10.1016/0896-6273(90)90107-Q.

Rosenblad, C. *et al.* (2019) 'Vector-mediated l-3,4-dihydroxyphenylalanine delivery reverses motor impairments in a primate model of Parkinson's disease', *Brain*, 142(8), pp. 2402–2416. doi: 10.1093/brain/awz176.

Rosenblum, S. *et al.* (2013) 'Handwriting as an objective tool for Parkinson's disease

diagnosis', *Journal of Neurology*, 260(9), pp. 2357–2361. doi: 10.1007/s00415-013-6996-x.

Roskoski, R. (2012) 'ERK1/2 MAP kinases: Structure, function, and regulation', *Pharmacological Research*. Elsevier Ltd, 66(2), pp. 105–143. doi: 10.1016/j.phrs.2012.04.005.

Ross, O. A. *et al.* (2011) 'Association of LRRK2 exonic variants with susceptibility to Parkinson's disease: a case-control study.', *The Lancet. Neurology*, 10(10), pp. 898–908. doi: 10.1016/S1474-4422(11)70175-2.

Roux, P. P. and Blenis, J. (2004) 'ERK and p38 MAPK-Activated Protein Kinases : a Family of Protein Kinases with Diverse Biological Functions ERK and p38 MAPK-Activated Protein Kinases : a Family of Protein Kinases with Diverse Biological Functions', *Microbiology and molecular biology reviews : MMBR*, 68(2), pp. 320–344. doi: 10.1128/MMBR.68.2.320.

Rowe, K. C. *et al.* (2012) 'Patterns of serotonergic antidepressant usage in prodromal Huntington disease.', *Psychiatry research*, 196(2–3), pp. 309–314. doi: 10.1016/j.psychres.2011.09.005.

Rub, C., Wilkening, A. and Voos, W. (2017) 'Mitochondrial quality control by the Pink1/Parkin system.', *Cell and tissue research*. Germany, 367(1), pp. 111–123. doi: 10.1007/s00441-016-2485-8.

Rubinfeld, H. and Seger, R. (2005) 'The ERK cascade', *Molecular Biotechnology*, 31(2), pp. 151–174. doi: 10.1385/MB:31:2:151.

Russell, D. W. (2007) 'AAV Vectors, Insertional Mutagenesis, and Cancer', *Molecular Therapy*. Elsevier, 15(10), pp. 1740–1743. doi: 10.1038/sj.mt.6300299.

Russell, S. *et al.* (2017) 'Efficacy and safety of voretigene neparvovec (AAV2-hRPE65v2) in patients with RPE65-mediated inherited retinal dystrophy: a randomised, controlled, open-label, phase 3 trial.', *Lancet (London, England)*, 390(10097), pp. 849–860. doi: 10.1016/S0140-6736(17)31868-8.

Ryu, H. H. and Lee, Y. S. (2016) 'Cell type-specific roles of RAS-MAPK signaling in learning and memory: Implications in neurodevelopmental disorders', *Neurobiology of Learning and Memory*. Elsevier Inc., 135, pp. 13–21. doi: 10.1016/j.nlm.2016.06.006.

Ryu, J. K. *et al.* (2004) 'Proactive transplantation of human neural stem cells prevents degeneration of striatal neurons in a rat model of Huntington disease', *Neurobiology of Disease*, 16(1), pp. 68–77. doi: https://doi.org/10.1016/j.nbd.2004.01.016.

Ryzhkova, A. I. *et al.* (2018) 'Mitochondrial diseases caused by mtDNA mutations: a mini-

review.', *Therapeutics and clinical risk management*, 14, pp. 1933–1942. doi: 10.2147/TCRM.S154863.

Saba-El-Leil, M. K. *et al.* (2003) 'An essential function of the mitogen-activated protein kinase Erk2 in mouse trophoblast development', *EMBO reports*, 4(10), pp. 964–968. doi: 10.1038/sj.embor.embor939.

Sairanen, M. *et al.* (2007) 'Chronic antidepressant treatment selectively increases expression of plasticity-related proteins in the hippocampus and medial prefrontal cortex of the rat', *Neuroscience*, 144(1), pp. 368–374. doi: 10.1016/j.neuroscience.2006.08.069.

Sakuma, T., Barry, M. A. and Ikeda, Y. (2012) 'Lentiviral vectors: basic to translational', *Biochemical Journal*, 443(3), pp. 603–618. doi: 10.1042/BJ20120146.

Samulski, R. J. and Muzyczka, N. (2014) 'AAV-Mediated Gene Therapy for Research and Therapeutic Purposes', *Annual Review of Virology*, 1(1), pp. 427–451. doi: 10.1146/annurev-virology-031413-085355.

Sanjo, H. *et al.* (2007) 'Extracellular signal-regulated protein kinase 2 is required for efficient generation of B cells bearing antigen-specific immunoglobulin G.', *Molecular and cellular biology*. United States, 27(4), pp. 1236–1246. doi: 10.1128/MCB.01530-06.

Santel, A. and Fuller, M. T. (2001) 'Control of mitochondrial morphology by a human mitofusin', *Journal of Cell Science*. The Company of Biologists Ltd, 114(5), pp. 867–874. Available at: https://jcs.biologists.org/content/114/5/867.

Sarantos, M. R. *et al.* (2013) 'Pizotifen Activates ERK and Provides Neuroprotection in vitro and in vivo in Models of Huntington's Disease', 1(2), pp. 195–210. doi: 10.3233/JHD-120033.Pizotifen.

Sarraf, S. A. *et al.* (2013) 'Landscape of the PARKIN-dependent ubiquitylome in response to mitochondrial depolarization.', *Nature*. England, 496(7445), pp. 372–376. doi: 10.1038/nature12043.

Satoh, Y. *et al.* (2007) 'Extracellular signal-regulated kinase 2 (ERK2) knockdown mice show deficits in long-term memory; ERK2 has a specific function in learning and memory.', *The Journal of neuroscience : the official journal of the Society for Neuroscience*, 27(40), pp. 10765–76. doi: 10.1523/JNEUROSCI.0117-07.2007.

Schapira, A. H. *et al.* (1990) 'Mitochondrial complex I deficiency in Parkinson's disease.', *Journal of neurochemistry*. England, 54(3), pp. 823–827. doi: 10.1111/j.1471-4159.1990.tb02325.x.

Schaser, A. J. *et al.* (2019) 'Alpha-synuclein is a DNA binding protein that modulates DNA repair with implications for Lewy body disorders', *Scientific Reports*. Springer US, 9(1), pp. 1–19. doi: 10.1038/s41598-019-47227-z.

Scherzinger, E. *et al.* (1999) 'Self-assembly of polyglutamine-containing huntingtin fragments into amyloid-like fibrils: implications for Huntington's disease pathology.', *Proceedings of the National Academy of Sciences of the United States of America*, 96(8), pp. 4604–4609. doi: 10.1073/pnas.96.8.4604.

Schiess, M. C. *et al.* (2000) 'Parkinson's disease subtypes: Clinical classification and ventricular cerebrospinal fluid analysis', *Parkinsonism and Related Disorders*, 6(2), pp. 69–76. doi: 10.1016/S1353-8020(99)00051-6.

Schmidt, N. and Ferger, B. (2001) 'Neurochemical findings in the MPTP model of Parkinson's disease.', *Journal of neural transmission (Vienna, Austria : 1996)*. Austria, 108(11), pp. 1263–1282. doi: 10.1007/s007020100004.

Schork, N. J. *et al.* (2009) 'Common vs. rare allele hypotheses for complex diseases.', *Current opinion in genetics & development*, 19(3), pp. 212–219. doi: 10.1016/j.gde.2009.04.010.

Schramm, C. *et al.* (2015) 'How to Capitalize on the Retest Effect in Future Trials on Huntington's Disease.', *PloS one*. United States, 10(12), p. e0145842. doi: 10.1371/journal.pone.0145842.

Schwanhausser, B. *et al.* (2011) 'Global quantification of mammalian gene expression control.', *Nature*. England, 473(7347), pp. 337–342. doi: 10.1038/nature10098.

Segura-Aguilar, J. *et al.* (2014) 'Protective and toxic roles of dopamine in Parkinson's disease', *Journal of Neurochemistry*, 129(6), pp. 898–915. doi: 10.1111/jnc.12686.

Selcher, J. C. *et al.* (2001) 'Mice lacking the ERK1 isoform of MAP kinase are unimpaired in emotional learning', *Learning and Memory*, 8(1), pp. 11–19. doi: 10.1101/lm.37001.

Sgambato, V. *et al.* (1998) 'Extracellular signal-regulated kinase (ERK) controls immediate early gene induction on corticostriatal stimulation.', *The Journal of neuroscience : the official journal of the Society for Neuroscience*. United States, 18(21), pp. 8814–8825.

Shahryari, A. *et al.* (2019) 'Development and Clinical Translation of Approved Gene Therapy Products for Genetic Disorders', 10(September). doi: 10.3389/fgene.2019.00868.

Shannon, K. M. and Fraint, A. (2015) 'Therapeutic advances in Huntington's Disease', *Movement Disorders*, 00(00), p. n/a-n/a. doi: 10.1002/mds.26331.

Shearwin, K. E., Callen, B. P. and Egan, J. B. (2005) 'Transcriptional interference--a crash course.', *Trends in genetics : TIG*, 21(6), pp. 339–345. doi: 10.1016/j.tig.2005.04.009.

Shelbourne, P. F. *et al.* (2007) 'Triplet repeat mutation length gains correlate with cell-type specific vulnerability in Huntington disease brain.', *Human molecular genetics*. England, 16(10), pp. 1133–1142. doi: 10.1093/hmg/ddm054.

Shen, Y. *et al.* (2000) 'Triple transduction with adeno-associated virus vectors expressing tyrosine hydroxylase, aromatic-L-amino-acid decarboxylase, and GTP cyclohydrolase I for gene therapy of Parkinson's disease.', *Human gene therapy*. United States, 11(11), pp. 1509–1519. doi: 10.1089/10430340050083243.

Shiflett, M. W. and Balleine, B. W. (2011) 'Contributions of ERK signaling in the striatum to instrumental learning and performance', *Computer*, 218(1), pp. 240–247. doi: 10.1038/jid.2014.371.

Shiflett, M. W., Brown, R. A. and Balleine, B. W. (2010) 'Acquisition and performance of goal-directed instrumental actions depends on ERK signaling in distinct regions of dorsal striatum in rats.', *The Journal of neuroscience : the official journal of the Society for Neuroscience*, 30(8), pp. 2951–2959. doi: 10.1523/JNEUROSCI.1778-09.2010.

Shin, J.-H. *et al.* (2011) 'PARIS (ZNF746) Repression of PGC-1α Contributes to Neurodegeneration in Parkinson's Disease', *Cell*, 144(5), pp. 689–702. doi: 10.1016/j.yjmcc.2010.12.015.Regulation.

Shlevkov, E. *et al.* (2016) 'Miro phosphorylation sites regulate Parkin recruitment and mitochondrial motility.', *Proceedings of the National Academy of Sciences of the United States of America*. United States, 113(41), pp. E6097–E6106. doi: 10.1073/pnas.1612283113.

Shojaee, S. *et al.* (2008) 'Genome-wide linkage analysis of a Parkinsonian-pyramidal syndrome pedigree by 500 K SNP arrays.', *American journal of human genetics*. United States, 82(6), pp. 1375–1384. doi: 10.1016/j.ajhg.2008.05.005.

Shu, Y. *et al.* (2016) 'Parkinson-Related LRRK2 Mutation R1628P Enables Cdk5 Phosphorylation of LRRK2 and Upregulates Its Kinase Activity', *PLOS ONE*. Public Library of Science, 11(3), pp. 1–13. doi: 10.1371/journal.pone.0149739.

Sieradzan, K. A. *et al.* (1999) 'Huntington's Disease Intranuclear Inclusions Contain Truncated, Ubiquitinated Huntingtin Protein', *Experimental Neurology*, 156(1), pp. 92–99. doi: https://doi.org/10.1006/exnr.1998.7005.

Silva, A. J. *et al.* (1997) 'A mouse model for the learning and memory deficits associated with

neurofibromatosis type I', *Nature Genetics*. Nature Publishing Group, 15, p. 281. Available at: https://doi.org/10.1038/ng0397-281.

Silvestri, L. *et al.* (2005) 'Mitochondrial import and enzymatic activity of PINK1 mutants associated to recessive parkinsonism.', *Human molecular genetics*. England, 14(22), pp. 3477–3492. doi: 10.1093/hmg/ddi377.

Simmons, A. D. A. *et al.* (2016) 'A small molecule p75NTR ligand normalizes signalling and reduces Huntington's disease phenotypes in R6/2 and BACHD mice.', *Human Molecular Genetics*, 15(25), pp. 492–4938.

Simmons, D. A. *et al.* (2011) 'Brief ampakine treatments slow the progression of Huntington's disease phenotypes in R6/2 mice', *Neurobiology of disease*. 2010/10/23, 41(2), pp. 436–444. doi: 10.1016/j.nbd.2010.10.015.

Simmons, D. a *et al.* (2009) 'Up-regulating BDNF with an ampakine rescues synaptic plasticity and memory in Huntington's disease knockin mice.', *Proceedings of the National Academy of Sciences of the United States of America*, 106(12), pp. 4906–4911. doi: 10.1073/pnas.0811228106.

Simmons, D. a *et al.* (2013) 'A small molecule TrkB ligand reduces motor impairment and neuropathology in R6/2 and BACHD mouse models of Huntington's disease.', *The Journal of neuroscience : the official journal of the Society for Neuroscience*, 33(48), pp. 18712–27. doi: 10.1523/JNEUROSCI.1310-13.2013.

Simpson, E. M. *et al.* (1997) 'Genetic variation among 129 substrains and its importance for targeted mutagenesis in mice.', *Nature genetics*. United States, 16(1), pp. 19–27. doi: 10.1038/ng0597-19.

Simuni, T. and Fernandez, H. H. (2013) 'Anxiety in Parkinson's Disease', *Milestones in Drug Therapy*, 24, pp. 17–29. doi: 10.1007/978-1-60761-429-6_2.

Skotte, N. H. *et al.* (2014) 'Allele-specific suppression of mutant huntingtin using antisense oligonucleotides: providing a therapeutic option for all Huntington disease patients.', *PloS one*, 9(9), p. e107434. doi: 10.1371/journal.pone.0107434.

Sliter, D. A. *et al.* (2018) 'Parkin and PINK1 mitigate STING-induced inflammation', *Nature*. Springer US, 561(7722), pp. 258–262. doi: 10.1038/s41586-018-0448-9.

Slow, E. J. *et al.* (2003) 'Selective striatal neuronal loss in a YAC128 mouse model of Huntington disease', *Human Molecular Genetics*, 12(13), pp. 1555–1567. doi: 10.1093/hmg/ddg169.

Smith, D. I. *et al.* (2006) 'Common fragile sites, extremely large genes, neural development and cancer.', *Cancer letters*. Ireland, 232(1), pp. 48–57. doi: 10.1016/j.canlet.2005.06.049.

Snyder, B. R. *et al.* (2010) 'Human multipotent stromal cells (MSCs) increase neurogenesis and decrease atrophy of the striatum in a transgenic mouse model for Huntington's disease.', *PloS one*. United States, 5(2), p. e9347. doi: 10.1371/journal.pone.0009347.

Soboleski, M. R., Oaks, J. and Halford, W. P. (2005) 'Green fluorescent protein is a quantitative reporter of gene expression in individual eukaryotic cells', *FASEB Journal*, 19(3), pp. 440–442. doi: 10.1096/fj.04-3180fje.

Song, D. D. *et al.* (2004) 'Enhanced substantia nigra mitochondrial pathology in human alpha-synuclein transgenic mice after treatment with MPTP.', *Experimental neurology*. United States, 186(2), pp. 158–172. doi: 10.1016/S0014-4886(03)00342-X.

Song, W. *et al.* (2010) 'ProNGF induces PTEN via p75NTR to suppress Trk-mediated survival signaling in brain neurons', *The Journal of neuroscience : the official journal of the Society for Neuroscience*, 30(46), pp. 15608–15615. doi: 10.1523/JNEUROSCI.2581-10.2010.

Sperling, R. A. *et al.* (2011) 'Toward defining the preclinical stages of Alzheimer's disease: recommendations from the National Institute on Aging-Alzheimer's Association workgroups on diagnostic guidelines for Alzheimer's disease.', *Alzheimer's & dementia : the journal of the Alzheimer's Association*. United States, 7(3), pp. 280–292. doi: 10.1016/j.jalz.2011.03.003.

Spillantini, M. G. *et al.* (1997) 'Alpha-synuclein in Lewy bodies.', *Nature*. England, pp. 839–840. doi: 10.1038/42166.

Spires, T. L. *et al.* (2004) 'Environmental enrichment rescues protein deficits in a mouse model of Huntington's disease, indicating a possible disease mechanism.', *The Journal of neuroscience : the official journal of the Society for Neuroscience*. United States, 24(9), pp. 2270–2276. doi: 10.1523/JNEUROSCI.1658-03.2004.

Squitieri, F. *et al.* (2015) 'Pridopidine, a dopamine stabilizer, improves motor performance and shows neuroprotective effects in Huntington disease R6/2 mouse model', *Journal of Cellular and Molecular Medicine*, 19(11), pp. 2540–2548. doi: 10.1111/jcmm.12604.

Srivastava, A. (2016) 'In vivo tissue-tropism of adeno-associated viral vectors.', *Current opinion in virology*, 21, pp. 75–80. doi: 10.1016/j.coviro.2016.08.003.

Srivastava, A., Lusby, E. W. and Berns, K. I. (1983) 'Nucleotide sequence and organization of the adeno-associated virus 2 genome.', *Journal of virology*. United States, 45(2), pp. 555–564.

Stansley, B. J. and Yamamoto, B. K. (2013) 'L-dopa-induced dopamine synthesis and oxidative stress in serotonergic cells.', *Neuropharmacology*, 67, pp. 243–251. doi: 10.1016/j.neuropharm.2012.11.010.

Starr, P. A. *et al.* (2008) 'Pallidal neuronal discharge in Huntington's disease: support for selective loss of striatal cells originating the indirect pathway.', *Experimental neurology*, 211(1), pp. 227–233. doi: 10.1016/j.expneurol.2008.01.023.

Stevens, D. A. *et al.* (2015) 'Parkin loss leads to PARIS-dependent declines in mitochondrial mass and respiration', *Proceedings of the National Academy of Sciences*, 112(37), pp. 11696–11701. doi: 10.1073/pnas.1500624112.

Stewart, H. J. *et al.* (2016) 'Optimizing Transgene Configuration and Protein Fusions to Maximize Dopamine Production for the Gene Therapy of Parkinson's Disease', *Human Gene Therapy Clinical Development*, 27(3), pp. 100–110. doi: 10.1089/humc.2016.056.

Stine, O. C. *et al.* (1993) 'Correlation between the onset age of Huntington's disease and length of the trinucleotide repeat in IT-15.', *Human molecular genetics*. England, 2(10), pp. 1547–1549. doi: 10.1093/hmg/2.10.1547.

Stocchi, F. *et al.* (2005) 'Intermittent vs continuous levodopa administration in patients with advanced Parkinson disease: a clinical and pharmacokinetic study.', *Archives of neurology*. United States, 62(6), pp. 905–910. doi: 10.1001/archneur.62.6.905.

Stojanovski, D. *et al.* (2012) 'Mechanisms of protein sorting in mitochondria.', *Cold Spring Harbor perspectives in biology*. United States, 4(10). doi: 10.1101/cshperspect.a011320.

Storch, A., Ludolph, A. C. and Schwarz, J. (2004) 'Dopamine transporter: involvement in selective dopaminergic neurotoxicity and degeneration.', *Journal of neural transmission (Vienna, Austria : 1996)*. Austria, 111(10–11), pp. 1267–1286. doi: 10.1007/s00702-004-0203-2.

Strong, T. V *et al.* (1993) 'Widespread expression of the human and rat Huntington's disease gene in brain and nonneural tissues.', *Nature genetics*. United States, 5(3), pp. 259–265. doi: 10.1038/ng1193-259.

Subramaniam, S. *et al.* (2009) 'Rhes, a Striatal Specific Protein, Mediates Mutant-Huntingtin Cytotoxicity', 324(5932), pp. 1327–1330. doi: 10.1126/science.1172871.Rhes.

Sudhakar, V. and Richardson, R. M. (2019) 'Gene Therapy for Neurodegenerative Diseases', *Neurotherapeutics*. Neurotherapeutics, 16(1), pp. 166–175. doi: 10.1007/s13311-018-00694-0.

Sui, X. *et al.* (2019) 'Hyposmia as a Predictive Marker of Parkinson's Disease: A Systematic Review and Meta-Analysis.', *BioMed research international*. United States, 2019, p. 3753786. doi: 10.1155/2019/3753786.

Sulzer, D. and Surmeier, D. J. (2013) 'Neuronal vulnerability, pathogenesis, and Parkinson's disease.', *Movement disorders : official journal of the Movement Disorder Society*, 28(1), pp. 41–50. doi: 10.1002/mds.25095.

Taanman, J. W. (1999) 'The mitochondrial genome: structure, transcription, translation and replication.', *Biochimica et biophysica acta*. Netherlands, 1410(2), pp. 103–123. doi: 10.1016/s0005-2728(98)00161-3.

Tabrizi, S. J. *et al.* (2019) 'Targeting huntingtin expression in patients with Huntington's disease', *New England Journal of Medicine*, 380(24), pp. 2307–2316. doi: 10.1056/NEJMoa1900907.

Tabrizi, S. J., Ghosh, R. and Leavitt, B. R. (2019) 'Huntingtin Lowering Strategies for Disease Modification in Huntington's Disease', *Neuron*. Elsevier Inc., 101(5), pp. 801–819. doi: 10.1016/j.neuron.2019.01.039.

Tanaka, A. *et al.* (2010) 'Proteasome and p97 mediate mitophagy and degradation of mitofusins induced by Parkin.', *The Journal of cell biology*. United States, 191(7), pp. 1367–1380. doi: 10.1083/jcb.201007013.

Tang, F.-L. *et al.* (2015) 'VPS35 in Dopamine Neurons Is Required for Endosome-to-Golgi Retrieval of Lamp2a, a Receptor of Chaperone-Mediated Autophagy That Is Critical for alpha-Synuclein Degradation and Prevention of Pathogenesis of Parkinson's Disease.', *The Journal of neuroscience : the official journal of the Society for Neuroscience*. United States, 35(29), pp. 10613–10628. doi: 10.1523/JNEUROSCI.0042-15.2015.

Tanik, S. A. *et al.* (2013) 'Lewy body-like alpha-synuclein aggregates resist degradation and impair macroautophagy.', *The Journal of biological chemistry*. United States, 288(21), pp. 15194–15210. doi: 10.1074/jbc.M113.457408.

Tanner, C. M. *et al.* (2011) 'Rotenone, paraquat, and Parkinson's disease.', *Environmental health perspectives*, 119(6), pp. 866–872. doi: 10.1289/ehp.1002839.

Telenius, H. *et al.* (1994) 'Somatic and gonadal mosaicism of the Huntington disease gene CAG repeat in brain and sperm', *Nature Genetics*. Nature Publishing Group, 6, p. 409. Available at: https://doi.org/10.1038/ng0494-409.

Thanvi, B. R. and Lo, T. C. N. (2004) 'Long term motor complications of levodopa: clinical

features, mechanisms, and management strategies', *Postgraduate Medical Journal*. The Fellowship of Postgraduate Medicine, 80(946), pp. 452–458. doi: 10.1136/pgmj.2003.013912.

The BDNF Study Group (1999) 'A controlled trial of recombinant methionyl human BDNF in ALS: The BDNF Study Group (Phase III).', *Neurology*. United States, 52(7), pp. 1427–1433. doi: 10.1212/wnl.52.7.1427.

Thiele, S. L., Warre, R. and Nash, J. E. (2012) 'Development of a unilaterally-lesioned 6-OHDA mouse model of Parkinson's disease', *Journal of Visualized Experiments*, (60), pp. 1–8. doi: 10.3791/3234.

Thomas, G. M. and Huganir, R. L. (2004) 'MAPK cascade signalling and synaptic plasticity.', *Nature reviews. Neuroscience*, 5(3), pp. 173–183. doi: 10.1038/nrn1346.

Todorovic, C. *et al.* (2009) 'Suppression of the MEK/ERK signaling pathway reverses depression-like behaviors of CRF2-deficient mice.', *Neuropsychopharmacology : official publication of the American College of Neuropsychopharmacology*, 34(6), pp. 1416–1426. doi: 10.1038/npp.2008.178.

Travessa, A. M. *et al.* (2017) 'Fifteen years of clinical trials in Huntington's disease: A very low clinical drug development success rate', *Journal of Huntington's Disease*, 6(2), pp. 157–163. doi: 10.3233/JHD-170245.

Trifunovic, A. *et al.* (2004) 'Premature ageing in mice expressing defective mitochondrial DNA polymerase.', *Nature*. England, 429(6990), pp. 417–423. doi: 10.1038/nature02517.

Tufekci, K. U. *et al.* (2012) 'Chapter Four - Inflammation in Parkinson's Disease', in Donev, R. (ed.) *Inflammation in Neuropsychiatric Disorders*. Academic Press (Advances in Protein Chemistry and Structural Biology), pp. 69–132. doi: https://doi.org/10.1016/B978-0-12-398314-5.00004-0.

Twelves, D., Perkins, K. S. and Counsell, C. (2002) 'Systematic review of incidence studies of Parkinson's disease', *Movement Disorders*, 18(1), pp. 19–31. doi: 10.1002/mds.10305.

Uhrig, S. *et al.* (2012) 'Successful target cell transduction of capsid-engineered rAAV vectors requires clathrin-dependent endocytosis', *Gene Therapy*, 19(2), pp. 210–218. doi: 10.1038/gt.2011.78.

Ünal, E. B., Uhlitz, F. and Blüthgen, N. (2017) 'A compendium of ERK targets', *FEBS Letters*, 591(17), pp. 2607–2615. doi: 10.1002/1873-3468.12740.

Ungerstedt, U. (1968) '6-Hydroxy-Dopamine Induced Degeneration of Central Monoamine

Neurons', *European Journal of Pharmacology*, 5(1), pp. 107–110. doi: 10.1016/0014-2999(68)90164-7.

Ungerstedt, U. (1971a) 'Postsynaptic supersensitivity after 6-hydroxy-dopamine induced degeneration of the nigro-striatal dopamine system.', *Acta physiologica Scandinavica. Supplementum*. England, 367, pp. 69–93.

Ungerstedt, U. (1971b) 'Striatal Dopamine Release after Amphetamine or Nerve Degeneration Revealed by Rotational Behaviour', *Acta Physiologica Scandinavica*, 82(S367), pp. 49–68. doi: 10.1111/j.1365-201X.1971.tb10999.x.

Unti, E. *et al.* (2017) 'Antipsychotic drugs in Huntington's disease.', *Expert review of neurotherapeutics*. England, 17(3), pp. 227–237. doi: 10.1080/14737175.2016.1226134.

van der Vaart, T. *et al.* (2011) 'Motor deficits in neurofibromatosis type 1 mice: The role of the cerebellum', *Genes, Brain and Behavior*, 10(4), pp. 404–409. doi: 10.1111/j.1601-183X.2011.00685.x.

Valente, E. M. *et al.* (2004) 'Hereditary Early-Onset Parkinson's Disease Caused by Mutations in PINK1', *Science*, 304(May), p. 4.

Valjent, E. *et al.* (2005) 'Regulation of a protein phosphatase cascade allows convergent dopamine and glutamate signals to activate ERK in the striatum.', *Proceedings of the National Academy of Sciences of the United States of America*, 102(2), pp. 491–496. doi: 10.1073/pnas.0408305102.

Valkovic, P. *et al.* (2015) 'Pain in Parkinson´s Disease: A Cross-Sectional Study of Its Prevalence, Types, and Relationship to Depression and Quality of Life', *PLOS ONE*. Public Library of Science, 10(8), pp. 1–11. doi: 10.1371/journal.pone.0136541.

Vantaggiato, C. *et al.* (2006) 'ERK1 and ERK2 mitogen-activated protein kinases affect Ras-dependent cell signaling differentially', *Journal of biology*, 5(5), pp. 1–15.

Varastet, M. *et al.* (1994) 'Chronic MPTP treatment reproduces in baboons the differential vulnerability of mesencephalic dopaminergic neurons observed in Parkinson's disease.', *Neuroscience*. United States, 63(1), pp. 47–56. doi: 10.1016/0306-4522(94)90006-x.

Varga, A. W. *et al.* (2000) 'Input-specific immunolocalization of differentially phosphorylated Kv4.2 in the mouse brain.', *Learning & memory (Cold Spring Harbor, N.Y.)*. United States, 7(5), pp. 321–332.

Vattakatuchery, J. J. and Kurien, R. (2013) 'Acetylcholinesterase inhibitors in cognitive

impairment in Huntington's disease: A brief review.', *World journal of psychiatry*, 3(3), pp. 62–64. doi: 10.5498/wjp.v3.i3.62.

Verny, C. *et al.* (2017) 'A randomized, double-blind, placebo-controlled trial evaluating cysteamine in Huntington's disease', *Movement Disorders*, 32(6), pp. 932–936. doi: 10.1002/mds.27010.

Vestergaard, P., Baastrup, P. C. and Petersson, H. (1977) 'Lithium treatment of Huntington's chorea', *Acta Psychiatrica Scandinavica*, 56(3), pp. 183–188. doi: 10.1111/j.1600-0447.1977.tb03561.x.

Vila, M. *et al.* (2000) 'Alpha-synuclein up-regulation in substantia nigra dopaminergic neurons following administration of the parkinsonian toxin MPTP.', *Journal of neurochemistry*. England, 74(2), pp. 721–729. doi: 10.1046/j.1471-4159.2000.740721.x.

Vilariño-Güell, C. *et al.* (2011) 'VPS35 mutations in Parkinson disease.', *American journal of human genetics*, 89(1), pp. 162–167. doi: 10.1016/j.ajhg.2011.06.001.

Vincow, E. S. *et al.* (2013) 'The PINK1-Parkin pathway promotes both mitophagy and selective respiratory chain turnover in vivo', *Proceedings of the National Academy of Sciences*, 110(16), pp. 6400–6405. doi: 10.1073/pnas.1221132110.

Volkmann, J. *et al.* (2004) 'Long-term results of bilateral pallidal stimulation in Parkinson's disease.', *Annals of neurology*. United States, 55(6), pp. 871–875. doi: 10.1002/ana.20091.

Volpicelli-Daley, L. A. *et al.* (2016) 'G2019S-LRRK2 Expression Augments alpha-Synuclein Sequestration into Inclusions in Neurons.', *The Journal of neuroscience : the official journal of the Society for Neuroscience*. United States, 36(28), pp. 7415–7427. doi: 10.1523/JNEUROSCI.3642-15.2016.

Vonsattel, J.-P. *et al.* (1985) 'Neuropathological Classification of Huntington's Disease', *Journal of Neuropathology & Experimental Neurology*, 44(6), pp. 559–577. doi: 10.1097/00005072-198511000-00003.

Wade, D. N., Mearrick, P. T. and Morris, J. L. (1973) 'Active transport of L-Dopa in the intestine', *Nature*, 242(5398), pp. 463–465. doi: 10.1038/242463a0.

Wade Harper, J., Ordureau, A. and Heo, J. M. (2018) 'Building and decoding ubiquitin hains for mitophagy', *Nature Reviews Molecular Cell Biology*. Nature Publishing Group, 19(2), pp. 93–108. doi: 10.1038/nrm.2017.129.

Wahlsten, D. *et al.* (2003) 'Different data from different labs: Lessons from studies of gene-

environment interaction', *Journal of Neurobiology*, 54(1), pp. 283–311. doi: 10.1002/neu.10173.

Wan, P. T. C. *et al.* (2004) 'Mechanism of activation of the RAF-ERK signaling pathway by oncogenic mutations of B-RAF', *Cell*, 116(6), pp. 855–867. doi: 10.1016/S0092-8674(04)00215-6.

Watson, S. G. and Leverenz, J. B. (2010) 'Profile of Cognitive Impairment in Parkinson Disease', *Brain Pathology*, 20(3), pp. 640–645. doi: 10.1111/j.1750-3639.2010.00373.x.Profile.

Watts, J. K. and Corey, D. R. (2012) 'Silencing disease genes in the laboratory and the clinic.', *The Journal of pathology*, 226(2), pp. 365–379. doi: 10.1002/path.2993.

Wehner, A. B. *et al.* (2016) 'The p75 neurotrophin receptor augments survival signaling in the striatum of pre-symptomatic Q175WT/HD mice', *Neuroscience*. IBRO, 324, pp. 297–306. doi: 10.1016/j.neuroscience.2016.02.069.

Weintraub, D. *et al.* (2003) 'Recognition and treatment of depression in Parkinson's disease.', *Journal of geriatric psychiatry and neurology*. United States, 16(3), pp. 178–183. doi: 10.1177/0891988703256053.

Weintraub, D. *et al.* (2010) 'Impulse control disorders in Parkinson disease: a cross-sectional study of 3090 patients.', *Archives of neurology*. United States, 67(5), pp. 589–595. doi: 10.1001/archneurol.2010.65.

Weintraub, D. and Burn, D. J. (2011) 'Parkinson's disease: The quintessential neuropsychiatric disorder', *Movement Disorders*, 26(6), pp. 1022–1031. doi: 10.1002/mds.23664.

West, A. B. *et al.* (2007) 'Parkinson's disease-associated mutations in LRRK2 link enhanced GTP-binding and kinase activities to neuronal toxicity.', *Human molecular genetics*. England, 16(2), pp. 223–232. doi: 10.1093/hmg/ddl471.

Wheeler, V. C. *et al.* (1999) 'Length-dependent gametic CAG repeat instability in the Huntington's disease knock-in mouse.', *Human molecular genetics*. England, 8(1), pp. 115–122. doi: 10.1093/hmg/8.1.115.

Wheeler, V. C. *et al.* (2002) 'Early phenotypes that presage late-onset neurodegenerative disease allow testing of modifiers in Hdh CAG knock-in mice.', *Human molecular genetics*. England, 11(6), pp. 633–640. doi: 10.1093/hmg/11.6.633.

Whitfield, A. C., Moore, B. T. and Daniels, R. N. (2014) 'Classics in chemical neuroscience:

Levodopa', *ACS Chemical Neuroscience*, 5(12), pp. 1192–1197. doi: 10.1021/cn5001759.

Whitmarsh, A. J. (2007) 'Regulation of gene transcription by mitogen-activated protein kinase signaling pathways', *Biochimica et Biophysica Acta (BBA) - Molecular Cell Research*, 1773(8), pp. 1285–1298. doi: https://doi.org/10.1016/j.bbamcr.2006.11.011.

Whitworth, A. J. and Pallanck, L. J. (2017) 'PINK1/Parkin mitophagy and neurodegeneration—what do we really know in vivo?', *Current Opinion in Genetics & Development*. Elsevier Ltd, 44, pp. 47–53. doi: 10.1016/j.gde.2017.01.016.

Wild, E. J. and Tabrizi, S. J. (2017) 'Therapies targeting DNA and RNA in Huntington's disease', *The Lancet Neurology*. Elsevier Ltd, 16(10), pp. 837–847. doi: 10.1016/S1474-4422(17)30280-6.

Wilms, H. *et al.* (2007) 'Inflammation in Parkinson's diseases and other neurodegenerative diseases: cause and therapeutic implications.', *Current pharmaceutical design*. United Arab Emirates, 13(18), pp. 1925–1928. doi: 10.2174/138161207780858429.

Winslow, A. R. *et al.* (2010) 'alpha-Synuclein impairs macroautophagy: implications for Parkinson's disease.', *The Journal of cell biology*. United States, 190(6), pp. 1023–1037. doi: 10.1083/jcb.201003122.

Wong, Y. C. and Krainc, D. (2017) 'alpha-synuclein toxicity in neurodegeneration: mechanism and therapeutic strategies.', *Nature medicine*. United States, 23(2), pp. 1–13. doi: 10.1038/nm.4269.

World Health Organisation (2017) 'Global action plan on the public health response to dementia 2017-2015'.

van der Worp, H. B. *et al.* (2010) 'Can animal models of disease reliably inform human studies?', *PLoS medicine*, 7(3), p. e1000245. doi: 10.1371/journal.pmed.1000245.

Wu, G. Y., Deisseroth, K. and Tsien, R. W. (2001) 'Spaced stimuli stabilize MAPK pathway activation and its effects on dendritic morphology.', *Nature neuroscience*, 4(2), pp. 151–8. doi: 10.1038/83976.

Wu, K., Politis, M. and Piccini, P. (2009) 'Parkinson disease and impulse control disorders: a review of clinical features, pathophysiology and management', *Postgraduate Medical Journal*, 85(1009), pp. 590 LP – 596. doi: 10.1136/pgmj.2008.075820.

Wu, Z., Yang, H. and Colosi, P. (2010) 'Effect of genome size on AAV vector packaging.', *Molecular therapy : the journal of the American Society of Gene Therapy*. United States, 18(1),

pp. 80–86. doi: 10.1038/mt.2009.255.

Xie, Y., Hayden, M. R. and Xu, B. (2010) 'BDNF overexpression in the forebrain rescues Huntington's disease phenotypes in YAC128 mice.', *The Journal of neuroscience : the official journal of the Society for Neuroscience*, 30(44), pp. 14708–14718. doi: 10.1523/JNEUROSCI.1637-10.2010.

Yamano, K., Matsuda, N. and Tanaka, K. (2016) 'The ubiquitin signal and autophagy: an orchestrated dance leading to mitochondrial degradation', *EMBO reports*, 17(3), pp. 300–316. doi: 10.15252/embr.201541486.

Yamano, K. and Youle, R. J. (2013) 'PINK1 is degraded through the N-end rule pathway.', *Autophagy*. United States, 9(11), pp. 1758–1769. doi: 10.4161/auto.24633.

Yan, J. Q. *et al.* (2014) 'Overexpression of Human E46K Mutant α-Synuclein Impairs Macroautophagy via Inactivation of JNK1-Bcl-2 Pathway', *Molecular Neurobiology*, 50(2), pp. 685–701. doi: 10.1007/s12035-014-8738-1.

Yan, S., Li, S. and Li, X.-J. (2019) 'Use of large animal models to investigate Huntington's diseases', *Cell Regeneration*, 8(1), pp. 9–11. doi: https://doi.org/10.1016/j.cr.2019.01.001.

Yang, D. *et al.* (2010) 'Expression of Huntington's disease protein results in apoptotic neurons in the brains of cloned transgenic pigs.', *Human molecular genetics*. England, 19(20), pp. 3983–3994. doi: 10.1093/hmg/ddq313.

Yang, L., Li, J. and Xiao, X. (2011) 'Directed evolution of adeno-associated virus (AAV) as vector for muscle gene therapy.', *Methods in molecular biology (Clifton, N.J.)*. United States, 709, pp. 127–139. doi: 10.1007/978-1-61737-982-6_8.

Yang, S.-H. *et al.* (2008) 'Towards a transgenic model of Huntington's disease in a non-human primate.', *Nature*. England, 453(7197), pp. 921–924. doi: 10.1038/nature06975.

Yhnell, E., Dunnett, S. B. and Brooks, S. P. (2016) 'A Longitudinal Motor Characterisation of the HdhQ111 Mouse Model of Huntington's Disease.', *Journal of Huntington's disease*, Preprint(Preprint), pp. 1–13. doi: 10.3233/JHD-160191.

Yoshiki, A. and Moriwaki, K. (2006) 'Mouse phenome research: Implications of genetic background', *ILAR Journal*, 47(2), pp. 94–102. doi: 10.1093/ilar.47.2.94.

You, H. *et al.* (2018) 'Molecular basis of dopamine replacement therapy and its side effects in Parkinson's disease', *Cell and Tissue Research*. Cell and Tissue Research, 373(1), pp. 111–135. doi: 10.1007/s00441-018-2813-2.

Yu, C. *et al.* (2018) 'Decreased BDNF Release in Cortical Neurons of a Knock-in Mouse Model of Huntington's Disease', *Scientific Reports*. Springer US, 8(1), pp. 1–11. doi: 10.1038/s41598-018-34883-w.

Yuan, J. and Zhao, Y. (2013) 'Evolutionary aspects of the synuclein super-family and sub-families based on large-scale phylogenetic and group-discrimination analysis.', *Biochemical and biophysical research communications*. United States, 441(2), pp. 308–317. doi: 10.1016/j.bbrc.2013.09.132.

Zeke, A. *et al.* (2016) 'JNK Signaling: Regulation and Functions Based on Complex Protein-Protein Partnerships', *Microbiology and Molecular Biology Reviews*. American Society for Microbiology Journals, 80(3), pp. 793–835. doi: 10.1128/MMBR.00043-14.

Zeng, X. S., Geng, W. S. and Jia, J. J. (2018) 'Neurotoxin-Induced Animal Models of Parkinson Disease: Pathogenic Mechanism and Assessment', *ASN Neuro*, 10. doi: 10.1177/1759091418777438.

Zhao, H. *et al.* (2017) 'Molecular mechanisms of brain-derived neurotrophic factor in neuro-protection: Recent developments', *Brain Research*, 1665, pp. 1–21. doi: https://doi.org/10.1016/j.brainres.2017.03.029.

Zheng, C. F. and Guan, K. L. (1994) 'Activation of MEK family kinases requires phosphorylation of two conserved Ser/Thr residues.', *The EMBO journal*. England, 13(5), pp. 1123–1131.

Zhu, J. J. *et al.* (2002) 'Ras and Rap control AMPA receptor trafficking during synaptic plasticity.', *Cell*. United States, 110(4), pp. 443–455. doi: 10.1016/s0092-8674(02)00897-8.

Zimprich, A. *et al.* (2004) 'Mutations in LRRK2 cause autosomal-dominant parkinsonism with pleomorphic pathology.', *Neuron*. United States, 44(4), pp. 601–607. doi: 10.1016/j.neuron.2004.11.005.

Zimprich, A. *et al.* (2011) 'A mutation in VPS35, encoding a subunit of the retromer complex, causes late-onset Parkinson disease.', *American journal of human genetics*. United States, 89(1), pp. 168–175. doi: 10.1016/j.ajhg.2011.06.008.

Zuccato, C. *et al.* (2001) 'Loss of Huntingtin-Mediated BDNF Gene Transcription in Huntington ' s Disease', 293(July), pp. 493–499.

Zuccato, C. *et al.* (2003) 'Huntingtin interacts with REST/NRSF to modulate the transcription of NRSE-controlled neuronal genes.', *Nature genetics*, 35(1), pp. 76–83. doi: 10.1038/ng1219.

Zuccato, C. *et al.* (2008) 'Systematic assessment of BDNF and its receptor levels in human

cortices affected by Huntington's disease', *Brain Pathology*, 18(2), pp. 225–238. doi: 10.1111/j.1750-3639.2007.00111.x.

Zuccato, C. and Cattaneo, E. (2007) 'Role of brain-derived neurotrophic factor in Huntington's disease.', *Progress in neurobiology*, 81(5–6), pp. 294–330. doi: 10.1016/j.pneurobio.2007.01.003.

Zuccato, C., Valenza, M. and Cattaneo, E. (2010) 'Molecular Mechanisms and Potential Therapeutical Targets in Huntington ' s Disease', *Physiol Rev*, 90, pp. 905–981. doi: 10.1152/physrev.00041.2009.

Zufferey, R. *et al.* (1997) 'Multiply attenuated lentiviral vector achieves efficient gene delivery in vivo.', *Nature biotechnology*. United States, 15(9), pp. 871–875. doi: 10.1038/nbt0997-871.

Zufferey, R. *et al.* (1998) 'Self-inactivating lentivirus vector for safe and efficient in vivo gene delivery.', *Journal of virology*. United States, 72(12), pp. 9873–9880.

Zufferey, R. *et al.* (1999) 'Woodchuck hepatitis virus posttranscriptional regulatory element enhances expression of transgenes delivered by retroviral vectors.', *Journal of virology*. United States, 73(4), pp. 2886–2892.